# DESIGN OF A CARDIAC PHANTOM

## FOR DEVELOPMENT OF ELECTROPHYSIOLOGY STUDIES

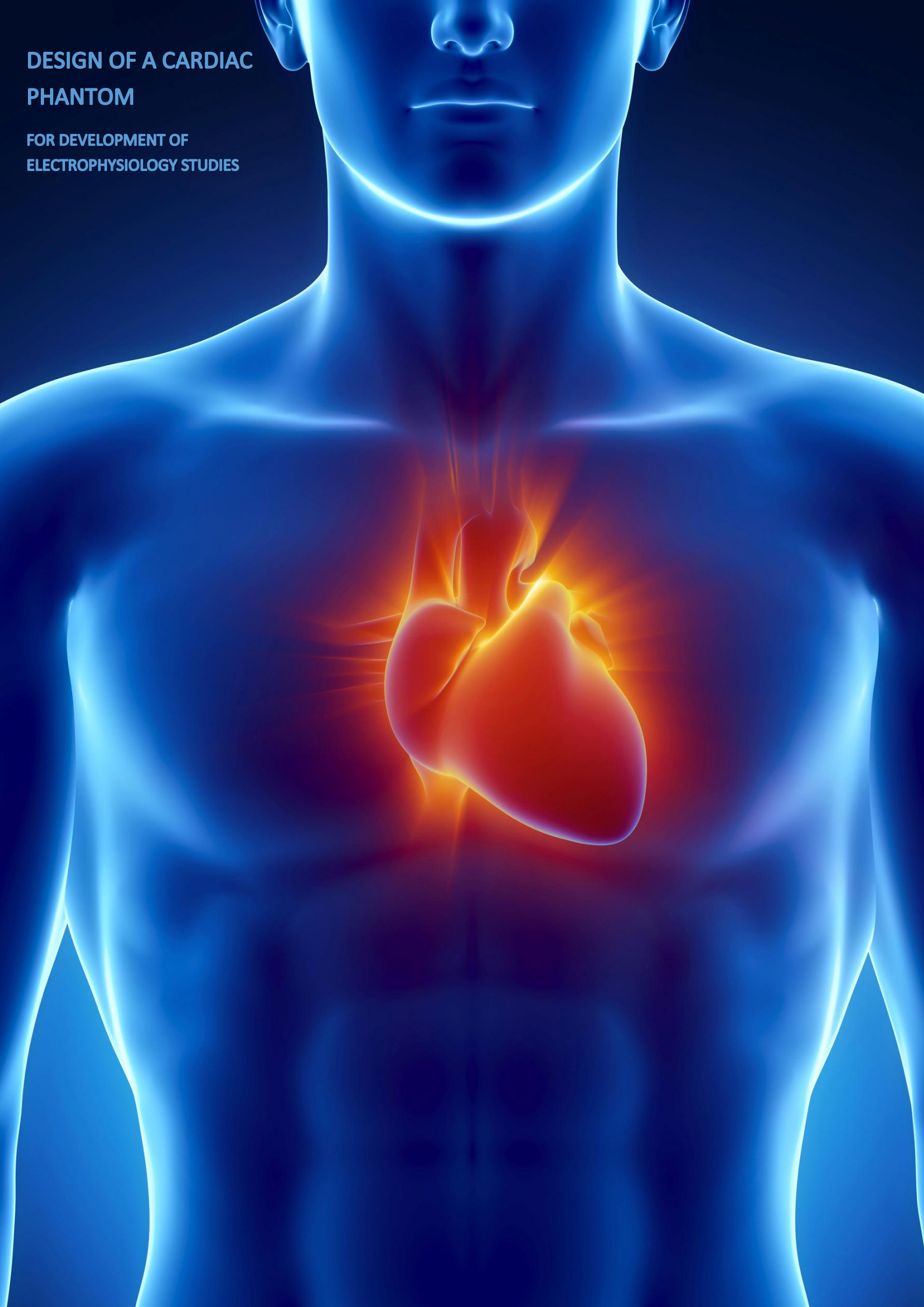

# DESIGN OF A CARDIAC PHANTOM

FOR DEVELOPMENT OF ELECTROPHYSIOLOGY STUDIES

BY

P.M.J. LUIK

IN PARTIAL FULFILMENT OF THE REQUIREMENTS FOR THE DEGREE OF

**MASTER OF SCIENCE**

IN BIOMEDICAL ENGINEERING

AT THE TECHNICAL UNIVERSITY OF DELFT

| | |
|---|---|
| Supervisors: | Dr. J.J. van den Dobbelsteen<br>Prof. Dr. B.H.W. Hendriks |
| Thesis committee: | Dr.ir. N. Tumer |

# Preface

The past year I have been working on my Master Thesis Project concerning the design of a cardiac phantom. This Master Thesis Project will be my last deliverable in order to obtain my Master degree in Biomedical Engineering, specialization in Medical Instruments and Medical Safety, at the Technical University (TU) of Delft. Under supervision of Professor Benno Hendriks at the Technical University Delft/Philips, and Doctor John van den Dobbelsteen at the Technical University Delft, this graduation project is conducted at the Technical University Delft. The project was performed in collaboration with the research department of Philips Healthcare in Best, the Netherlands. The objective of this Master Thesis Project was to develop an anthropomorphic left atrium (LA) phantom containing the dielectric properties similar to the human heart in the frequency range of 10 kHz – 20 kHz. The steps taken to achieve this objective are described in this thesis.

Approximately one year of hard work and dedication lead to the accomplishment of this Master Thesis Project. The entire project was a great experience, involving loads of new theoretical information and gaining practical skills. This project would not have been possible without the help of people from both the TU Delft and Philips. I would like to thank my supervisors Professor Benno Hendriks, for helping me with his expert information and John van den Dobbelsteen, who helped me with all facilities needed throughout this project. Moreover, I would like to thank Jan van Frankenhuyzen, who offered me great help and insights regarding 3D printing. Furthermore, Jeroen Bastemeijer from the TU Delft and Mischa Megens from Philips offered me great help with their electrical engineering-related knowledge.

# Abstract

**Introduction** Atrial fibrillation (AF) is the most common form of arrythmia. Without treatment, the heart rhythm usually becomes permanently disrupted and can lead to various heart related complications as stroke or heart failure. Cardiac phantoms are needed for the development of electrophysiological instruments and for training and education of electrophysiologist. A tissue mimicking phantom is an accurate model of organs or tissues mimicking the real life like scenario for a desired goal. Currently, no cardiac phantoms are available containing all requirements needed.

**Objective** Therefore, as a first step towards an applicable cardiac phantom for development of electrophysiology studies, this Master Thesis focused on the design of an anatomically anthropomorphic left atrium (LA) phantom mimicking the dielectric properties of human heart tissue in the frequency range of 10 kHz – 20 kHz.

**Methods** To assess this research goal, the objective was divided into 3 subgoals:

*1. Evaluate different tissue mimicking materials with additives to meet the main phantom requirements.*

Three promising types of phantoms were examined: agar-, gellan gum- and polyvinyl alcohol-cryogel-based (PVA-C) phantoms. The dielectric properties and stiffness of the phantoms were manipulated by varying the concentrations of materials and by using additives. Graphite powder, charcoal powder, salt and sodium acetate were examined for increasing the electrical conductivity and oil, sugar and PVC for decreasing its relative permittivity.

*2. Extensively evaluate the most promising cardiac phantom materials.*

The most promising phantom tissue materials, based on the main phantom requirements, was used for the final design of a LA phantom. The cardiac phantom was prepared four times for extensive examination based on all phantom requirements.

*3. Develop a phantom design with comparable anatomy.*

As a last step, the phantom was fabricated with comparable anatomy. In this part, a suitable mould was prepared in order to get a hollow shaped phantom.

**Results** A 13,0wt% PVA, 0,15wt% salt and 0,05wt% sodium acetate and tap water solution was used for the final LA phantom design. The flexible cardiac phantom is easily made, affordable and has a shelf life of at least 1 month. The average difference between the target values and the mean of all four prepared cardiac phantom samples is 21.9% and 15.0% for permittivity and conductivity, respectively. Storing the phantoms in an aqueous liquid results in diffusion of salt and sodium acetate and water absorption of the phantom material. Stability is reached after 1 week. Finally, a cylinder-shaped hollow cardiac phantom is produced, with the use of a 3D printed mould, as comparable shape of the LA.

**Conclusion** Producing a cardiac phantom of PVA is proved to be a good model. This research shows the design of a low cost, easily produced hollow shaped cardiac phantom consisting of 13.0wt% PVA, 0.15wt% salt and tap water. Even though more future work needs to be done for the development of a cardiac phantom, this research functions as a proof of concept for the development of a flexible phantom with possibilities to manipulate the dielectric properties and to create a hollow shaped phantom. The use of PVA as tissue mimicking material (TMM) and the use of 3D printed PVA for creation of the hollow shapes shows promising results for future development.

# Contents

# List of figures

# List of tables

# Abbreviations

| | |
|---|---|
| AC | Alternating current |
| AF | Atrial fibrillation |
| DIW | Deionized water |
| ECG | Electrocardiograph |
| EC-meter | Electrical conductivity meter |
| EM | Electromagnetic |
| EP | Electrophysiology |
| IEGM | Intracardiac electrogram |
| LA | Left atrium |
| LV | Left ventricle |
| $NaN_3$ | Sodium azide |
| PLA | Polylactic acid |
| PVA | Polyvinyl alcohol |
| PVA-C | Polyvinyl alcohol cryogel |
| PVC | Polyvinyl chloride |
| PVI | Pulmonary vein isolation |
| PVP | Polyvinyl pyrrolidone |
| RF | Radiofrequency |
| TMMs | Tissue mimicking materials |

# 1. Introduction

Atrial fibrillation (AF) is the irregular beating of the atrial chambers, almost always too fast, due to chaotic uncoordinated electrical activity throughout the atria. Without treatment, the heart rhythm usually becomes permanently disrupted over time and can lead to various heart-related complications such as stroke [1] or heart failure. [2] 62% of all daily hospitalizations of the cardiovascular department in the Netherlands are from patients with atrial fibrillation. Currently, 380.000 people in the Netherlands have AF and [3] one quarter of the entire population above the age of 40 will have AF [4]. AF is the most common form of arrhythmia [5]. Moreover, recent research came to new insights about the treatment of AF, where more early rhythm control treatment can lead to fewer strokes and infarcts [6]. Mostly, AF can be treated with pulmonary vein isolation (PVI). PVI is an electrophysiologic minimally invasive procedure where electrode catheters are guided through the veins into the heart where it will eliminate the abnormal electrical activity around the pulmonary veins. To eliminate the abnormal electrical activity, commonly radiofrequency (RF) energy is used where the cardiac tissue will respond to the electromagnetic (EM) energy due to its dielectric properties causing scarring of the cardiac tissue.

A tissue mimicking phantom is an accurate model of organs or tissues mimicking the real life like scenario for a desired goal. An accurate anatomical dielectric phantom of the human heart could be extremely important for multiple experiments regarding reliability, accuracy and training purposes of multiple medical treatments in a controlled way, leading to better patient outcomes [7]. In order to obtain the desired properties in a phantom, the production process can be altered, the concentrations can be altered, or additives can be used.

## 1.1 Problem statement

Currently, validation of new electrophysiological instruments is performed on rigid cardiac phantoms and therefore lack correct tactile feedback [8]. Furthermore, trainings for electrophysiologists are experience-based and contain training in real patients. Cardiac phantoms can be used for the development of electrophysiological instruments and for training entities. These trainings can be divided into trainings for cardiologists to become electrophysiologists and trainings for electrophysiologists when new medical instruments are implemented in the hospital. According to the knowledge of the writer, no cardiac phantoms exist containing all requirements needed that it can be used for development of electrophysiology studies. Experimenting and training in phantoms ensures a safe and controlled environment. Therefore, cardiac phantoms are needed for development of electrophysiology technologies.

## 1.2 Objective

As a first step towards an applicable cardiac phantom for development of electrophysiology studies, the aim of this Master Thesis is:

---

*'Develop a LA phantom mimicking the dielectric values of human heart tissue in the frequency range of 10 kHz – 20 kHz.'*

---

To assess this research goal, it will be divided into 3 subgoals:

1. *Evaluate different tissue mimicking materials with additives to meet the main phantom requirements.*
2. *Extensively evaluate the most promising cardiac phantom materials.*
3. *Develop a phantom design with comparable anatomy.*

## 1.3 Thesis outline

To systematically address and report all findings, this Thesis has been subdivided into four parts:

### Part I: Theory

Previous to this Master Thesis a literature study [9] has been performed to obtain the required background knowledge. This part will explain the background information needed for this Master Thesis Project and is divided into the following chapters:

Chapter 2 gives an overview of the theoretical background information about the human heart and its dielectric properties.

Chapter 3 gives an overview of the theoretical background information about AF and its diagnosis and treatment.

Chapter 4 summarizes possible phantom materials reviewed in the previous literature study [9].

### Part II: Research of phantom materials

This part explains the research process for finding the most promising tissue mimicking materials (TMMs) for the development of a LA phantom.

Chapter 5 displays the requirements and wishes of the LA phantom. The requirements were set up based on the desired goal and the desires of the supervisors and Philips Healthcare.

Chapter 6 explains the evaluation method for the sample phantoms made in this part.

Chapter 7 describes stepwise the design process of the sample phantom production. At the end, most promising sample phantoms will be compared and evaluated to find the most promising TMM for the design of the final LA phantom.

### Part III: Cardiac phantom design

This part will elaborate on the most promising TMMs found in the previous part. In this part, the phantom materials will be extensively evaluated.

Chapter 8 explains the evaluation method for the final LA phantom.

Chapter 9 summarizes all retrieved results to evaluate the final LA phantom.

### Part IV: Evaluation

This part will evaluate the results and findings of this Master Thesis project.

Chapter 10 contains the overall discussion of the results of this Master Thesis and describes the limitations of this research and recommendations for further future research.

Chapter 11 contains the overall conclusions to finalize this Master Thesis project.

PART I:

# Theory

At the beginning of this Master Thesis Project a literature study [9] was performed to obtain the required knowledge about the human heart and its anatomy, mechanical and dielectric properties, diseases and treatments and possible tissue mimicking materials. This chapter will provide the most important background information needed for this Master Thesis Project. Beginning with the dielectric properties of human heart tissue, its diseases and treatments and ending with promising TMMs.

# 2. Dielectric properties human heart tissue

This chapter describes the basics of electrical impedance and the dielectric properties of human heart tissue. First, some general terminology will be explained. Thereafter, the dielectric properties of human tissue and in specific human heart tissue will be explained in more detail.

## 2.1 Electrical impedance general

Electrical impedance (Z), hereafter referred to as 'impedance', is a measure of the opposition of a material to the applied electrical current [10]. Applying a direct current (DC), the impedance is just the resistance of the material. Applying an alternating current (AC), the impedance consists of a real part, the resistance (R), and an imaginary part, the reactance (X). Therefore, seen in Figure 1, the impedance can also be expressed in the polar form as magnitude (|Z|) and phase angle (θ) . [11] The resistance quantifies the drop in voltage of the current passing through the tissue, and the reactance reflects the time delay between the exploring current wave and the voltage wave and therefore, taking the effect of the electrical capacitance of the material into account [12] [13] [14].

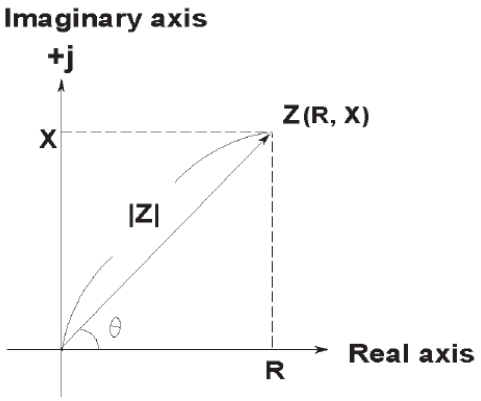


*Figure 1: Impedance vector Z(R,X) consists of a real part (R) and an imaginary part (X). With |Z| the magnitude and (ϑ) the phase angle* [11]

## 2.2 Electrical impedance of biological tissue

The dielectric properties of biological tissue determine the response of the tissue to an applied EM field [7]. Because biological cell membranes have capacitive properties, myocardial tissue is not purely resistive. Therefore, an AC should be applied to take the electrical capacitance of myocardial tissue into account [10][15][16]. For biological tissue, two things occur when applying an EM field which is described by the dielectric properties, the absolute permittivity, ε, and the electrical conductivity, σ, hereafter referred to as 'permittivity' and 'conductivity' respectively.

The permittivity describes its ability to trap or store charge, or to rotate dipole molecules. When the molecule's positive and negative charge centres do not coincide, an electric dipole moment exist. Applying an EM field changes the orientation of the dipoles so they can align along the applied field, producing a field inside the dielectric which opposes the applied field, called polarization, and is expressed by the permittivity. [17] Mostly, the relative permittivity, $\varepsilon_r$, of biological tissues is used, also known as the dielectric constant, and describes the ratio of stored electrical energy by an applied voltage within the tissue, ε, relative to the stored electrical energy within vacuum, $\varepsilon_0$, a physical constant [18]. Water molecules are dipole molecules and have therefore a high dielectric constant

[19]. Hence, high-water-content tissues, like human heart tissue, have a higher dielectric constant than low-water-content tissues which is about 10 times as large [20]. The conductivity describes its ability to transport charge, which are the ionic currents flowing in the biological tissue [21]. Applying an EM field triggers oxidation-reduction (redox) reactions between the electrode and the tissue [22], resulting in flowing of electrical current. The averaged conductivity is the effective conductivity. For inhomogeneous tissue as cardiac tissue the effective conductivity is the averaged conductivity of a hypothetical homogeneous tissue mimicking the potential distribution found outside the inhomogeneous tissue [22].

The dielectric properties are completely described by the complex relative permittivity (ε*):

$$\varepsilon^* = \varepsilon' - j\,\varepsilon'' \qquad (1)$$

with ε' the real part, indicating the degree of polarization (εr = ε') and ε'' its imaginary part, indicating the dielectric losses (energy converted into heat and dissipates). The imaginary part can be described by:

$$\varepsilon'' = \frac{\sigma}{\omega\,\varepsilon_0} \qquad (2)$$

with σ the total conductivity of the material, $\varepsilon_0$ the permittivity within vacuum and ω as the angular frequency. [23] Both, permittivity and conductivity vary with frequency and temperature [23].

A decrease in the permittivity is associated with an increase of the conductivity and can be categorized in three main steps α, β and ϒ, seen in Figure 2, characterizing a type of relaxation occurring in a specific frequency range and is typical for all tissues [24]. Dielectric relaxation denotes the adjustment of polarization in response to the applied EM field, where dielectric dispersion denotes the dependence of permittivity on frequency with the relaxation time as time constant [18]. α-Relaxation occurs at low frequencies in the range of 10 Hz – 10 kHz and is due to the counter-ionic environment surrounding the membrane surface [18][13][17]. β-Relaxation occurs in the frequency range of 10 kHz – 10 MHz and its time constant depends on the conduction in tissue and the capacitive coupling through cell membranes [18][13]. Lastly, the γ-relaxation occurs in the GHz frequency range and is due to the orientation of the dipoles (due to the polarization of water molecules) causing polarization [18][13][17]. [24][25]

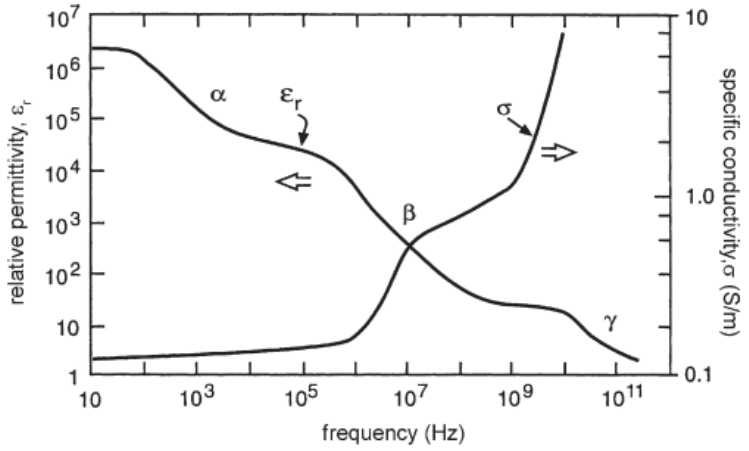


*Figure 2: Ideal representation of conductivity and permittivity of biological tissues as a function of frequency with the three major α, β and ϒ relaxations categories [32]*

The Cole-Cole model is generally used to describe the dielectric relaxation in biological tissues [17]. Here, each relaxation region is characterized by a single time constant, τ, and the complex relative permittivity (ε*) as a function of angular frequency (ω) is expressed with the Cole-Cole equation:

$$\varepsilon^*(\omega) = \varepsilon_\infty + \frac{\varepsilon_s - \varepsilon_\infty}{1+(j\omega\tau)^{1-\alpha}} \quad (3)$$

with $\varepsilon_\infty$ the permittivity at field frequencies where $\omega\tau >> 1$, $\varepsilon_s$ the permittivity at $\omega\tau << 1$, $j^2 = -1$ and $\alpha$ the distribution parameter as a measure of the broadening of the dispersion. The magnitude of the dispersion is described as [17][26][27]

$$\Delta\varepsilon = \varepsilon_s - \varepsilon_\infty. \quad (4)$$

By selecting appropriate parameters to each tissue, equation (3) can be used to predict the dielectric behaviour over a desired frequency range. S. Gabriel et al. (1996) made a parametric model for predicting the dielectric properties of biological tissues as a function of frequency in the frequency range of 10 Hz to 100 GHz [26] treating all biological tissues as homogeneous. This model describes the dielectric properties of human tissues in terms of multiple Cole-Cole dispersion:

$$\varepsilon^*(\omega) = \varepsilon_\infty + \sum_n \frac{\varepsilon_s - \varepsilon_\infty}{1+(j\omega\tau)^{1-\alpha_n}} + \frac{\sigma_i}{j\omega\varepsilon_0} \quad (5)$$

with $\sigma_i$ the static ionic conductivity, $\varepsilon_0$ the vacuum permittivity and the rest of the parameters described as in equation (3) [17][26]. Here, each successive summation of the Cole-Cole mode is plotted, emphasizing the contribution of each dispersion to the final model. The value for $\varepsilon_\infty$ was fixed at 4 for high-water-content tissues. Graphs were made showing the dielectric properties of several biological tissues they received with their parametric model and compared these outcomes with values found in literature [25] and experiments [28], seen in Appendix A for the plots made for human heart tissue. Databases based on the founding's of C. Gabriel et al. (1996) [29] of the dielectric properties for all tissues at a specific frequency at body temperature were made for the frequency range of 10 Hz – 100 GHz; The Foundation for Research on Information Technologies (IT'IS) database [30]. Little is found in literature about conductivity measured at frequencies below 100 Hz because of occurrence of errors in this frequency range, with electrode polarization and lead inductance as the two main sources of systematic error [17]. This will be more elaborated further on.

# 3. AF

This chapter briefly describes the most common form of arrythmia, AF, how it can be diagnosed with an electrophysiology (EP) study, and how it can be treated with RF cardiac catheter ablation.

## 3.1 Arrythmia

Arrythmia is a malfunction of the conduction system of the heart resulting in forms of the cardiac rhythm to be either too slow, bradycardia, too fast, tachycardia, or irregular [31][32]. AF, a form of supraventricular tachycardia, is the most common arrythmia [5] and is the irregular beating of the atrial chambers, mostly always too fast, due to chaotic uncoordinated electrical activity throughout the atria, Figure 3. This results in the atrium to fibrillate at 350 beats per minute up to 600 in extreme cases [33] and having a heart rate of 100 – 175 beats per minute, compared to a normal heart rate of 60 – 100 beats per minute [34]. AF can cause a reduction in the hearts efficiency and may make you feel tired and weak. AF normally does not cause life threatening problems if it is treated properly. If it is not treated properly, AF can be the cause of blood clots, stroke, heart failure and other complications [35].

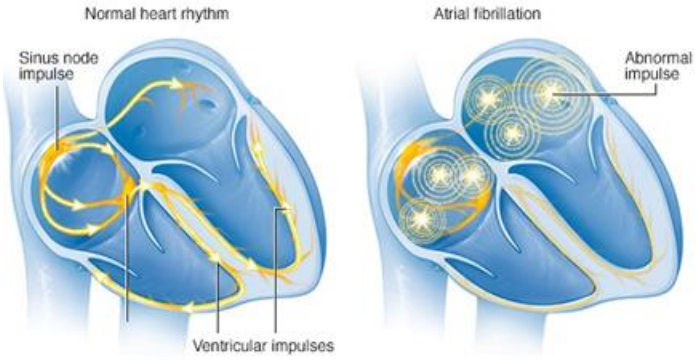


*Figure 3: Electrical activity during (left) normal heart rhythm and (right) atrial fibrillation* [36]

## 3.2 EP study

For the diagnosis of arrythmia, the hearts electrical activity can be recorded. An electrocardiograph (ECG) is a graphic record of the hearts activity showing a composite of all the action potentials generated by conductive and contractile cells in the myocardium. While the cause and precise location of the arrhythmia cannot be detected with an ECG, an EP study can be helpful for the diagnosis of a broad spectrum of cardiac arrhythmias [31]. An EP study is a minimally invasive study where electrode catheters are inserted into blood vessels, mostly in the groin, and are guided through the blood vessels into proper intracardiac positions with the use of X-ray fluoroscopy imaging guidance, allowing imaging of the soft body tissue [37]. Here, the electrical activity of the heart can be recorded, intracardiac electrogram (IEGM), and paced [31] allowing the doctor to locate the origin of the arrhythmia. An IEGM is the recording made of the cardiac electrical activity from an electrode catheter and is essentially an ECG recorded from within the heart. The IEGM records the depolarization phases of the cardiac tissue between the electrodes using relatively low frequencies (< 100 kHz) in order to avoid sparking [38].

## 3.3 RF cardiac catheter ablation

### 3.3.1 Introduction

Cardiac catheter ablation, hereafter referred to as 'ablation', is a minimally invasive technique for the treatment of arrythmia. During ablation procedures, faulty tissue in the heart will be destroyed in order to restore the normal cardiac rhythm. Different ablation methods are used, like RF ablation (100 kHz – 1.5 MHz), microwave ablation (915 MHz or 2420 MHz), cryoablation (tissue freezing to -70 °C), laser ablation (980 nm laser light) [31] and high-intensity focused ultrasound (20 kHz – 200 MHz) [39]. RF cardiac catheter ablation is the most common procedure for treating AF [40]. During this procedure, RF ablation catheters are guided into the heart and pushed up against the heart wall where high-energy is used leading to desiccation and coagulation necrosis of the underlying tissue, creating scar tissue, at the aberrant pacing pathways [31]. RF ablation of cardiac arrhythmia uses a sinusoidal AC at frequencies between 100 kHz – 1.5 MHz [39]. Here, the current oscillates too rapidly for the myocardium to depolarize and to induce arrhythmia. The heat is generated due to EM dissipation caused by the dielectric cardiac tissue properties [23]. The water molecules in cardiac tissue rotate due to the EM-energy causing frictional heating and results in necrosis when tissue temperature exceeds 50 °C [41]. Tissue properties change after death therefore, the creation of ablative lesions during RF ablation forms an electrical barrier to prevent electrical impulses from propagating through the damaged cardiac tissue to surrounding healthy tissue stopping the abnormal electrical signals from propagating to the rest of the heart causing AF [42]. Ablative lesions changes the conductivity [22], and are usually associated with impedance drops of 5-10 Ω. [43]

### 3.3.2 PVI

AF often originate from the four pulmonary veins entering the LA and can be cured with PVI. While ablation procedures are minimally invasive, mapping systems are used for creating a 3D map of the heart's anatomy. Most mapping systems use X-ray. Philips launched a new mapping system, the KODEX-EPD, where with the use of dielectric sensing detailed images of the heart's anatomy can be made without using X-ray and contrast dye [44]. With ablation procedures first, an EP study is performed in order to find the focus of the abnormal electrical signal. Once found, the focus will be destroyed with ablation. There are often more than one focus which will be eliminated by creating lines of ablation. During PVI, ablation lines are created around the pulmonary veins at the entry point from the LA, preventing abnormal electrical activity from within the veins to get into the atrium and triggering AF. [40]

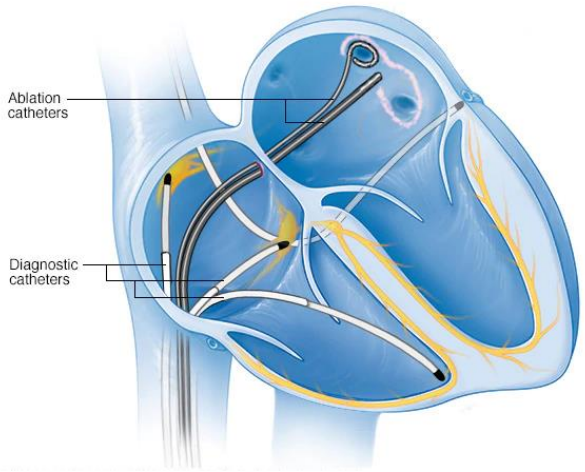


*Figure 4: Catheters during PVI procedure* [36]

# 4. Phantom materials

This chapter provides an overview of different phantom materials reviewed in the prior literature review [9]. The most promising base materials, according to the prior literature review, will be explained. Thereafter, additives for manipulating the dielectric properties found in the prior literature review will be displayed.

## 4.1 Introduction

A tissue mimicking phantom is an accurate model of organs or tissues mimicking the real life like scenario for a desired goal. Phantoms can be used for multiple purposes, including testing and optimisation of surgical equipment, testing and optimisation of imaging systems and for comparison between systems. Depending on the goal of the phantom, certain properties are more important than others. A homogeneous replication of the dielectric properties of human heart tissue can give an approximate simulation of their response and contribution to the overall impedance of a part of the human heart [45]. An accurate anatomical dielectric cardiac phantom could be extremely important for multiple experiments regarding reliability and accuracy of multiple medical treatments and diagnostics, leading to better patient outcomes [7]. Phantoms mimicking dielectric properties of human tissues, have already been developed [46][47]. However, cardiac phantoms mimicking the dielectric properties have not yet been extensively examined and developed [48][49][50]. Moreover, there are to the writers knowledge no cardiac phantoms which can be used for development of electrophysiology studies. In order to produce the correct tissue mimicking phantom, a base material has to be chosen with the correct additive materials to create the properties required for the phantom.

## 4.2 Base material

In the literature study previous to this Master Thesis Project [9] TMMs with additives to control the conductivity and permittivity were reviewed. In the literature study [9] it was concluded that agar and gelatin are the most used TMMs for the development of dielectric phantoms, but they seem to struggle with its shelf life, stability and mechanical stiffness. PVA-C and gellan gum seem to be the most promising TMMs with PVA-C the most promising. However, these materials have not been extensively used for the development of dielectric phantoms. Therefore, in this research project, multiple TMMs will be used in order to evaluate which phantom design will be best suited for the design goal.

### 4.2.1 Agar and gelatin

Most dielectric phantoms found in literature were fabricated with agar or gelatin as base material [48][50]. These gels are easy to fabricate, inexpensive and can form homogeneous phantoms [51]. Agar is a biopolymer and derived from cell membranes of some species of seaweed and red algae [52]. Gelatin is an aqueous based material, consisting of peptides and proteins derived from collagen of animal tissue [52]. The major drawback of these base materials is the reduced shelf life [53][54]. Preservatives can be added such as sodium azide ($NaN_3$) and sodium dehydroacetate [52], benzoic acid [55] or formaldehyde (carcinogenic substance [56]) [57]. Precaution is needed when using these preservatives [58].

### 4.2.2 PVA-C

PVA hydrogel is a biocompatible non-toxic synthetic insulating polymer [51][59]. PVA is commonly used as TMM due to its repeatability, biocompatibility, low cost, long shelf life and excellent mechanical properties [60]. PVA solutions can be chemically or physically crosslinked and can thereby be transformed into flexible solid hydrogels. Physical crosslinking occurs with the use of freeze-thaw cycles and forming PVA-cryogel (PVA-C), which is relatively easy to produce and can be moulded into complex shapes [61]. The degree of crosslinking is dependent on the concentration of PVA-powder, the freezing and thawing times and the number of freeze-thaw cycles [62]. Physical crosslinking addresses toxicity issues compared to chemical crosslinking. PVA has a high water-content and therefore exhibit mechanical properties similar to biological tissues [63]. Compared to agar-based phantoms, PVA-C based phantoms show an improved strength and shelf-life [64]. The ionic conductivity of PVA-C based phantoms depends on variables such as polymer polarity, water content, salt/ions, and hydrogel structure [65]. Moreover, increasing the amount of freeze-thaw cycles will decrease the conductivity of PVA [64], the permittivity is independent of the number of freeze-thaw cycles [62].

### 4.2.3 Gellan gum

Gellan gum is a low costly anionic polysaccharide and forms a gel during cooling of the heated gellan gum solution due to a disorder-order coil-helix transition occuring [66]. High-acyl gellan gum provides a soft and elastic texture with a very homogeneous structure, suitable for mimicking soft tissues [67] [52]. When storing under correct storage conditions, gellan gum can have a long shelf life [68]. Preservatives as sodium propionate can be used to increase its shelf life [69].

## 4.3 Dielectric additives

Most soft human tissues and liquids (i.e., excluding adipose tissue and cortical bone) have an electrical conductivity [48] and relative permittivity greater than water at frequencies below 100 MHz [70]. Additives mostly found in the previous literature study [9] for manipulating the dielectric properties are shown in Table 1 and will be evaluated individually. The arrows in the figure indicates if the additive will increase or decrease its dielectric value of water-based phantoms.

*Table 1: Dielectric additives, '↑' indicates the additive will increase its dielectric value of water-based phantom tissues, '↓'indicates the additives will decrease the dielectric value of water-based phantom tissues and '~' indicates contradiction in literature.*

| **Additives** | **Affects σ** | **Affects $\varepsilon_r$** |
|---|---|---|
| Acetone | ↑ | ~ |
| Conductive components*: Metals, carbon based materials, conductive polymers | ↑ | ↑ |
| Ethanol/ethanediol | | ↓ |
| Glycine | | ↑ |
| Isopropanol | ↑ | |
| Lignin | Non-systematic | Non-systematic |
| Oil** | ↓ | ↓ |
| PVC | ↓ | ↓ |
| PVP | | ↓ |
| Salt | ↑ | |
| $NaN_3$ | ↑ | |
| Sugar/sucrose | ↓ | ↓ |

* Al powder, brass powder, carbon black, carbon nanotubes, graphite, graphite/nickel nanoparticles, graphene ink

** Mixture of 50% kerosene and 50% safflower oil, vegetable oil

### 4.3.1 Acetone and isopropanol

Acetone can be used to aid mixing with high concentrations of graphite and carbon black [71]. A. Santorelli et al. (2015) stated that adding small volumes of acetone, the overall permittivity would be increased [72]. Which is in contrary with the low value of the relative permittivity of acetone [73]. B. McDermott et al. (2018) concluded acetone would increase the conductivity of mixtures [71]. However, no values of the increase in conductivity are shown in the study. The same amount of isopropanol instead of acetone was used. Using the isopropanol was found to significantly increases conductivity for any given TMM, resulting in way higher conductivity values than the values of human heart tissue. However, the resultant mixtures were more friable than those that contained acetone or no mixing aid. Hence, it was preferable not to use isopropanol if possible. It is hypothesized that the increase in conductivity is a result of improved dispersion of graphite and carbon black in isopropanol and acetone. Moreover, alcohols are known to prevent agglomeration of these materials resulting in more conducting pathways. [71]

### 4.3.2 Conductive components

Metals, carbon based materials, or conductive polymers are typically used in polymers to increase its conductivity. When the electrical percolation threshold is exceeded, conductive pathways are formed within the nonconductive polymer matrix. Typically the electrical properties of the composite will improve, but the mechanical properties will deteriorate. [59] A lot of methods can be used to mix conductive components in polymers, with solution casting as the most common. Problems may arise when incorporating electroactive components into a polymeric material due to lack of complete understanding of the structure-property relationships of the component materials, leading to unexpected interactions between the component materials. [59]

### 4.3.3 Ethanol/ ethanediol

M. Robinson et al. (1991) [74] and S.A. Lopez-Haro et al. (2011) [75] used ethanediol in gelatin and ethanol in agarose for measurements of the dielectric properties. Ethanol has a low relative permittivity and will decrease the relative permittivity of aqueous phantom mixtures [70].

### 4.3.4 Glycine

Glycine will increase the relative permittivity [70]. M. Hagmann et al. (1992) used for their dielectric muscle phantoms glycine, formamide and urea. Glycine causes the greatest increase in relative permittivity [70]. Also in the study of Y. Yu et al. (2019) glycine was added to agar and gelatin to increase its relative permittivity [76].

### 4.3.5 Oil

M. Lazebnik et al. (2005) [77] created oil-in-gelatin phantoms with a solution of 50% kerosene and 50% safflower oil. The more amount of oil in the gelatin mixture, the lower the relative permittivity and the lower the conductivity. Oil has very low permittivity and conductivity.

### 4.3.6 PVC

Polyvinyl chloride (PVC) can be used for the fabrication of mechanically stable phantoms with relatively long shelf lives. PVC can be used as base material, but can also be added for manipulating the dielectric properties of the phantom. H. Kato et al. (1987) added PVC powder to agar-based phantoms [78]. Moreover, PVC has a low relative permittivity [79][80] and can decrease the phantoms conductivity [81][78].

### 4.3.7 PVP

Polyvinyl pyrrolidone (PVP) is a readily available, water-soluble non-toxic polymer and can be added to lower the relative permittivity [48].

### 4.3.8 Salt

In most studies, NaCl is used to control the phantoms conductivity. All reviewed studies can be found in the previous literature study [9]. In the studies of R.K. Chen and A.J. Shih (2013) [67] and M. Miyakawa et al. (1995) [69] salt (NaCl) was added to gellan gum to increase its electrical conductivity. S. Jiang et al. (2013) fabricated homogeneous phantoms with the use of PVA-C and NaCl [82]. In this study NaCl was added to affect the micro-structure morphology of the PVA phantom instead of looking at the conductivity. The addition of NaCl would disrupt the intra PVA chains and promote the interactions between polymer chains, which could shorten the gelling time. In studies of M. Kandadai et al. (2012) [47], Q. Duan et al. (2014) [55] and M. Kandadai et al. (2012) [47] agar-base phantoms were made, also using NaCl to control its conductivity.

### 4.3.9 Sodium azide

Sodium azide is very poisonous therefore, precautions are needed when using this product [58]. It is deadly when swallowing the product, when it is in contact with the skin or inhaling the product. It may cause damage to organs when prolonged or repeated exposure. When in contact with acids, a very toxic gas will be formed. [83] H. Kato and T. Ishida (1987) concluded that an increase in $NaN_3$ in agar-

based phantoms will increase the conductivity but this influence is not frequency dependent in the frequency range of 5-40 MHz.

### 4.3.10 Sucrose

Sucrose decreases the relative permittivity of water-based phantoms [55] while it has a low relative permittivity [70]. Polyethylene powder is a more expensive form of sucrose [84] and will also lower the relative permittivity.

PART II:

# Research of phantom materials

In this part, the approach towards the TMMs for the final cardiac phantom design will be described. First, a list of requirements and wishes is set up. Thereafter, the methods used for the evaluation of the requirements will be described. A more extensively inspection will be performed on the final LA phantom. In this part, multiple 'sample phantoms' will be prepared and examined based on the main phantom requirements. This is an iterative process where different combinations will be used and compared to each other. Finally, all results will be described, discussed and concluded with the use of a Harris Profile.

# 5. Requirements

The requirements are set up based on findings in literature and the desires of Philips Healthcare. Based on the possibilities and desires, the requirements are divided into 'Main requirements', which are the most important requirements, and 'Additional requirements', which are less important, as seen in Table 2.

*Table 2: Requirements cardiac phantom*

| Main Requirements |
|---|
| 1. The electrical conductivity in the frequency range of 10 kHz – 20 kHz is similar to human heart tissue |
| 2. The relative permittivity in the frequency range of 10 kHz – 20 kHz is similar to human heart tissue |
| 3. The phantom should be stored in a solution mimicking the conductivity values of human blood |
| 4. The phantom is homogeneous |
| 5. The mechanical stiffness is similar to that of human heart tissue |
| 6. Shelf life of at least one month |

| Additional requirements |
|---|
| 1. The anatomy is similar to the anatomy of the LA |
| 2. Inexpensive to produce |
| 3. Ease of manufacturing |
| 4. Reproducible; same recipe should give the same results |
| 5. Stable over time; the phantom should retain its dielectric properties over at least one month |

# 6. Evaluation methods

The sample phantoms will be evaluated based on the main phantom requirements and will be done less extensively than with the final cardiac phantom design. Therefore, this chapter will describe the methods used for the examination of the samples phantoms in order to meet these requirements.

## 6.1 Dielectric properties

### 6.1.1 Impedance measurements

An impedance analyser (4192A LF HP), provided by Philips, will be used for the measurements of the dielectric properties in combination with the same needle-needle electrode configuration as S. Poompavai and V. Gowri Sree (2018) [85], seen in Figure 6. Therefore, Figure 5 shows how to connect the two-needle electrode to the impedance analyser. Moreover, this needle-needle electrode configuration can be seen as two parallel cylinders of length L, radius r and distance b measured in meters. If b >> r, the capacitance (C) in Farads can be calculated as:

$$C = \frac{\pi \varepsilon_0 \varepsilon_r}{\ln\left(\frac{b}{r}\right)} L \tag{6}$$

[86][87] and the conductance (G) in Siemens (S) can be calculated as:

$$G = \frac{\pi \sigma}{\ln\left(\frac{b}{r}\right)} L \tag{7}$$

with $\varepsilon_0$ = 8.854 x $10^{-12}$ and σ the electrical conductivity in S/m [85][88]. With the use of the software LabVIEW (NI LabVIEW 2013) the impedance analyser will automatically measure the capacitance and conductance in the frequency range of 10 kHz – 1 MHz with 21 equally distributed steps and will store the measured data. When substituting the capacitance and conductance into formula (6) and (7), the relative permittivity and electrical conductivity can be measured respectively with formula (8) and (9).

$$\varepsilon_r = \frac{C \ln\left(\frac{b}{r}\right)}{\pi \varepsilon_0 L} \tag{8}$$

$$\sigma = \frac{G \ln\left(\frac{b}{r}\right)}{\pi L} \tag{9}$$

With the use of MATLAB all measured values of the phantom tissues can be substituted into formula (8) and (9) to measure the relative permittivity and electrical conductivity respectively at all measured frequencies. All measurements will be conducted at room temperature (20°C - 23°C), the impedance analyser should be warmed up (> 30 min) and the ambient temperature should be 23°C ± 5°C [89].

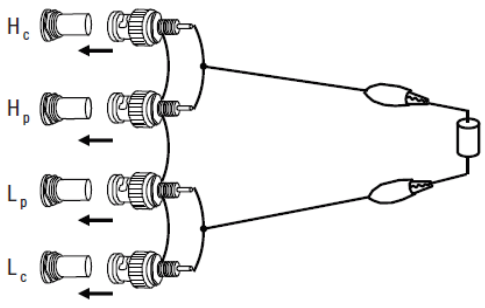


*Figure 5: Connection image for the two-needle configuration* [11]

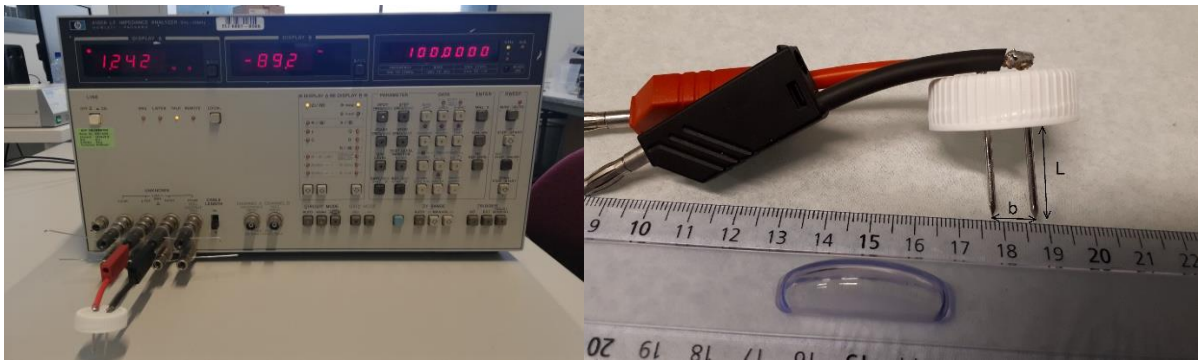


*Figure 6 Set-up for the impedance measurements, left: complete set-up, right: needle electrode configuration with length L and distance b*

### 6.1.2 Repeatability impedance measurements

To evaluate the repeatability of the needle electrode impedance measurements, 27 homogeneous phantom tissues without additives were prepared and measured three times. Repeatability will be measured as the maximum percentage variation between the measured values and the mean of the measured values per phantom over all frequency points, averaged over all 27 phantoms [90]. Therefore, various homogeneous phantoms without additives were prepared and measured three times at different sides. Figure 7 shows an example of the results of repeated measurements in a gellan gum-based phantom. In total 27 phantoms were prepared and measured for repeatability; 9 phantoms per base material. The average of all 27 maximum percentage variation between the measured values and the mean of the measured values over all frequency points is 11% and 4% for permittivity and conductivity respectively. Most greater variation occur at the higher frequencies. Appendix B 'B2 Repeatability tests' shows all results of the repeatability tests.

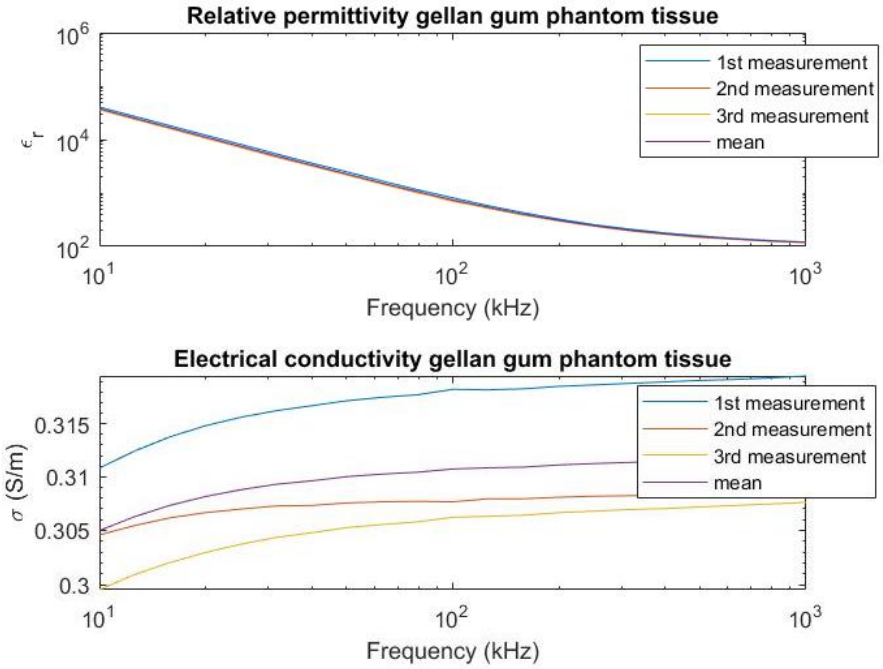


*Figure 7: Repeatability test for gellan gum-based phantom*

### 6.1.3 Target values

For the design of an anthropomorphic LA phantom, the dielectric properties of the phantom at room temperature (20°C – 23°C) should mimic the dielectric properties of human heart tissue at body temperature (37°C) in the frequency range of 10 kHz – 20 kHz which complies with the frequency range used in EP study. For this Master Thesis, measured dielectric values of porcine heart tissue at room temperature will be used as target values. The measurements of the target values will be performed using the same equipment and method as the measurements on the phantom tissues. Porcine heart tissue is often used as animal model for human heart tissue, because of the great resemblance anatomically and physically. Also seen in Appendix A, comparison between dielectric values of human heart tissue compared to porcine heart tissue shows great resemblance [25]. But, differences between porcine heart tissue and human heart tissue must be taken into account for further research [91]. Moreover, as a second comparison, dielectric values of human heart tissue at body temperature derived from the database IT'IS [30] will be used, a common used reference in literature [16].

Accuracy will be the percentage variation between the measured values and the target values over all frequency points [64]. Ideally, the measured values of the phantom tissue are considered to be accepted when they are in the range of ±10% on the target values, the measured porcine heart tissue values. This accepted tolerance range is in agreement with the study of V. Lopresto et al. (2011) [92]. In order for the accepted tolerance range of ± 10% to comply with the results retrieved from the repeatability tests, the accepted tolerance range will be ± 11% and ± 10% for permittivity and conductivity respectively. However, this research project serves as a proof of concept and therefore the accepted tolerance range is desired and not a requirement.

For the impedance measurements of the target values, a piece of porcine heart tissue, Figure 8, was brought to room temperature. For repeatability, the measurements were conducted four times. The first measurement measured the cardiac tissue in the frequency range of 10 kHz – 1 MHz with 21 equally distributed steps, the second, third and fourth measurement measured the tissue in the frequency range of 10 Hz – 1 MHz with steps of 51, 51 and 21 respectively. The results are showed in Figure 9. The repeatability is measured to be 9.22% and 1.7% for permittivity and conductivity respectively, within the frequency range of 10 kHz – 1 MHz, and therefore complies with the results of the repeatability tests.

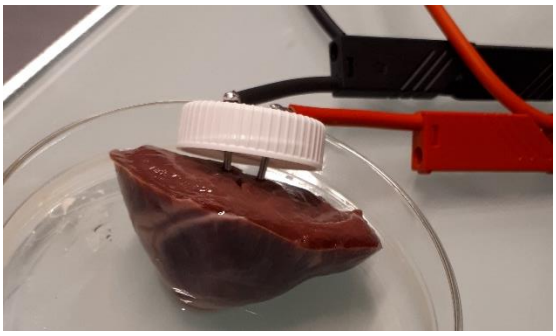

*Figure 8: Piece of porcine heart tissue during impedance measurements*

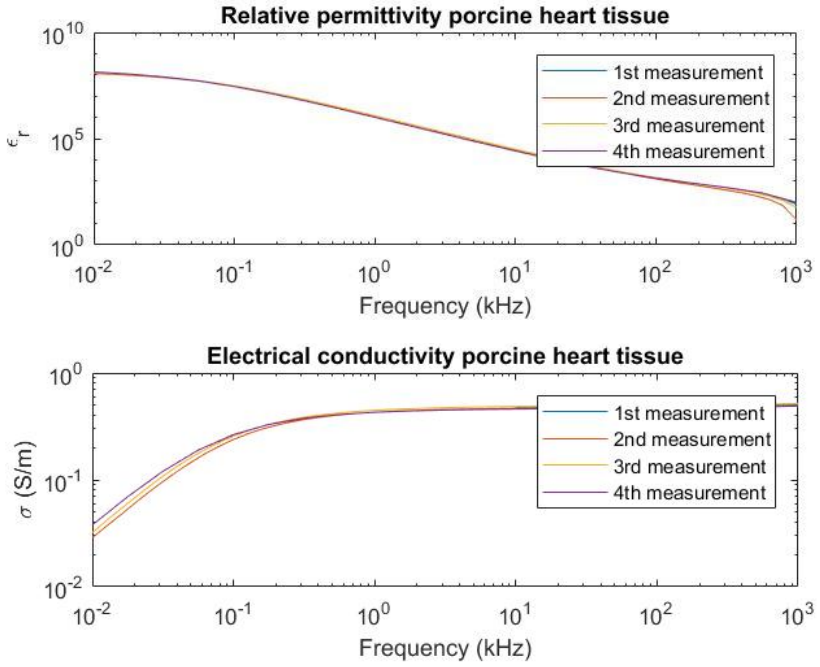


*Figure 9: Measured dielectric values of porcine heart tissue, measured with the 2-electrode measurement set-up*

The maximum percentage variation of the first measurement compared to the mean measurement in the frequency range of 10 kHz – 20 kHz is measured to be 5.4% and 0.8% for permittivity and conductivity respectively and complies with the repeatability tests. Therefore, the first measurement will be accepted as the target values of the porcine heart tissue for the phantom tissue. Figure 10 shows the comparison between the dielectric values of human heart tissue at body temperature derived from the database IT'IS [30] and the results of the porcine heart tissue which will function as the target values.

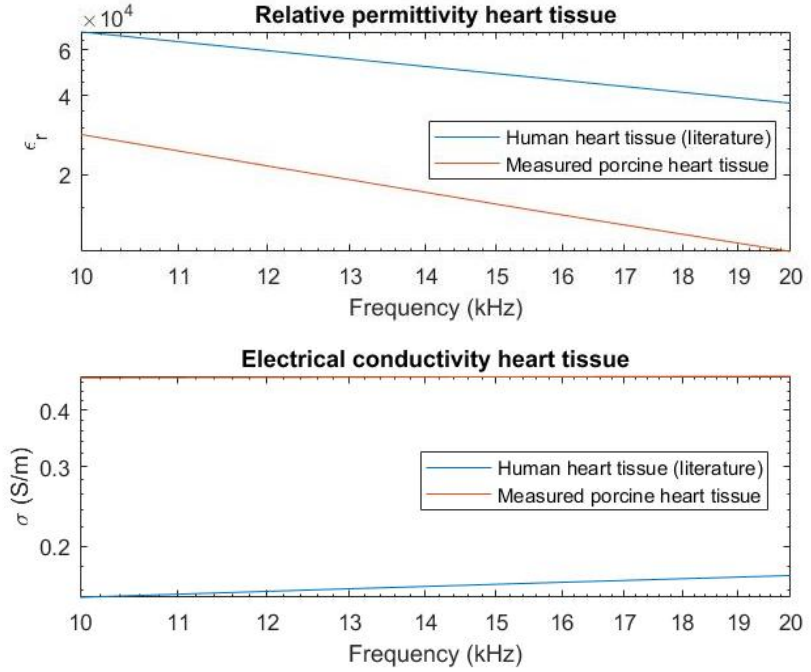


*Figure 10: Two target dielectric values: measured porcine heart tissue and dielectric values derived from the database IT'IS* [30]

## 6.2 Storage solution

The LA phantom should be stored in a solution mimicking the conductivity values of human blood. According to The Foundation for Research on Information Technologies (IT'IS) database [30], the conductivity of human blood is 0.7 S/m. In order to mimic this conductivity value in the 'storage solution', a saline solution will be prepared. Therefore an electrical conductivity-meter (EC-meter) (Online aquarium spullen) with an accuracy of ± 2% full scale, will be used to measure the conductivity of the storage solution. Results showed a solution made of 0.15 wt% salt in tap water mimics the conductivity value of blood. Therefore, the phantoms will be stored in the 0.15 wt% saline solution, hereafter referred to as 'storage solution'. All results of measured conductivity values of solutions can be seen in Appendix C.

## 6.3 Homogeneity

In order to examine the homogeneity of the phantoms, all impedance measurements will be performed three times at different sides of the sample phantom. The phantom is considered to be homogeneous, when the measurements are within the repeatability ranges of the impedance analyser. Repeatability tests showed a maximum percentage variation between the measured values and the mean of the measured values of 11% and 4% for permittivity and conductivity. Therefore, phantoms are said to be homogeneous when repeated measurements at various sides of the phantom shows 11% and 4% or lower variation for permittivity and conductivity, respectively.

## 6.4 Mechanical stiffness

The final LA phantom should give the same haptic feedback as human heart tissue. Therefore, for the 'sample phantoms' a haptic and visual inspection will be performed. The elastance of the phantom materials can be manipulated by varying the weight percentage (wt%) of the base material and additives. All wt% mentioned in this Master Thesis refers to the weight of the material relative to the weight of water used. According to literature, the more wt% base material, the stiffer the phantom [93]. It will be examined if this will apply to all materials. Moreover, multiple freeze-thaw cycles will increase the mechanical stiffness of PVA-C phantoms. The stiffness of the phantom will be influenced by the freezing time, freezing temperature and the rate of the freeze-thaw cycle [63].

## 6.5 Shelf life

The shelf life of the phantom should be at least one month. This signifies the phantom should remain their shape, no rupture of the phantom should occur and no growth of mould should occur. A visual inspection will be performed.

## 6.6 Discussion

A few discussion points will be presented in this subchapter, containing measurements performed in this chapter.

### Impedance measurements

Errors may arise during impedance measurements. Using the two-needle electrode configuration, the potential differences sensed between the electrodes includes the voltage due to the current flowing through the polarization impedance at the electrode-tissue interface at lower frequencies [18]. Ions in the phantom material tend to move towards the electrode-tissue interface, leading to the

development of ionic double layers in such regions: electrical double layer. Resulting in a rapid voltage drop in these layers, implying an enormous electrical polarization of the material and a near-absence of the electric field in the bulk sample at low frequencies. This effect is called electrode polarization and can be reduced by using a four-needle electrode configuration. In a four-electrode method, the two outer electrodes apply the current and the two inner electrodes sense the voltage differences. The voltage is measured with a very high input impedance, ensuring practically no current flows in the sensing electrodes and avoids electrode polarization. [94][16] Moreover, using the two-terminal configuration also contains unwanted elements, parasitics. While the four terminals of the impedance analyser are connected to each other as shown in Figure 5, lead inductances, lead resistances and stray capacitance between the two leads are added. [11][95] Moreover, the accuracy of the impedance measurements can be influenced by [96]:

- Contamination of electrode surfaces
- Geometry of electrodes and phantom tissue
- Frequency change
- Temperature changes

### Target values

The measured porcine heart values serve as target values. In Figure 10, the dielectric values of the measured porcine heart tissue and of human heart tissue derived from the database IT'IS [30] are shown. A big difference between the two values are shown in the figure. Differences between the measured cardiac tissue and the cardiac tissue derived from the database can be explained by differences between porcine heart tissue and human heart tissue [25][91], differences in measurements due to differences in temperature (porcine heart tissue is measured at room temperature, human heart tissue values are of cardiac tissue at body temperature) [23], differences between measurement equipment, electrode configuration and translation of measurements into permittivity and conductivity. Using the same equipment, electrodes and methods reduces errors occurring. Because this project serves as a proof of concept, mimicking the measured porcine values is a good target for the cardiac phantom design. In addition, it is unclear whether the values of human heart tissue derived from the database IT'IS are the absolute values. A very high permittivity insinuates electrode polarization occurred [94][16]. Moreover, cardiac tissue is inhomogeneous and therefore shows variability in dielectric properties. The variation of values ranges from about ± 5-10% above 100 MHz to ± 15-25% at lower frequencies [28].

At the beginning of this Master Thesis, it was desired to measure the impedance in the frequency range of 10 kHz – 1 MHz. Therefore, all measurements performed in this part contain measurements performed in this frequency range. As for the accepted tolerance range of ± 11% and ± 10% for permittivity and conductivity respectively, they serve as desired values. However, this research project serves as a proof of concept and therefore the accepted tolerance range is not a requirement. In addition, because cardiac tissue is

### Storage solution

The storage solution only mimics the conductivity values of human blood and not the permittivity values. For future work, the permittivity should also be mimicked in the storage solution. However, this research serves as a proof of concept. Because of the limited time of this project, it is chosen to only mimic the conductivity. Moreover, the storage solution is only measured using the EC-meter,

while the device measures with an accuracy of ± 2% full scale according to the instruction manual of the device. However, in the study of H.W. Choi et al. (2011) [97] the conductivity values of human blood are compared to a 0.45% saline solution (4.5g salt per litre water) and 0.9% saline solution (9g salt per litre water), as seen in Figure 11.

All experiments in this project will be conducted at room temperature (20°C - 23°C), therefore it is expected that a saline solution slightly below 0.45% saline will give the same conductivity values as the conductivity value of human blood, 0.7 S/m. However, the found storage solution does not seem to match. Furthermore, it is not mentioned whether saline solutions reported in Figure 11 are sterile saline or non-sterile saline. In all probability, these results are of sterile saline. This is of great importance while, as seen in Appendix C, a great difference between conductivity values of tap water and distilled water is shown.

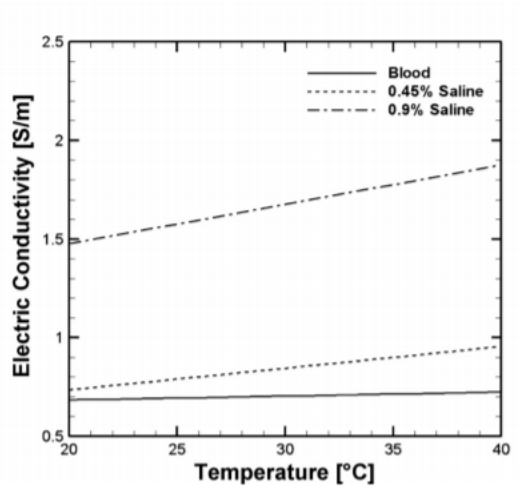


*Figure 11: Conductivity values of human blood, 0.45% saline solution and 0.9% saline solution varied with temperature, figure from H.W. Choi et al. (2011)* [97]

## 6.7 Conclusion

Table 3 gives an overview of all evaluation points for the sample phantoms, with the definition and accepted ranges as described in this chapter.

*Table 3: Evaluation methods for sample phantoms*

| Requirement phantom | Definition | Accepted ranges |
|---|---|---|
| Dielectric properties | Phantom should mimic measured dielectric properties of porcine heart tissue | ± 11% for permittivity and ± 10% and conductivity |
| Storage solution | All phantoms should be stored in a solution of 0.15 wt% salt in tap water, which mimics the conductivity value of blood | - |
| Homogeneity | Phantom should be homogeneous | Variation of repeated measurements at various sides of the phantom should be ≤11% for permittivity and ≤4% for conductivity |
| Mechanical stiffness | Phantom should give the same haptic feedback as human heart tissue | - |
| Shelf life | Length of time of the phantom without becoming unusable | > 1 month |

# 7. Sample phantoms

This chapter describes the production process of the sample phantoms. An experimental method is used to evaluate the effects of different additives in three types of base materials. The 'sample phantoms' will be evaluated based on the material properties of the main requirements, this will be done less extensively than for the final phantom design. First, the most promising additives and base materials of the previous literature study will be selected. Thereafter, an experimental method will be used to find the most promising phantom materials for the final LA phantom design. This process is conducted in a few steps. Each subsequent step is affected by the prior step, therefore the results of all steps individually will be reviewed, discussed, and concluded. To conclude which phantom design will be most promising for the final cardiac phantom, all results will be described, discussed and concluded with the use of a Harris Profile. The following steps will be conducted:

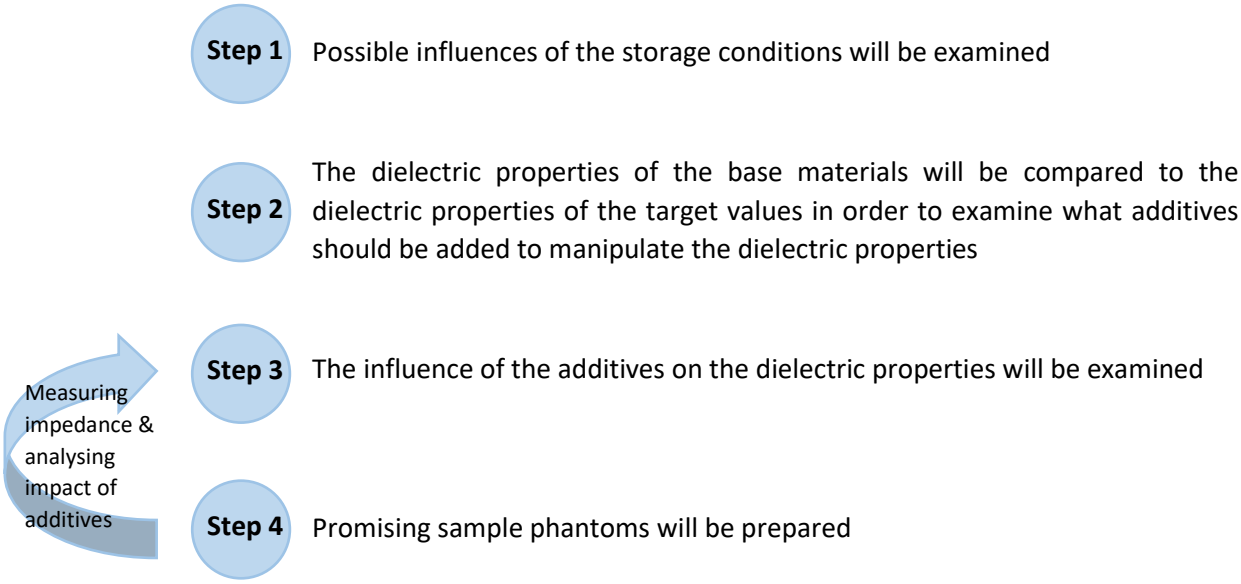


## 7.1 Phantom preparation

### 7.1.1 TMMs

Three base materials will be evaluated: agar, gellan gum and PVA. Gellan gum and PVA are the most promising base materials for the development of a dielectric cardiac phantom according to the previous literature study [9]. Agar is mostly used as base material for dielectric phantom fabrication and resulted in the research project of P.G.T. van Berckel to have a longer shelf life compared to gelatin [98]. The base materials used in this research project are: PVA-C (99+% hydrolyzed, molecular weight 89000-98000, Sigma Aldrich), commercially available Agar powder (Agar Agar powder, De Kruidenbaron) and High acyl Gellan Gum (Gellan Gum LT100, Special Ingredients).

According to the previous literature study [9] promising additives to control its relative permittivity are ethanol, glycine and PVP. Promising additives for controlling its conductivity are salt and acetone (acetone in combination with metals or carbon based materials). And for controlling both conductivity and permittivity are metals, carbon based materials, oil, PVC and sugar. It was chosen to experiment

with all these additives except for PVP and metals while these materials are costly and the outcomes are not certain to be positive for this research. As for the carbon based materials, graphite powder and charcoal powder will be used while these materials seem promising and are low costly commercially available. Moreover, ammonia was also examined for controlling its permittivity while ammonia has a low permittivity [99]. Therefore, the additives which will be examined in this research project are bioethanol (≥95% Ethanol, Selchemie), glycine (100% glycine amino acid powder, My Vegan), Poly(vinyl chloride) powder (Average Mw 62,000, average Mn 35,000, Sigma Aldrich), ammonia (Sel), salt (Fijn zeezout, JOZO), acetone (Etos), sunflower oil (AH Basic), granulated sugar (Kristal suiker, AH), activated charcoal powder (Original powdere by nature superfoods) and graphite powder (Grafietpoeder 99%, natuurlijke kwaliteit, Werken met merken). Sodium acetate (Natrium acetaat, Van Beekum Specerijen) will be used as preservative for the gellan gum- and agar-based phantoms and for the phantom preparation with the use of oil, a surfactant (dishwashing detergent (afwasmiddel Original, AH)) will be used to act as emulsifier and therefore decreasing the surface tension between the oil and water. Using a dish washing detergent as surfactant was based on the study of M. Lazebnik et al. (2005) [77].

### 7.1.2 Working protocol

As for the phantom preparation, the amounts of additives and base materials will be varied and evaluated based on the requirements as described in the previous chapter. The protocols for the phantom preparations are based on literature and own findings. All phantoms will be composed of 100ml tap water, deionized water or 0.9% saline. The mould which will be used for the phantoms will be a silicone ice-cube mould (Dotz) in order to make phantoms with dimensions of 3.3x3.3x3.3 cm. The phantoms should be stored in a closed container refrigerated in the storage solution to prevent it from drying out and to avoid air contact [100]. All phantoms prepared during this research project are shown in Appendix B.

#### Agar

The working protocols for the agar-based phantoms is partly based on findings of T. Kao et al. (2008) [101] and will be as follows: Pre-weigh all ingredients. Put a beaker on the stove, heat the water until 85°C and keep at this temperature. When using salt as additive, add salt while magnetically stirring for 5 minutes until the mixture is completely dissolved. Add Agar powder and preservative to the mixture and mix for 15 minutes more. Afterwards, gradually add the additives while magnetically stirring until mixture is homogenously mixed. Remove the beaker from the stove, pour the mixture into a mould and allow it to cool down and solidify.

#### Gellan gum

The working protocols for the gellan gum-based phantoms were partly based on the findings of R. Mao et al. (2001) [68] and will be as follows: Pre-weigh all ingredients. Put the beaker on the stove and heat the water until 85°C. Add the additives and preservative while magnetically stirring until the mixture is homogeneously mixed while keeping the mixture are 85°C. Then, disperse gellan gum gradually in the mixture. After the mixture is completely mixed, heat up the mixture until 100°C and mix for 15 minutes more. Water losses due to evaporation should be corrected by adding water of approximately 80°C - 90°C. Remove the beaker from the stove and pour the mixture into a mould. Allow the mixture to cool down at room temperature and to solidify.

#### PVA-C

The working protocols for the PVA-C-based phantoms is partly based on the findings of E. Repetti (2019) [102] and will be as follows: Pre-weigh all ingredients. Fill the beaker with water at room temperature. Add all additives while magnetically stirring until mixture is homogeneously mixed. Add

gradually PVA powder to the mixture with continued stirring and stir for 5 minutes more. Heat up the mixture until 96°C and mix for 60 minutes. After mixing, pour the mixture into a mould and allow to cool down till room temperature. When using graphite powder, charcoal powder, PVC and/or glycine as additive, continue stirring while cooling down the mixture until room temperature. After the mixture is cooled down, start the freeze-thaw cycle. Put the mould with mixture for 24 hours in the freezer. After 24 hours, thaw the mixture for 24 hours at room temperature.

## 7.2 Step 1: Storage conditions

### 7.2.1 Methods

As predefined, the phantoms should be stored refrigerated in a closed container in the storage solution. In this subchapter the influence of the storage condition on its shelf life and stability will be examined. Because the storage solution is a 0.15 wt% saline solution, salt diffusion might occur and should be examined. Therefore, the stability will be tested by measuring the dielectric properties of the sample phantoms before storage and after storage. The storage conditions will be examined per base material separately.

### 7.2.2 Results

Appendix B 'B3 Shelf life' shows the shelf life with other storing conditions for all base materials and Appendix B 'B4 Salt diffusion' gives more results regarding salt diffusion. However, the shelf life reported in Appendix B gives an approximation. Other conditions might influence the shelf life, like touching the phantoms more often would stimulate mould growth. Shelf life and stability when storing according the correct storage conditions will be described below.

#### Agar

Multiple agar phantoms were produced and stored according to the previous explained conditions. For all phantoms, mould growth appeared after three weeks storage as seen in Figure 12. Moreover, salt diffusion occurs when storing agar phantoms in a saline solution. Figure 13 shows the change in dielectric values over 5 days of an agar phantom prepared by mixing 6g agar powder to 100ml of tap water and afterwards stored in a 0.9% saline solution. The dielectric properties were measured immediately after the phantom was prepared and cooled down to room temperature; day 1. Thereafter, the agar phantom was stored in a 0.9% saline solution and the dielectric properties were measured after 1 day and after 5 days of storage. Here, the maximum percentage variation between the measured values and the mean of the measured values over all frequency points is 66% and 61% for permittivity and conductivity respectively.

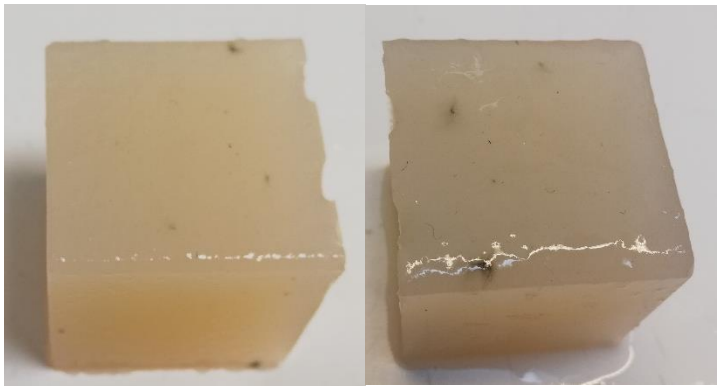

*Figure 12: 5.66 wt% agar phantom mould growth; left: after three weeks, right: after five weeks*

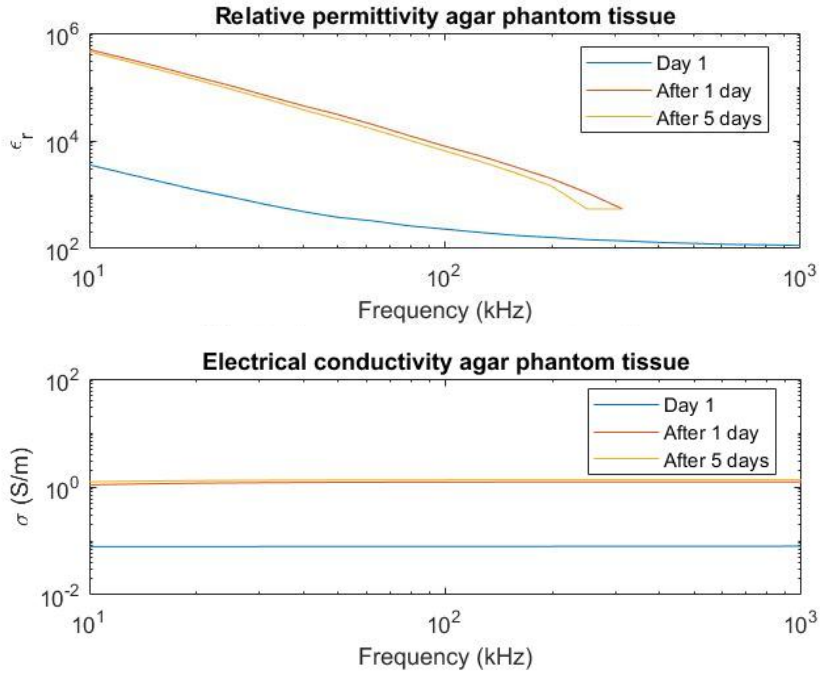


*Figure 13: Salt diffusion 5.7 wt% agar phantom prepared with tap water, stored in 0.9% saline. Top: Relative permittivity, bottom: electrical conductivity*

### Gellan gum

Multiple gellan gum phantoms were produced and stored according to the previous explained conditions. For all phantoms, the shelf life is more than 1 month. But, on average 5% of the gellan gum material seperates after three weeks of storage, seen in Figure 14. Moreover, the gellan gum phantoms absorb in two weeks' time on average 69% water by weight. Furthermore, salt diffusion occurs when storing gellan gum phantoms in a saline solution. A 2.9wt% gellan gum phantom tissue was prepared with tap water and stored for one week in a 0.9% saline solution. The maximum percentage variation between the measured values and the mean of the measured values over all frequency points is 62% and 54% for permittivity and conductivity respectively.

*Figure 14: Gellan gum phantom stored in saline solution where phantom material gets loose. Left: storage for 2 weeks, right: storage for 3 weeks*

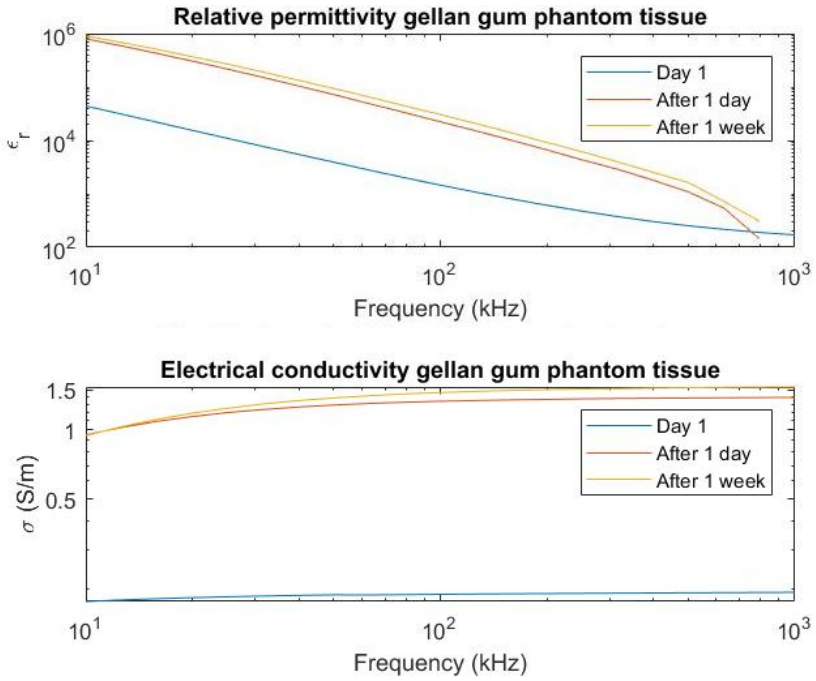


*Figure 15: Salt diffusion 2.9wt% gellan gum phantom prepared with tap water, stored in 0.9% saline. Top: Relative permittivity, bottom: electrical conductivity*

### PVA-C

Multiple PVA-C phantoms were produced and stored according to the previous explained conditions. For all phantoms, the shelf life is more than 1 month. PVA-C phantoms absorb in two weeks' time on average 48% water, Figure 16. Furthermore, a PVA-C phantom prepared by mixing 10g PVA-powder with 100ml tap water was stored in a 0.9% saline solution. The dielectric properties were measured after the phantom underwent 1 freeze-thaw cycle and the phantom was at room temperature; day 1. Afterwards, the PVA-C phantom was stored in a 0.9% saline solution and the dielectric properties were measured after 1 day and after 1 week of storage. Results are shown in Figure 17. Here, the maximum percentage variation between the measured values and the mean of the measured values over all frequency points is 66% and 56% for permittivity and conductivity respectively.

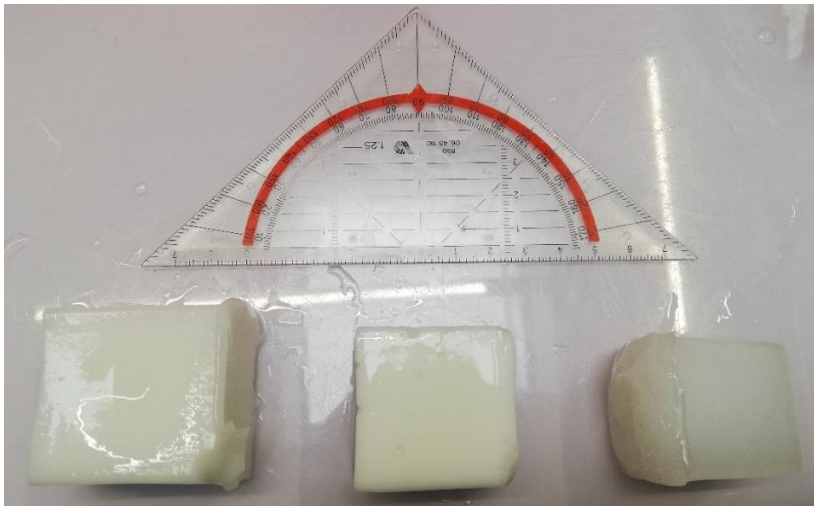

*Figure 16: Change in size of PVA-C phantom tissues due to water absorption & drying out of the phantom. Left phantom: stored for 1 week in water. Middle phantom: stored for 1 day in water. Right phantom: stored for 2 days in air.*

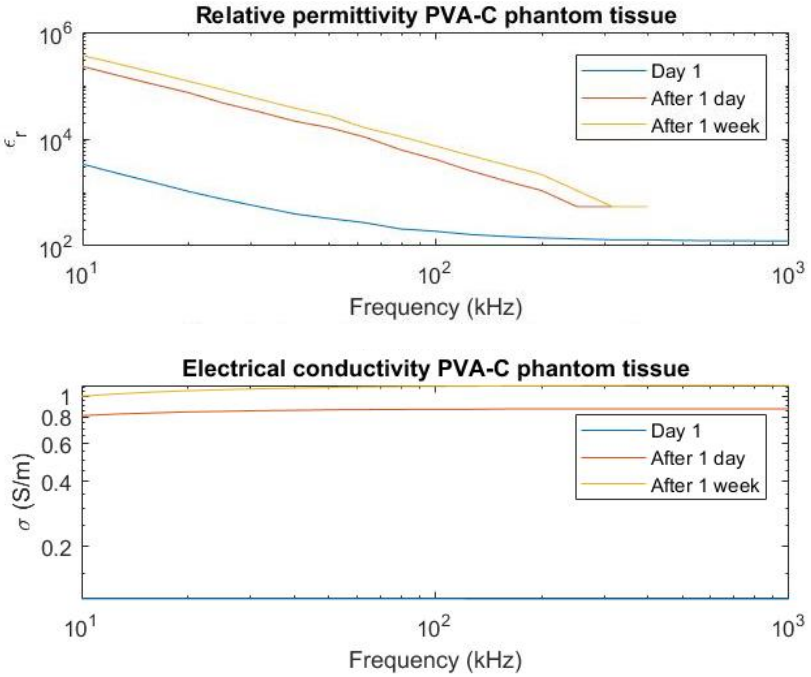


*Figure 17: Salt diffusion in 9.1wt% PVA phantom prepared with tap water, stored in 0.9% saline. Top: Relative permittivity, bottom: electrical conductivity*

### 7.2.3 Discussion and conclusion

As for the agar phantoms, the shelf life did not realize the required 1 month. The gellan gum and PVA-C phantom tissues did realize the required shelf life of at least 1 month. But, the gellan gum phantom tissue seems to result in material separation when stored in a liquid. Moreover, water absorption occurs in the gellan gum and PVA-C phantoms, which might affect the dielectric properties and should be investigated during stability tests which will be examined in Part III [64]. Finally, salt diffusion occurs in all phantom tissues when stored in water [103]. The maximum percentage variations between the measured values and the mean over all frequency points is for all phantoms much greater compared to the variation seen in PVA-C phantom due to water absorption.

## 7.3 Step 2: Base materials

### 7.3.1 Methods

Due to salt diffusion occurring in all phantoms, all phantoms should be prepared with the same saline solution as the storage solution. Moreover, no additional salt can be added for increasing the conductivity. In this step, sample phantoms with the storage solution will be prepared without additives. The dielectric properties will be measured and compared to the target values in order to examine how the dielectric properties should be manipulated. Because at this stage of the phantom preparation, the wt% of the base materials can still variate due to possible effects on the stiffness of the phantoms, various phantoms will be prepared with different wt% of base material.

### 7.3.2 Results

Results of an agar-based, gellan gum-based and PVA-C-based phantom tissues are shown in Figure 18, Figure 19 and Figure 20 respectively and are representable for all phantom tissues made. In Appendix B ‘B5 Base materials in comparison with target values’ all results and possible influences of varying with wt% are shown.

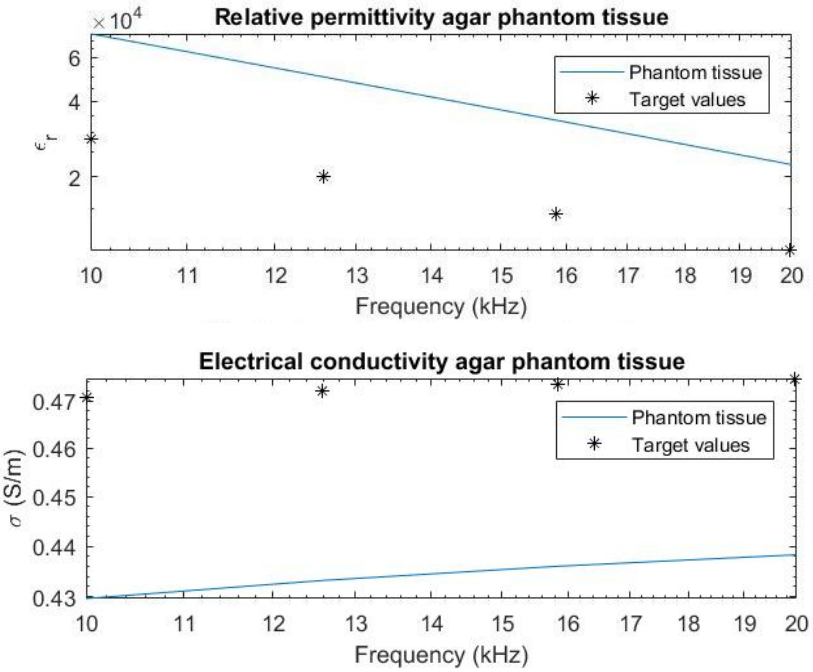


*Figure 18: 5.7wt% agar phantom compared to target values*

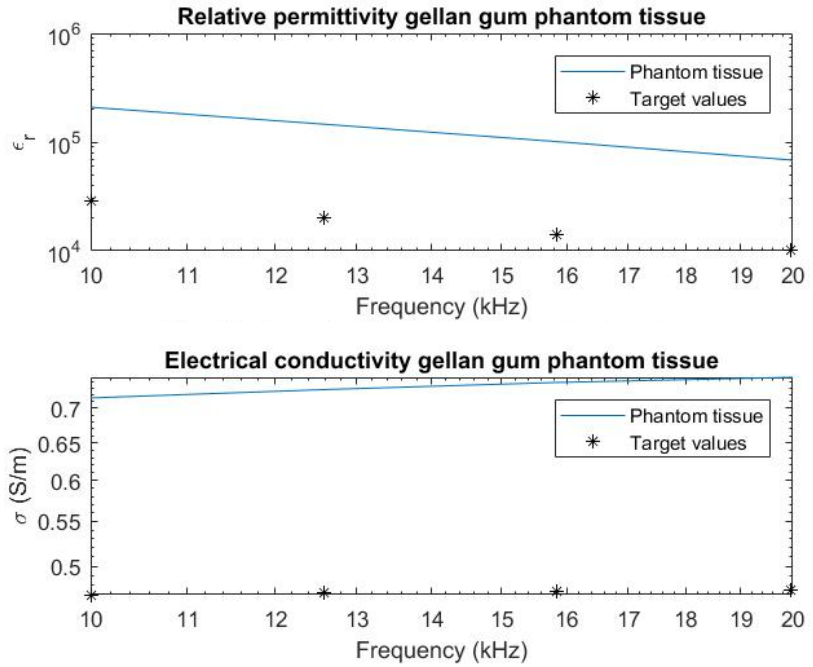


*Figure 19: 2.9wt% gellan gum phantom compared to target values*

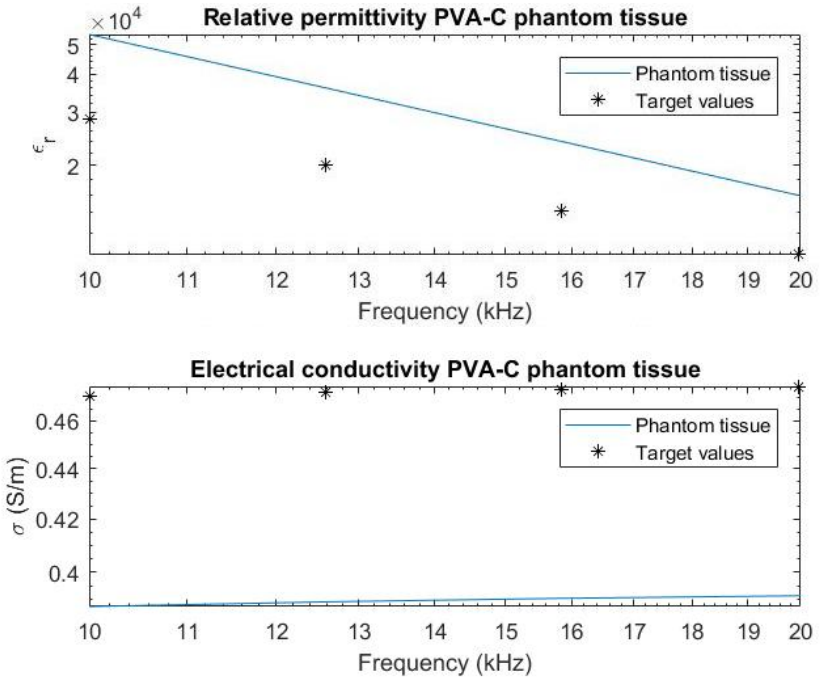


*Figure 20: 13.0 wt% PVA-C phantom compared to target values*

### 7.3.3 Discussion and conclusion

Results show that for agar-based phantoms the permittivity should decrease and the conductivity should increase with the use of additives. For gellan gum-based phantoms both the permittivity and conductivity should be decreased and for PVA-C-based phantoms the permittivity should be decreased and the conductivity should be increased. Table 4 gives a clear overview of the results.

*Table 4: Dielectric values of base materials compared to the target values. (↑) indicates the dielectric value of the phantom tissue should be increased and (↓) indicates the dielectric value of the phantom tissue should be decreased in order to get the same dielectric values as the target values.*

| Base material | Permittivity | Conductivity |
|---|---|---|
| **Agar** | ↓ | ↑ |
| **Gellan gum** | ↓ | ↓ |
| **PVA-C** | ↓ | ↑ |

## 7.4 Step 3: Additives

### 7.4.1 Methods

Table 1 shows if the additive should increase or decrease the dielectric values of the phantom tissue when added according to literature. In this step it will be examined if this is in line with own findings when preparing phantom samples with additives. Multiple sample phantoms will be prepared with one additive. Thereafter, the measured dielectric properties will be compared to the properties of the sample phantom with the same mixture without the additive. An increase or decrease of the dielectric values is said to occur when the mean percentage variation between the measured values and the mean of the measured values over all frequency points exceeds the accepted tolerance range of 11% and 10% for permittivity and conductivity respectively.

Moreover, according to literature sugar diffusion occurs in aqueous solutions [104]. While salt diffusion occurs when the phantoms will be stored in the storage solution, sugar will also be tested on diffusion. A phantom will be prepared with added sugar and will be stored in the same solution as it will be prepared in. Impedance measurements will be performed over a period of one week to examine whether diffusion might occur.

### 7.4.2 Results

Table 5 shows the expected results compared to the actual results. Here, a slight change indicates the mean percentage variation lies between 11% - 22% for permittivity and 10% - 20% for conductivity. Additionally, it was examined if antifrost, the surfactant and the preservative used would change the dielectric values. Antifrost might be needed for the PVA-C phantoms when using closed rigid moulds. Graphics of all results of the impedance measurements are shown in 'Appendix B' 'B8 Increase/decrease of additives'.

*Table 5: Dielectric additives, '↑' indicates the additive will increase its dielectric value, '↓'indicates the additives will decrease the dielectric value and '~' indicates contradiction in literature.*

| **Additives** | **Affects $\varepsilon_r$** | | **Affects σ** | |
|---|---|---|---|---|
| | **According to literature** | **Result** | **According to literature** | **Result** |
| **Acetone** | ~ | ↓ Slightly | ↑ | No influence |
| **Ammonia** | ↓ | ↓ Slightly | | No influence |
| **Antifrost** | | ↑ Slightly | | No influence |
| **Charcoal powder** | ↑ | ↑ | ↑ | ↑ Slightly |
| **Ethanol** | ↓ | ↓ Slightly | | No influence |
| **Glycine** | ↑ | No influence | | No influence |
| **Graphite powder (+ acetone)** | ↑ | ↑ | ↑ | ↑ |
| **Oil (+ surfactant)** | ↓ | ↓ | ↓ | No influence |
| **Preservative (sodium acetate)** | | ↑ | | ↑ |
| **PVC** | ↓ | ↓ | ↓ | ↓ |
| **Salt** | | ↑ | ↑ | ↑ |
| **Sugar** | ↓ | ↓ | ↓ | ↓ |

To examine whether sugar diffusion occurs, a 13.0wt% PVA phantom is made with 28.6wt% sugar and is stored in the same solution as it is prepared in. Figure 21 shows the results where the maximum percentage variation between the measured values and the mean of the measured values over all frequency points is 62% and 26% for permittivity and conductivity respectively.

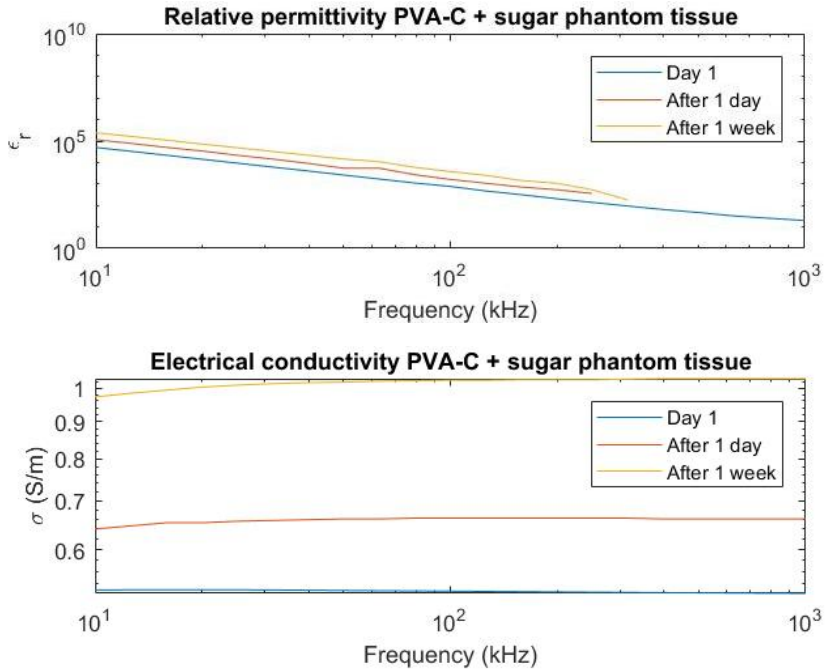


*Figure 21: PVA-C phantom with added sugar tested on diffusion*

### 7.4.3 Discussion and conclusion

A good match with literature and own results is shown. After this examination, it is clear what influence the additives have on the phantom materials, seen in Table 5. Furthermore, diffusion of sugar is tested and an enormous increase in permittivity and conductivity is shown in Figure 21, indicating sugar diffusion occurred. Therefore, sugar will not be used for the sample phantoms.

## 7.5 Step 4: Sample phantoms preparation

### 7.5.1 Methods

After it was examined what the effect of the additives would be on the dielectric values, the sample phantoms can be prepared. Therefore, for manipulating the dielectric properties of the phantom materials the additives shown in Table 6 will be used in order to mimic the target dielectric values. Multiple phantoms will be prepared and examined based on the measured dielectric values. First, phantoms with one additive with different wt% will be prepared and analysed. For the second batch of phantom preparation, the trend seen for the dielectric values, the 'ease' of mixing and a haptic and visual inspection will be taken into account. This experimental process will continue until a good fit for the phantom samples can be realised.

*Table 6: Additives used for manipulating the dielectric properties*

| **Agar** | |
|---|---|
| **Permittivity (↓)** | **Conductivity (↑)** |
| Oil | Graphite powder |
| PVC | Charcoal powder |
| | Sodium acetate |
| **Gellan gum** | |
| **Permittivity (↓)** | **Conductivity (↓)** |
| Oil | Oil |
| PVC | PVC |
| **PVA-C** | |
| **Permittivity (↓)** | **Conductivity (↑)** |
| Oil | Graphite powder |
| PVC | Charcoal powder |
| | Sodium acetate |

### 7.5.2 Results

The dielectric values of all succeeded phantoms were measured and compared to the target values. Appendix B 'B7 Sample phantoms' shows all results. In this subchapter, only the most promising prepared phantoms will be reported per base material.

#### Agar

5.7wt% agar phantoms were prepared while this appeared to result into the best possible stiffness. Less base material resulted in too brittle phantoms and more base material resulted in too stiff phantoms. Graphite resulted as a good additive for increasing the conductivity, but also increased the permittivity while this value should be decreased. Hence, it was chosen to combine graphite and oil as additive. In line with this theory, the same was done with charcoal. However, charcoal resulted to have no effect on the dielectric values. Agar with added PVC resulted in a more brittle phantom, but could be mixed homogeneously. Agar phantoms with oil were prepared and resulted in a good decrease in permittivity. However, the phantoms did not pass the visual inspection as can be seen in Figure 22. Moreover, agar did not mix well with sodium acetate, seen in Figure 22, the phantom did not solidify. Of all agar phantoms made, Figure 23 shows the best resulted phantoms per additive used regarding the dielectric values. Phantom 'A2' of Figure 23 resulted as the most promising agar-based phantom material. But, as a result the 5.7wt% agar phantoms did not pass the haptic inspection while the phantoms are still too stiff and more brittle than elastic what is desired.

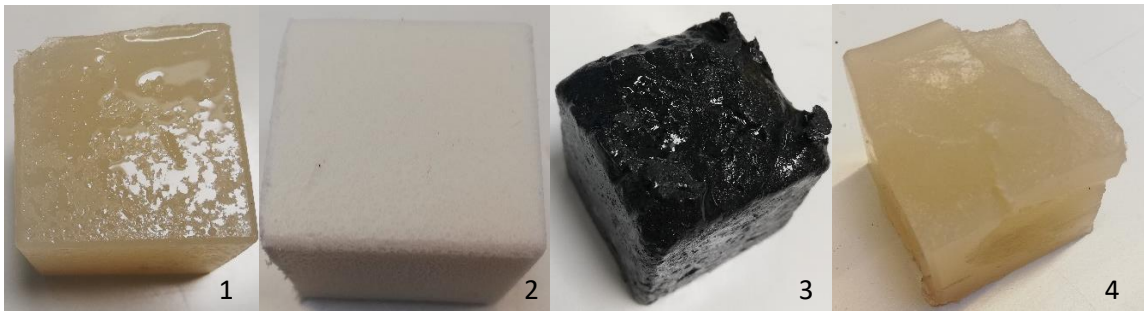


*Figure 22: Agar phantoms. 1: oil as additive, 2: PVC as additive, 3: graphite & oil as additive, 4: sodium acetate as additive*

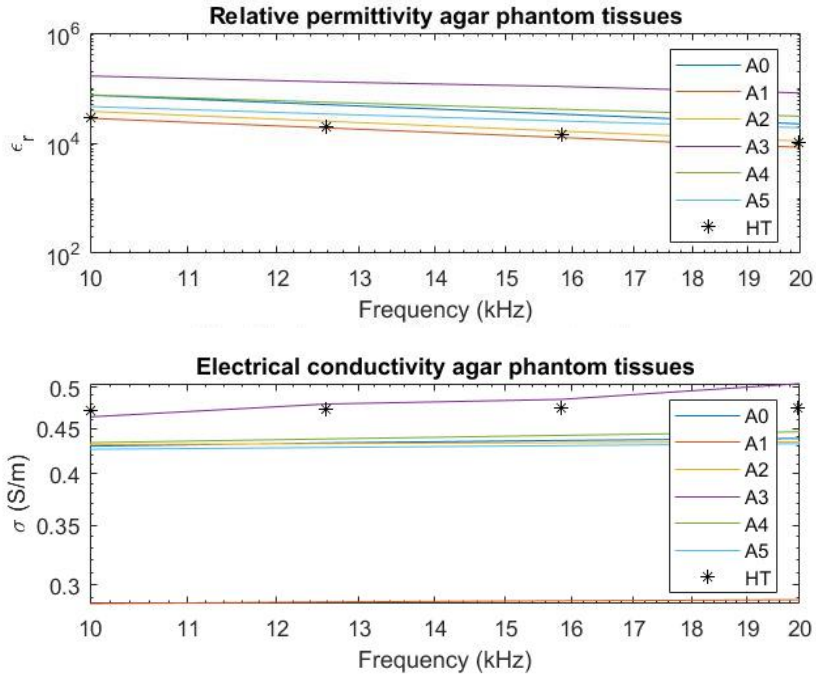


*Figure 23: 5.7wt% agar phantoms closest to the target values (HT), with A0: no additives, A1: 16.7wt% PVC, A2: 23.1wt% oil, A3: 9.1wt% graphite, A4: 2.9wt% charcoal, A5: 28.6wt% oil & 2.9wt% charcoal*

### Gellan gum

2.8wt% gellan gum-based phantoms were prepared with oil and PVC to decrease the dielectric values of the phantom tissue. Both, oil and PVC as additive resulted in a homogenous prepared phantom tissue as seen in Figure 24. Phantom preparation above 16.7wt% PVC did not succeed, while the mixture gets clumpy. Figure 25 shows the results for the best prepared gellan gum-based phantoms. Dielectric measurements resulted in phantoms GG1 and GG2 as seen in Figure 25 to be the most promising gellan gum-based phantom materials.

*Figure 24: Gellan gum phantoms, left: oil as additive, right: PVC as additive*

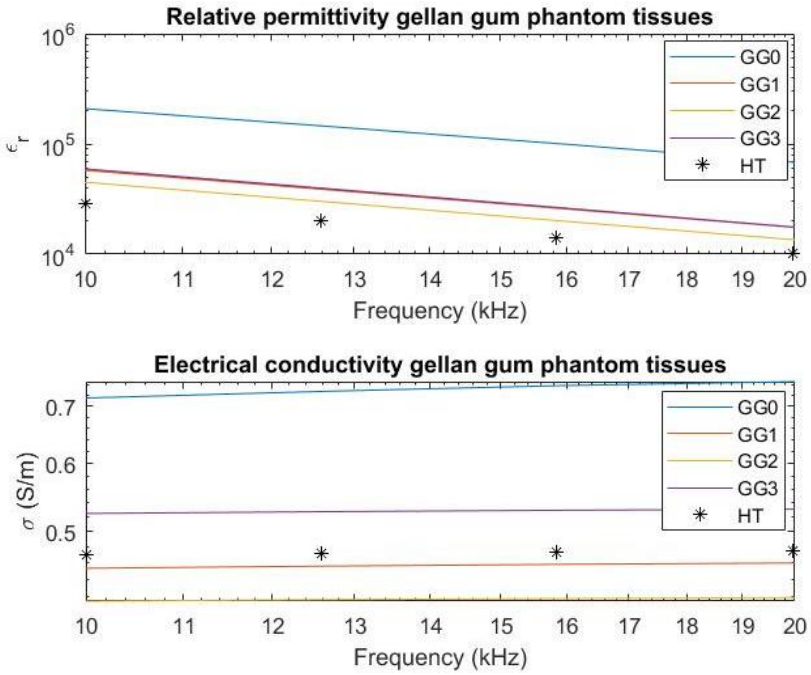


*Figure 25: 2.9wt% gellan gum phantoms closest to the target values (HT), with GG0: no additives, GG1: 16.7wt% oil, GG2: 23.1wt% oil, GG3: 16.7wt% PVC*

### PVA-C

For the PVA-based phantom tissue, 13.0wt% PVA-powder resulted in a good phantom stiffness and was used for the sample phantom preparations. Charcoal did not manipulate the conductivity as expected, as seen in Figure 27. Moreover, charcoal precipitates even when using small amounts of charcoal (4.8wt%). Adding graphite did influence the conductivity and permittivity, but also increases the stiffness of the phantom. 13.0wt% PVA-based phantoms with added graphite resulted in too stiff phantom tissues and therefore the wt% of PVA powder was decreased. Results are shown in Figure 28. Also, graphite precipitates when using high amounts of graphite powder (20.0wt%). This is noticed when touching the phantom tissue, it can be felt that the bottom of the phantom tissue is much stiffer than the rest of the phantom. Added PVC resulted in both a decrease in permittivity and a decrease in conductivity. But, also PVC powder precipitates when using high amounts of PVC (16.7wt%), seen in Figure 26. Therefore, lower amounts of PVC powder (4.8wt%) was used in combination with sodium acetate. Furthermore, oil is used in combination with sodium acetate for decreasing its permittivity and increasing its conductivity respectively. Figure 29 shows the results of the best prepared 13.0wt% PVA-based phantoms and Figure 30 shows all phantom tissues closest to the target values with P1 and P2 as the most closest to the target values.

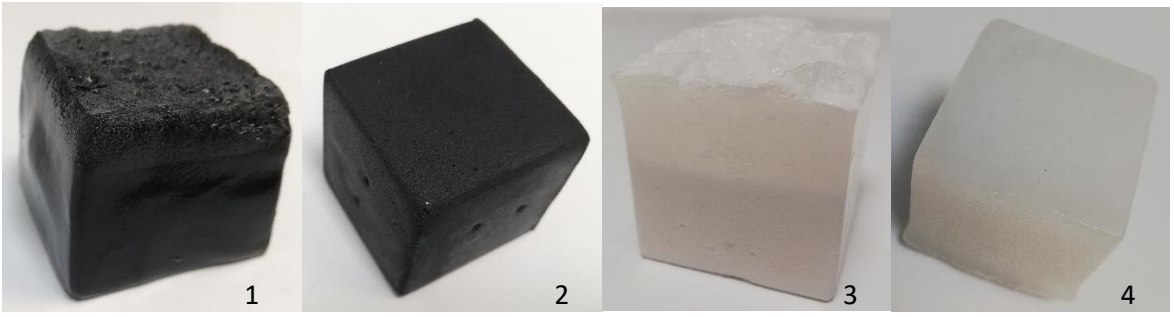


*Figure 26: PVA-C phantoms. 1: charcoal as additive, 2: graphite as additive, 3: PVC as additive, 4: sodium acetate as additive*

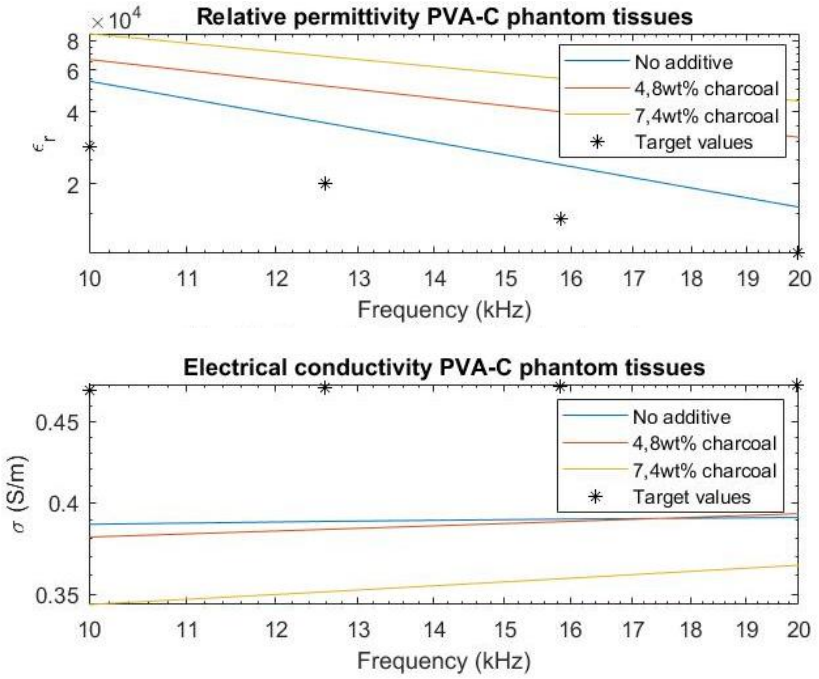


*Figure 27: Influence of different wt% charcoal on 13.0wt% PVA-C phantom tissues*

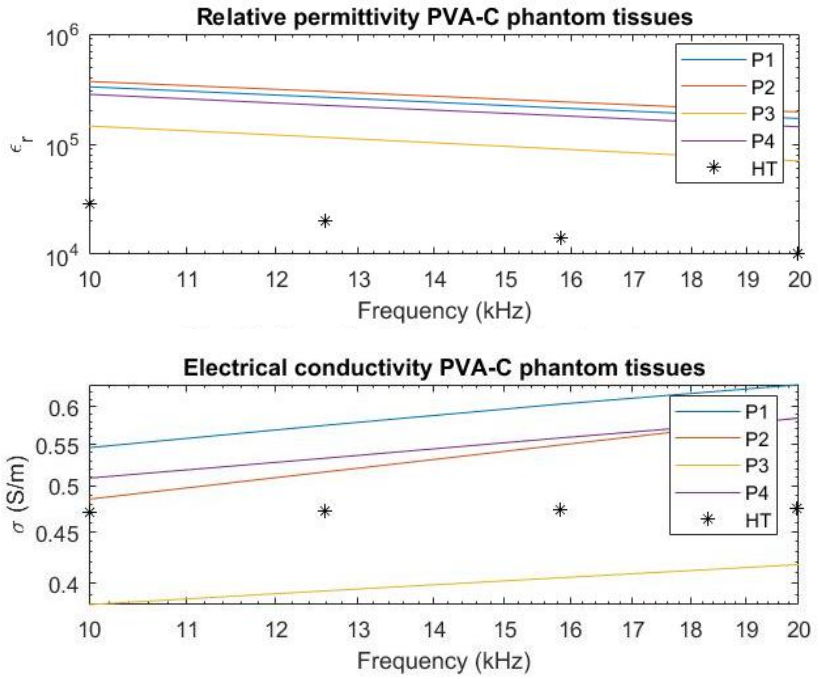


*Figure 28: Influence of different wt% graphite and PVA compared to target values (HT), with P1: 9.1wt% PVA & 23.1wt% graphite, P2: 10.7wt% PVA & 23.1wt% graphite, P3: 13.0wt% PVA & 20.0wt% graphite, P4: 13.0wt% PVA & 25.9wt% graphite*

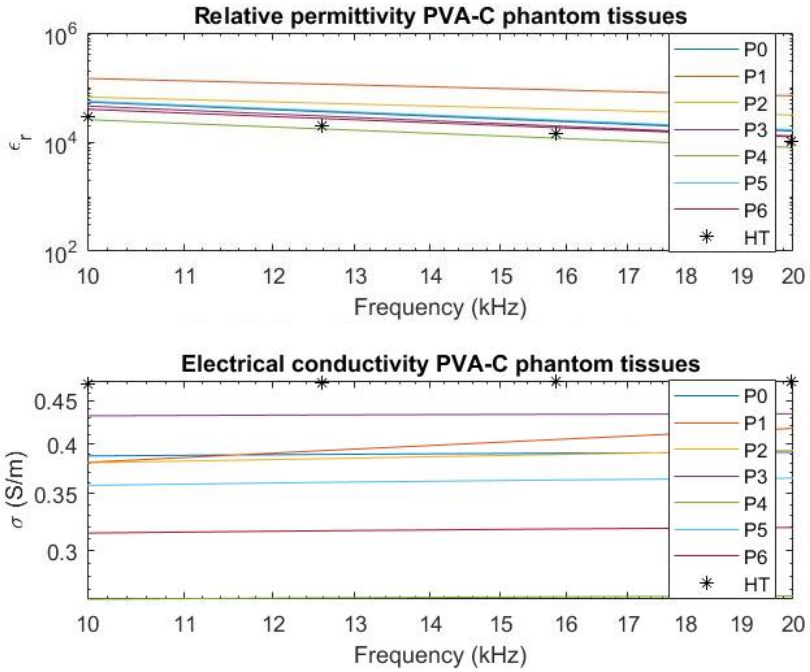


*Figure 29: 13.0wt% PVA-C phantoms closest to the target values (HT), with P0: no additives, P1: 20.0wt% graphite, P2: 4.8wt% charcoal, P3: 0.05wt% sodium acetate, P4: 33.3wt% oil, P5: 0.07wt% sodium acetate & 4.8wt% PVC, P6: 0.07wt% sodium acetate & 33.3wt% oil*

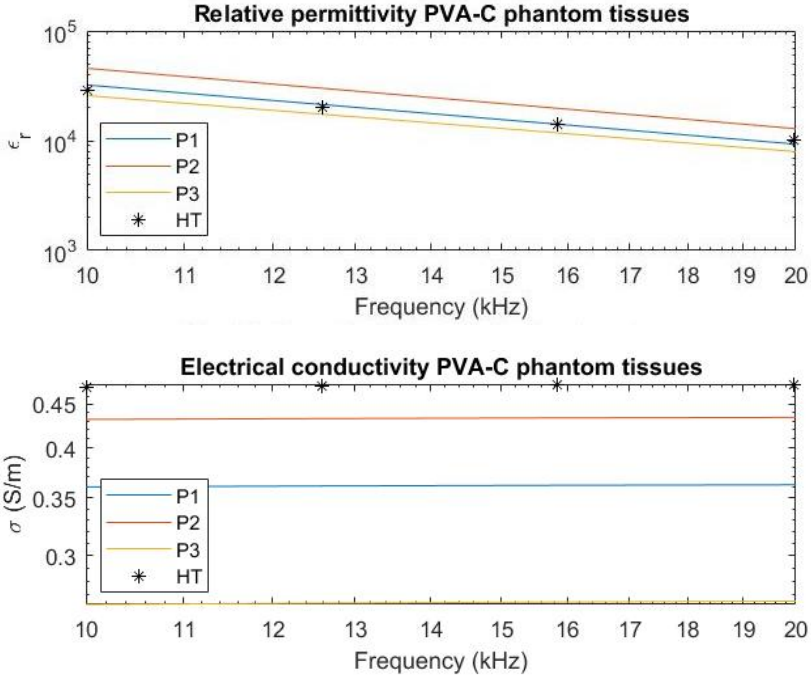


*Figure 30: PVA-C phantoms closest to the target values (HT), with P1: 10.7wt% PVA, 0.01wt% sodium acetate & 31.0wt% oil, P2: 13.0wt% PVA & 0.05wt% sodium acetate, P3: 13.0wt% PVA & 33.3wt% oil*

### 7.5.3 Discussion and conclusion

Some challenges during the preparation of the phantoms were encountered. Agar-based phantoms did not always solidify. Solidification of agar-based phantoms is dependent on the procedures taken, the ratios of each ingredient [105] and the pH-value of the mixture [106]. Preparing gellan gum-based

phantoms cannot be done easily. Water evaporates quickly and should be refilled before the mixture gets lumpy. Gellan gum powder can be added to water or saline between 80 - 85 °C. After the gellan gum powder is completely mixed, the mixture should be heated to 100 °C. Again, evaporated water should be refilled. When water is refilled, the water should not be below 80 °C, otherwise the mixture will get lumpy. Moreover, when water is refilled, make sure the 'new' mixture is heated to 100°C, otherwise the gellan gum mixture will not become solid when cooling down. When the mixture is finished, the gellan gum can be poured into a mould. When pouring the gellan gum mixture, it becomes very quickly solid. Therefore, the mixture should be poured quickly into the mould. Additives as PVC, graphite and charcoal easily precipitates in PVA-C-based phantoms. The optimum wt% base material for agar was 5.7wt% and for gellan gum 2.9wt%. No significant change in stiffness is seen in the gellan gum-based phantoms when changing the wt% gellan gum powder. As for PVA-C-based phantom, 13.0wt% base material resulted to be a good match regarding the stiffness (when no graphite is added). A variation in the amount of PVA-powder would give good results as well.

Furthermore, sodium acetate resulted in a big increase of the phantoms conductivity. And oil resulted in a big decrease of the phantoms permittivity, but resulted in oily phantoms which is not desired. Charcoal powder does not seem to influence the electrical conductivity considerably for all phantoms made. This could be due to the percolation threshold which is not achieved. Therefore, higher amounts of charcoal were added in the PVA-C phantoms to check whether the percolation threshold would be achieved. However, this resulted in precipitation of the charcoal powder in the PVA-C phantom. Moreover, the percolation threshold for the conductive components charcoal and graphite varies with base material used. Literature showed that the percolation threshold for carbon black in many composites corresponds to approximately 3-15 wt% carbon black [107]. Carbon black with a polyethylene terephthalate resin has a low percolation value of 0.58wt% [108]. Carbon in other forms, like carbon nanotubes, show different percolation values [109]. However, the percolation threshold of active charcoal is unknown. The percolation threshold of graphite lies much higher [110].

## 7.6 Discussion and conclusion

To conclude which phantom material will be the best fit for the final cardiac phantom, a Harris profile will be used. Therefore, all most promising phantom tissues as described in this chapter will be evaluated and compared to each other. This evaluation will be based on the predefined requirements and will be described per property. In the previous subchapter, the phantom tissues with dielectric values closest to the target values were previewed. These phantom tissues, the most promising phantom tissues, will be compared to each other and are defined as shown in Table 7.

*Table 7: Most promising phantom tissues*

| Phantom tissue | Ingredients |
|---|---|
| **A1** | 5.7wt% agar + 23.1wt% oil |
| **G1** | 2.9wt% gellan gum + 16.7wt% oil |
| **G2** | 2.9wt% gellan gum + 23.1wt% oil |
| **P1** | 10.7wt% PVA + 0.1wt% sodium acetate + 31.0wt% oil |
| **P2** | 13.0wt% PVA + 0.05wt% sodium acetate |

### 7.6.1 Dielectric properties

Figure 31 shows the dielectric values of these most promising phantom, with the average percentage difference between the phantom tissue and the measured cardiac tissue in the frequency range of 10 kHz – 20 kHz shown in Table 8. For all phantoms shown in this part, not all dielectric values are within the predefined accepted tolerance range.

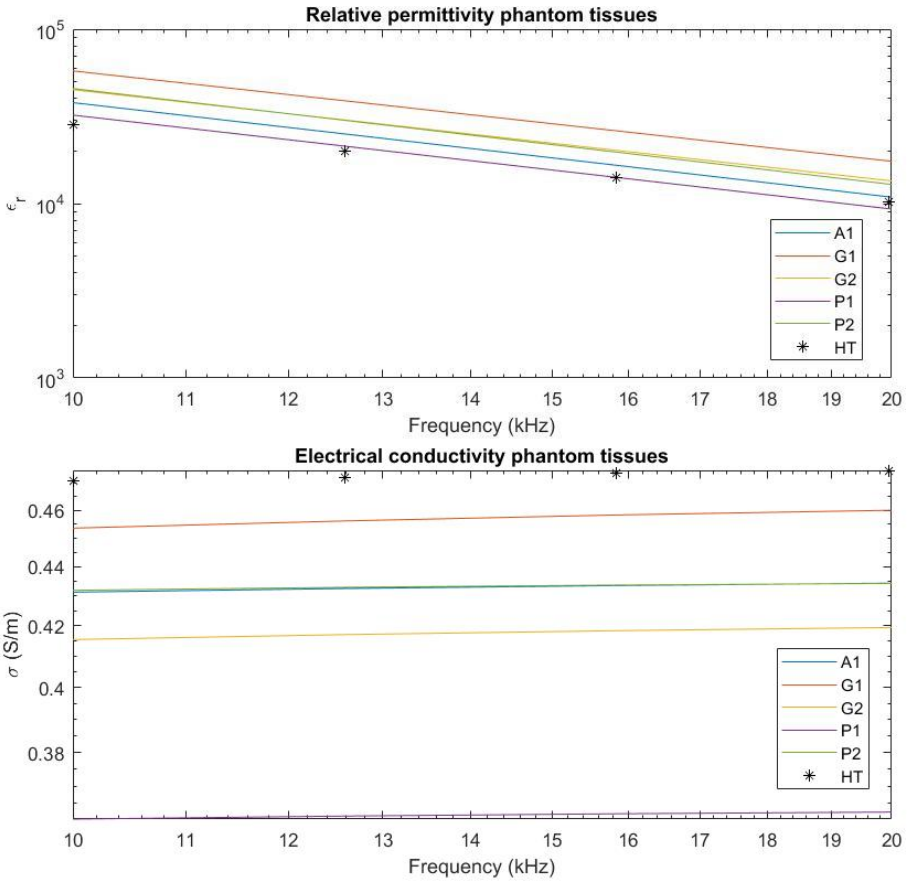


*Figure 31: Phantoms closest to the target values (HT)*

*Table 8: Average difference between phantom tissue and target values (HT)*

| Sample phantom tissue | Average difference between phantom tissue and HT (%) | |
|---|---|---|
| | **Permittivity** | **Conductivity** |
| **A1** | 20.8 | 8.4 |
| **G1** | 88.4 | 3.3 |
| **G2** | 46.1 | 11.7 |
| **P1** | 7.1 | 23.5 |
| **P2** | 44.2 | 8.4 |

### 7.6.2 Storage

The final cardiac phantom should be stored in a saline solution, the predefined 'storage solution', containing the same conductivity as blood. It can be concluded that agar-, gellan gum- and PVA-C-based phantom tissues can be stored in the appropriate solution. But, in all stored phantoms salt diffusion occurs. Moreover, gellan gum- and PVA-C-based phantom tissues, absorb water what might result in a decrease of the dielectric properties [64]. Furthermore, storing gellan gum-based phantom tissues in the storage solution results in phantom material separation (approximately 5% material over 3 weeks storage time). As for the phantoms G1 and G2, the oil with surfactant seems to escape resulting in a cloudy storage solution, Figure 32.

*Figure 32: Phantom tissue G1 in storage solution*

### 7.6.3 Homogeneity

As predefined, phantoms are said to be homogeneous when repeated measurements at various sides of the phantom shows 11% and 4% or lower variation for permittivity and conductivity, respectively. Table 9 shows the results for the homogeneity tests, with the average percentage difference between the measured value of the phantom tissue and the mean value of the phantom tissue together with the maximum percentage difference. All phantoms pass the homogeneity test, except for phantom G2 which shows a maximum difference of 11.8% between the measured permittivity and the mean.

*Table 9: Homogeneity results of most promising phantom samples*

| Sample phantom tissue | Average difference between measured value and the mean, (Maximum difference) (%) | |
|---|---|---|
| | **Permittivity** | **Conductivity** |
| **A1** | 3.6 (5.1) | 2.3 (2.4) |
| **G1** | 8.8 (10.6) | 2.6 (2.8) |
| **G2** | 8.7 (11.8) | 3.0 (3.2) |
| **P1** | 2.1 (2.8) | 2.1 (2.1) |
| **P2** | 4.9 (6.5) | 1.6 (1.6) |

### 7.6.4 Mechanical stiffness

The mechanical stiffness in this chapter is only haptic and visually examined. Agar-based phantoms do not seem to get the desired elasticity. Moreover, results showed that agar-based phantom tissues with oil as additive are not easily prepared and the oil does not seem to mix well with the phantom tissue, as seen in Figure 33, resulting in no solidification of the phantom (left in the figure) or a too tough phantom (right in the figure). Gellan gum-based phantoms are extremely elastic, do not break easily but need to be stiffer. The mechanical stiffness of the PVA-C-based phantom tissues can be easily manipulated by changing the wt% of PVA powder and changing the amounts of freeze-thaw cycles. As for sample phantom P1, the addition of oil gives an oily phantom, seen in Figure 34 on the left. Phantom 'P2' results in a slightly translucent phantom tissue with desired mechanical properties, Figure 34 on the right.

*Figure 33: Agar-based phantom tissues with oil as additive. Left: oil with surfactant, right: oil*

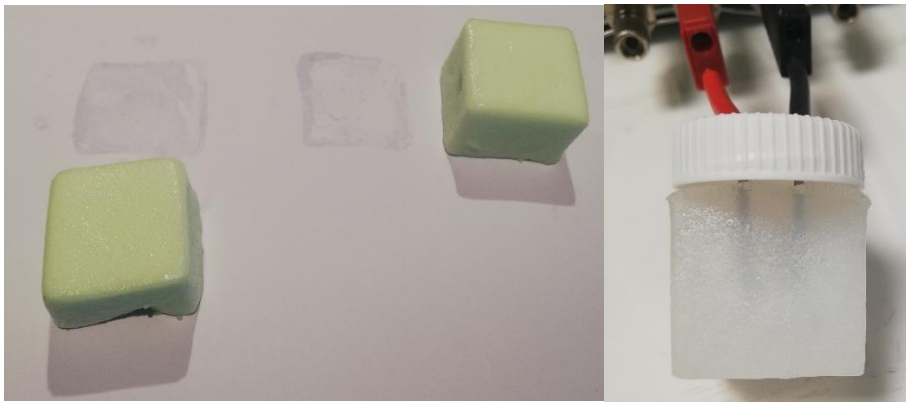

*Figure 34: PVA-C phantom sample tissues. Left: 'P1', showing oily resulted phantoms. Right: 'P2', showing the slight translucent phantom*

### 7.6.5 Shelf life

As for the shelf life of the phantoms, mould growth appeared after three weeks of storing the agar-based phantoms. The gellan gum- and PVA-C-based phantoms appeared to have a shelf life of at least one month.

### 7.6.6 Harris profile

A Harris profile will be used to give an overview of all results of this subchapter. Here, all most promising phantom tissues will be evaluated and compared to each other, in order to find the best fit for the cardiac phantom TMMs. Table 10 shows the Harris profile, resulting in phantom sample tissue 'P2' as the best fit for the cardiac phantom TMM.

*Table 10: Harris Profile, evaluation on the main requirements*

| | **Phantom tissue** | | | | | | | | | | | | | | | | | | | |
|---|---|---|---|---|---|---|---|---|---|---|---|---|---|---|---|---|---|---|---|---|
| | **A1** | | | | **G1** | | | | **G2** | | | | **P1** | | | | **P2** | | | |
| **Property** | -- | - | + | ++ | -- | - | + | ++ | -- | - | + | ++ | -- | - | + | ++ | -- | - | + | ++ |
| Conductivity | | | | ■ | | | | ■ | | | ■ | ■ | | | ■ | | | | | ■ |
| Permittivity | | | ■ | | | ■ | | | | | ■ | | | | | ■ | | | ■ | |
| Storage | | | | ■ | | ■ | | | | ■ | | | | | | ■ | | | | ■ |
| Homogeneous | | | | ■ | | | ■ | | | | ■ | | | | | ■ | | | | ■ |
| Mechanical stiffness | ■ | | | | | | ■ | | | | ■ | | | | ■ | | | | | ■ |
| Shelf life | ■ | | | | | | | ■ | | | | ■ | | | | ■ | | | | ■ |

PART III:

# Cardiac phantom design

In this part, the most promising sample phantom will be extensively examined to evaluate if the phantom material meets all requirements needed for the development of the LA phantom. This evaluation will be done more elaborately than in the previous chapter. First, the methods used for the evaluation of all requirements will be described. Thereafter, cardiac phantom samples will be prepared four more times for the final evaluation. The evaluation on all main requirements will be described separately in this part and the evaluation on all additional requirements will be described together. Finally, all results will be discussed and concluded.

# 8. Evaluation methods

Table 2 shows all requirements needed for the final cardiac phantom. In the previous part, sample phantoms were evaluated based on the main requirements. In this part, the most promising sample phantom will be evaluated more elaborately based on all requirements. The most promising sample phantom will be produced four more times, the cardiac phantom samples, and will be evaluated as shown in this chapter. Some methods are equal to the methods described in Chapter 6 and will therefore be only referred to Chapter 6. Additional and/or extended methods will be described in this chapter.

## 8.1 Dielectric properties

### 8.1.1 Impedance measurements

All dielectric measurements will be performed six times on the cardiac phantom samples at room temperature. The 2-needle electrode configuration as used in Chapter 6.1.1 cannot be used for measurements at the cardiac phantom because of the thin walls; the needles of the 2-needle electrode are too long. Moreover, as already discussed in Chapter 6.6, electrode polarisation can occur when using a 2-needle electrode. This can be limited using a 4 point needle electrode as already seen in Chapter 6.1.1. Therefore, Philips provided a 4-needle electrode as seen in Figure 35. Figure 36 shows the connection image of the 4-terminal configuration, which can also reduce the effects of lead impedances and contact resistances as compared to the 2-terminal configuration. The signal current path and the voltage sensing leads are independent when using the 4-terminal configuration. Hence, the voltage sensing leads do not detect the voltage drop caused by the lead inductances, lead resistances and contact resistances on the current leads. [11] The 4-point needle electrode is fabricated with high precision and is made in duplicate. In that way, at Philips measurements can be performed at the exact same way and conditions as measurements at the TU Delft. Moreover, the new needle electrode will be connected to the same impedance analyser as described in Chapter 6.1.1. First, the 2-needle electrode method will be compared to the new 4-needle electrode method.

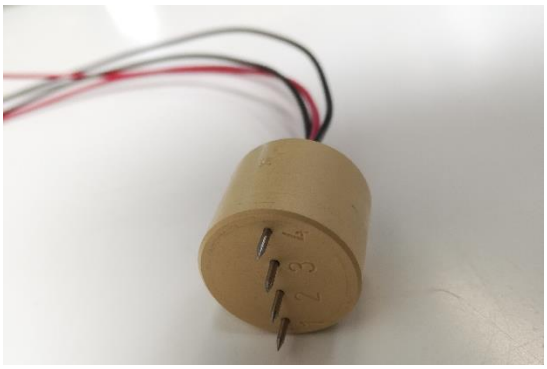

*Figure 35: Four needle electrode, with the distance between the needles b = 5.0 mm, radius of the needles r = 0.5mm and length of the needles L = 5.0mm*

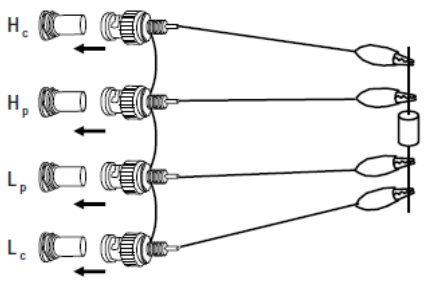


*Figure 36: Connection image for the four-needle electrode method* [11]

For the comparison of the 'old' method using the 2-needle electrode and the 'new' method using the 4-needle electrode, measurements were done six times on two phantom samples. Figure 37 shows the results of the measured Capacitance in Farads (F) and the measured Conductance in Siemens (S). Figure 45 shows comparisons of all 3 methods used: in blue the 'old' 2-needle electrode method, in red the 'new' 4-needle electrode method using all 4 needles and in yellow the 'new' 4-needle electrode using only 2 needles. It is expected that the capacitance would decrease using the 4-needle electrode because less electrode polarisation should occur and results are in agreement with this expectation. But, it is not expected the conductance would decrease. Because the 4-neelde electrode is made with precision, it is chosen to use the 4-needle electrode for all further measurements. But, because the 4-needle electrode is not working as expected, a 2-point measurement will be performed using the 4-needle electrode. So, only wire 2 and 3 will be used and therefore the 4-needle electrode will function as a 2-needle electrode configuration. Appendix D shows the results of the 3 methods used on the second phantom, giving the same results.

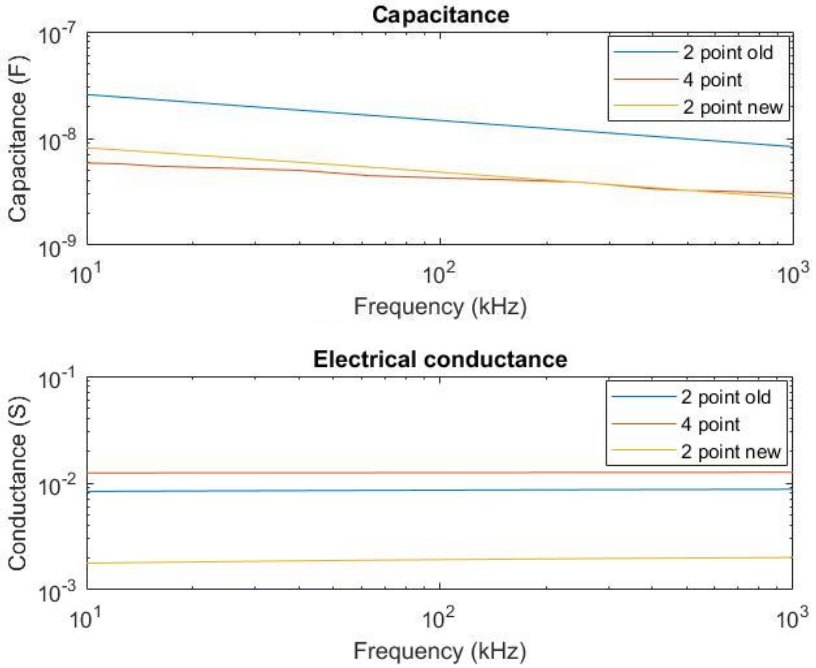


*Figure 37: Comparison between the 'old' 2-needle electrode (2 point old), the 4-needle electrode (4 point) and the 4-needle electrode functioning as a 2-needle electrode (2 point new)*

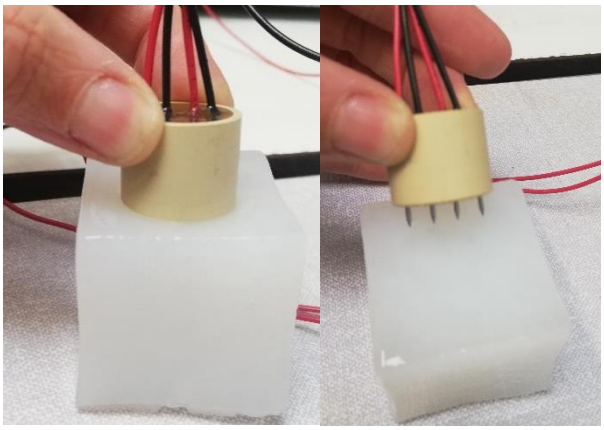

*Figure 38: Dielectric measurements with the four needle electrode*

### 8.1.2 Target values

New measurements will be performed using the 4-needle electrode with the 2-needle electrode method. The measurements will be conducted on porcine heart tissue in the frequency range of 10kHz – 20kHz with 21 equally distributed steps and will function as the new target values. All previously performed impedance measurements, were measured in parallel mode parameters of capacitance and conductance. In this part, new measurements are conducted on the porcine heart tissue, but are measured in series mode parameters in forms of magnitude, $|Z|$, and phase angle, $\theta$. For converting the impedance in the polar form into the rectangular-coordinate form R + jZ, the following formulas can be used

$$Rs = |Z| \cos\theta \quad (10)$$

$$Xs = |Z| \sin\theta \quad (11)$$

with Rs the series resistance and Xs the series reactance. Series and parallel mode impedance values are identical. But, Rs is not equal to the parallel resistance Rp except when the Xs = 0 and the parallel susceptance equals zero (Bp = 0). Using the susceptance can be easier for parallel combinations of real and imaginary components of the impedance. In which case

$$\frac{1}{Z} = \frac{1}{R+jX} = Y = G + jB \quad (12)$$

where Y represents admittance, G conductance, and B susceptance. However, the series and parallel mode parameters are related with each other by using the following equations, which are functions of the dissipation factor (D) [11],

$$D = \frac{Rs}{Xs} = \omega CsRs \quad (13)$$

$$Gp = \frac{Rs}{Rs^2 + Xs^2} \quad (14)$$

$$Cs = Cp(1+D^2) \quad (15)$$

with $\omega = 2\pi f$ the angular frequency, Cs the series capacitance and Gp the parallel conductance. By substituting equation (15) into (13), the formula for converting the Rs and Xs into Cp is

$$Cp = \frac{1}{\omega Xs\,(1+D^2)} \quad (16)$$

with D equals $\frac{Rs}{Xs}$ . [11] Now, the previous found formulas (8) and (9) can be used for rewriting the parallel capacitance and parallel conductance into the relative permittivity and electrical conductivity respectively can be used.

For validation, two phantom samples were measured four times. The first measurement is performed by measuring the capacitance and conductance in parallel mode parameters and the second measurement is performed by measuring the magnitude and phase angle of the impedance in series mode parameters. These two measurements are performed directly after each other without moving the electrodes in the phantom sample. Thereafter, this process is conducted three more times. Results are shown in Figure 39. Results of the second phantom sample are shown in Appendix E.

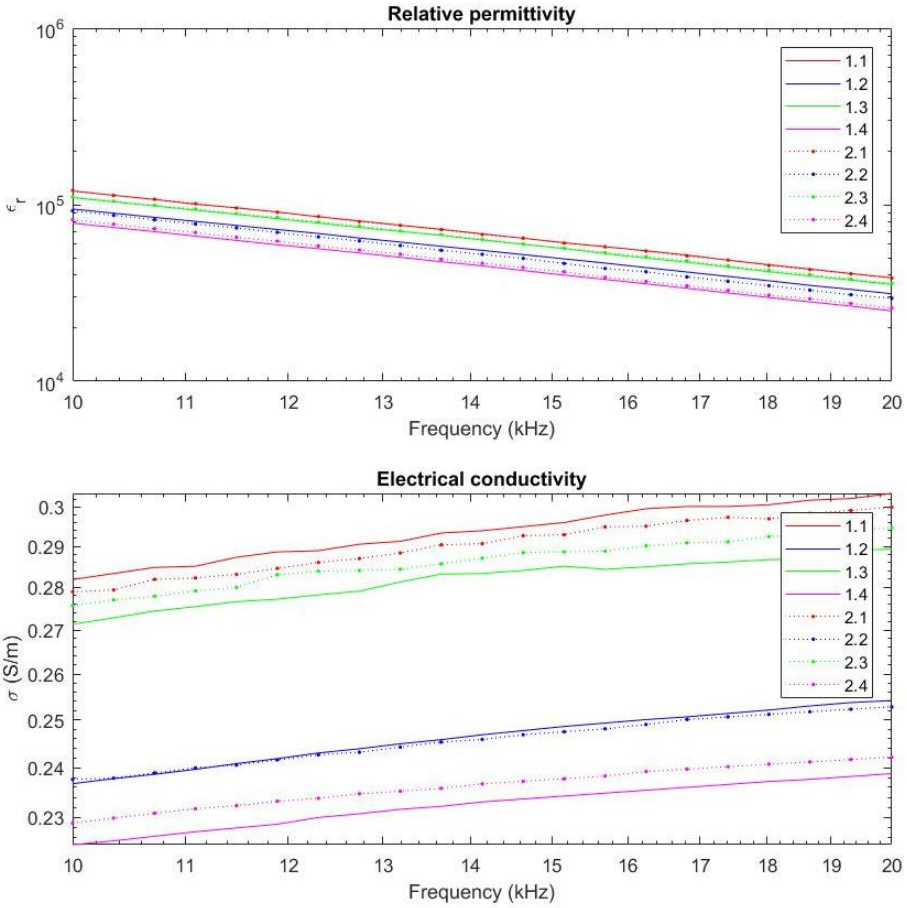


*Figure 39: Comparison between measured capacitance and conductance in parallel mode parameters (1.1 - 1.4) and measured magnitude and phase angle in series mode parameters (2.1 – 2.4)*

The new measurements on the same porcine heart tissue as described in Chapter 6.1.3 are repeated 5 times, Figure 40. Results are shown in Figure 41 and will function as target values in this chapter. Moreover, as comparison between the old measurement method used and the new measurement method used, in Figure 42 the methods are compared to the dielectric values of human heart tissue derived from the database IT'IS [30].

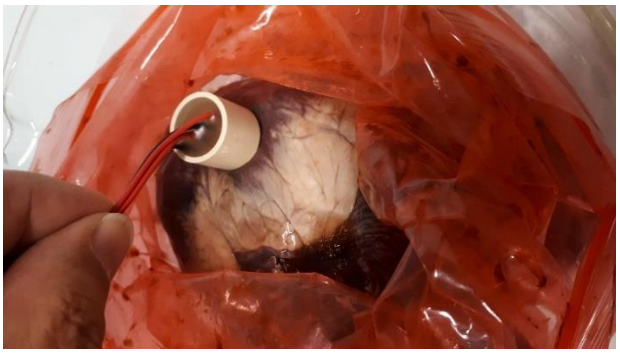

*Figure 40: Measurements on porcine heart tissue with 4-points needle electrode*

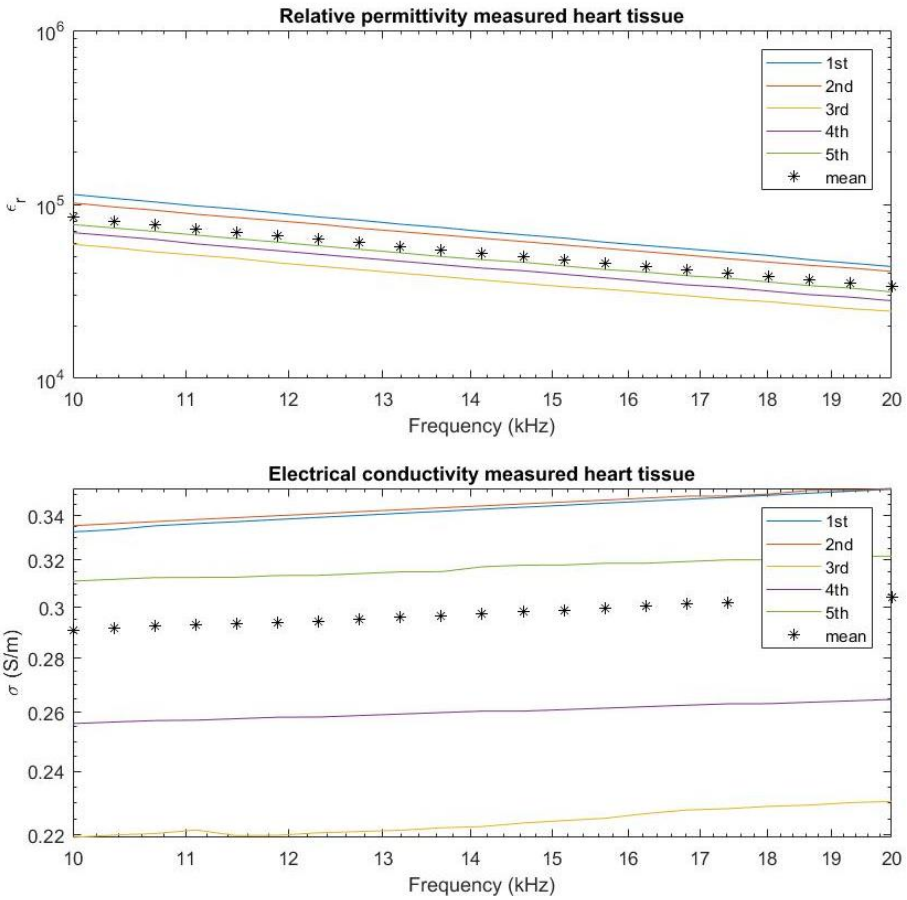


*Figure 41: Measurements performed in porcine heart tissue*

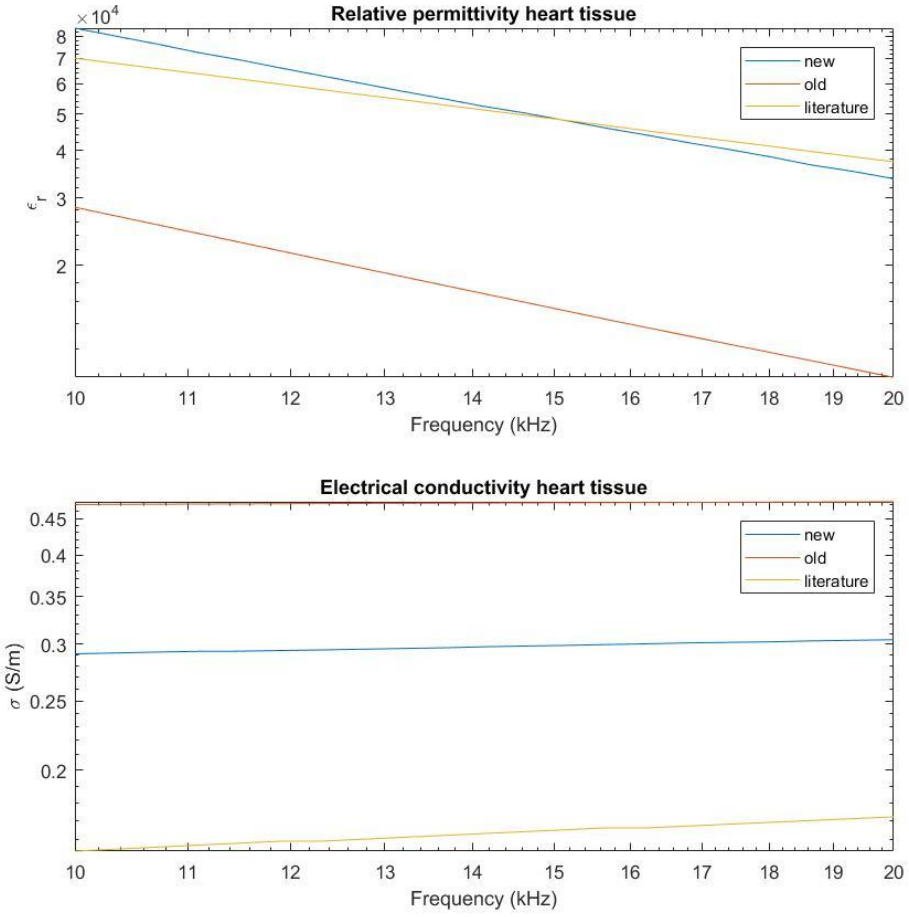


*Figure 42: Comparison between new measurements on porcine heart tissue and the old measurements of porcine heart tissue and the dielectric values of human heart tissue derived from the database IT'IS* [30]

## 8.2 Storage solution

The cardiac phantom tissue will be stored in a 0.15wt% saline solution (0.15wt% salt in tap water) and therefore mimicking the conductivity value of human blood. Because salt diffusion occurs, the cardiac phantom tissue should be prepared with the same solution as it will be stored in. Moreover, it will be examined whether sodium acetate diffusion will occur. Therefore, two PVA-based phantom materials will be produced with tap water. The two phantom materials will be made out of the same mixture, where sodium acetate will be added to one of the two mixtures. Impedance measurements will be performed on both sample phantoms when finished and will afterwards be stored in tap water. After a period of time, impedance measurements will be conducted on both of the phantom samples for comparison. As a second step, the storage solution will be measured with an EC-meter and with the impedance analyser for comparison. In Part II a saline solution of 0.15wt% salt in tap water was used as storage solution. The storage solution was measured with the EC-meter. For validation, multiple saline solutions are prepared and measured together with the previous defined storage solution, with the EC-meter and the impedance analyser using the new needle-electrode. The saline solutions are prepared by diluting 0.9% saline solution (Baxter Viapack NaCl 0,9% Fysiologisch Serum Voor Irrigatie 1000ml, New Pharma) with distilled water. Figure 43 shows the results.

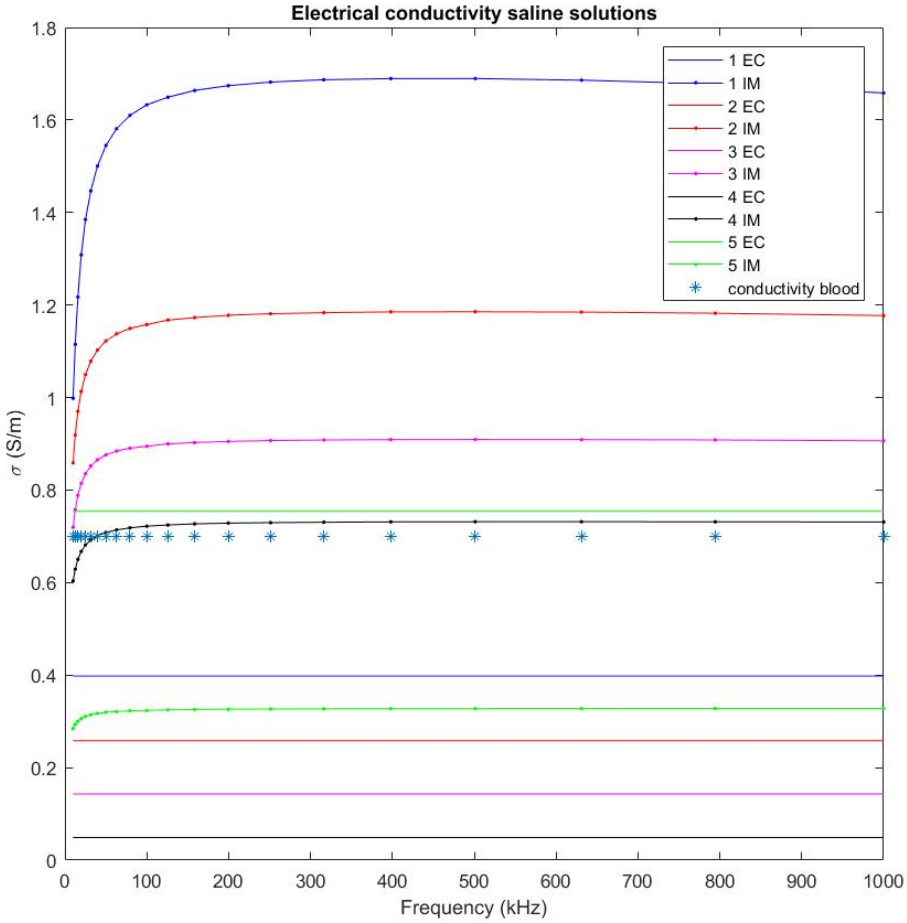


*Figure 43: Comparison between measurements performed with an EC-meter (EC) and measurements performed with the impedance analyser (IM). (1) 0.9% saline, (2) 0.6% saline, (3), 0.45% saline, (4) 0.36% saline, (5) storage solution of 0.15wt% salt in tap water and conductivity blood derived from database IT'IS* [30]

## 8.3 Homogeneity

As predefined, phantoms are said to be homogeneous when repeated measurements at various sides of the phantom shows 11% and 4% or lower variation for permittivity and conductivity respectively. The cardiac phantom samples will be measured 6 times, each at a side of the cubic shaped cardiac phantom sample.

## 8.4 Mechanical stiffness

The mechanical properties of human heart tissue are anisotropic, varies within the heart and is dependent on the timing of the cardiac cycle [49]. Because the mechanical properties varies, literature shows diverse values of the mechanical stiffness. Most literature report the myocardial Young's modulus of the left ventricle (LV). According to L.A. Reis et al. (2016) the Young's modulus of the human myocardium ranges from 20 kPa (end of diastole) to 500 kPa (end of systole) [111], which corresponds to the values of the myocardial ventricles reported in the study of L. Korn (2018) [49]. In the studies of A. Arani et al. (2017) [112] and Kolipaka et al. (2011) [113] lower values of the left ventricular myocardial Young's modulus are reported; 8.2 kPa and 5.64 ± 1 kPa in end-systole respectively. The Young's modulus of cardiac tissue and the myocardium is comparable [114]. The available data in literature that quantifies the passive mechanical properties of human heart tissue, and more

specifically of the LA, is very limited. F. Nemavhola (2017) [115] performed biaxial tensile tests on porcine tissue of the LV, mid-wall and right ventricle (RV) resulting in Young's moduli approximately between 30 – 45 kPa in the RV in the cross fibre direction and longitudinal direction respectively. For this graduation project it is of importance that the phantom tissue gives approximately the same haptic feedback as human heart tissue. But, in order to quantitatively examine the stiffness of the cardiac phantom, compression tests will be performed to examine the Young's modulus. Because the Young's modulus of the LA is lower than that of the LV [116], it is chosen that the Young's modulus of the phantom tissue should range between 10 kPa – 50 kPa.

In order to meet the mechanical requirement, the cardiac phantom samples will be tested with a compression test additional to the haptic examination. An uniaxial compression test will be performed using a linear stage (PRO-115, Aerotech, USA/UK) to exert force on the phantoms via a square object with a surface area of 1600 $mm^2$. For measuring the force, a 22N Force Sensor (LSB200, FUTEK, USA) will be mounted between the square surface and the linear stage. The Young's modulus (E) can be calculated by measuring the elastic, reversible deformation (strain) in the linear region (at low strain values, typically < 20%) of the stress-strain curve by dividing the uniaxial stress with the strain:

$$E = \frac{F/A}{\Delta L/L_0} \tag{17}$$

with F the force, A the phantoms surface, ΔL the change in height of the phantom and $L_0$ the initial height of the phantom [114]. The phantoms surface will be 33x33 mm and the initial height 33 mm. All tests will be carried out at room temperature. K. Verma et al. (2018) examined the compressive behaviour of human heart tissue [117]. Results showed that the Young's modulus is strain rate dependent. Therefore, four different strain rates will be tested; 0.003/s, 0.05/s, 0.063/s and 0.1/s. In order to match the strain rate, the compression speed of the linear stage will be set to 0.1 mm/s, 1.65 mm/s 2.08 mm/s and 3.3 mm/s. The raw data of the compression test will consist of the measured output voltage, the speed of the linear stage and the position of the linear stage. First, the force sensor has to be calibrated in order to convert the output voltage to a measured force. Thereafter, the measured force can be used to calculate the stress. The calculations will be done using MATLAB.

The measured Young's moduli of the four cardiac phantom samples will be compared to studies that measured the Young's moduli of PVA-C tissue, A.H.A. Wahab et al. (2019) [93], and of cardiac tissue, M.S. Sirry et al. (2016) [118]. While little literature is found about uniaxial compression tests on human heart tissue, the mechanical properties in the study of M.S. Sirry et al. (2016) are characterised for rat myocardium. K. Verma et al. (2018) [117] performed compression tests on human heart tissue, but used a very low strain rate (0.001/s). To match this strain rate with the cardiac phantom samples, a compression speed of 0.033 mm/s should be used. However, the lowest possible compression speed of the linear stage is 0.1 mm/s. Because the Young's modulus is strain rate dependent, it is chosen to mimic the study of M.S. Sirry et al. (2016) [118]. M.S. Sirry et al. (2016) used a preload to 1g, while this effect can be negligible, the compression tests performed in this project will not use a preload. All other conditions will be replicated. Although, M.S. Sirry et al. (2016) measured a higher Young's modulus (145 kPa) compared to the desired range for the cardiac phantom (10 kPa – 50 kPa) the compression test will be replicated for comparison of the cardiac phantom tissue. Furthermore, compression tests will be conducted on multiple variations of the cardiac phantom sample in order to examine the influence of varying the wt% PVA-powder and multiple freeze-thaw cycles on the stress-strain relationship.

## 8.5 Shelf life

As for the evaluation of the shelf life, the same haptic and visual inspection will be performed as described in Chapter 6.5.

## 8.6 Anatomy

Literature showed that the thickest part of the LA, at the anterior wall, is approximately 4-5 mm and the thinnest part, posterior or anterior aspect of the atrium, is approximately 3 mm [119]. Because the phantom material is flexible and should not collapse when the cardiac phantom contains the hollow shapes, it will be chosen to make the wall of the cardiac phantom 5 mm. Two simplified versions for the LA will be made: a cylinder and a sphere. Both shapes will contain 4 hollow tubes, representing the pulmonary veins.

For the mould preparation, the desired shape should be made in duplicate with an overall increase in size of 5 mm normal to the surface, which can be done using the 3D modelling software Rhino. The smaller shape will be named 'inner core' and the increased shape will be named 'outer core'. The inner core represents the hollow shape. The outer core will be used to make a negative image in a solid structure, the outer mould. The inner core should fit perfectly with a range of 5 mm in the outer mould. Both, the inner core and the outer mould can be 3D printed ensuring a reproducible mould. The inner core should be printed with dissolvable PVA, using the Ultimaker3. The outer mould can be printed with polylactic acid (PLA), using the Ultimaker2 or Ultimaker3 when PVA support material is needed. Make sure a filling hole is present and a few smaller holes for releasing air inside the closed mould.

When both moulds are printed, the inside of the outer mould can be coated with Smooth-On XTC-3D [120] to make the mould watertight. Thereafter, the inner core should be placed within the outer mould and the cardiac phantom material can be poured into the mould. Make sure no air bubbles are trapped inside the mould. The filled mould can be placed inside the freezer for the freeze-thaw cycle to solidify the phantom material. When the freeze-thaw cycle is completed, the inner core should be dissolved in the storage solution of the cardiac phantom material ensuring no salt diffusion. Appendix F will explain all points of attention during the mould preparation. While the hollow cylinder shaped cardiac phantom should not collapse, the wt% of PVA powder can be altered to manipulate its stiffness and multiple freeze-thaw cycles can be used. However, this will affect the dielectric properties of the cardiac phantom tissue and therefore impedance measurements should be performed also on these variations of the cardiac phantom.

## 8.7 Additional requirements

The additional requirements contain the anatomy of the phantom explained in the previous subchapter, the costs for fabrication of the cardiac phantom, the ease of manufacturing, the reproducibility of the phantom production and the stability of the dielectric properties over time. Because the cardiac phantom fabricated in this project serves as a proof of concept, no real cost analysis will be done. The costs will be calculated and will be given in a range. The ease of manufacturing contains the phantom material fabrication process, the mould making and mould filling process. As for the reproducibility, four phantom samples will be prepared and the impedance measurements will be compared to each other. If the maximum percentage variation between the mean of the measured values over all frequency points of all four phantom samples does not exceed the previous defined repeatability values of 11% and 4% for permittivity and conductivity respectively, than the cardiac phantom tissue is said to be reproducible. As for the stability, in Chapter 7.2 it was

mentioned that PVA-C phantoms absorb water what might influence the dielectric properties [64]. Therefore, to examine what the influence on the dielectric properties is of the water absorption, a 9.1wt% PVA phantom was prepared with 0.9% saline and stored in 0.9% saline. Figure 44 shows the results of repeated impedance measurements with 1 day and 1 week in between. Here, the maximum percentage variation between the measured values and the mean of the measured values over all frequency points is 22% and 9% for permittivity and conductivity respectively.

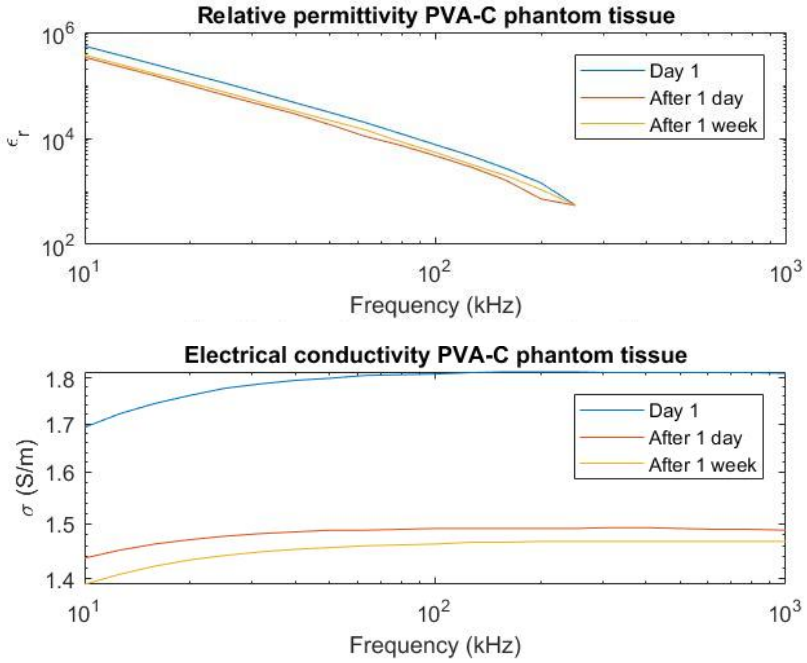


*Figure 44: PVA-C phantom tissue prepared with 9.1wt% PVA powder prepared with 0.9% saline solution, stored in 0.9% saline solution*

In this chapter, impedance measurements will be performed over a period of time in order to see whether the PVA-C phantoms will become stable at a time after storage. Here a cardiac phantom sample will be compared to a phantom sample containing no additives. All actions will be performed simultaneously in order to obtain equal conditions.

## 8.8 Discussion

This subchapter will discuss all measurements performed in this chapter.

### Dielectric measurements

As for the comparison between the 4-point needle and the 2-point needle electrode, it is expected that the capacitance would decrease using the 4-needle electrode because less electrode polarisation should occur and the results agree. However, it is not expected that the conductance would increase. [28][94][16] Because the 4-neelde electrode is made with precision, it was decided to use the 4-needle electrode for all further measurements. Since the 4-needle electrode is not working as expected, a 2-point measurement will be performed using the 4-needle electrode. So, only wire 2 and 3 will be used and therefore the 4-needle electrode will function as a 2-needle electrode configuration. Figure 45 shows comparisons of all 3 methods used: in blue the 'old' 2-needle electrode method, in red the 'new' 4-needle electrode method using all 4 needles and in yellow the 'new' 4-needle electrode using only 2

needles. The figure shows the results of the 3 methods used on the second phantom, showing the same results.

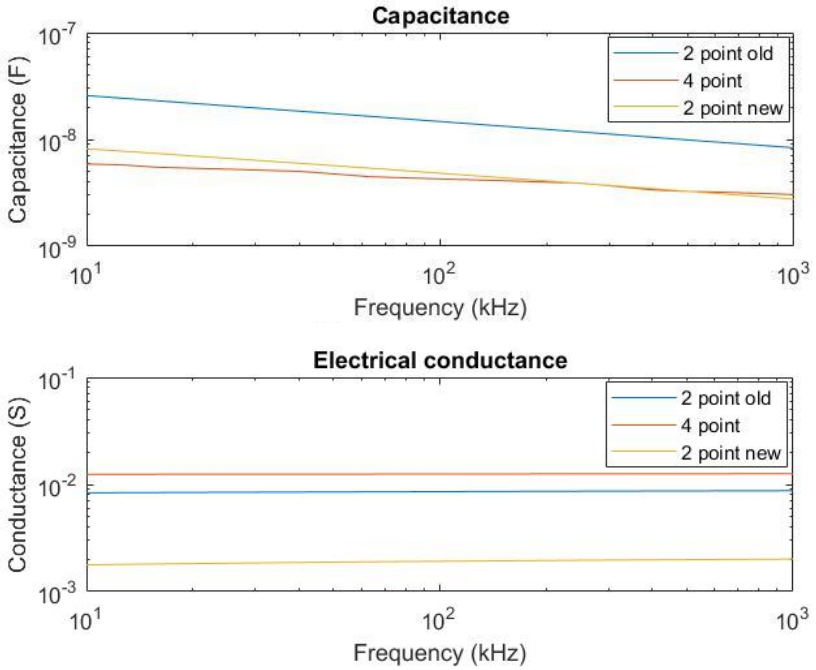


*Figure 45: Comparison between the 'old' 2-needle electrode (2 point old), the 4-needle electrode (4 point) and the 4-needle electrode functioning as a 2-needle electrode (2 point new)*

## Storage solution

Figure 43 shows the results of the comparison between the measurements conducted with the EC-meter and the impedance analyser. Here, it can be seen that the measurements of the EC-meter does not match the measurements performed with the impedance analyser. Moreover, results show that a 0.36% saline solution comes close to the conductivity values of human blood.

## Stability

Water absorption occurs in PVA-C phantoms, what might affect the dielectric properties [64]. This is demonstrated in the measurements of the PVA-C phantom, Figure 44. Because the amount of salt in the phantom tissue is equal to the amount of salt in the storage solution, no salt diffusion can take place. But, as results show, a decrease in permittivity and conductivity is seen which proves the absorption of water changes the dielectric properties. This decrease of dielectric values should be considered for all dielectric measurements.

## 8.9 Conclusion

Table 11 gives an overview of all requirements for the final cardiac phantom with the definition and accepted ranges for the evaluation methods.

*Table 11: Evaluation methods for final cardiac phantom tissue*

| Requirement phantom | Definition | Accepted ranges |
|---|---|---|
| Dielectric properties | Phantom mimics measured dielectric properties of porcine heart tissue | ± 11% for permittivity and ± 10% and conductivity |
| Storage solution | All phantoms are stored in a solution of 0.15 wt% salt in tap water, which mimics the conductivity value of blood | - |
| Homogeneity | Phantom is homogeneous | Variation of repeated measurements at various sides of the phantom should be ≤11% for permittivity and ≤4% for conductivity |
| Mechanical stiffness | Phantom gives the same haptic feedback as human heart tissue | The Young's modulus of the phantom tissue should range between 10 kPa – 50 kPa |
| Shelf life | Length of time of the phantom without becoming unusable | ≥ 1 month |
| Anatomy | The phantom has the same anatomy as the LA | The phantom can be produced in the desired shape: cylinder and sphere. With an overall wall thickness of 5mm |
| Inexpensive to produce | Low costly materials for the phantom preparation | - |
| Ease of manufacturing | Easy mixing procedure for the phantom material fabrication, easy mould preparation and easy mould filling process | - |
| Reproducible | Repeated cardiac phantom production should give same results | Maximum variation of the measured dielectric values of the mean of all reproduced cardiac phantoms should be ≤11% for permittivity and ≤4% for conductivity |
| Stable over time | The cardiac phantom retains its dielectric properties over time | ≥ 1 month |

# 9. Results final LA phantom

In this chapter, the most promising 'sample phantom' will be extensively examined based on all predefined requirements. First, the methods for the cardiac phantom tissue preparation will be explained. The final LA phantom tissue will be prepared four more times, the cardiac phantom samples, and will be evaluated based on the requirements as described in the previous chapter. All results will be reviewed per main requirements separately, the additional requirements will be reviewed together in one subchapter. Except for the additional requirements regarding the anatomy of the phantom, this chapter will be explained separately.

## 9.1 Cardiac phantom production

For the preparation of the cardiac phantom material, first pre weigh all ingredients as seen in Table 15. Fill the beaker with the saline solution (storage solution) at room temperature. Add sodium acetate while magnetically stirring until mixture is completely mixed. Gradually add PVA powder to the mixture with continued stirring and stir for 5 minutes more. Cover the beaker with aluminium foil to minimize water evaporation. Evaporated water can be supplemented with distilled water. Heat up the mixture until 96°C and mix for 60 minutes. Turn off the stove and allow the mixture to cool down till room temperature with continued stirring. When the mixture is cooled down, pour the mixture into the mould and start the freeze-thaw cycle. Put the mould filled with the phantom mixture for 24 hours in the freezer. After 24 hours, thaw the mixture for 24 hours at room temperature. Remove the mould carefully from the phantom tissue and store in the storage solution which is the same saline solution used for the phantom preparation. Allow the 3D-printed inner core to dissolve.

*Table 12: Ingredients for the cardiac phantom tissue*

| Ingredients | Weight (g) | Wt% |
|---|---|---|
| Saline solution | 100 | - |
| PVA powder | 15 | 13,0 |
| Sodium acetate | 0,05 | 0,05 |

## 9.2 Dielectric properties

Figure 46 shows the results of the four cardiac phantom samples and the target values. Table 13 shows the average percentage variation between the cardiac phantom samples and the target values.

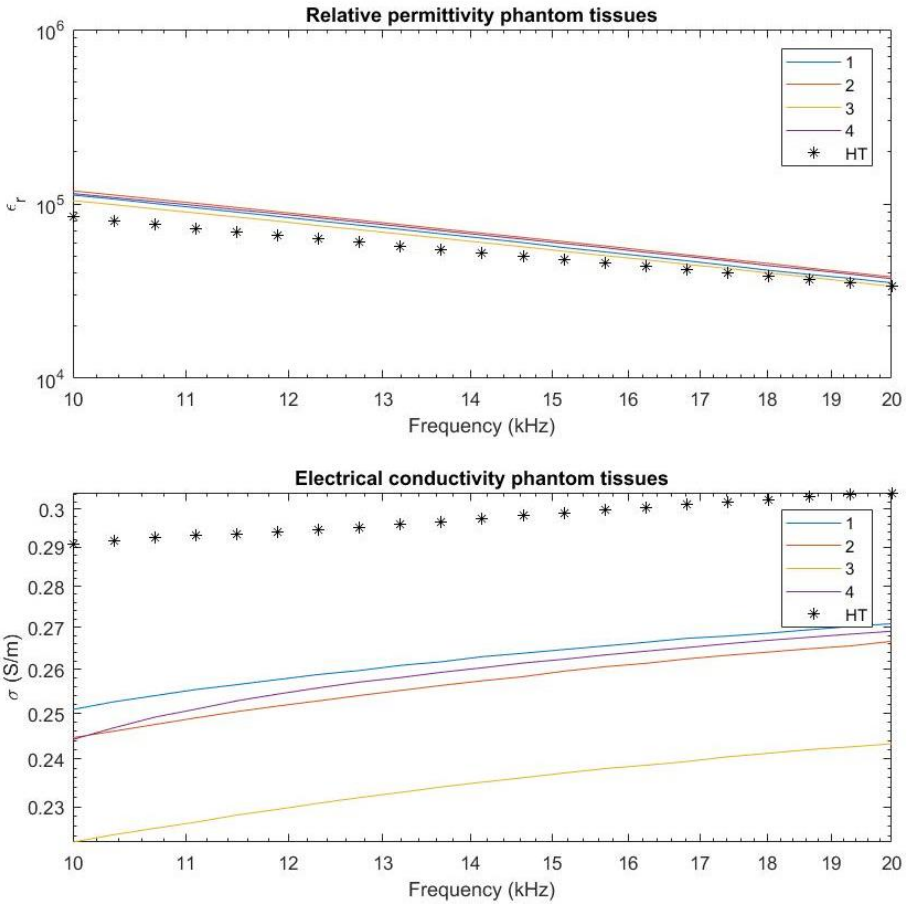


*Figure 46: Results of the dielectric measurements of the four cardiac phantom samples (1 – 4) compared to the target values (HT)*

*Table 13: Average percentage difference between hear phantom samples and the target values*

| Cardiac phantom sample | Average difference between cardiac phantom and HT (%) | |
|---|---|---|
| | Permittivity | Conductivity |
| **1** | 20.0 | 11.9 |
| **2** | 28.7 | 13.7 |
| **3** | 13.6 | 21.3 |
| **4** | 25.4 | 12.9 |
| **Mean** | 21.9 | 15.0 |

As for the anatomy of the cardiac phantom, which will be described in Chapter 9.7, phantoms were prepared with an increase in wt% PVA-powder and underwent an extra freeze-thaw cycle. This can affect the dielectric properties and is therefore examined. Figure 47 shows the results of the cardiac phantom sample (HP0), the cardiac phantom sample composed of 16.7wt% PVA-powder (HP1), the

cardiac phantom sample composed of 16.7wt% PVA-powder which underwent an extra freeze-thaw cycle (HP2) and the target values (HT).

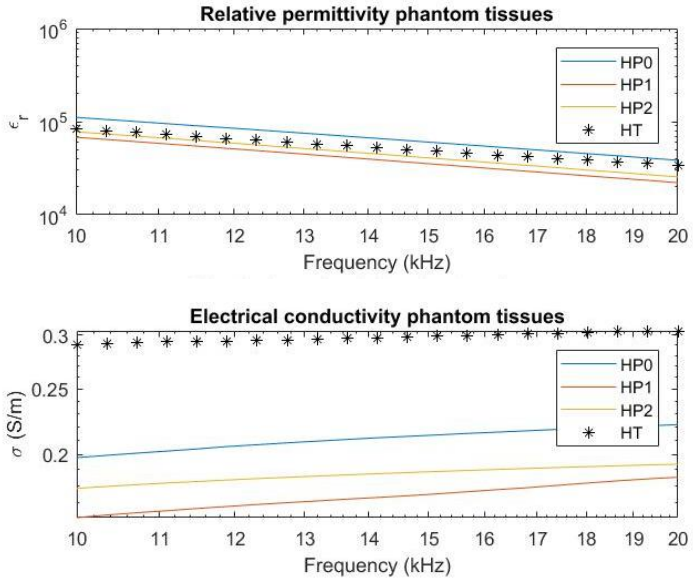


*Figure 47: Comparison between cardiac phantom sample (HP0), cardiac phantom sample made with 16.7wt% PVA-powder and 1 freeze-thaw cycle (HP1), cardiac phantom sample made with 16.7wt% PVA-powder and 2 freeze-thaw cycles (HP2) and the target values (HT)*

## 9.3 Storage

As already concluded in Chapter 7.2, the predefined storage conditions gives good results. PVA-C phantoms absorb in two weeks' time on average 48% water what influences the dielectric properties. Moreover, salt diffusion occurs and therefore the cardiac phantom should be stored in the same solution as its prepared with. As a final check, it is examined whether the sodium acetate will diffuse out of the cardiac phantom. Figure 48 shows the results of the phantom with added sodium acetate (P) and the phantom without additives (N). Measurements where conducted before storage (0), after 1 week of storage in tap water (1), after 2 weeks storage (2) and after 3 weeks storage (3).

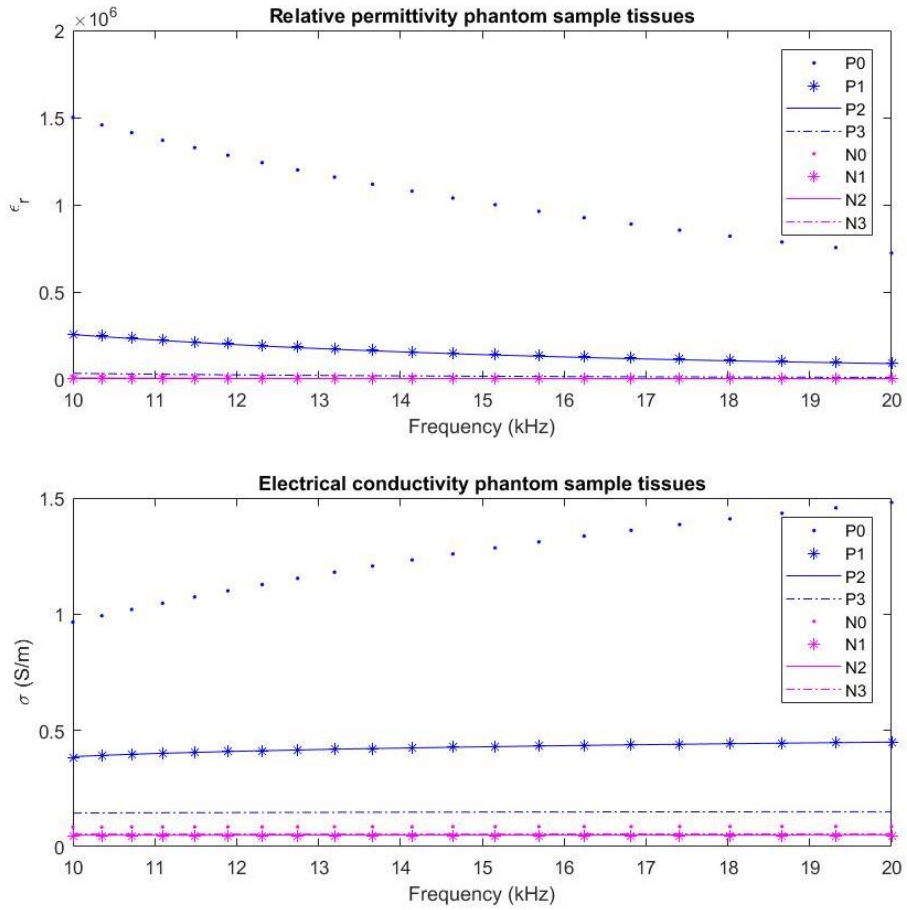


*Figure 48: Sodium acetate diffusion. Phantom P prepared with sodium acetate and tap water, phantom N without additives. Measurements taken before storage in tap water (0), after 1 week storage (1), after 2 weeks storage (2), after 3 weeks storage (3)*

Chapter 8.2 reported a 0.36% saline solution results in a solution with conductivity values more closer to the conductivity values of blood as reported in the database IT'IS [30] than the storage solution used for the cardiac phantom preparation. Therefore, a cardiac phantom sample is prepared with a 0.36% saline solution instead of the storage solution as reported. Results are shown in Figure 49.

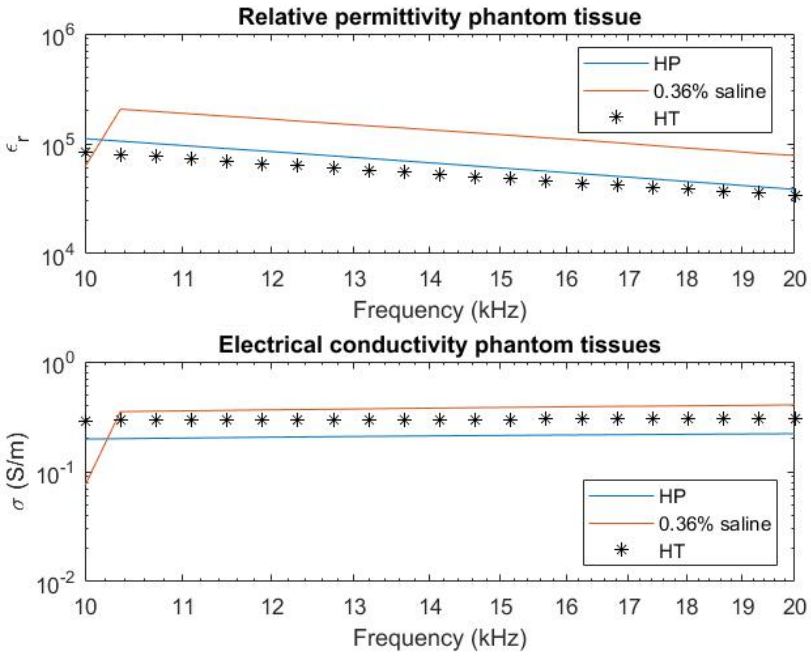


*Figure 49: Comparison cardiac phantom sample (HP) with cardiac phantom tissue prepared with 0.36% saline and the target values (HT)*

## 9.4 Homogeneity

As for the homogeneity tests, all four cardiac phantom samples were measured six times each at a different side. Results are shown in Table 14. Appendix G shows all results of the impedance measurements performed on cardiac phantom sample 1 – 4.

*Table 14: Results homogeneity tests of the cardiac phantom samples*

| **Cardiac phantom sample** | **Average difference between measured value and the mean, (Maximum difference) (%)** | |
|---|---|---|
| | **Permittivity** | **Conductivity** |
| **1** | 5.7 (7.4) | 2.9 (3.1) |
| **2** | 6.0 (6.3) | 2.4 (2.8) |
| **3** | 18.8 (19.0) | 18.2 (19.1) |
| **4** | 4.8 (6.9) | 2.3 (4.4) |
| **Mean** | 8.8 (9.9) | 6.5 (7.4) |

## 9.5 Mechanical stiffness

Figure 50 shows the setup for the compression tests. First, the noise is measured and the force sensor is calibrated for all four strain rates. Thereafter, the force is used for the calculation of the stress in MATLAB. Here, the data is filtered by a moving average to create a clear line. All compression tests are performed at room temperature. Figure 51 shows the results from the compression tests of one of the four phantoms. It can be seen that for the higher strains, the stress differs per strain rate used. For the smaller strains, the measured stresses are comparable. The average of all four measurements per strain rate is shown in Figure 52. Measured stresses are comparable at low strains, therefore, the Young's modulus should be calculated at low strains (< 15%).

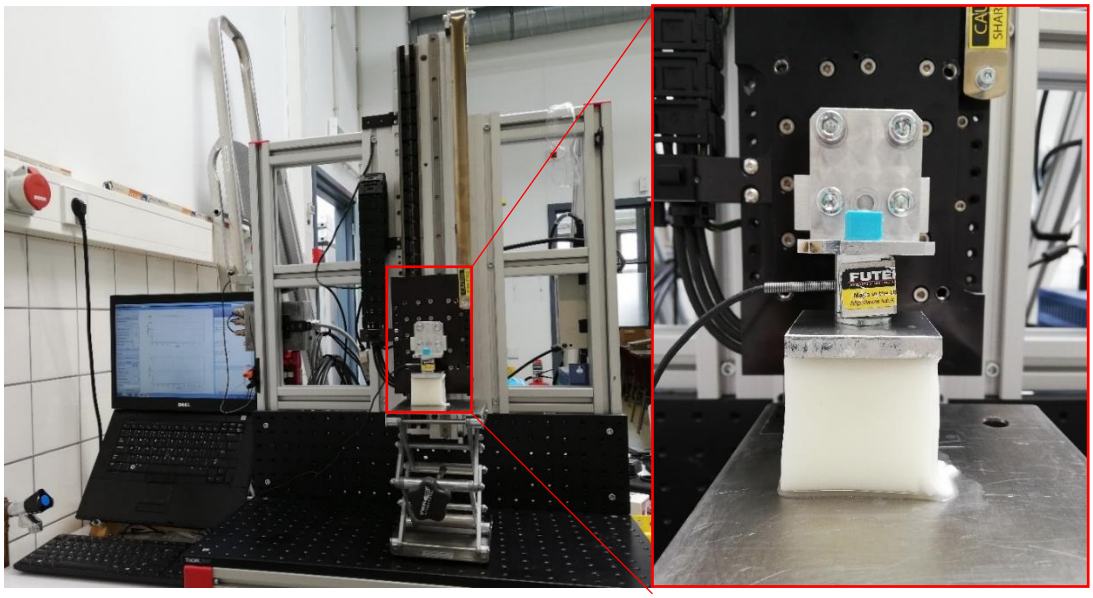

*Figure 50: Setup of compression tests*

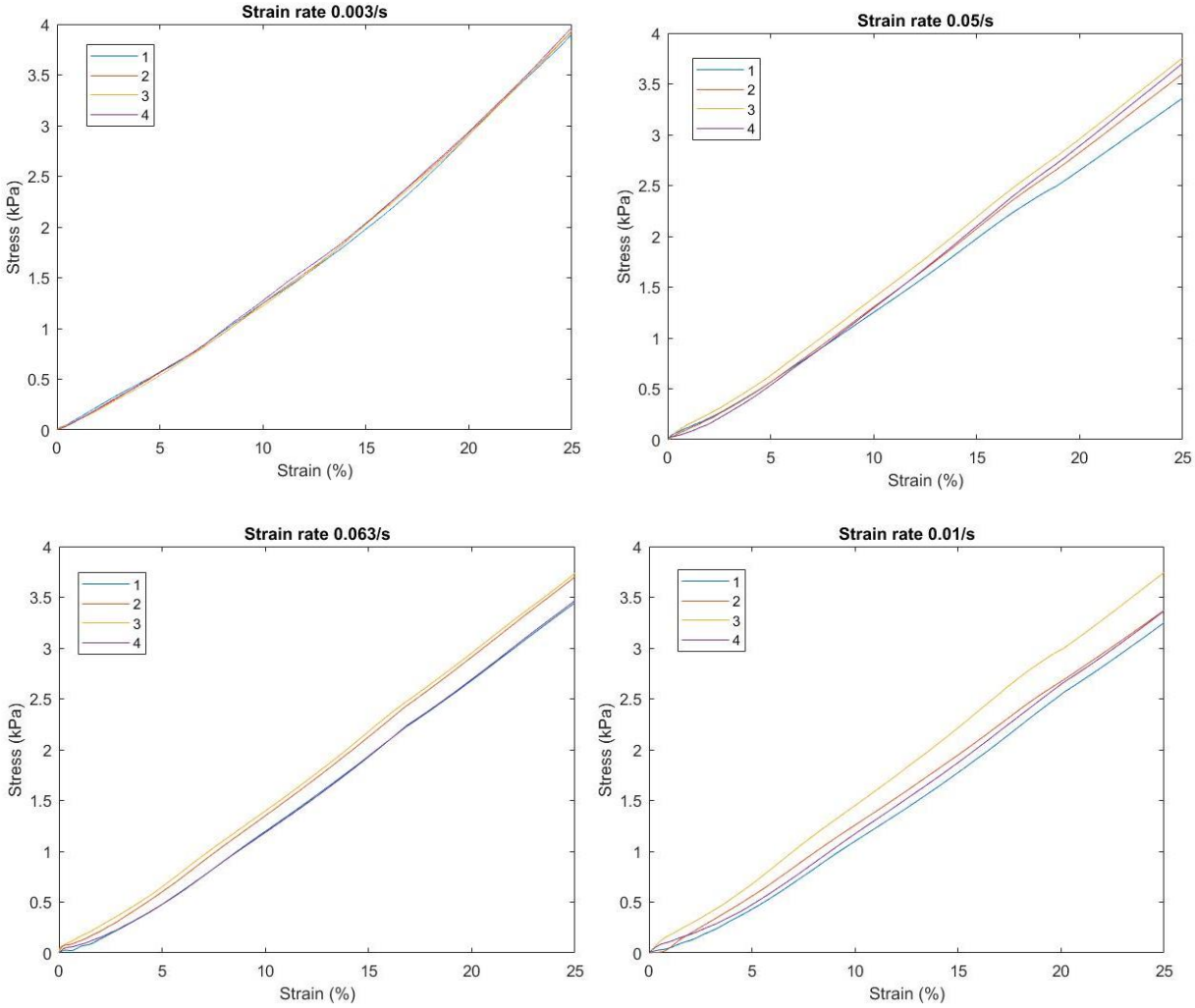


*Figure 51: Stress strain curves of one phantom with different strain rates*

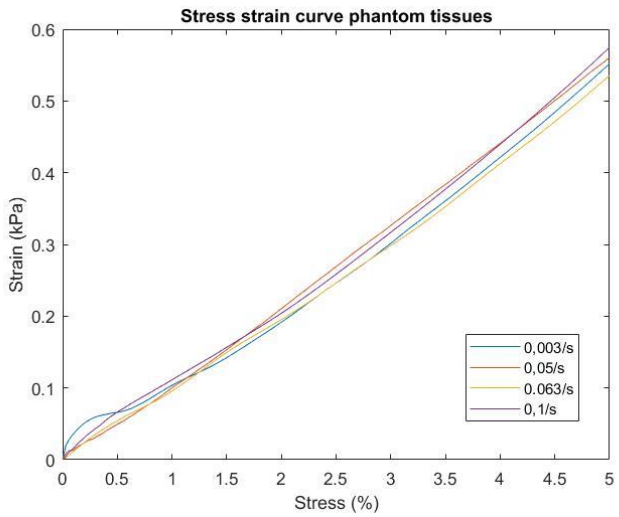


*Figure 52: Mean stress-strain responses of one phantom at four different strain rates*

The Young's modulus (E) of all four cardiac phantom samples at all four strain rates are calculated at 15% strain using MATLAB. Results are shown in Table 15, see 'Appendix B' 'B8 Boxplots of calculated Young's moduli of the cardiac phantom samples' for boxplots made. The Young's modulus of the cardiac phantom sample at strain rate 0.003/s at 25% strain is calculated to be 17.0 ± 1.5 kPa which is not near the values found in the study of M.S. Sirry et al. (2016) [118] where a Young's modulus of 145 kPa was measured.

*Table 15: Young's moduli of the cardiac phantom samples*

| Sample tissue | E (kPa) ± SD |
|---|---|
| Cardiac phantom sample at 0.003/s | 13.5 ± 1.3 |
| Cardiac phantom sample at 0.05/s | 14.0 ± 1.4 |
| Cardiac phantom sample at 0.063/s | 12.9 ± 1.5 |
| Cardiac phantom sample at 0.1/s | 12.3 ± 1.5 |
| **Mean** | **13.2 ± 1.4** |

Multiple phantom samples underwent the compression tests to examine the influence of varying the wt% PVA-powder and multiple freeze-thaw cycles on the stress-strain relationship. The left figure of Figure 53 shows the results of the compression tests performed on two phantoms with varying wt% PVA-powder. It is clearly seen that the stress strain curve of Phantom 2 containing more wt% PVA-powder gives a steeper curve than of Phantom 1, resulting in a higher Young's modulus. Furthermore, compression tests were performed after the phantom underwent 1 freeze-thaw cycle and after the phantom underwent 2 freeze-thaw cycles. Results are shown in Figure 53 on the right, where it can be seen that the phantom which underwent 2 freeze-thaw cycles has a higher Young's modulus than the phantom which underwent 1 freeze-thaw cycle.

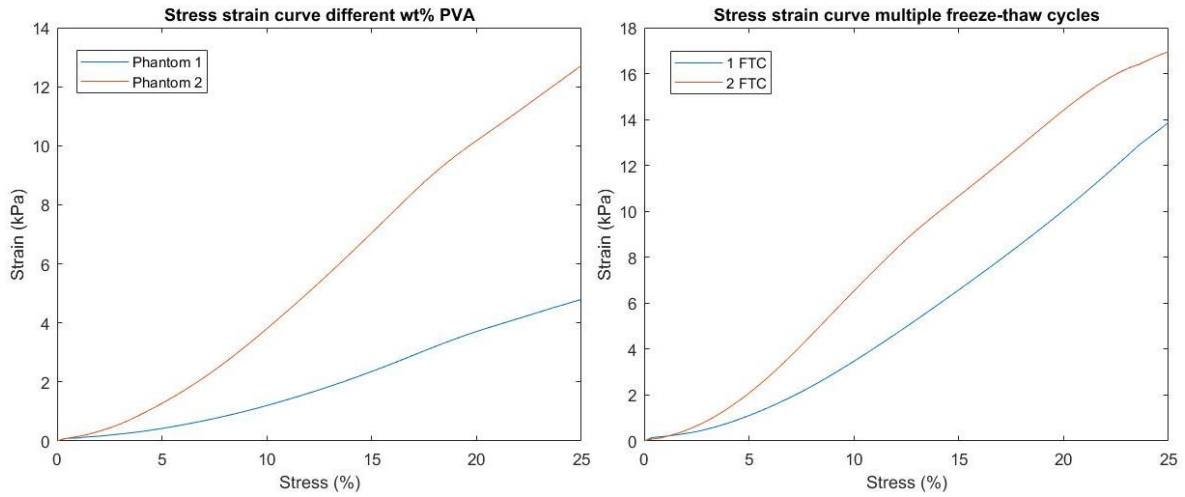


*Figure 53: Stress strain curve of two PVA-C phantom tissues. Left: different wt% PVA, with Phantom 1: 13.0wt% PVA, Phantom 2: 16.7wt% PVA. Right: different freeze-thaw cycles, with 1 freeze-thaw cycle (1 FTC) and two freeze-thaw cycles (2FTC)*

All resulted Young's moduli are shown in Table 16 together with values derived from the study of A.H.A. Wahab et al. (2019) [93]. Here it can be seen that the Young's modulus of the cardiac phantom sample composed of 0.36% saline is comparable to the Young's modulus found for a 10wt% PVA phantom tissue with 1 freeze-thaw cycle as reported in the study of A.H.A. Wahab et al. (2019) [93]. Furthermore, the Young's modulus of the cardiac phantom sample composed of 16.7wt% PVA and which underwent 2 freeze-thaw cycles is comparable to that of the 15wt% PVA phantom which underwent 1 freeze-thaw cycle as reported in the study of A.H.A. Wahab et al. (2019) [93].

*Table 16: Young's moduli of performed compression tests and derived from literature*

| Tissue | Additional | E (kPa) |
|---|---|---|
| Cardiac phantom sample | Mean four cardiac phantom sample at different strain rates | 13.2 ± 1.4 |
| Cardiac phantom sample | Fifth phantom sample at strain rate 0.063/s | 15.7 ± 2.0 |
| Cardiac phantom sample | Composed of 0.36% saline | 21.0 ± 1.8 |
| Cardiac phantom sample | Composed of 16.7wt% PVA (1 freeze-thaw cycle) | 43.9 ± 5.3 |
| Cardiac phantom sample | Composed of 16.7wt% PVA (2 freeze-thaw cycles) | 71.1 ± 6.1 |
| 10wt% PVA phantom (1 freeze-thaw cycle) | Derived from the study of A.H.A. Wahab et al. (2019) [93] | 25 ± 4 |
| 15wt% PVA phantom (1 freeze-thaw cycle) | Derived from the study of A.H.A. Wahab et al. (2019) [93] | 91 ± 42 |

## 9.6 Shelf life

As already seen in Chapter 7.2, the shelf life of the cardiac phantom tissues resulted to be at least one month, which complies with the requirement.

## 9.7 Anatomy

Figure 54 shows the 3D printed cylinder mould, with the outer mould of grey PLA and the inner mould composed of white dissolvable PVA. Four pins, shaped in truncated cones, were printed to secure the outer moulds to each other. Diameters of the pins used are shown in Appendix F. The PVA inner core is secured at the top and bottom of the cylinder to the outer mould to secure the inner core exactly in the middle of the outer mould. Therefore, an overall wall thickness of 5mm can be ensured. At the top and bottom four holes were created in the 3D printed design for air bubbles to escape and to fill the mould with the cardiac phantom material. The cylinder shaped phantom resulted in good appearance, Figure 55. On the down side, air bubbles were still trapped in the mould resulting in air bubbles in the final phantom. The sphere shaped phantom did not succeed and more care in the mould preparation should be taken.

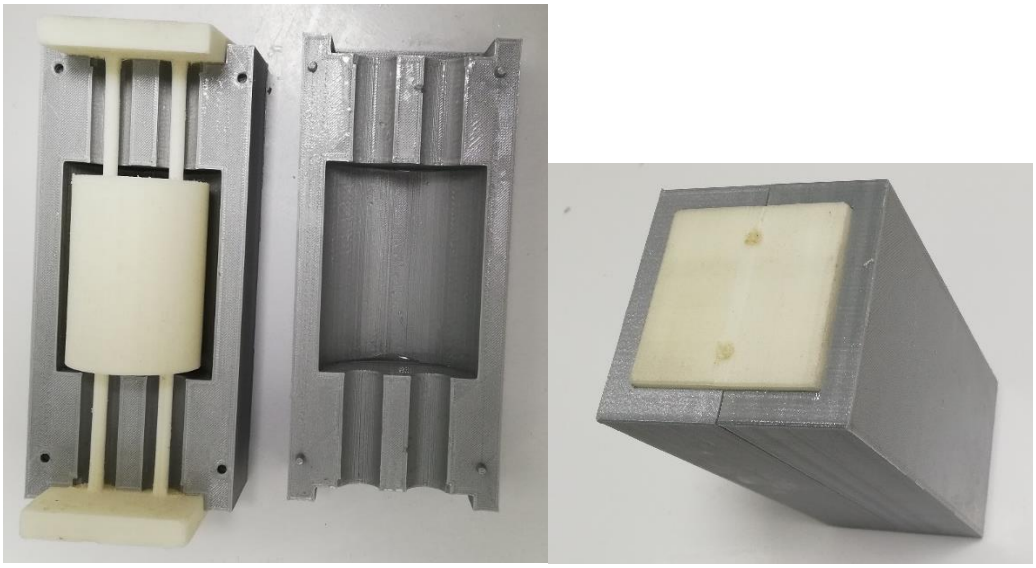

*Figure 54: 3D printed cylinder mould*

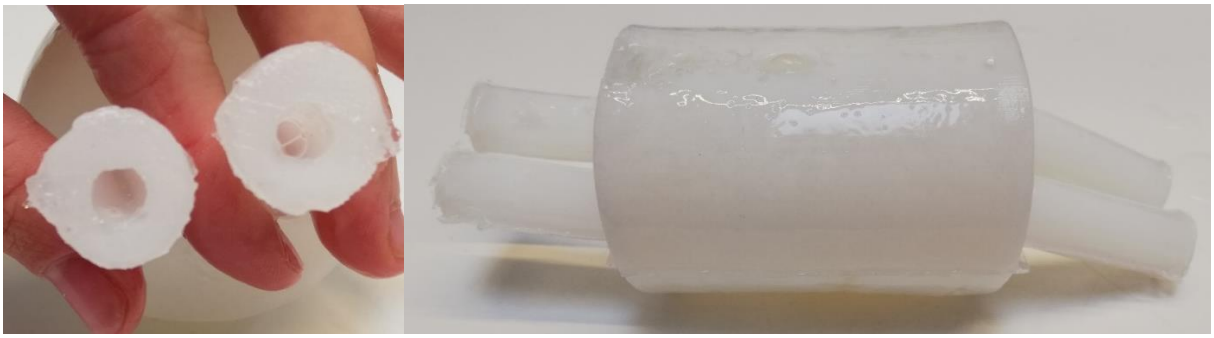

*Figure 55: Cylinder shaped phantom*

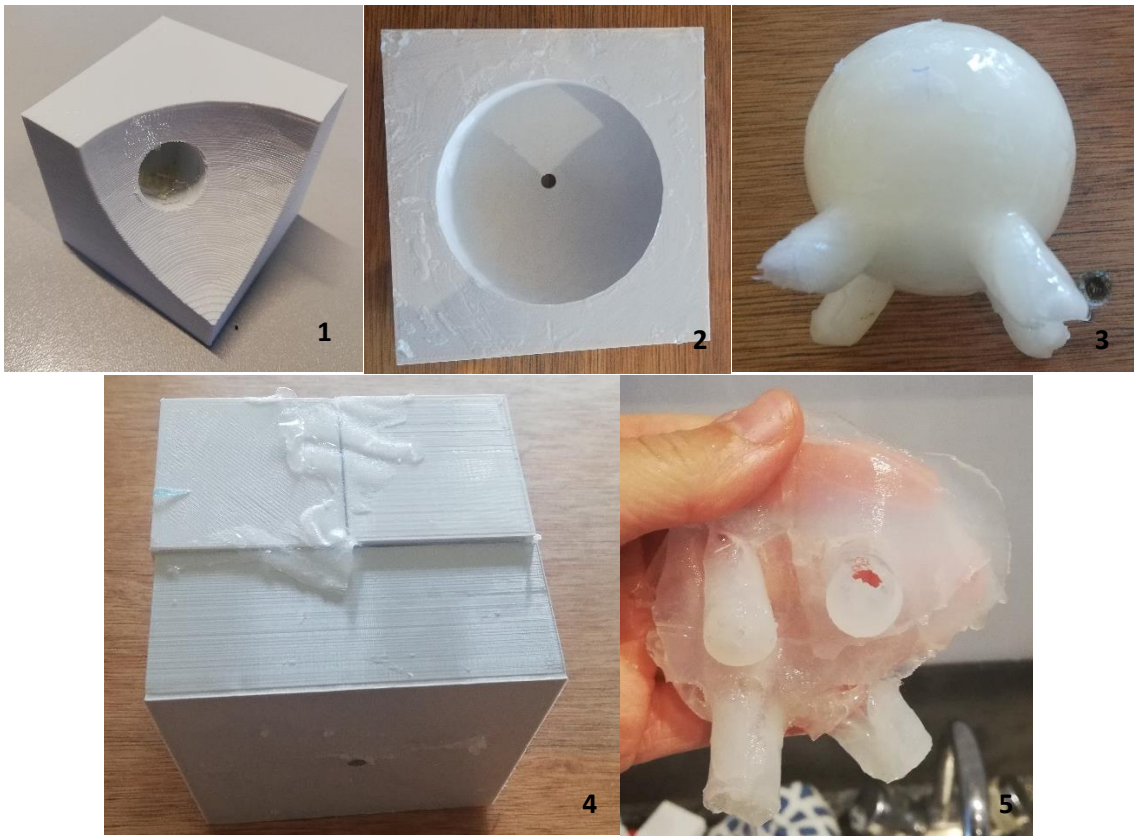


*Figure 56: 3D printed sphere shaped mould. (1) One of the four smaller outer moulds to slide over one of the four cylinders of the inner mould. (2) The big outer mould. (3) The PVA-printed inner core. (4) The resulted 3D printed mould. (5) The failed sphere shaped cardiac phantom*

## 9.8 Additional requirements

No real cost analysis is done for the cardiac phantom. However, the only more expensive materials are PVA-powder, PVA-filament and PLA-filament for the 3D printer. The costs for the cardiac phantom materials used and for the mould preparation ranges between 50 - 80 euro. Moreover, the cardiac phantom material is easily made. The mould preparation for the cardiac phantom material with correct anatomy is challenging. But, once the correct mould is prepared the mould can be printed repeatably. As for the reproducibility, Figure 46 already showed the dielectric values of all four phantoms made. Table 17 shows the results of the reproducibility tests. Figure 57 shows the results for the stability tests where the cardiac phantom sample is compared to a PVA-C phantom sample without additives with same PVA-powder/tap water ratio. Both phantoms were simultaneously made, measured and stored.

*Table 17: Reproducibility results of cardiac phantom samples*

| **Cardiac phantom sample** | **Average difference between mean value of cardiac phantom sample and the mean of all cardiac phantom samples (Maximum difference) (%)** | |
|---|---|---|
| | **Permittivity** | **Conductivity** |
| **1** | 1.6 (3.0) | 3.6 (4.2) |
| **2** | 5.6 (6.2) | 1.4 (1.7) |
| **3** | 6.9 (7.2) | 7.4 (7.6) |
| **4** | 2.9 (3.5) | 2.4 (2.6) |

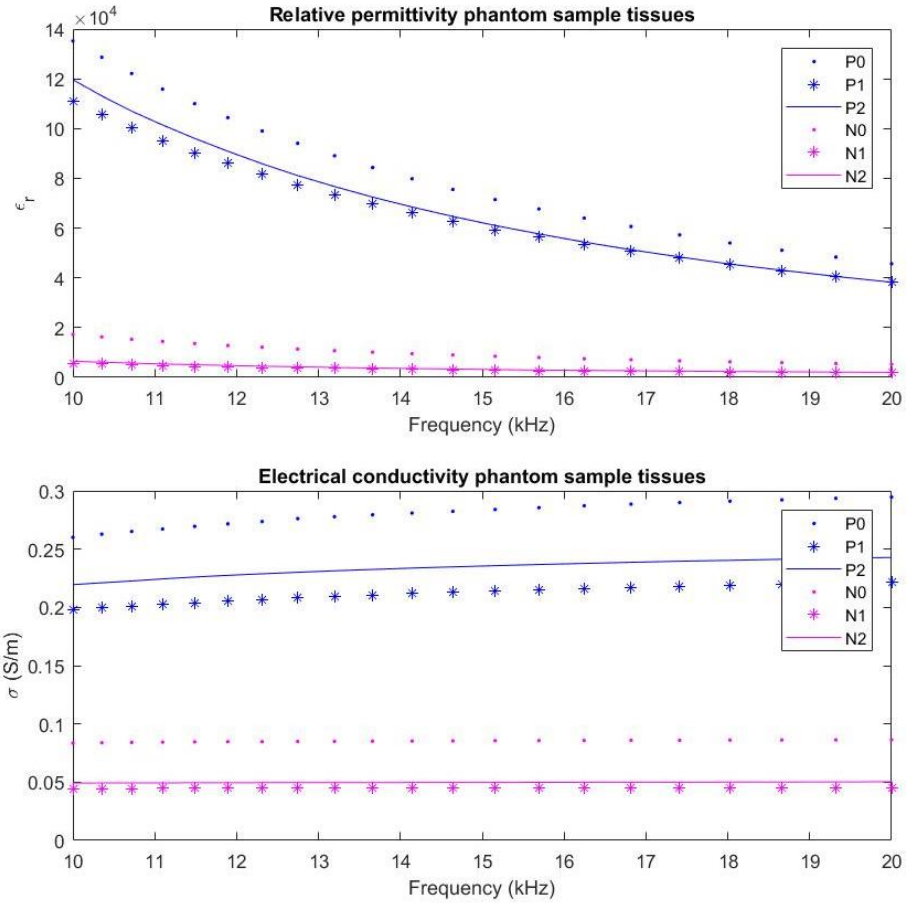


*Figure 57: Stability tests. Phantom P as the cardiac phantom sample, phantom N without additives. Measurements taken before storage in tap water (0), after 1 week storage (1), after 2 weeks storage (2)*

## 9.9 Discussion and conclusion

### 9.9.1 Dielectric properties

It can be concluded that the accepted tolerance range of ±11% and ±10% for permittivity and conductivity is not achieved. The dielectric values of the cardiac phantom sample come close but should come closer. Moreover, a decrease in permittivity and conductivity is shown with an increase in wt% PVA-powder. Increasing its freeze-thaw cycles does not seem to affect the dielectric properties significantly.

### 9.9.2 Storage

#### Sodium acetate

It can be concluded that sodium acetate diffusion occurs when stored in the storage solution. The phantom sample with added sodium acetate was stored in tap water. Results as seen in Figure 48 show the phantoms become stable after 1 week storage, whereas the measurements of P1 and P2 are equal and the measurements of N1 and N2. After measurements of P2 and N2 were conducted, the storage liquid (tap water) got refreshed expecting no change of dielectric values would occur between measurement P2 and P3. However, results show the opposite. It can be seen that the dielectric values of P3 come near the values of N3, suggesting sodium acetate diffusion took place. This signifies, all dielectric measurements performed on the cardiac phantom samples after stability is reached are of the cardiac phantom composition without sodium acetate. So therefore, the measurements

performed after 1 week of storage are of phantoms composed of 13.0wt% PVA, 0.15wt% salt and tap water.

### Storage solution

A phantom sample produced with 0.36% sterile saline was compared to the cardiac phantom sample prepared as described in Chapter 9.1. Results show the conductivity values of the 0.36% saline cardiac phantom sample better mimic the conductivity values of the target values (HT). As for the permittivity values, the cardiac phantom sample (HP) better mimics the permittivity values of the target values.

## 9.9.3 Homogeneity

All cardiac phantom samples prepared are within the predefined range for homogeneity, except for phantom number 3. Figure 58 shows the results of the six impedance measurements performed on cardiac phantom sample 3. It can be seen that the 6$^{th}$ measurement deviates from the rest of the measurements. As described, al cardiac phantom samples were measured six times. The 6$^{th}$ measurement of all cardiac phantom samples was measured at the top of the phantom sample. For some cardiac phantom samples, a layer arose on top of the liquid form of cardiac phantom sample (before the freeze-thaw cycle). This layer eventually resulted in a much stiffer layer on top of the phantom sample compared to the rest of the sample. This layer should be avoided when the phantom undergoes the freeze-thaw cycle. It was decided to not remove this layer by cutting, while this could influence impedance measurements and compression tests results. Moreover, this deviation of the 6$^{th}$ measurement is also seen in the fourth cardiac phantom sample, seen in Appendix G.

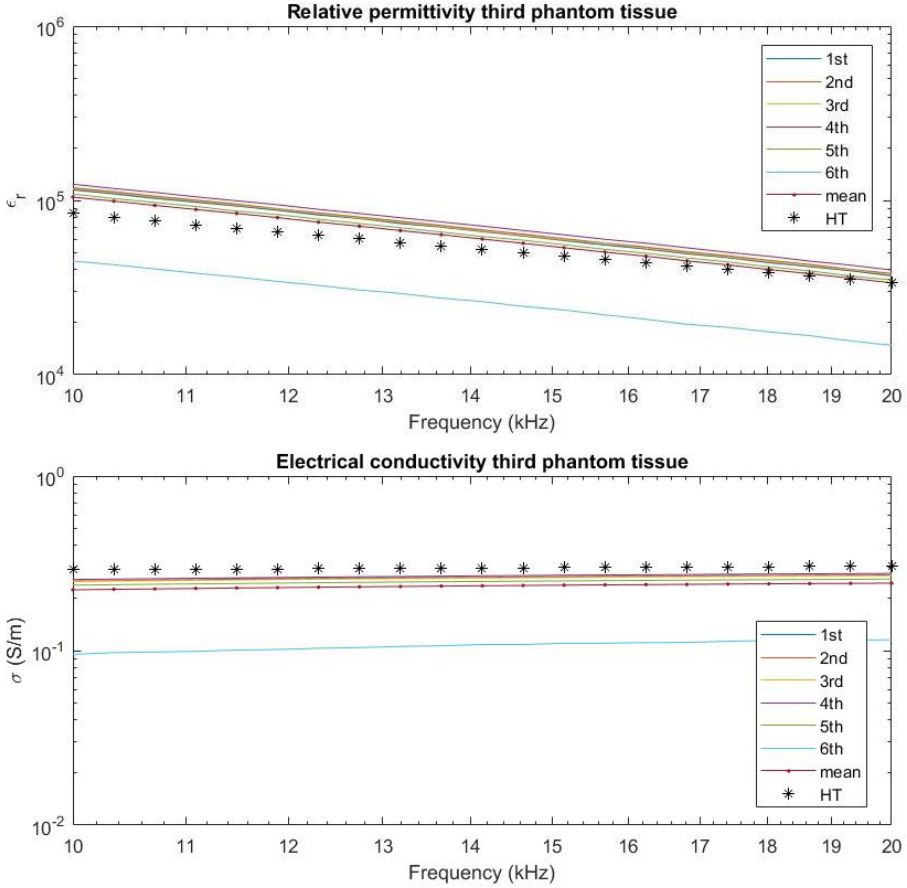


*Figure 58: Results of impedance measurements of cardiac phantom sample 3, with 1$^{st}$ – 6$^{th}$ all 6 measurements performed each at a different side of the phantom, the mean and the target values (HT)*

### 9.9.4 Mechanical stiffness

Very few uniaxial compression tests are performed on cardiac tissues. Mostly biaxial tensile tests are performed, while the mechanical stiffness of cardiac tissue varies in fibre length direction and the cross-section. Moreover, the Young's modulus should be calculated in the linear region. However, most biological tissues such as human heart tissue respond nonlinear to compression at strains higher than 10% [117][121]. Therefore, the Young's modulus of cardiac tissue should be calculated at low strains while M.S. Sirry et al. (2016) [118] measured the Young's modulus between 25% - 30% strain. Furthermore, uniaxial compression tests as performed in this Master Thesis are not very accurate measurements. Determining the 'zero' for the compression tests on your phantom samples is challenging. The surface of the sample should be exactly the same at every sight of the phantom. Then, the phantom should perfectly line with the compression surface that the phantom tissue does not touch the compression surface, but does touch the compression surface as soon as the measurements starts. In literature, it is not explained how the 'zero' is specified. Therefore, it was chosen to specify the 'zero' in this project as the first positive measurement point of all positive consecutive points. Also, the measured Young's modulus of the cardiac phantom composed of 16.7wt% PVA (1 freeze-thaw cycles) is measured after the phantom was stored for 3 days in liquid while the Young's modulus of the same cardiac phantom which underwent 2 freeze-thaw cycles is measured without storing the phantom in liquid. This could influence the results. Furthermore, according to S. Jiang et al. (2013), the addition of NaCl to PVA-C phantoms would disrupt the intra PVA chains and promote interaction between the polymer chains. Therefore, the gelling time would shorten [82] and the crystallinity would increase resulting in a stiffer phantoms [103]. This could be used when the cardiac phantom material should be stiffer.

### 9.9.5 Anatomy

In the previous literature study, a way of fabricating a cardiac phantom in desired shape was mentioned using a silicone mould. The referred study, of J. Laing et al. (2018) [122], described a way of fabricating a hollow patient-specific cardiac phantom of PVA-C. Figure 59 shows the fabrication process as reported in their study. For the mould fabrication in this Master Thesis, this process as described in Figure 59 was also considered as an option. However, using this process results in a phantom containing an open end while the inside blood pool model has to be pulled out by stretching the flexible heart model. In this project, it was desired to create a closed hollow phantom where only the pulmonary veins are open. Moreover, a 3D printed mould ensures a more repeatable phantom preparation in desired shape.

In addition, a new design for the cylinder shaped phantom was created as seen in Figure 60. This is the exact same mould as used in Chapter 9.7 with three more added holes for releasing the air bubbles. The resulted cylinder-shaped cardiac phantoms showed air bubbles at the top of the bigger cylinder. The filled mould was placed horizontally as seen in the lower figure of Figure 60. Whether these air releasing holes would fully resolve the trapped air bubbles problem is uncertain and unfortunately due to the limited time for this Master Thesis project this was not realised.

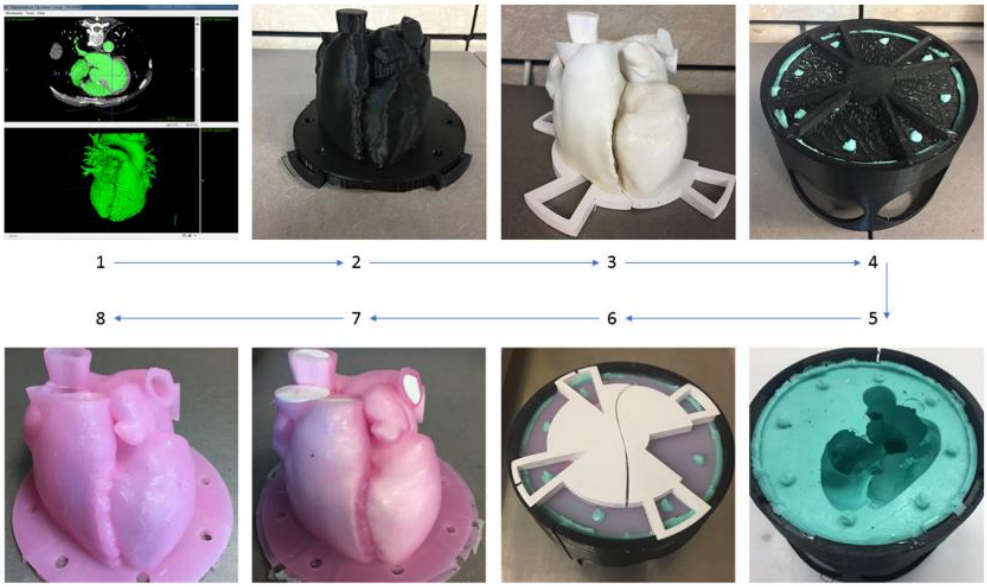


*Figure 59: Workflow showing the manufacturing of a patient-specific cardiac model. Step 1) Displaying the initial blood pool segmentation. Step 2) The thickened 3-D printed blood pool model. Step 3) The 3-D printed blood model. Step 4) The silicone mould generation using the 3-D printed container. Step 5) The completed silicon mould. Step 6) The silicone mould with the blood pool model aligned within. Step 7) The completed silicone model with the blood pool model inside. Step 8) The completed hollow silicone model.* [122]

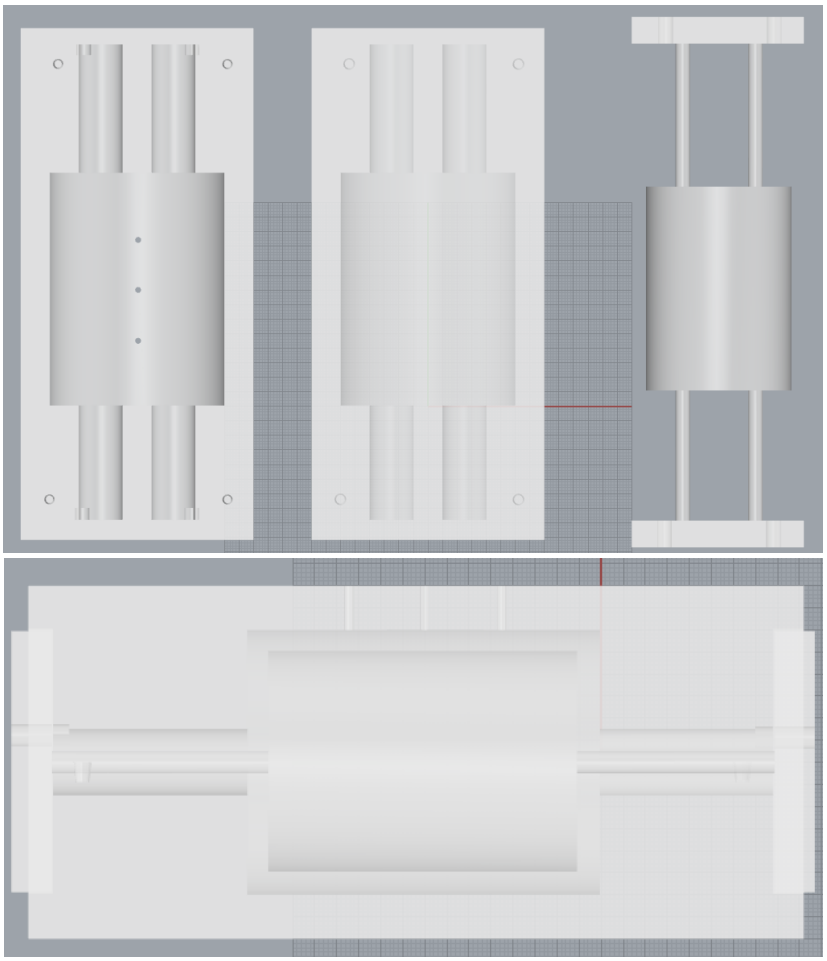

*Figure 60: New cylinder mould model, containing 3 extra holes for releasing air bubbles*

### 9.9.6 Additional requirements

The costs for the cardiac phantom materials used and for the mould preparation ranges between 50 - 80 euro, which is considered to be low. However, considering the time spent for preparing the material, preparing the mould, printing the mould, filling the mould and finally dissolving the PVA 3D-printed inner core, the cardiac phantom is more expensive. Furthermore, as defined previously, the cardiac phantom is said to be reproducible if the maximum percentage variation between the mean of the measured values over all frequency points of all four phantom samples does not exceed the previous defined repeatability values of 11% and 4% for permittivity and conductivity respectively. As Table 17 shows, cardiac phantom number 3 does not comply with the repeatability tests regarding its conductivity value. When preparing the phantom materials, water easily evaporates and should be refilled precisely. However, if this is not done correctly, the dielectric measurements could vary resulting in a deviation between multiple prepared cardiac phantoms. Moreover, cardiac phantom samples became stable after 1 week of storage.

PART IV:

# Evaluation

In this part, all most important results and findings will be reviewed and discussed. Moreover, recommendations for further research will be given and the Master Thesis project will be concluded.

# 10. Discussion and recommendations

This chapter contains the overall discussion of this Master Thesis and recommendations for further research. The goal of this chapter is to reflect on the most important results of this Master Thesis to determine the research contribution of this research project. The most important results of the research parts Part II and Part III will be reflected. Furthermore, the most important limitations will be reviewed. Finally, recommendations for further research will be given based on findings obtained during this research project.

## 10.1 Most important results and interpretations

### Part II: Research of phantom materials

Cardiac phantoms mimicking the dielectric properties already have been developed [48][49][50]. However, the cardiac phantoms found in literature either contain a different frequency range of interest, have a limited shelf life, or do not take the mechanical properties of human heart tissue into account. Therefore, none of the cardiac phantoms found in literature can be used for development of electrophysiology studies. Hence, in part II, three most promising base materials, according to the prior literature review [9], agar, gellan gum and PVA-C were examined with additives to manipulate the dielectric properties. Relevant studies for the production of homogeneous phantoms were mimicked and useful information about promising additives was extracted from literature [68][101][102]. First, a storage solution was produced with 0.15wt% salt in tap water, mimicking the conductivity values of human blood tissue according to the database IT'IS [30], a common used reference in literature [16]. Additives used were graphite powder, charcoal powder and sodium acetate for increasing the electrical conductivity and oil and PVC for decreasing its relative permittivity.

Experiments showed that the addition of sodium acetate results in a great increase of the phantoms conductivity. Moreover, oil results in a great decrease of the phantoms permittivity. However, the addition of oil resulted in oily phantoms which is not desired. Also, oil and other additives in agar-based phantoms sometimes caused solidification problems of the phantom. Solidification of agar-based phantoms is dependent on the procedures taken, the ratios of each ingredient [105] and the pH-value of the mixture [106]. Using graphite (> 20.0wt%), charcoal (> 4.8wt%) or PVC (> 16.7wt%) as additive, precipitation occurs in PVA-C phantoms. Furthermore, charcoal powder did not affect the conductivity as desired. This could be due to the percolation threshold of charcoal powder which varies per form of charcoal and base material used [107][108][109].

As a result, five sample phantoms with closest dielectric values to the target values were compared to each other and evaluated based on the main requirements of the cardiac phantom. All results of the five most promising sample phantoms are shown in Table 18. Agar phantoms did not get the desired elasticity and did not realize the required shelf life. Gellan gum phantoms are difficult to prepare. As prepared, they resulted in too soft and not always homogeneously phantoms. Phantom P2 of Table 18 resulted to be the most promising cardiac phantom and is further investigated in Part III. However, all sample phantoms produced in this part were measured without storing the phantoms. This is examined in Part III in order to comply with the additional requirement concerning the stability of the phantom. Water absorption influenced the dielectric properties [64] and therefore could have influenced the results for examining the most promising phantom material. Therefore, all phantoms should be measured after 1 week of storage. Furthermore, it is decided to only mimic the conductivity values of human blood in the storage solution because of the limited time of the project. Moreover, this research project serves as a proof of concept and therefore only manipulating the conductivity

values of the storage solution is a good first step towards the cardiac phantom which eventually can be used for development of electrophysiology studies. Ultimately, the permittivity also should be mimicked in the storage solution which can influence the dielectric properties of the cardiac phantom.

*Table 18: Results of most promising sample phantoms, all composed of 0.15wt% salt in tap water*

| Properties | Most promising phantom samples | | | | |
|---|---|---|---|---|---|
| | **A1** | **G1** | **G2** | **P1** | **P2** |
| Ingredients* | 5.7wt% agar<br>23.1wt% oil | 2.9wt% GG<br>16.7wt% oil | 2.9wt% GG<br>23.1wt% oil | 10.7wt% PVA<br>0.1wt% s.a.<br>31.0wt% oil | 13.0wt% PVA<br>0.05wt% s.a. |
| Dielectric properties (%)** | $\varepsilon_r$ : 20.8<br>σ : 8.4 | $\varepsilon_r$ : 88.4<br>σ : 3.3 | $\varepsilon_r$ : 46.1<br>σ : 11.7 | $\varepsilon_r$ : 7.1<br>σ : 23.5 | $\varepsilon_r$ : 44.2<br>σ : 8.4 |
| Storage | - Salt diffusion | - Salt diffusion<br>- Water absorption<br>- Phantom material separation<br>- Cloudy storage solution | - Salt diffusion<br>- Water absorption<br>- Phantom material separation<br>- Cloudy storage solution | - Salt diffusion<br>- Water absorption | - Salt diffusion<br>- Water absorption |
| Homogeneity (%)*** | $\varepsilon_r$ : 3.6<br>σ : 2.3 | $\varepsilon_r$ : 8.8<br>σ : 2.6 | $\varepsilon_r$ : 8.7<br>σ : 3.0 | $\varepsilon_r$ : 2.1<br>σ : 2.1 | $\varepsilon_r$ : 4.9<br>σ : 1.6 |
| Mechanical stiffness | Too stiff, brittle and oily | Too soft and elastic | Too soft and elastic | Good stiffness but oily | Good stiffness |
| Shelf life | < 3 weeks | > 1 month | > 1 month | > 1 month | > 1 month |

* GG = Gellan gum
s.a. = Sodium acetate
**The average percentage difference between phantom tissue and target values
***The average percentage difference between measured value and the mean

## Part III: Cardiac phantom design

In this part, the most promising phantom sample was prepared four more times and extensively evaluated based on all phantom requirements. Hence, the cardiac phantom tissue evaluated in Part III consists of 13.0wt% PVA, 0.15wt% salt, 0.05wt% sodium acetate and tap water.

### *Main requirement 1 & 2: The electrical conductivity and relative permittivity in the frequency range of 10 kHz – 20 kHz is similar to human heart tissue*

In order to compare the dielectric properties of the cardiac phantoms and the target values, the average percentage difference over all frequency points was measured which is in line with the method used in the study of N. Arteaga-Marrero et al. (2019) [64]. Ideally, the measured values of the phantom tissue are considered to be accepted when they are in the range of ± 11% and ± 10% for permittivity and conductivity respectively on the target values and complies with repeatability tests performed. The accepted tolerance range is based on the study of V. Lopresto et al. (2011) [92]. However, the dielectric properties of the cardiac phantom samples are not within the desired accepted tolerance range. The mean of all four cardiac phantom samples produced varies from the target values with 21.9% and 15.0% for permittivity and conductivity, respectively.

Differences found between the used target values and the dielectric values of human heart tissue derived from the database IT'IS [30] can be explained by differences between dielectric properties of porcine heart tissue and human heart tissue [25][91]. Moreover, dielectric properties are temperature dependent and the porcine heart tissue is measured at room temperature, while the human heart tissue values are of tissue at body temperature [23]. Furthermore, differences between measurement equipment, electrode configuration and translation of measurements into the dielectric values permittivity and conductivity can cause differences in results.

### *Main requirement 3: The phantom should be stored in a solution mimicking the conductivity values of human blood*

PVA-C phantoms should be stored refrigerated in a closed container in liquid [102]. When stored in a liquid, water absorption takes place and salt diffusion occurs when stored in a solution with different salt composition, influencing the dielectric properties [64]. Moreover, it is resulted that sodium acetate diffusion also occurs. Therefore, all results are based on a phantom tissue composed of 13.0wt% PVA, 0.15wt% salt and tap water.

### *Main requirement 4: The phantom is homogeneous*

Phantoms are said to be homogeneous when repeated measurements at various sides of the phantom shows 11% and 4% or lower variation for permittivity and conductivity, respectively. The mean percentage of variation between the measured value and the mean is on average 8.8 and 6.5 for permittivity and conductivity, respectively. For three of the four cardiac phantom samples prepared it can be said to be homogeneous. The strong deviation seen in the supposing non-homogeneous phantom is caused by the $6^{th}$ measurement. The $6^{th}$ measurement of all cardiac phantom samples was measured at the top of the phantom sample. For some cardiac phantom samples, a layer arose on top of the liquid form of cardiac phantom sample (before the freeze-thaw cycle). This layer eventually resulted in a much stiffer layer on top of the phantom sample compared to the rest of the sample and resulted in a much rougher surface. This layer should be avoided when the phantom undergoes the freeze-thaw cycle. It was decided to not remove this layer by cutting, while this could influence impedance measurements and compression tests results.

### *Main requirement 5: The mechanical stiffness is similar to that of human heart tissue*

For this research project, it was of importance to fabricate a flexible cardiac phantom giving approximately the same haptic feedback as human heart tissue. The cardiac phantom succeeded in the haptic evaluation. Moreover, uniaxial compression tests were performed to calculate the Young's modulus of the cardiac phantoms. However, comparison between calculated Young's moduli of the cardiac phantoms and human heart tissue is rather difficult. Literature shows diverse values of the Young's moduli of human heart tissue, while the mechanical properties are anisotropic, varies within the heart and is dependent on timing of the cardiac cycle [49]. Nevertheless, in order to meet the mechanical requirement the cardiac phantom approximately gives the same haptic feedback as human heart tissue. In addition, the stiffness of PVA-C phantoms can be easily manipulated by changing the wt% of PVA-powder [93], changing the freezing time, freezing temperature and the rate of the freeze-thaw cycle [63]. Furthermore, according to S. Jiang et al. (2013), the addition of NaCl to PVA-C phantoms would disrupt the intra PVA chains and promote interaction between the polymer chains. Therefore, the gelling time would shorten [82] and the crystallinity would increase resulting in a stiffer phantom [103]. Changing these elements, also influences the dielectric properties and should therefore be taken into account.

### *Main requirement 6: Shelf life of at least one month*

Storing the cardiac phantom in the storage solution results in a sufficiently long shelf life (> 1 month).

*Addition requirement 1: The anatomy is similar to the anatomy of the LA*

In this project, a cardiac phantom in the shape of a simplified version of the LA is successfully produced. The final cardiac phantom is cylindrically shaped and contains 4 hollow tubes representing the four pulmonary veins. In order to create such a closed hollow phantom with only four small openings of the pulmonary veins, an outer mould 3D-printed with PLA and a solvable inner mould 3D-printed with PVA is used. This simplified version is a good first step in the possibilities for the production of the cardiac phantom with correct anatomy.

*Additional requirement 2: Inexpensive to produce*

*Additional requirement 3: Ease of manufacturing*

*Additional requirement 4: Reproducible; same recipe should give the same results*

*Additional requirement 5: Stable over time; the phantom should retain its dielectric properties over at least one month*

The cardiac phantom is an inexpensive (50 – 80 euros), easily produced phantom. For evaluation of the reproducibility of the cardiac phantom design, the average percentage difference between the cardiac phantom samples and the mean of all cardiac phantom samples was calculated. The phantom is said to be reproducible if these values do not exceed the defined repeatability values of 11% and 4% for permittivity and conductivity, respectively. Results show all four produced cardiac phantoms can said to be reproducible, except for one of the four phantoms produced which does not comply regarding its conductivity value. When preparing the phantom materials, water easily evaporates and should be refilled precisely. Therefore, the dielectric measurements could vary resulting in a deviation between multiple prepared cardiac phantoms. Storing the phantom in liquid, water absorption and diffusion influences the dielectric properties of the phantom. Stability of the cardiac phantom is reached in 1 week. However, it can be more extensively investigated if the phantom will reach its stability after a shorter period.

## 10.2 Limitations of experiment

Promising phantoms have been made, but some technical limitations have occurred during this research project which may have influenced the results obtained. At first, the storage solution made in Part II was only measured with an EC-meter with an accuracy of ± 2% full scale assuming the device measured the conductivity accurate enough. To continuously use the same storage solution for the phantom preparation and for the storage, the amount of salt and tap water was weighted rather than making a saline solution and measuring the conductivity with the EC-meter. Therefore, all sample phantom were prepared with the same storage solution. Nevertheless, the storage solution was measured in Part III with the new 4-point needle electrode and resulted in different conductivity values as measured with the EC-meter. New sterile saline solutions were prepared and a 0.36% saline solution resulted to have a conductivity more closer to human blood as the used storage solution of 0.15wt% salt in tap water. This result is in good agreement with results found in the study of H.W. Choi et al. (2011) [97]. Using a different storage solution will affect the dielectric values of the cardiac phantom. Therefore, the correct storage solution with high accuracy must be made in advance.

Furthermore, the used electrode method for the impedance measurements was greatly based on accessibility and therefore ease of manufacturing because of the limited time for this research project. Determining the best possible electrode method for the cardiac phantom tissue is very specific and needs thorough investigation. The main error occurring when using a two-needle electrode configuration is electrode polarization which as example can be limited by using a four-needle electrode configuration or adapting the formula used for deriving the dielectric properties

[18][11][94][16]. Therefore, for limiting errors, the dielectric values of the porcine heart tissue measured with the same equipment and same method is best suited as target values for this research project which serves as a proof of concept.

## 10.3 Recommendations for further research

This section contains the recommendations for further research based on the findings obtained during this research project. Five recommendations will be given regarding TMMs for manipulating the dielectric properties of the cardiac phantom in order to ultimately get the desired dielectric properties. Before measuring the dielectric properties of the cardiac phantom, two things are of importance. First, a correct storage solution mimicking both the conductivity and permittivity of human blood should be prepared. Thereafter, the storage solution should be used for the cardiac phantom preparation. Second, all measurements of the cardiac phantom tissues should be measured after stability is reached. In this research project, the stability was measured after 1 week, 2 weeks and 2,5 weeks of storage and was concluded stability is reached after 1 week. However, it can be examined whether stability is reached in less than 1 week storage.

### Further development cardiac phantom

This research project showed the design of a cardiac phantom. However, the storage solution mimicking the dielectric conductivity values of human blood can become more identical to the dielectric properties of human blood. Moreover, the permittivity of the storage solution should also be mimicked eventually. Because of diffusion occurring when storing the cardiac phantom in the storage solution, the cardiac phantom should be made of the storage solution. This would influence the dielectric properties of the cardiac phantom. After the correct storage solution is fabricated, the cardiac phantom of PVA can be prepared. Changing the amount of PVA powder in the cardiac phantom will affect the dielectric properties (and stiffness) and can therefore be manipulated into the desired dielectric properties. For increasing its stiffness, multiple freeze-thaw cycles can be performed. This will not affect the dielectric properties proportionally. Moreover, it can be examined whether increasing the amount of salt in the phantom mixture results in a stiffer phantom. After the freeze-thaw cycle, the excessive salt will leave the phantom by diffusion when storing the phantom in the storage solution. Figure 61 shows the variants of the cardiac phantom tissue fabricated in this project.

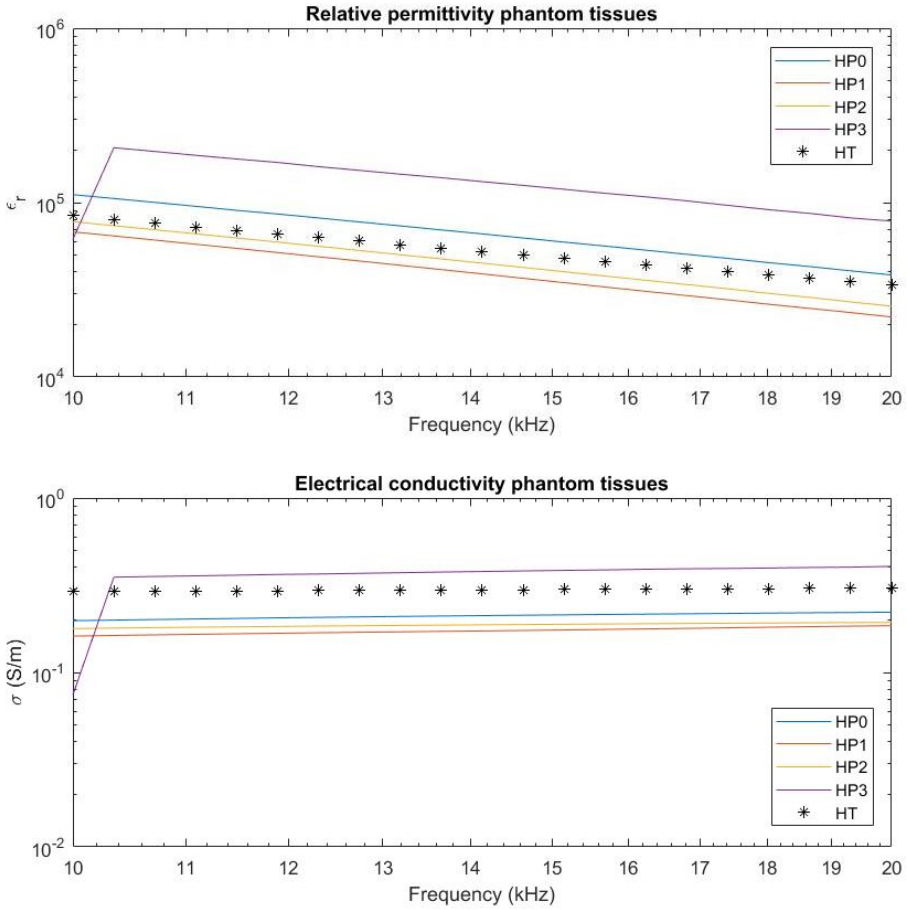


*Figure 61: Comparison between final cardiac phantom tissue (HP0), cardiac phantom tissue prepared with 16.7wt% (HP1), cardiac phantom tissue prepared with 16.7wt% and 2 freeze-thaw cycles (HP2), cardiac phantom tissue prepared with 0.36% saline (HP3) and the target values (HT)*

## Oil as additive

In Chapter 7 the most promising phantoms were compared to each other. Here, the other promising PVA phantom was prepared with the addition of oil. But, this phantom resulted in an undesired oily phantom. It can be examined whether the use of a different oil/surfactant ratio, a different oil or a different surfactant will result in a phantom without feeling oily. Moreover, it has to be examined whether the oil will not diffuse when stored in the storage solution. Figure 62 shows the dielectric properties of prepared PVA-C phantoms of this project. These values seen are the phantom values without storing the phantoms. Moreover, the dielectric properties will change when using the correct storage solution. Thereafter, the dielectric properties can be manipulated by varying the wt% of PVA powder and the wt% of oil to get the desired values.

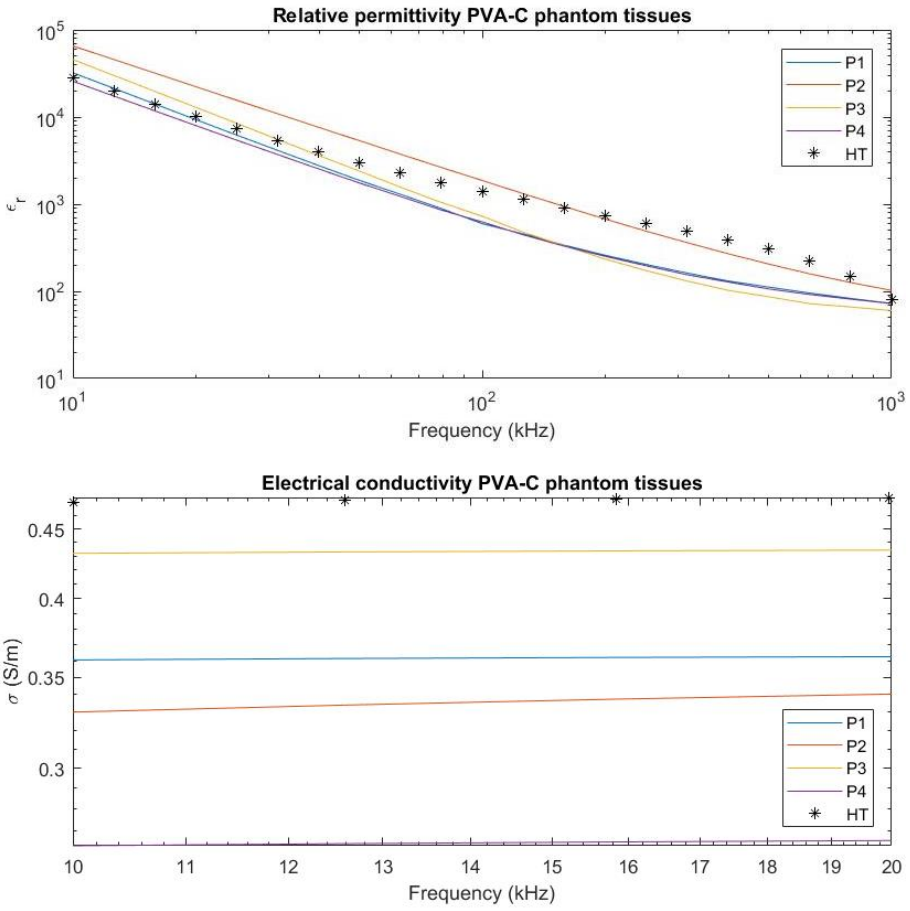


*Figure 62: Comparison PVA-C phantoms with adding oil. With P1 – P4 explained in Table 19 and HT the target values*

*Table 19: Ingredients of PVA-C phantoms as shown in figure above made with the storage solution*

| Phantom number | P1 | P2 | P3 | P4 |
|---|---|---|---|---|
| **PVA-powder (wt%)** | 10.7 | 13.0 | 13.0 | 13.0 |
| **Sodium acetate (wt%)** | 0.1 | - | 0.05 | - |
| **Oil (wt%)** | 31.0 | 23.1 | - | 33.3 |
| **Surfactant (wt%)** | 4.9 | 4.8 | - | 5.2 |

## PVC as additive

PVC can be added for decreasing the phantoms permittivity. But, PVC precipitates when using > 16.7wt% PVC powder. However, it can be examined whether a different PVC powder will result in a homogeneous phantom. Moreover, the mixing procedure is based on the study of H. Kato and T. Ishida (1987) [78] where PVC powder is added to an agar-based phantom. Therefore, it should be examined whether a different mixing procedure would result in a homogenous PVA phantom.

## PVP as additive

In this research project, it was decided to not use PVP as additive. However, it still can be examined whether PVP would be a good additive for decreasing the permittivity of the phantom material [48].

### Use of different base material

Three promising base materials are examined in this research project. According to the prior literature review performed [9], the base materials hydroxylethyl cellulose, polyurethane, polyester resin and epoxy resin could be promising for the fabrication of a flexible cardiac phantom. However, hydroxylethyl cellulose has a very short shelf life [123][84] and is therefore not recommended as base material for the cardiac phantom. Therefore, polyurethane, polyester resin and epoxy resin can be examined for a new design of a cardiac phantom. Moreover, polyurethane comes in a variety of different elasticities while it can be mixed with different ratios. Therefore, it can range in forms of more elastic to more tougher materials [71]. When using resins, addition of additives can be challenging for creating a homogeneous phantom [124]. Using a polyester resin with low degree of filling makes it easier to mix additives homogeneously [79].

# 11. Conclusion

The objective of this project was to develop an anthropomorphic cardiac phantom. The most important criteria for the development of the phantom was to create a flexible phantom containing the same dielectric properties as human heart tissue. In order to assess this goal, the objective was divided into 3 subgoals:

1. *Evaluate different tissue mimicking materials with additives to meet the main phantom requirements.*

Results showed agar- and gellan gum-based phantoms are not appropriate as base material for a cardiac phantom design. PVA-C resulted to be a good phantom model for the heart design. Potential additives for manipulating the dielectric properties are graphite, sodium acetate and salt for manipulating the conductivity and oil, PVC and for manipulating the permittivity. However, sodium acetate, salt and sugar resulted to diffuse when the phantom is stored in liquid. Therefore, diffusion should be taken into account when preparing the storage solution and the phantom material. Graphite (> 20.0wt%) and PVC (> 16.7wt%) resulted in precipitation of the additive.

2. *Extensively evaluate the most promising cardiac phantom materials.*
3. *Develop a phantom design with comparable anatomy.*

This Master Thesis project shows the design of a low cost (50 – 80 euros), easily produced hollow shaped cardiac phantom consisting of 13.0wt% PVA, 0.15wt% salt and tap water. The amount of salt is based on the composition of the storage solution mimicking the conductivity values of human blood. Still a lot of future work needs to be done for the development of a cardiac phantom, yet this research serves as a proof of concept for the development of a flexible phantom with possibilities to manipulate the dielectric properties and to create a hollow shaped phantom. The use of PVA as TMM and the use of 3D printed PVA for creation of the hollow shapes shows promising results for future development.

# References


[1] "Stroke – Op2Lysis." [Online]. Available: https://www.op2lysis.com/?page_id=590&lang=en. [Accessed: 23-Jun-2020].

[2] "Boezemfibrilleren: van kwaad tot erger | Hartstichting."

[3] "Bekijk de cijfers over hart- en vaatziekten | Hartstichting." [Online]. Available: https://www.hartstichting.nl/hart-en-vaatziekten/feiten-en-cijfers-hart-en-vaatziekten. [Accessed: 20-Jun-2020].

[4] F. Yntema, "Onderzoek: vaker hartritme herstellen kan leiden tot minder beroertes en infarcten," *NOS*, 2020.

[5] J. Thomas and G. Whitworth, "Atrial fibrillation: Facts, Statistics, and You," *Healthline*, 2018. [Online]. Available: https://www.healthline.com/health/living-with-atrial-fibrillation/facts-statistics-infographic#1.

[6] P. Kirchhof *et al.*, "Early Rhythm-Control Therapy in Patients with Atrial Fibrillation.," *N. Engl. J. Med.*, p. NEJMoa2019422, Aug. 2020.

[7] S. Salahuddin *et al.*, "Demonstration of dielectric heterogeneity of previously assumed homogeneous tissues: Examination of the heart," *IET Conf. Publ.*, vol. 2018, no. CP741, 2018.

[8] "3D human heart anatomy model - TurboSquid 1283134." [Online]. Available: https://www.turbosquid.com/3d-models/3d-human-heart-anatomy-model-1283134. [Accessed: 22-Jun-2020].

[9] P. M. J. Luik, "Literature review. Dielectric heart phantom," 2020.

[10] R. Pethig, "Phantoms for hyperthermia and impedance tomography," *Physics in Medicine and Biology*, vol. 36, no. 12. pp. 1559–1563, 1991.

[11] *Agilent Impedance Measurement Handbook A guide to measurement technology and techniques*. Agilent Technologies, 2013.

[12] G. Amorós-Figueras *et al.*, "Endocardial infarct scar recognition by myocardial electrical impedance is not influenced by changes in cardiac activation sequence," *Hear. Rhythm*, vol. 15, no. 4, pp. 589–596, Apr. 2018.

[13] Y. Zou and Z. Guo, "A review of electrical impedance techniques for breast cancer detection," *Medical Engineering and Physics*, vol. 25. Elsevier BV, pp. 79–90, 2003.

[14] J. Cinca *et al.*, "Changes in myocardial electrical impedance induced by coronary artery occlusion in pigs with and without preconditioning: Correlation with local ST-segment potential and ventricular arrhythmias," *Circulation*, vol. 96, no. 9, pp. 3079–3086, Nov. 1997.

[15] W. H. W. Tang and W. Tong, "Measuring impedance in congestive heart failure: Current options and clinical applications," *American Heart Journal*, vol. 157, no. 3. pp. 402–411, Mar-2009.

[16] J. Z. Tsai, H. Cao, S. Tungjitkusolmun, E. J. Woo, V. R. Vorperian, and J. G. Webster, "Dependence of apparent resistance of four-electrode probes on insertion depth," *IEEE Trans. Biomed. Eng.*, vol. 47, no. 1, pp. 41–48, 2000.

[17] D. Miklavcic, N. Pavselj, and F. X. Hart, "Electric properties of tissues," *Wiley Encycl. Biomed. Eng.*, p. 12, 2006.

[18] J. Jossinet, “Elementary electrodynamics,” IOS Press Bioelectronics, 2008.

[19] B. L. Beck, K. A. Jenkins, J. R. Rocca, and J. R. Fitzsimmons, “Tissue-equivalent phantoms for high frequencies,” *Concepts Magn. Reson. Part B Magn. Reson. Eng.*, vol. 20, no. 1, pp. 30–33, Feb. 2004.

[20] K. S. Moon, H. Do Choi, A. K. Lee, K. Y. Cho, H. G. Yoon, and K. S. Suh, “Dielectric properties of epoxy-dielectrics-carbon black composite for phantom materials at radio frequencies,” *J. Appl. Polym. Sci.*, vol. 77, pp. 1294–1302, Aug. 1999.

[21] M. r. Neuman, “The biomedical engineering handbook - Chapter 48, Biopotential Electrodes,” 2000.

[22] B. He, *Modeling and Imaging of Bioelectrical Activity, Principles and Applications*. Plenum Publishers, 2004.

[23] C. Rossmanna and D. Haemmerich, “Review of temperature dependence of thermal properties, dielectric properties, and perfusion of biological tissues at hyperthermic and ablation temperatures,” *Crit. Rev. Biomed. Eng.*, vol. 42, no. 6, pp. 467–492, Jun. 2014.

[24] J. R. Bourne, “Biomedical Engineering.” p. 484, 1996.

[25] C. Gabriel, S. Gabriel, and E. Corthout, “The dielectric properties of biological tissues: I. Literature survey,” 1996.

[26] S. Gabriel, R. W. Lau, and C. Gabriel, “The dielectric properties of biological tissues: III. Parametric models for the dielectric spectrum of tissues,” 1996.

[27] K. S. Cole and R. H. Cole, “Dispersion and absorption in dielectrics I. Alternating current characteristics,” *J. Chem. Phys.*, vol. 9, no. 4, pp. 341–351, 1941.

[28] S. Gabriel, R. W. Lau, and C. Gabriel, “The dielectric properties of biological tissues: II. Measurements in the frequency range 10 Hz to 20 GHz,” 1996.

[29] C. Gabriel, “Compilation of the Dielectric Properties of Body Tissues at RF and Microwave Frequencies.” 1996.

[30] “Dielectric Properties » IT’IS Foundation.” [Online]. Available: https://itis.swiss/virtual-population/tissue-properties/database/dielectric-properties/. [Accessed: 09-Dec-2019].

[31] R. N. Fogoros, *Electrophysiologic testing*, vol. 36. 2006.

[32] “Arrhythmia,” *National Heart, Lung, and Blood Institute*, 2019. [Online]. Available: https://www.nhlbi.nih.gov/health-topics/arrhythmia. [Accessed: 10-Oct-2019].

[33] T. Newman, “Arrhythmia: Causes, symptoms, types, and treatment,” *Medical News Today*, 2017. [Online]. Available: https://www.medicalnewstoday.com/articles/8887.php. [Accessed: 11-Oct-2019].

[34] C. et Al., “Arrythmia display - US6721594B2 - Foreign patent documents,” *United States Patent*, 2004. [Online]. Available: https://patents.google.com/patent/US6721594B2/en. [Accessed: 25-Oct-2019].

[35] J. Park, S. Lee, and M. Jeon, “Atrial fibrillation detection by heart rate variability in Poincare plot,” *Biomed. Eng. Online*, vol. 8, Dec. 2009.

[36] “Pulmonary vein isolation - Mayo Clinic.” [Online]. Available: https://www.mayoclinic.org/tests-procedures/pulmonary-vein-isolation/about/pac-

20384996. [Accessed: 09-Oct-2019].

[37] T. Reiter *et al.*, "Direct cooling of the catheter tip increases safety for CMR-guided electrophysiological procedures," *J. Cardiovasc. Magn. Reson.*, vol. 14, no. 1, 2012.

[38] S. Weiss *et al.*, "In Vivo Evaluation and Proof of Radiofrequency Safety of a Novel Diagnostic MR-Electrophysiology Catheter," 2010.

[39] S. K. Stephen Huang, "Radio-frequency catheter ablation of cardiac arrhythmias: Appraisal of an evolving therapeutic modality," *Am. Heart J.*, vol. 118, no. 6, pp. 1317–1323, 1989.

[40] "Atrial fibrillation ablation - Mayo Clinic." [Online]. Available: https://www.mayoclinic.org/tests-procedures/atrial-fibrillation-ablation/about/pac-20384969. [Accessed: 23-Oct-2019].

[41] W. W. B. Chik *et al.*, "High spatial resolution thermal mapping of Radiofrequency ablation Lesions using a novel thermochromic liquid crystal myocardial phantom," *J. Cardiovasc. Electrophysiol.*, vol. 24, no. 11, pp. 1278–1286, 2013.

[42] "Catheter Ablation | National Heart, Lung, and Blood Institute (NHLBI)," *National Heart, Lung, and Blood Institute*. [Online]. Available: https://www.nhlbi.nih.gov/health-topics/catheter-ablation. [Accessed: 23-Oct-2019].

[43] E. Buch, N. G. Boyle, and K. Shivkumar, "Catheter Ablation: Technical aspects," in *Cardiac Electrophysiology: From Cell to Bedside*, Elsevier, 2016, pp. 1199–1207.

[44] "Philips lanceert nieuwste generatie van KODEX-EPD systeem - Nieuws | Philips." [Online]. Available: https://www.philips.nl/a-w/about/news/archive/standard/about/news/press/2020/20200826-catharina-ziekenhuis-gebruikt-als-eerste-in-nederland-een-nieuwe-techniek-voor-de-behandeling-van-boezemfibrilleren.html. [Accessed: 05-Oct-2020].

[45] G. Anand, A. Lowe, and A. Al-Jumaily, "Tissue phantoms to mimic the dielectric properties of human forearm section for multi-frequency bioimpedance analysis at low frequencies," *Mater. Sci. Eng. C*, vol. 96, pp. 496–508, Mar. 2019.

[46] R. Ortega-Palacios, L. Leija, and A. Vera, "Tumor breast phantom vs breast phantom Microwave ablation: Thermal experimentation and electric property measurements," in *CCE 2012 - 2012 9th International Conference on Electrical Engineering, Computing Science and Automatic Control*, 2012.

[47] M. A. Kandadai, J. L. Raymond, and G. J. Shaw, "Comparison of electrical conductivities of various brain phantom gels: Developing a 'Brain Gel Model,'" *Mater. Sci. Eng. C*, vol. 32, pp. 2664–2667, 2012.

[48] C. Ianniello *et al.*, "Synthesized tissue-equivalent dielectric phantoms using salt and polyvinylpyrrolidone solutions," *Magn. Reson. Med.*, vol. 80, no. 1, pp. 413–419, Jul. 2018.

[49] L. Korn *et al.*, "Heart phantom with electrical properties of heart muscle tissue," *Curr. Dir. Biomed. Eng.*, vol. 4, no. 1, pp. 97–100, Sep. 2018.

[50] C. Ianniello *et al.*, "Design and construction of a tissue-mimicking phantom to validate electrical properties mapping techniques based on magnetic resonance," in *2015 1st URSI Atlantic Radio Science Conference, URSI AT-RASC 2015*, 2015.

[51] P. Li, Z. Yang, and S. Jiang, "Tissue mimicking materials in image-guided needle-based interventions: A review," *Mater. Sci. Eng. C*, vol. 93, pp. 1116–1131, Dec. 2018.

[52] A. Dabbagh, B. Johan, J. Abdullah, C. Ramasindarum, N. Hayaty, and A. Kasim, “Tissue-Mimicking Gel Phantoms for Thermal Therapy Studies,” *Ultrason. Imaging*, vol. 36, no. 4, pp. 291–316, 2014.

[53] R. J. Sadleir, F. Neralwala, T. Te, and A. Tucker, “A controllably anisotropic conductivity or diffusion phantom constructed from isotropic layers.,” *Ann. Biomed. Eng.*, vol. 37, no. 12, pp. 2522–2531, Dec. 2009.

[54] E. Porter, J. Fakhoury, R. Oprisor, M. Coates, and M. Popovic, “Improved tissue phantoms for experimental validation of microwave breast cancer detection,” in *EuCAP 2010 - The 4th European Conference on Antennas and Propagation*, 2010.

[55] Q. Duan *et al.*, “Characterization of a dielectric phantom for high-field magnetic resonance imaging applications,” *Med. Phys.*, vol. 41, no. 10, Oct. 2014.

[56] “Formaldehyde | RIVM.” [Online]. Available: https://www.rivm.nl/tabak/rook/schadelijke-stoffen-in-tabaksrook/formaldehyde. [Accessed: 31-Mar-2020].

[57] P. T. Nguyen, A. M. Abbosh, and S. Crozier, “Thermo-Dielectric Breast Phantom for Experimental Studies of Microwave Hyperthermia,” *IEEE Antennas Wirel. Propag. Lett.*, vol. 15, pp. 476–479, 2016.

[58] K. Ito, K. Furuya, Y. Okano, and L. Hamada, “Development and characteristics of a biological tissue-equivalent phantom for microwaves,” *Electron. Commun. Japan, Part I Commun. (English Transl. Denshi Tsushin Gakkai Ronbunshi)*, vol. 84, no. 4, pp. 67–77, 2001.

[59] A. J. Patton, L. A. Poole-Warren, and R. A. Green, “Mechanisms for Imparting Conductivity to Nonconductive Polymeric Biomaterials,” *Macromol. Biosci.*, vol. 16, pp. 1103–1121, Aug. 2016.

[60] K. J. M. Surry, H. J. B. Austin, A. Fenster, and T. M. Peters, “Poly(vinyl alcohol) cryogel phantoms for use in ultrasound and MR imaging,” *Phys. Med. Biol.*, vol. 49, no. 24, pp. 5529–5546, Dec. 2004.

[61] G. Lamouche *et al.*, “Review of tissue simulating phantoms with controllable optical, mechanical and structural properties for use in optical coherence tomography,” *Biomed. Opt. Express*, vol. 3, no. 6, p. 1381, Jun. 2012.

[62] N. N. K. Getangama, J. R. De Bruyn, and J. L. Hutter, “Dielectric Spectroscopy of Polyvinyl Alcohol Hydrogels and Nanocomposites,” 2015.

[63] A. Iravani, J. Mueller, and A. M. Yousefi, “Producing homogeneous cryogel phantoms for medical imaging: A finite-element approach,” *J. Biomater. Sci. Polym. Ed.*, vol. 25, no. 2, pp. 181–202, Jan. 2014.

[64] N. Arteaga-Marrero, E. Villa, J. González-Fernández, Y. Martín, and J. Ruiz-Alzola, “Polyvinyl alcohol cryogel phantoms of biological tissues for wideband operation at microwave frequencies,” *PLoS One*, vol. 14, no. 7, pp. 1–17, Jul. 2019.

[65] H. Palza, P. A. Zapata, and C. Angulo-Pineda, “Electroactive smart polymers for biomedical applications,” *Materials*, vol. 12. MDPI AG, p. 24, 16-Jan-2019.

[66] E. R. Morris, K. Nishinari, and M. Rinaudo, “Gelation of gellan - A review,” *Food Hydrocolloids*, vol. 28, no. 2. pp. 373–411, Aug-2012.

[67] R. K. Chen and A. J. Shih, “Multi-modality gellan gum-based tissue-mimicking phantom with targeted mechanical, electrical, and thermal properties,” *Phys. Med. Biol.*, vol. 58, pp. 5511–

5525, 2013.

[68] R. Mao, J. Tang, and B. G. Swanson, “Water holding capacity and microstructure of gellan gels,” *Carbohydr. Polym.*, vol. 46, pp. 365–371, 2001.

[69] M. Miyakawa, N. Takahashi, and S. Hoshina, “A method for observing the three-dimensional patterns of electromagnetic power absorbed by the human body-the gel phantom of the human body used to study the electromagnetic environmental problem,” *Electron. Commun. Japan (Part I Commun.*, vol. 78, no. 8, pp. 99–112, Aug. 1995.

[70] M. J. Hagmann, R. L. Levin, L. Calloway, A. J. Osborn, and K. R. Foster, “Muscle-Equivalent Phantom Materials for 10–100 MHz,” *IEEE Trans. Microw. Theory Tech.*, vol. 40, no. 4, pp. 760–762, 1992.

[71] B. McDermott *et al.*, “Stable tissue-mimicking materials and an anatomically realistic, adjustable head phantom for electrical impedance tomography,” *Biomed. Phys. Eng. Express*, vol. 4, no. 1, p. 13, Jan. 2018.

[72] A. Santorelli, O. Laforest, E. Porter, and M. Popovic, “Image Classification for a Time-Domain Microwave Radar System: Experiments with Stable Modular Breast Phantoms,” 2015.

[73] “Dielectric constants of common solvents,” *University of Washington*. .

[74] M. P. Robinson, M. J. Richardson, J. L. Green, and A. W. Preece, “New materials for dielectric simulation of tissues,” *Phys. Med. Biol.*, vol. 36, no. 12, pp. 1565–1571, 1991.

[75] S. A. López-Haro, C. J. Trujillo, A. Vera, and L. Leija, “An agarose based phantom embedded in an in vitro liver tissue to simulate tumors: First experience,” in *Pan American Health Care Exchanges, PAHCE 2011 - Conference, Workshops, and Exhibits. Cooperation / Linkages: An Independent Forum for Patient Care and Technology Support*, 2011, pp. 233–236.

[76] Y. Yu, A. Lowe, G. Anand, and A. Kalra, “Tissue phantom to mimic the dielectric properties of human muscle within 20 Hz and 100 kHz for biopotential sensing applications,” in *Proceedings of the Annual International Conference of the IEEE Engineering in Medicine and Biology Society, EMBS*, 2019, pp. 6490–6493.

[77] M. Lazebnik, E. L. Madsen, G. R. Frank, and S. C. Hagness, “Tissue-mimicking phantom materials for narrowband and ultrawideband microwave applications,” *Phys. Med. Biol.*, vol. 50, pp. 4245–4258, Sep. 2005.

[78] H. Kato and T. Ishida, “Development of an agar phantom adaptable for simulation of various tissues in the range 5-40 MHz,” *Phys. Med. Biol.*, vol. 32, no. 2, pp. 221–226, 1987.

[79] P. Wust, H. Fähling, J. Berger, A. Jordan, G. Mönich, and R. Felix, “Solid materials with high dielectric constants for hyperthermia applications,” *Int. J. Hyperth.*, vol. 14, no. 2, pp. 183–193, 1998.

[80] A. T. Mobashsher and A. M. Abbosh, “Artificial human phantoms: Human proxy in testing microwave apparatuses that have electromagnetic interaction with the human body,” *IEEE Microw. Mag.*, vol. 16, no. 6, pp. 42–62, Jul. 2015.

[81] A. Raveendran, M. T. Sebastian, and S. Raman, “Applications of Microwave Materials: A Review,” *J. Electron. Mater.*, vol. 48, no. 5, pp. 2601–2634, 2019.

[82] S. Jiang, Z. Su, X. Wang, S. Liu, and Y. Yu, “Development of a new tissue-equivalent material applied to optimizing surgical accuracy,” *Mater. Sci. Eng. C*, vol. 33, no. 7, pp. 3768–3774, Oct. 2013.

[83] V. P. Chemicals, “Veiligheidsinformatieblad.”

[84] G. Hartsgrove, A. Kraszewski, and A. Surowiec, “Simulated biological materials for electromagnetic radiation absorption studies,” *Bioelectromagnetics*, vol. 8, no. 1, pp. 29–36, 1987.

[85] S. Poompavai and V. Gowri Sree, “Dielectric Property Measurement of Breast—Tumor Phantom Model Under Pulsed Electric Field Treatment,” *IEEE Trans. Radiat. Plasma Med. Sci.*, vol. 2, no. 6, pp. 608–617, Sep. 2018.

[86] L. K. Baxter, *Capacitive Sensors*. 1997.

[87] E. Terzic, J. Terzic, R. Nagarajah, and M. Alamgir, “Chapter 2 Capacitive Sensing Technology,” in *A Neural Network Approach to Fluid Quantity Measurement in Dynamic Environments*, 2012, pp. 11–37.

[88] T. Yamamoto and K. Koshiji, “Electromagnetic high-hydrous gel phantom at a low-frequency band-improvement in the electrical characteristics by using a carbon microcoil and investigation of its mechanism-,” in *IFMBE Proceedings*, 2015, vol. 51, pp. 1383–1386.

[89] HP, “Operation and service manual Model 4192A LF IMPEDANCE ANALYZER.” p. 115, 1983.

[90] B. L. Oliveira, “Microwave Breast Imaging: Experimental tumour phantoms for the evaluation of new breast cancer diagnosis systems,” *Biomed. Phys. Eng. Express*, vol. 4, p. 17, 2018.

[91] P. P. Lelovas, N. G. Kostomitsopoulos, and T. T. Xanthos, “A comparative anatomic and physiologic overview of the porcine heart,” *J. Am. Assoc. Lab. Anim. Sci.*, vol. 53, no. 5, pp. 432–438, Sep. 2014.

[92] V. Lopresto, R. Pinto, R. Lodato, G. A. Lovisolo, and M. Cavagnaro, “Design and realisation of tissue-equivalent dielectric simulators for dosimetric studies on microwave antennas for interstitial ablation,” *Phys. Medica*, vol. 28, no. 3, pp. 245–253, Jul. 2011.

[93] A. H. A. Wahab *et al.*, “Developing functionally graded PVA hydrogel using simple freeze-thaw method for artificial glenoid labrum,” *J. Mech. Behav. Biomed. Mater.*, vol. 91, pp. 406–415, Mar. 2019.

[94] R. Plonsey, “Bioelectric Phenomena,” in *Wiley Encyclopedia of Electrical and Electronics Engineering*, John Wiley & Sons, Inc., 1999.

[95] P. Ben Ishai, M. S. Talary, A. Caduff, E. Levy, and Y. Feldman, “Electrode polarization in dielectric measurements: A review,” *Measurement Science and Technology*, vol. 24, no. 10. Institute of Physics Publishing, pp. 102001–102022, 27-Aug-2013.

[96] “Conductivity Theory and Practice.” SAS, Radiometer Analytical, pp. 1–50, 2004.

[97] H. W. Choi *et al.*, “Conductance catheter measurements of lumen area of stenotic coronary arteries: theory and experiment,” *J Appl Physiol*, vol. 111, pp. 758–765, 2011.

[98] P. G. T. van Berckel, “Developing a Breast Phantom to Test and Validate the Smart Electrosurgical Knife,” 2020.

[99] “Relative Permittivity - the Dielectric Constant.” [Online]. Available: https://www.engineeringtoolbox.com/relative-permittivity-d_1660.html. [Accessed: 19-Jul-2020].

[100] R. M. Souza, T. Q. Santos, D. P. Oliveira, R. M. Souza, A. V. Alvarenga, and R. P. B. Costa-Felix,

"Standard operating procedure to prepare agar phantoms," *J. Phys. Conf. Ser.*, vol. 733, no. 1, 2016.

[101] T. J. Kao, G. J. Saulnier, D. Isaacson, T. L. Szabo, and J. C. Newell, "A versatile high-permittivity phantom for EIT," *IEEE Trans. Biomed. Eng.*, vol. 55, no. 11, pp. 2601–2607, Nov. 2008.

[102] E. Repetti, "Design and develop a 3D printed medical phantom and mechanical characteristics bronchial tree geometrical able to replicate lungs and as human tissue," 2019.

[103] S. Paţachia, C. Florea, C. Friedrich, and Y. Thomann, "Tailoring of poly(vinyl alcohol) cryogels properties by salts addition," *Express Polym. Lett.*, vol. 3, no. 5, pp. 320–331, May 2009.

[104] H. C. Price, J. Mattsson, and B. J. Murray, "Sucrose diffusion in aqueous solution," *Phys. Chem. Chem. Phys.*, vol. 18, no. 28, pp. 19207–19216, 2016.

[105] E. Ohmae *et al.*, "Stable tissue-simulating phantoms with various water and lipid contents for diffuse optical spectroscopy," 2018.

[106] S. K. Kim, *Handbook of Marine Macroalgae*. Chichester, UK: John Wiley & Sons, Ltd, 2011.

[107] J. Li, P. C. Ma, W. S. Chow, C. K. To, B. Z. Tang, and J. K. Kim, "Correlations between percolation threshold, dispersion state, and aspect ratio of carbon nanotubes," *Adv. Funct. Mater.*, vol. 17, no. 16, pp. 3207–3215, Nov. 2007.

[108] H.-J. Choi, M. sung Kim, D. Ahn, S. Young Yeo, and S. Lee, "electrical percolation threshold of carbon black in a polymer matrix and its application to antistatic fibre," *Sci. Rep.*, vol. 9, p. 12, 2019.

[109] A. Battisti, A. A. Skordos, and I. K. Partridge, "Percolation threshold of carbon nanotubes filled unsaturated polyesters," *Compos. Sci. Technol.*, vol. 70, no. 4, pp. 633–637, Apr. 2010.

[110] J. Garrett and E. Fear, "Stable and Flexible Materials to Mimic the Dielectric Properties of Human Soft Tissues," *IEEE Antennas Wirel. Propag. Lett.*, vol. 13, pp. 599–602, 2014.

[111] L. A. Reis, L. L. Y. Chiu, N. Feric, L. Fu, M. Radisic, and A. Chemistry, "Biomaterials in myocardial tissue engineering," *J Tissue Eng Regen Med.*, vol. 10, no. 1, pp. 11–28, 2016.

[112] A. Arani *et al.*, "Cardiac MR Elastography for Quantitative Assessment of Elevated Myocardial Stiffness in Cardiac Amyloidosis," *J. Magn. Reson. Imaging*, vol. 46, pp. 1361–1367, 2017.

[113] A. Kolipaka *et al.*, "A Feasibility Study: MR Elastography as a Method to Compare Stiffness Estimates in Hypertrophic Obstructive Cardiomyopathy and in Normal Volunteers," *Proc. Intl. Soc. Mag. Reson. Med.*, vol. 19, p. 274, 2011.

[114] C. F. Guimarães, L. Gasperini, A. P. Marques, and R. L. Reis, "The stiffness of living tissues and its implications for tissue engineering," *Nature Reviews Materials*, vol. 5, no. 5. Nature Research, pp. 351–370, 01-May-2020.

[115] F. Nemavhola, "Biaxial quantification of passive porcine myocardium elastic properties by region," *Eng. Solid Mech.*, vol. 5, no. 3, pp. 155–166, 2017.

[116] N. Momtahan *et al.*, "Automation of Pressure Control Improves Whole Porcine Heart Decellularization," *Tissue Eng. - Part C Methods*, vol. 21, no. 11, pp. 1148–1161, Nov. 2015.

[117] K. Verma, S. Mukherjee, P. Gaur, A. Chawla, R. Malhotra, and S. Lalwani, "High strain rate compressive behaviour of human heart," *Int. J. Exp. Comput. Biomech.*, vol. 4, no. 2/3, p. 152, 2018.

[118] M. S. Sirry *et al.*, “Characterisation of the mechanical properties of infarcted myocardium in the rat under biaxial tension and uniaxial compression,” *J. Mech. Behav. Biomed. Mater.*, 2016.

[119] K. Wang, S. Yen Ho, D. G. Gibson, and R. H. Anderson, “Architecture of atrial musculature in humans,” 1995.

[120] “Smooth-On XTC-3D Epoxyhars - 3DJake Nederland.” [Online]. Available: https://www.3djake.nl/smooth-on/xtc-3d-epoxyhars?sai=702&gclid=CjwKCAjwwab7BRBAEiwAapqpTNgV7mV5QoHfYMA0tQ88G0YpP_6tPma58g1N3w4r-g5JqS7adGzVkxoCtHoQAvD_BwE. [Accessed: 22-Sep-2020].

[121] T. A. Krouskop, T. M. Wheeler, F. Kallel, B. S. Garra, and T. Hall, “Elastic moduli of breast and prostate tissues under compression,” *Ultrason. Imaging*, vol. 20, no. 4, pp. 260–274, 1998.

[122] J. Laing, J. Moore, R. Vassallo, D. Bainbridge, M. Drangova, and T. Peters, “Patient-specific cardiac phantom for clinical training and preprocedure surgical planning,” *J. Med. Imaging*, vol. 5, no. 02, p. 1, Mar. 2018.

[123] P. R. Stauffer *et al.*, “Phantom and animal tissues for modelling the electrical properties of human liver,” *Int. J. Hyperth.*, vol. 19, no. 1, pp. 89–101, 2003.

[124] J. B. Li *et al.*, “A New Head Phantom With Realistic Shape and Spatially Varying Skull Resistivity Distribution,” *IEEE Trans. Biomed. Eng.*, vol. 61, no. 2, pp. 254–263, 2014.

[125] J. L. Schwartz and G. A. R. Mealing, “Dielectric properties of frog tissues in vivo and in vitro,” *Phys. Med. Biol.*, vol. 30, no. 2, pp. 117–124, 1985.

[126] G. M. Hahn *et al.*, “Some heat transfer problems associated with heating by ultrasound, microwaves, or radio frequency,” *Ann. N. Y. Acad. Sci.*, vol. 335, no. 1, pp. 327–346, 1980.

[127] D. Xu, L. Liu, and Z. Jiang, “Measurement of the dielectric properties of biological substances using an improved open-ended coaxial line resonator method,” *IEEE Trans. Microw. Theory Tech.*, vol. 35, no. 12, pp. 1424–1428, 1987.

[128] A. Surowiec, S. S. Stuchly, L. Eidus, and A. Swarup, “In vitro dielectric properties of human tissues at radiofrequencies,” *Phys. Med. Biol.*, vol. 32, no. 5, pp. 615–621, 1987.

[129] H. P. Schwan, “Electrical properties measured with alternating currents; body tissues,” *Handb. Biol. Data ed WS Spector*, 1956.

[130] H. P. SCHWAN, “Electrical properties of tissue and cell suspensions.,” *Adv. Biol. Med. Phys.*, vol. 5, pp. 147–209, 1957.

[131] H. P. Schwan, “Electric characteristics of Tissues,” 1963.

# Appendices

## Appendix A

**Findings from literature and experiments of S. Gabriel et al (1996) [25]**

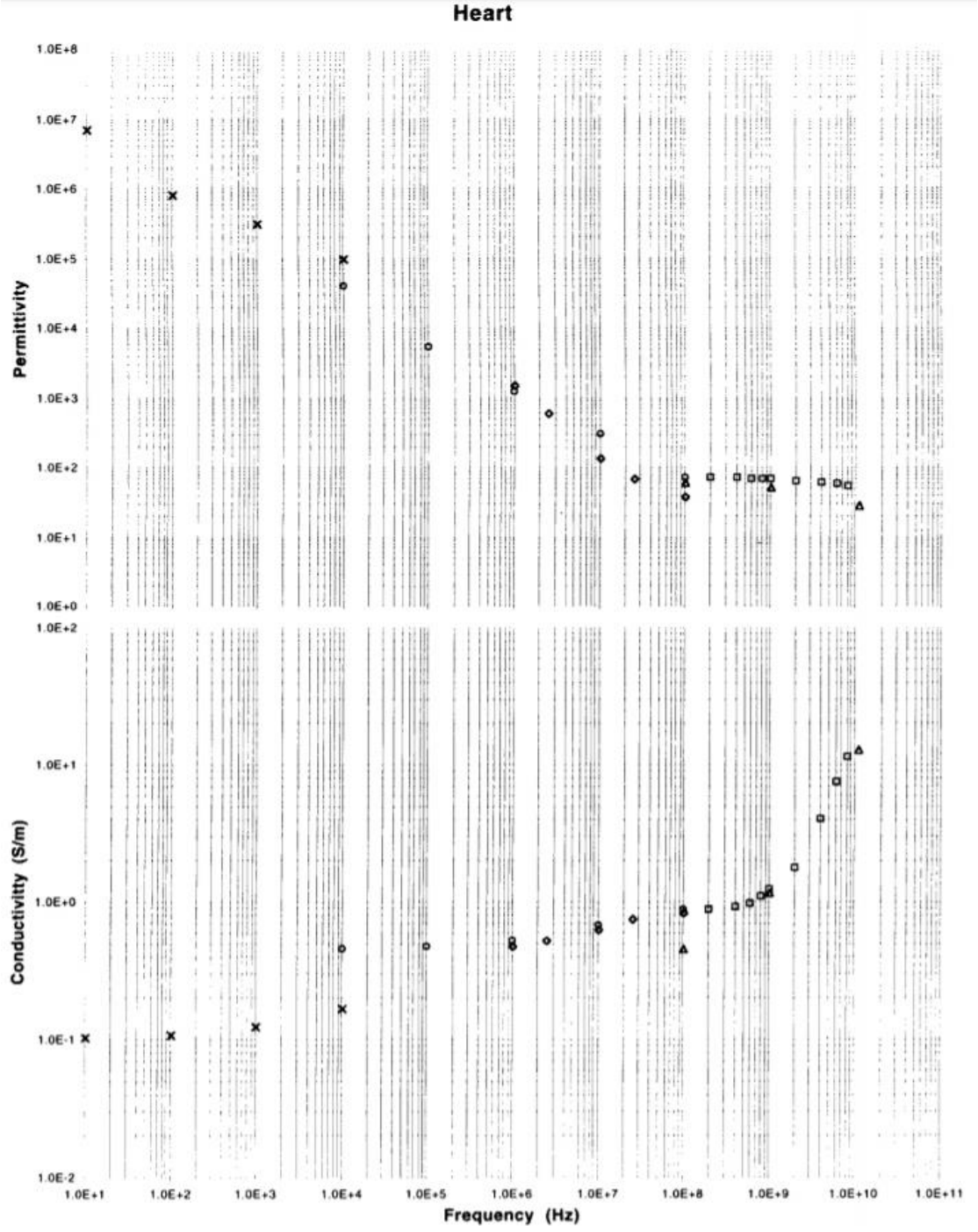


□ Bullfrog (In vivo) at 22°C (2E8 – 8E9 Hz) [125]
◊ Porcine (In vivo) at 34 – 36°C (1E6 – 1E8 Hz) [126]
Δ Canine at 20°C ± 1°C (1E8 – 1E10 Hz) [127]
○ Human at 36.8°C (1E4 – 1E8 Hz) [128]
x Canine (In situ) at 37°C (1E1 – 1E4 Hz) [129] [130] [131]

*Figure 63: Survey of permittivity and conductivity of tissues in the frequency range 10 Hz to 100 GHz at temperatures as low as 20 °C* [25]

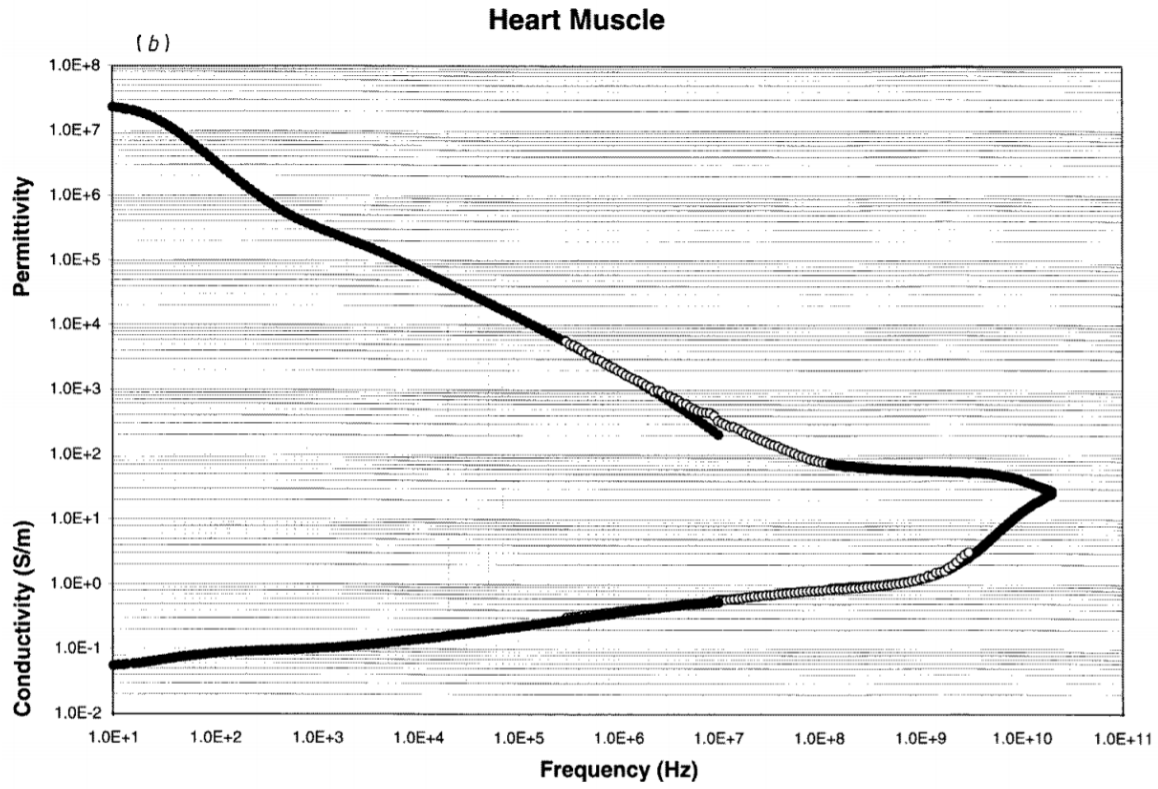


*Figure 64: The permittivity and conductivity of bovine heart muscle tissue from measurements at body temperature on three experimental arrangements with overlapping frequency coverage* [28]

# Appendix B

**All phantom preparations**

## B1 All prepared phantoms

**Mixing procedures of all prepared phantoms**

| Phantom number* | Materials** | Amount (g) | Mixing order | Temperature (°C) | Time (minutes) | Additional information*** |
|---|---|---|---|---|---|---|
| **1** | PVA | 10 | 2 | 20 – 85 | 60 | |
| | Salt | 2 | 1 | 20 | 10 | |
| | DEMI water | 100 | 1 | 20 | | |
| **2** | PVA | 10 | 2 | 20 – 85 | 60 | |
| | Salt | 10 | 1 | 20 | 10 | |
| | DEMI water | 100 | 1 | 20 | | |
| **3** | PVA | 10 | 2 | 32.5 – 95 | 60 | |
| | Graphite | 25 | 1 | 20 – 65 – 32.5 | 45 | |
| | Tap water | 100 | 1 | 19.5 – 85 | 60 | |
| **4** | PVA | 10 | 1 | 85 | 45 | |
| | Graphite | 25 | 2 | | | |
| | Tap water | 100 | 1 | | | |
| **5** | Agar | 3 | 2 | 85 | 3 | After 3 min. clumpy |
| | Tap water | 50 | 1 | 85 | | Very stiff and brittle |
| **6** | Agar | 2 | 2 | 85 | 15 | Very stiff and brittle |
| | Tap water | 50 | 1 | 85 | | |
| **7** | PVA | 10 | 2 | 20 – 85 | 60 | Clumpy while mixing |
| | Glycine | 20 | 1 | 20 | 10 | |
| | Tap water | 100 | 1 | | | |
| **8** | Agar | 2 | 2 | 85 | 15 | Brittle |
| | Tap water | 100 | 1 | 85 | | |
| **9** | Agar | 2 | 2 | 85 | 15 | |
| | Salt | 10 | 1 | 85 | 10 | |
| | Tap water | 100 | 1 | | | |
| **10** | Agar | 2 | 2 | 85 | 15 | Releases graphite |
| | Graphite | 25 | 3 | 85 | 30 | |
| | Tap water | 100 | 1 | 85 | | |
| **11** | Agar | 2 | 2 | 85 | 15 | Too soft |
| | Glycine | 10 | 3 | 85 | 15 | |
| | Tap water | 100 | 1 | 85 | | |
| **12** | PVA | 5 | 1 | 20 – 85 | 60 | Clumpy while mixing |
| | Glycine | 10 | 2 | 85 - 90 | 120 | |

| | | | | | | |
|---|---|---|---|---|---|---|
| | Tap water | 100 | 1 | | | |
| **13** | PVA | 5 | 1 | 20 – 85 | 60 | |
| | Glycine | 10 | 1 | | | |
| | Tap water | 100 | 1 | | | |
| **14** | PVA | 5 | 1 | 20 – 85 | 120 | |
| | Glycine | 10 | 1 | | | |
| | Tap water | 100 | 1 | | | |
| **15** | PVA | 5 | 1 | 20 – 85 – 20 | 60 min at 85 °C | |
| | Glycine | 10 | 1 | | | |
| | Tap water | 100 | 1 | | | |
| **16** | PVA | 5 | 2 | 20 - 85 | 70 | |
| | Graphite | 25 | 1 | 20 | 5 | |
| | Acetone | 100 | 1 | | | |
| | Tap water | 1 | 1 | | | |
| **17** | Agar | 2 | 2 | 85 | 15 | Releases graphite |
| | Graphite | 25 | 3 | 85 | 30 | |
| | Tap water | 100 | 1 | 85 | | |
| | Acetone | 1 | 3 | | | |
| **18** | PVA | 5 | 2 | 20 - 85 | 70 | Charcoal precipitated |
| | Charcoal | 3 | 1 | 20 | 5 | |
| | Tap water | 100 | 1 | | | |
| **19** | PVA | 5 | 1 | 20 - 85 | 80 | |
| | Glycine | 10 | 1 | | | |
| | Acetone | 100 | 1 | | | |
| | Tap water | 1 | 1 | | | |
| **20** | Agar | 2 | 2 | 85 | 15 | Releases charcoal |
| | Charcoal | 3 | 3 | 85 | 30 | |
| | Tap water | 100 | 1 | 85 | | |
| **21** | Gellan gum | 1 | 2 | 95 | | Clumpy while mixing |
| | Tap water | 50 | 1 | 95 | | |
| **22** | Gellan gum | 1 | 1 | 20 – 95 | | Clumpy while mixing |
| | Tap water | 50 | 1 | | | |
| **23** | Gellan gum | 0,6 | 2 | 20 – 98 | 50 | Sticky phantom |
| | Tap water | 50 | 1 | | | |
| **24** | Gellan gum | 1 | 2 | 95 – 98 | 50 | |
| | Tap water | 50 | 1 | | | |
| **25** | Gellan gum | 2 | 2 | 95 – 98 | 50 | More brittle |
| | Tap water | 100 | 1 | | | |
| | Glycine | 10 | 3 | 95 | 40 | |
| **26** | Gellan gum | 3 | 2 | 95 – 98 | 50 | Sticky phantom |
| | Tap water | 100 | 1 | | | |
| | Graphite | 25 | 3 | 95 – 98 | 40 | |

| | | | | | | |
|---|---|---|---|---|---|---|
| **27** | Gellan gum | 3 | 2 | 95 – 98 | 50 | |
| | Tap water | 100 | 1 | | | |
| | Charcoal | 3 | 3 | 95 – 98 | 40 | |
| **28** | Gellan gum | 3 | 2 | 95 – 98 | 50 | Clumpy while adding Salt |
| | Tap water | 100 | 1 | | | |
| | Salt | 10 | 3 | 95 – 98 | | |
| **29** | Gellan gum | 3 | 3 | 95-98 | 50 | No solidification |
| | Tap water | 100 | 1 | | | |
| | Salt | 10 | 2 | 85-95 | 5 | |
| **30** | Agar | 2 | 2 | 85 | 15 | |
| | Glycine | 10 | 3 | 85 | 30 | |
| | Tap water | 100 | 1 | 85 | | |
| **31** | Agar | 2 | 2 | 85 | 15 | |
| | Glycine | 10 | 3 | 85 | 30 | |
| | Tap water | 100 | 1 | 85 | | |
| | Acetone | 1 | 3 | | | |
| **32** | Gellan gum | 3 | 3 | 95-98 | 50 | No solidification |
| | Tap water | 100 | 1 | 85 | | |
| | Salt | 10 | 2 | 85-95 | 5 | |
| **33** | Gellan gum | 3 | 3 | 95-98 | 50 | |
| | Tap water | 100 | 1 | 85 | | |
| | Salt | 5 | 2 | 85-95 | 5 | |
| **34** | Gellan gum | 3 | 2 | 95-98 | 50 | |
| | Tap water | 100 | 1 | | | |
| | Glycine | 10 | 3 | 95 | 40 | |
| **35** | Agar | 3 | 2 | 85 | 15 | |
| | Tap water | 100 | 1 | 85 | | |
| **36** | Gellan gum | 3 | 2 | 95-98 | 50 | |
| | DIW | 100 | 1 | 85 | | |
| **37** | Gellan gum | 3 | 2 | 95-98 | 50 | |
| | DIW | 100 | 1 | 85 | | |
| | Sodium acetate | 1 | 2 | | | |
| **38** | Agar | 4 | 2 | 85 | 15 | |
| | Tap water | 100 | 1 | 85 | | |
| **39** | PVA | 5 | 2 | 20 - 85 | 60 | |
| | Charcoal | 3 | 1 | 20 | 5 | |
| | Tap water | 100 | 1 | | | |
| **41** | Gellan gum | 3 | 3 | 95 | 50 | |
| | DIW | 80 | 1 | 85 | | |
| | Salt | 5 | 2 | 85-95 | 5 | |
| | Sodium acetate | 1 | 2 | | | |
| **42** | Gellan gum | 3 | 2 | 95-98 | 50 | |
| | Tap water | 100 | 1 | | | |
| | Charcoal | 3 | 3 | 95-98 | 40 | |

| | | | | | | |
|---|---|---|---|---|---|---|
| | Sodium acetate | 1 | 2 | | | |
| **43** | Gellan gum | 3 | 3 | 95-98 | 50 | No solidification |
| | DIW | 80 | 1 | 85 | | |
| | Salt | 5 | 2 | 85-95 | 5 | |
| | Sodium acetate | 1 | 2 | | | |
| **44** | Gellan gum | 3 | 3 | 98-100 | 50 | No solidification |
| | DIW | 60 | 1 | 85 | | |
| | Salt | 5 | 2 | 85-95 | 5 | |
| | Sodium acetate | 1 | 2 | | | |
| **45** | Gellan gum | 3 | 2 | 98-100 | 50 | No solidification |
| | Tap water | 100 | 1 | | | |
| **46** | Gellan gum | 3 | 2 | 98-100 | 50 | |
| | Tap water | 100 | 1 | | | |
| **47** | Gellan gum | 3 | 3 | 98-100 | 50 | No solidification |
| | DIW | 100 | 1 | 85 | | |
| | Salt | 5 | 2 | 85-95 | 5 | |
| | Sodium acetate | 1 | 2 | | | |
| **48** | Gellan gum | 3 | 3 | 98-100 | 50 | No solidification |
| | DIW | 100 | 1 | 85 | | |
| | Salt | 5 | 2 | 85-95 | 5 | |
| | Sodium acetate | 1 | 2 | | | |
| **49** | Gellan gum | 3 | 3 | 98-100 | 50 | No solidification |
| | DIW | 75 | 1 | 85 | | |
| | Salt | 5 | 2 | 85-95 | 5 | |
| | Sodium acetate | 1 | 2 | | | |
| **50** | Gellan gum | 3 | 2 | 95-98 | 50 | No solidification |
| | DIW | 100 | 1 | | | |
| | Glycine | 10 | 3 | 95 | 40 | |
| | Sodium acetate | 1 | 2 | | | |
| **51** | PVA | 5 | 1 | 20-85 | 70 | Softer compared to PVA with tap water |
| | DIW | 100 | 1 | | | |
| **52** | PVA | 5 | 2 | 20-85 | 70 | Wet and brittle |
| | DIW | 100 | 1 | | | Phantom broke |
| | Salt | 10 | 1 | 20 | 10 | |
| **53** | PVA | 5 | 2 | 20 - 85 | 60 | |
| | Charcoal | 3 | 1 | 20 | 5 | |
| | DIW | 100 | 1 | | | |
| **54** | PVA | 5 | 1 | 20 - 85 | 60 | Brittle |
| | Glycine | 10 | 1 | | | |

| | | | | | | |
|---|---|---|---|---|---|---|
| | DIW | 100 | 1 | | | |
| **55** | PVA | 5 | 2 | 20 - 85 | 60 | |
| | Graphite | 10 | 1 | 20 | 5 | |
| | Tap water | 100 | 1 | | | |
| **56** | Gellan gum | 5 | 2 | 99 – 100 | | |
| | DIW | 100 | 1 | 98 | | |
| **57** | Agar | 6 | 2 | 85 | 15 | |
| | Tap water | 100 | 1 | 85 | | |
| **58** | Agar | 6 | 2 | 85 | 15 | |
| | DIW | 100 | 1 | 85 | | |
| **59** | Agar | 6 | 2 | 85 | 15 | |
| | DIW | 100 | 1 | 85 | | |
| | Sodium acetate | 2 | 2 | | | |
| **60** | Agar | 6 | 3 | 85 | 15 | |
| | DIW | 100 | 1 | 85 | | |
| | Salt | 10 | 2 | 85 | 10 | |
| | Sodium acetate | 2 | 3 | | | |
| **61** | Agar | 6 | 2 | 85 | 15 | |
| | Graphite | 25 | 3 | 85 | 15 | |
| | DIW | 100 | 1 | 85 | | |
| | Sodium acetate | 2 | 2 | | | |
| | Acetone | 1 | 3 | | | |
| **62** | Agar | 6 | 2 | 85 | 15 | |
| | Charcoal | 4 | 3 | 85 | 15 | |
| | DIW | 100 | 1 | 85 | | |
| | Sodium acetate | 2 | 2 | | | |
| | Acetone | 1 | 3 | | | |
| **63** | Agar | 6 | 2 | 85 | 15 | |
| | Glycine | 10 | 3 | 85 | 30 | |
| | Sodium acetate | 2 | 2 | 85 | | |
| | DIW | 100 | 1 | | | |
| | Acetone | 1 | 3 | | | |
| **64** | Gellan gum | 5 | 2 | 99-100 | 40 | |
| | DIW | 100 | 1 | | | |
| **65** | Gellan gum | 5 | 2 | 99-100 | 40 | |
| | DIW | 100 | 1 | | | |
| | Sodium acetate | 2 | 2 | | | |
| **66** | Gellan gum | 4 | 2 | 99-100 | 40 | |
| | DIW | 100 | 1 | | | |
| **67** | Gellan gum | 4 | 2 | 99-100 | 40 | |
| | DIW | 100 | 1 | | | |

| | | | | | | |
|---|---|---|---|---|---|---|
| | Sodium acetate | 2 | 2 | | | |
| **68** | Gellan gum | 4 | 3 | 99-100 | 40 | No solidification |
| | DIW | 100 | 1 | | | |
| | Sodium acetate | 2 | 2 | | | |
| | Salt | 10 | 2 | | 5 | |
| **69** | Gellan gum | 4 | 2 | 99-100 | 40 | Hard to mix |
| | DIW | 100 | 1 | | | |
| | Graphite | 21 | 3 | 99-100 | 30 | |
| | Sodium acetate | 2 | 2 | | | |
| | Acetone | 2 | 3 | | | |
| **70** | Gellan gum | 4 | 2 | 99-100 | 40 | |
| | DIW | 100 | 1 | | | |
| | Glycine | 25 | 3 | 99-100 | 30 | |
| | Sodium acetate | 2 | 2 | | | |
| **71** | PVA | 5 | 1 | 20-85 | 70 | Too soft |
| | 0.9% saline | 100 | 1 | | | |
| **72** | PVA | 5 | 1 | 20-85 | 70 | Too soft |
| | DIW | 100 | 1 | | | |
| **73** | Agar | 6 | 2 | 85 | 15 | |
| | Sodium acetate | 2 | 2 | 85 | | |
| | 0.9% saline | 100 | 1 | 85 | | |
| **74** | Gellan gum | 4 | 2 | 99-100 | 40 | |
| | 0.9% saline | 100 | 1 | | | |
| | Sodium acetate | 2 | 2 | | | |
| **75** | Gellan gum | 4 | 2 | 99-100 | 40 | |
| | 0.9% saline | 100 | 1 | | | |
| | Graphite | 60 | 3 | 99-100 | 30 | |
| | Sodium acetate | 2 | 2 | | | |
| | Acetone | 2 | 3 | | | |
| **76** | Agar | 6 | 2 | 85 | 15 | |
| | Sodium acetate | 2 | 2 | 85 | | |
| | 0.9% saline | 100 | 1 | | | |
| | Acetone | 1 | 3 | | | |
| | Graphite | 80 | 3 | 85 | 15 | Mix by hand |
| **77** | PVA | 10 | 1 | 20-85 | 70 | |
| | 0.9% saline | 100 | 1 | | | |
| **78** | PVA | 10 | 2 | 20-85 | 70 | |
| | 0.9% saline | 100 | 1 | | | |
| | Graphite | 60 | 1 | 20 | 5 | |
| **79** | PVA | 10 | 2 | 20-85 | 70 | Brittle |

| | | | | | | |
|---|---|---|---|---|---|---|
| | Tap water | 100 | 1 | | | Phantom broke |
| | Salt | 12 | 1 | 20 | 5 | |
| **80** | Agar | 6 | 2 | 85 | 15 | |
| | DIW | 100 | 1 | 85 | | |
| **81** | Agar | 6 | 2 | 85 | 15 | |
| | Tap water | 100 | 1 | 85 | | |
| **82** | Agar | 6 | 2 | 85 | 15 | |
| | 0.9% saline | 100 | 1 | 85 | | |
| **83** | Agar | 4 | 2 | 85 | 15 | |
| | Tap water | 100 | 1 | 85 | | |
| **84** | Gellan gum | 4 | 2 | 99-100 | 40 | |
| | Tap water | 100 | 1 | | | |
| **85** | Gellan gum | 4 | 2 | 85-100 | 40 | |
| | 0.9% saline | 100 | 1 | | | |
| **86** | Gellan gum | 4 | 3 | 95-98 | 40 | Clumpy while mixing |
| | DIW | 100 | 1 | | | |
| | Salt | 5 | 2 | 95 | 5 | |
| **87** | PVA | 10 | 1 | 20-85 | 70 | |
| | Tap water | 100 | 1 | | | |
| **88** | PVA | 10 | 1 | 20-85 | 70 | |
| | DIW | 100 | 1 | | | |
| **89** | PVA | 5 | 1 | 20-85 | 70 | |
| | Tap water | 100 | 1 | | | |
| **90** | PVA | 5 | 1 | 20-85 | 70 | |
| | Tap water | 100 | 1 | | | |
| | Sodium acetate | 2 | 1 | | | |
| **91** | PVA | 5 | 1 | 20 - 85 | 60 | Precipitation of glycine |
| | Glycine | 10 | 1 | | | |
| | Tap water | 100 | 1 | | | |
| **92** | Gellan gum | 4 | 3 | 85-100 | 40 | |
| | Tap water | 100 | 1 | | | |
| | Salt | 5 | 2 | 85 | 5 | |
| **93** | Gellan gum | 4 | 3 | 85-100 | 40 | Too soft & brittle |
| | Tap water | 100 | 1 | | | |
| | Glycine | 20 | 2 | 85 | 10 | |
| **94** | Gellan gum | 3 | 3 | 85-100 | 40 | |
| | Tap water | 100 | 1 | | | |
| | Salt | 5 | 2 | 85 | 3 | |
| **95** | Agar | 6 | 3 | 85 | 15 | |
| | Tap water | 100 | 1 | 85 | | |
| | Salt | 10 | 2 | 85 | 5 | |
| **96** | Agar | 6 | 2 | 85 | 15 | |
| | Glycine | 10 | 3 | 85 | 30 | |
| | Tap water | 100 | 1 | | | |

| | | | | | | |
|---|---|---|---|---|---|---|
| **97** | PVA | 6 | 1 | 20 - 90 | 60 | No homogeneous mixture |
| | 0.9% saline | 100 | 1 | | | |
| | Glycine | 10 | 1 | | | |
| **98** | PVA | 6 | 1 | 20 - 90 | 60 | |
| | 0.9% saline | 100 | 1 | | | |
| **99** | PVA | 6 | 1 | 20-90 | 70 | |
| | Tap water | 100 | 1 | | | |
| | Sodium acetate | 1 | 1 | | | |
| **100** | Gellan gum | 3 | 2 | 99-100 | 40 | |
| | Tap water | 100 | 1 | | | |
| **101** | Gellan gum | 3 | 2 | 85-100 | 40 | |
| | 0.9% saline | 100 | 1 | | | |
| **102** | Gellan gum | 3 | 2 | 85-100 | 40 | |
| | DIW | 100 | 1 | | | |
| **103** | Agar | 6 | 2 | 85 | 15 | |
| | Sodium acetate | 1 | 2 | | | |
| | Tap water | 100 | 1 | 85 | | |
| **104** | Agar | 6 | 2 | 85 | 15 | |
| | Glycine | 10 | 3 | 85 | 30 | |
| | 0.9% saline | 100 | 1 | 85 | | |
| **105** | Agar | 6 | 2 | 85 | 15 | Stored in saline |
| | 0.9% saline | 100 | 1 | | | |
| **106** | Agar | 6 | 2 | 85 | 15 | Stored in tap water |
| | 0.9% saline | 100 | 1 | | | |
| **107** | Agar | 6 | 2 | 85 | 15 | Stored in saline |
| | Tap water | 100 | 1 | | | |
| **108** | Agar | 6 | 2 | 85 | 15 | Stored in tap water |
| | Tap water | 100 | 1 | | | |
| **109** | Agar | 6 | 1 | 85 | 15 | |
| | 0.9% saline | 100 | 1 | | | |
| | Acetone | 2 | 1 | | | |
| **110** | Agar | 6 | 1 | 85 | 15 | |
| | Tap water | 100 | 1 | | | |
| | acetone | 2 | 1 | | | |
| **111** | PVA | 6 | 1 | 20-95 | 70 | |
| | Tapwater | 100 | 1 | | | |
| **112** | PVA | 6 | 2 | 20-95 | 60 | Turn off stove and continue mixing till room temperature |
| | Tapwater | 100 | 1 | | | |

| | | | | | | |
|---|---|---|---|---|---|---|
| | Graphite | 10 | 1 | 20 | 5 | Precipitation of graphite |
| **113** | Agar | 6 | 1 | 85 | 15 | |
| | Tap water | 100 | 1 | | | |
| **114** | Agar | 6 | 2 | 85 | 15 | |
| | Tap water | 100 | 1 | | | |
| | Salt | 2 | 1 | 85 | 5 | |
| **115** | Agar | 6 | 2 | 85 | 15 | |
| | Tap water | 100 | 1 | | | |
| | Salt | 3 | 1 | 85 | 5 | |
| **116** | Agar | 6 | 2 | 85 | 15 | |
| | Tap water | 100 | 1 | | | |
| | Graphite | 20 | 3 | 85 | 15 | |
| | Acetone | 2 | 3 | | | |
| **117** | PVA | 6 | 2 | 20-95 | 60 | Turn off stove and continue mixing till room temperature |
| | Tap water | 100 | 1 | | | |
| | Charcoal | 2 | 1 | 20 | 5 | Precipitation of charcoal |
| **118** | Agar | 6 | 2 | 85 | 15 | |
| | Tap water | 100 | 1 | | | |
| | Charcoal | 2 | 3 | 85 | 15 | |
| **119** | Agar | 6 | 2 | 85 | 15 | |
| | Tap water | 100 | 1 | | | |
| | Glycine | 5 | 3 | 85 | 30 | |
| | Sodium acetate | 0,5 | 2 | | | |
| **120** | Gellan gum | 4 | 2 | 85-100 | 40 | |
| | Tap water | 100 | 1 | | | |
| **121** | PVA | 6 | 2 | 20 - 85 | 60 | Turn off stove and continue mixing |
| | Tap water | 100 | 1 | | | |
| | Glycine | 10 | 1 | 20 | 5 | Precipitation of glycine |
| | Sodium acetate | 0,5 | 1 | 20 - 85 | 60 | |
| **122** | Gellan gum | 5 | 2 | 85-100 | 40 | |
| | Tap water | 100 | 1 | | | |
| **123** | Gellan gum | 3 | 2 | 85-100 | 40 | |
| | Tap water | 100 | 1 | | | |
| **124** | Gellan gum | 3 | 2 | 85-100 | 40 | |
| | Tap water | 100 | 1 | | | |
| | Sodium acetate | 1 | 2 | | | |
| **125** | Gellan gum | 4 | 2 | 85 | 40 | |

| | | | | | | |
|---|---|---|---|---|---|---|
| | Tap water | 100 | 1 | 85 | | |
| | Graphite | 10 | 3 | 85 -100 | 40 | Mix graphite with hot water before mixing with gellan gum mixture |
| **126** | Gellan gum | 4 | 2 | 85 | 40 | |
| | Tap water | 100 | 1 | 85 | | |
| | Charcoal | 2 | 3 | 85 -100 | 40 | |
| **127** | Gellan gum | 4 | 3 | 85-100 | 40 | |
| | Tap water | 100 | 1 | 85 | | |
| | Glycine | 5 | 2 | 85 | 10 | |
| | Sodium acetate | 0,5 | 2 | | | |
| **128** | Agar | 6 | 2 | 85 | 15 | |
| | Tap water | 100 | 1 | | | |
| | Graphite | 30 | 3 | 85 | 15 | |
| | Acetone | 7 | 3 | | | |
| **129** | Agar | 6 | 2 | 85 | 15 | |
| | Tap water | 100 | 1 | | | |
| | Graphite | 25 | 3 | 85 | 15 | |
| | Acetone | 5 | 3 | | | |
| **130** | Agar | 6 | 2 | 85 | 15 | |
| | Tap water | 100 | 1 | | | |
| | Charcoal | 3 | 3 | 85 | 15 | |
| **131** | Agar | 6 | 2 | 85 | 15 | |
| | Tap water | 100 | 1 | | | |
| | Salt | 0,5 | 1 | 85 | 5 | |
| **132** | Gellan gum | 4 | 3 | 85-100 | 40 | |
| | Tap water | 100 | 1 | 85 | | |
| | Glycine | 10 | 2 | 85 | 10 | |
| | Sodium acetate | 0,5 | 2 | | | |
| **133** | Gellan gum | 4 | 3 | 85 | 30 | |
| | Tap water | 100 | 1 | 85 | | |
| | Glycine | 5 | 2 | 85 | 5 | |
| | Charcoal | 2 | 4 | 85 -100 | 40 | Mix charcoal with hot water before mixing with gellan gum mixture |
| **134** | Gellan gum | 4 | 2 | 85 | 40 | |
| | Tap water | 100 | 1 | 85 | | |
| | Graphite | 5 | 3 | 85 -100 | 40 | Mix graphite with hot water before mixing with gellan gum mixture |
| **135** | Gellan gum | 3 | 3 | 85-100 | 40 | |

| | | | | | | |
|---|---|---|---|---|---|---|
| | Tap water | 100 | 1 | | | |
| | Salt | 1 | 2 | 85 | 3 | |
| **136** | PVA | 10 | 1 | 20 - 90 | 60 | |
| | 0.9% saline | 100 | 1 | | | |
| **137** | PVA | 12 | 1 | 20 - 90 | 60 | |
| | 0.9% saline | 100 | 1 | | | |
| **138** | PVA | 15 | 1 | 20 - 90 | 60 | |
| | 0.9% saline | 100 | 1 | | | |
| **139** | Gellan gum | 4 | 2 | 85-100 | 40 | |
| | Tap water | 100 | 1 | | | |
| **140** | Agar | 6 | 1 | 85 | 15 | |
| | Tapwater | 100 | 1 | | | |
| **141** | PVA | 15 | 1 | 20 | 15 | |
| | 0.9% saline | 100 | 1 | | | |
| | Oil | 10 | 2 | 20-90 | 50 | |
| **142** | PVA | 15 | 1 | 20 | 15 | |
| | 0.9% saline | 100 | 1 | | | |
| | Oil | 15 | 2 | 20-90 | 50 | |
| **143** | PVA | 15 | 1 | 20 | 15 | |
| | 0.9% saline | 100 | 1 | | | |
| | Ammonia | 10 | 2 | 20-90 | 50 | |
| **144** | PVA | 15 | 1 | 20 | 15 | |
| | 0.9% saline | 100 | 1 | | | |
| | Ammonia | 20 | 2 | 20-90 | 50 | |
| **145** | PVA | 15 | 2 | 20-90 | 50 | Turn off stove and continue mixing |
| | 0.9% saline | 100 | 1 | | | Stiffer phantom |
| | Glycine | 5 | 1 | 20-90 | 10 | |
| **146** | PVA | 15 | 2 | 20-90 | 50 | |
| | 0.9% saline | 100 | 1 | | | |
| | Sugar | 30 | 1 | 20-90 | 10 | |
| **147** | PVA | 15 | 2 | 20-90 | 50 | |
| | 0.9% saline | 100 | 1 | | | |
| | Sugar | 40 | 1 | 20-90 | 10 | |
| **148** | PVA | 10 | 1 | 20-90 | 60 | |
| | 0.9% saline | 100 | 1 | | | |
| | Antifrost | 5 | 1 | | | |
| **149** | PVA | 12 | 2 | 20-90 | 60 | |
| | 0.9% saline | 100 | 1 | | | |
| | Ethanol | 60 | 1 | 20 | 5 | |
| **150** | PVA | 12 | 2 | 20-90 | 60 | |
| | 0.9% saline | 100 | 1 | | | |
| | Ethanol | 40 | 1 | 20 | 5 | |
| **151** | PVA | 12 | 2 | 20-90 | 60 | |
| | 0.9% saline | 100 | 1 | | | |
| | Ethanol | 70 | 1 | 20 | 5 | |
| **152** | PVA | 15 | 1 | 20 | 15 | |

| | | | | | | |
|---|---|---|---|---|---|---|
| | 0.9% saline | 100 | 1 | | | |
| | Oil | 15 | 2 | 20-90 | 50 | |
| | Surfactant | 5 | 2 | | | |
| **153** | PVA | 15 | 1 | 20 | 15 | |
| | 0.9% saline | 100 | 1 | | | |
| | Oil | 15 | 2 | 20-90 | 50 | |
| | Surfactant | 10 | 2 | | | |
| **154** | PVA | 10 | 1 | 20-95 | 60 | |
| | Tap water | 100 | | | | |
| **155** | PVA | 15 | 1 | 20-95 | 60 | |
| | 0.9% saline | 100 | | | | |
| **156** | PVA | 10 | 2 | 20-90 | 50 | |
| | 0.9% saline | 100 | 1 | | | |
| | Sugar | 40 | 1 | 20-90 | 10 | |
| **157** | PVA | 15 | 2 | 20-90 | 50 | |
| | 0.9% saline | 100 | 1 | | | |
| | Sugar | 50 | 1 | 20-90 | 10 | |
| **158** | PVA | 10 | 2 | 20-90 | 50 | |
| | 0.9% saline | 100 | 1 | | | |
| | Sugar | 30 | 1 | 20-90 | 10 | |
| **159** | PVA | 15 | 2 | 20-90 | 50 | |
| | 0.9% saline | 100 | 1 | | | |
| | Sugar | 60 | 1 | 20-90 | 10 | |
| **160** | PVA | 15 | 2 | 20-90 | 50 | |
| | 0.9% saline | 100 | 1 | | | |
| | Glycine | 20 | 1 | 20-90 | 10 | |
| **161** | PVA | 15 | 1 | 20 | 15 | No soap bubble formation |
| | 0.9% saline | 100 | 1 | | | |
| | Oil | 30 | 2 | 20-90 | 50 | |
| | Surfactant | 5 | 2 | | | |
| **162** | PVA | 15 | 2 | 20-95 | 60 | |
| | Tap water | 100 | 1 | 20 | 5 | |
| | Salt | 0,15 | 1 | | | |
| **163** | PVA | 15 | 2 | 20 | 10 | |
| | Tap water | 100 | 1 | 20 | 5 | |
| | Salt | 0,15 | 1 | | | |
| | Oil | 10 | 3 | 20-95 | 60 | |
| | Surfactant | 1,5 | 3 | | | |
| **164** | PVA | 15 | 2 | 20 | 10 | |
| | Tap water | 100 | 1 | 20 | 5 | |
| | Salt | 0,15 | 1 | | | |
| | Oil | 20 | 3 | 20-95 | 60 | |
| | Surfactant | 2 | 3 | | | |
| **165** | PVA | 15 | 2 | 20-95 | 60 | |
| | Tap water | 100 | 1 | 20 | 5 | |
| | Salt | 0,15 | 1 | | | |
| | Sugar | 20 | 1 | | | |

| | | | | | | |
|---|---|---|---|---|---|---|
| **166** | PVA | 15 | 2 | 20-95 | 60 | |
| | Tap water | 100 | 1 | 20 | 5 | |
| | Salt | 0,15 | 1 | | | |
| | Sugar | 50 | 1 | | | |
| **167** | PVA | 15 | 2 | 20 | 10 | |
| | Tap water | 100 | 1 | 20 | 5 | |
| | Salt | 0,15 | 1 | | | |
| | Oil | 30 | 3 | 20-95 | 60 | |
| | Surfactant | 5 | 3 | | | |
| **168** | PVA | 15 | 2 | 20 | 10 | |
| | Tap water | 100 | 1 | 20 | 5 | |
| | Salt | 0,15 | 1 | | | |
| | Oil | 50 | 3 | 20-95 | 60 | |
| | Surfactant | 5,5 | 3 | | | |
| **169** | PVA | 15 | 2 | 20 | 60 | Turn off stove and continue mixing |
| | Tap water | 100 | 1 | 20 | 5 | Precipitation of graphite |
| | Salt | 0,15 | 1 | | | Stiffer phantoms |
| | Graphite | 25 | 1 | | | |
| | Acetone | | | | | |
| **170** | PVA | 15 | 2 | 20 | 60 | Turn off stove and continue mixing |
| | Tap water | 100 | 1 | 20 | 5 | Stiffer phantom |
| | Salt | 0,15 | 1 | | | Precipitation of graphite |
| | Graphite | 35 | 1 | | | |
| | Acetone | | | | | |
| **171** | PVA | 15 | 2 | 20 | 60 | Turn off stove and continue mixing |
| | Tap water | 100 | 1 | 20 | 5 | Precipitation of charcoal |
| | Salt | 0,15 | 1 | | | |
| | Charcoal | 5 | 1 | | | |
| | Acetone | | | | | |
| **172** | PVA | 15 | 2 | 20 | 60 | Turn off stove and continue mixing |
| | Tap water | 100 | 1 | 20 | 5 | Precipitation of charcoal |
| | Salt | 0,15 | 1 | | | |
| | Charcoal | 8 | 1 | | | |
| | Acetone | | | | | |
| **173** | PVA | 15 | 2 | 20 | 60 | |
| | Tap water | 100 | 1 | 20 | 5 | |
| | Salt | 0,15 | 1 | | | |

| | | | | | | |
|---|---|---|---|---|---|---|
| | Sodium acetate | 0,5 | 1 | | | |
| **174** | PVA | 15 | 2 | 20 | 60 | |
| | Tap water | 100 | 1 | 20 | 5 | |
| | Salt | 0,15 | 1 | | | |
| | Sodium acetate | 0,1 | 1 | | | |
| **175** | Agar | 6 | 2 | 85 | 15 | |
| | Tap water | 100 | 1 | | | |
| | Salt | 0,15 | 1 | 85 | 5 | |
| **176** | Gellan gum | 3 | 3 | 85-100 | 40 | |
| | Tap water | 100 | 1 | | | |
| | Salt | 0,15 | 2 | 85 | 3 | |
| **177** | Agar | 6 | 2 | 85 | 10 | |
| | Tap water | 100 | 1 | | | |
| | Salt | 0,15 | 1 | 85 | 5 | |
| | Graphite | 15 | 3 | 85 | 15 | |
| **178** | Agar | 6 | 2 | 85 | 10 | |
| | Tap water | 100 | 1 | | | |
| | Salt | 0,15 | 1 | 85 | 5 | |
| | Graphite | 20 | 3 | 85 | 15 | |
| **179** | Agar | 6 | 2 | 85 | 10 | |
| | Tap water | 100 | 1 | | | |
| | Salt | 0,15 | 1 | 85 | 5 | |
| | Graphite | 10 | 3 | 85 | 15 | |
| **180** | Agar | 6 | 2 | 85 | 10 | |
| | Tap water | 100 | 1 | | | |
| | Salt | 0,15 | 1 | 85 | 5 | |
| | Charcoal | 2 | 3 | 85 | 15 | |
| **181** | Agar | 6 | 2 | 85 | 10 | |
| | Tap water | 100 | 1 | | | |
| | Salt | 0,15 | 1 | 85 | 5 | |
| | Charcoal | 3 | 3 | 85 | 15 | |
| **182** | Agar | 6 | 2 | 85 | 10 | Hard to mix |
| | Tap water | 100 | 1 | | | |
| | Salt | 0,15 | 1 | 85 | 5 | |
| | Oil | 30 | 3 | 85 | 15 | |
| | Surfactant | 4 | 3 | | | |
| **183** | Agar | 6 | 2 | 85 | 10 | Hard to mix |
| | Tap water | 100 | 1 | | | |
| | Salt | 0,15 | 1 | 85 | 5 | |
| | Oil | 40 | 3 | 85 | 15 | |
| | Surfactant | 5 | 3 | | | |
| **184** | Agar | 6 | 2 | 85 | 10 | |
| | Tap water | 100 | 1 | | | |
| | Salt | 0,15 | 1 | 85 | 5 | |
| | Oil | 40 | 3 | 85 | 15 | |
| | Surfactant | 6 | 3 | | | |

| | | | | | | |
|---|---|---|---|---|---|---|
| | Graphite | 20 | 4 | | | |
| **185** | Agar | 6 | 2 | 85 | 10 | |
| | Tap water | 100 | 1 | | | |
| | Salt | 0,15 | 1 | 85 | 5 | |
| | Oil | 40 | 3 | 85 | 15 | |
| | Surfactant | 6 | 3 | | | |
| | Charcoal | 3 | 4 | | | |
| **186** | Gellan gum | 3 | 3 | 85-100 | 40 | Less stiff compared to 185 |
| | Tap water | 100 | 1 | | | |
| | Salt | 0,15 | 2 | 85 | 3 | |
| | Oil | 20 | 2 | | 5 | |
| | Surfactant | 2 | | | | |
| **187** | Gellan gum | 3 | 3 | 85-100 | 40 | Less stiff compared to 185 |
| | Tap water | 100 | 1 | | | |
| | Salt | 0,15 | 2 | 85 | 3 | |
| | Oil | 30 | 2 | | 5 | |
| | Surfactant | 5 | | | | |
| **188** | Agar | 6 | 2 | 85 | 10 | |
| | Tap water | 100 | 1 | | | |
| | Antifrost | 5 | 3 | | 5 | |
| **189** | Agar | 6 | 2 | 85 | 10 | |
| | Tap water | 100 | 1 | | | |
| | Oil | 10 | 3 | | 5 | |
| **190** | Agar | 6 | 2 | 85 | 10 | |
| | Tap water | 100 | 1 | | | |
| | Oil | 10 | 3 | | 5 | |
| | Surfactant | 1 | 3 | | | |
| **191** | Agar | 6 | 2 | 85 | 15 | No solidification |
| | Tap water | 100 | 1 | | | |
| | Sodium acetate | 1 | 2 | | | |
| **192** | PVA | 15 | 2 | 20 | 60 | Turn off stove and continue mixing |
| | Tap water | 100 | 1 | 20 | 5 | Precipitation of charcoal |
| | Charcoal | 5 | 1 | 20 | | |
| **193** | PVA | 15 | 2 | 20 | 60 | |
| | Tap water | 100 | 1 | 20 | 5 | |
| | Sodium acetate | 1 | 1 | | | |
| **194** | PVA | 12 | 2 | 20 | 60 | Turn off stove and continue mixing |
| | Tap water | 100 | 1 | 20 | 5 | Precipitation of graphite |

| | | | | | | |
|---|---|---|---|---|---|---|
| | Salt | 0,15 | 1 | | | |
| | Graphite | 30 | 1 | | | |
| | Acetone | | | | | |
| **195** | PVA | 12 | 3 | 20 | 60 | Turn off stove and continue mixing |
| | Tap water | 100 | 1 | 20 | 5 | Clumpy phantom |
| | Salt | 0,15 | 1 | | | |
| | Graphite | 35 | 1 | | | |
| | Acetone | | | | | |
| | Oil | 40 | 2 | | 5 | |
| | Surfactant | 5 | 2 | | | |
| **196** | PVA | 12 | 3 | 20 | 60 | Turn off stove and continue mixing |
| | Tap water | 100 | 1 | 20 | 5 | |
| | Salt | 0,15 | 1 | | | |
| | Graphite | 40 | 1 | | | |
| | Acetone | | | | | |
| | Oil | 50 | 2 | | 5 | |
| | Surfactant | 5,5 | | | | |
| **197** | PVA | 10 | 2 | 20 | 60 | Turn off stove and continue mixing |
| | Tap water | 100 | 1 | 20 | 5 | Precipitation of graphite |
| | Salt | 0,15 | 1 | | | |
| | Graphite | 30 | 1 | | | |
| | Acetone | | | | | |
| **198** | PVA | 10 | 3 | 20 | 60 | Turn off stove and continue mixing |
| | Tap water | 100 | 1 | 20 | 5 | |
| | Salt | 0,15 | 1 | | | |
| | Graphite | 35 | 1 | | | |
| | Acetone | | | | | |
| | Oil | 40 | 2 | | 5 | |
| | Surfactant | 5 | 2 | | | |
| **199** | PVA | 10 | 3 | 20 | 60 | Turn off stove and continue mixing |
| | Tap water | 100 | 1 | 20 | 5 | |
| | Salt | 0,15 | 1 | | | |
| | Graphite | 40 | 1 | | | |
| | Acetone | | | | | |
| | Oil | 50 | 2 | | 5 | |
| | Surfactant | 5,5 | 2 | | | |

| | | | | | | |
|---|---|---|---|---|---|---|
| **200** | PVA | 12 | 3 | 20 | 60 | Turn off stove and continue mixing |
| | Tap water | 100 | 1 | 20 | 5 | |
| | Salt | 0,15 | 1 | | | |
| | Graphite | 40 | 1 | | | |
| | Acetone | | | | | |
| | Oil | 40 | 2 | | 5 | |
| | Surfactant | 5 | 2 | | | |
| **201** | PVA | 10 | 3 | 20 | 60 | Turn off stove and continue mixing |
| | Tap water | 100 | 1 | 20 | 5 | |
| | Salt | 0,15 | 1 | | | |
| | Graphite | 40 | 1 | | | |
| | Acetone | | | | | |
| | Oil | 40 | 2 | | 5 | |
| | Surfactant | 5 | 2 | | | |
| **202** | Gellan gum | 3 | 3 | 85-100 | 40 | |
| | Tap water | 100 | 1 | | | |
| | Salt | 0,15 | 2 | 85 | 3 | |
| | Oil | 15 | 2 | | 5 | |
| | Surfactant | 1 | 3 | 85-100 | 40 | |
| **203** | Gellan gum | 3 | 3 | 85-100 | 40 | |
| | Tap water | 100 | 1 | | | |
| | Salt | 0,15 | 2 | 85 | 3 | |
| | Oil | 17 | 2 | | 5 | |
| | Surfactant | 1,5 | | | | |
| **204** | Gellan gum | 3 | 3 | 85-100 | 40 | |
| | Tap water | 100 | 1 | | | |
| | Salt | 0,15 | 2 | 85 | 3 | |
| | Oil | 18 | 2 | | 5 | |
| | Surfactant | 1,5 | | | | |
| **205** | Agar | 6 | 2 | 85 | 10 | |
| | Tap water | 100 | 1 | | | |
| | Salt | 0,15 | 1 | 85 | 5 | |
| | Graphite | 25 | 3 | | | |
| **206** | PVA | 10 | 2 | 20 | 60 | |
| | Tap water | 100 | 1 | 20 | 5 | |
| | Salt | 0,15 | 1 | | | |
| **207** | PVA | 10 | 2 | 20 | 5 | Precipitation of PVC |
| | Tap water | 100 | 1 | 20 | 5 | |
| | Salt | 0,15 | 1 | | | |
| | PVC | 20 | 3 | | 60 | Turn off stove and continue mixing |

| | | | | | | |
|---|---|---|---|---|---|---|
| **208** | PVA | 10 | 2 | 20 | 5 | Precipitation of PVC |
| | Tap water | 100 | 1 | 20 | 5 | |
| | Salt | 0,15 | 1 | | | |
| | PVC | 40 | 3 | | 60 | Turn off stove and continue mixing |
| **209** | Agar | 6 | 2 | 85 | 10 | |
| | Tap water | 100 | 1 | | | |
| | Salt | 0,15 | 1 | 85 | 5 | |
| | PVC | 20 | 3 | | | |
| **210** | Agar | 6 | 2 | 85 | 10 | |
| | Tap water | 100 | 1 | | | |
| | Salt | 0,15 | 1 | 85 | 5 | |
| | PVC | 30 | 3 | | | |
| **211** | Gellan gum | 3 | 3 | 85-100 | 40 | |
| | Tap water | 100 | 1 | | | |
| | Salt | 0,15 | 2 | 85 | 3 | |
| | PVC | 20 | 2 | | 5 | |
| **212** | Gellan gum | 3 | 3 | 85-100 | 40 | Clumpy while mixing |
| | Tap water | 100 | 1 | | | |
| | Salt | 0,15 | 2 | 85 | 3 | |
| | PVC | 40 | 2 | | 5 | |
| **213** | Gellan gum | 3 | 3 | 85-100 | 40 | |
| | Tap water | 100 | 1 | | | |
| | Salt | 0,15 | 2 | 85 | 3 | |
| | PVC | 5 | 2 | | 5 | |
| **214** | PVA | 15 | 2 | 20 | 60 | |
| | Tap water | 100 | 1 | 20 | 5 | |
| | Salt | 0,15 | 1 | | | |
| | Sodium acetate | 0,05 | 1 | | | |
| **215** | PVA | 12 | 2 | 20 | 60 | |
| | Tap water | 100 | 1 | 20 | 5 | |
| | Salt | 0,15 | 1 | | | |
| **216** | Agar | 6 | 2 | 85 | 10 | |
| | Tap water | 100 | 1 | | | |
| | PVC | 20 | 3 | 85 | 10 | |
| **217** | PVA | 12 | 4 | 20 | 60 | Turn off stove and continue mixing |
| | Tap water | 100 | 1 | 20 | 5 | |
| | Salt | 0,15 | 1 | | | |
| | PVC | 5 | 2 | | | |
| | Oil | 40 | 3 | | | |
| | Surfactant | 5 | 3 | | | |
| | Graphite | 40 | 3 | | | |

| | | | | | | |
|---|---|---|---|---|---|---|
| **220** | PVA | 12 | 4 | 20 | 60 | Turn off stove and continue mixing |
| | Tap water | 100 | 1 | 20 | 5 | |
| | Salt | 0,15 | 1 | | | |
| | PVC | 5 | 2 | | | |
| | Oil | 30 | 3 | | | |
| | Surfactant | 4 | 3 | | | |
| | Graphite | 40 | 3 | | | |
| **223** | PVA | 15 | 2 | 20 | 60 | |
| | Tap water | 100 | 1 | 20 | 10 | |
| | Salt | 0,15 | 1 | | | |
| | Sodium acetate | 0,07 | 1 | | | |
| | PVC | 5 | 1 | | | |
| **224** | PVA | 15 | 3 | 20 | 60 | |
| | Tap water | 100 | 1 | 20 | 10 | |
| | Salt | 0,15 | 1 | | | |
| | Sodium acetate | 0,07 | 1 | | | |
| | Oil | 50 | 2 | | 5 | |
| | Surfactant | 5,5 | 2 | | | |
| **225** | PVA | 17,64705882 | 3 | 20 | 60 | |
| | Tap water | 100 | 1 | 20 | 10 | |
| **226** | Gellan gum | 3 | 3 | 85-100 | 40 | |
| | Tap water | 100 | 1 | | | |
| | Salt | 0,15 | 2 | 85 | 3 | |
| | Oil | 18 | 2 | | 5 | |
| | Surfactant | 1,5 | | | | |
| **227** | Gellan gum | 3 | 3 | 85-100 | 40 | |
| | Tap water | 100 | 1 | | | |
| | Salt | 0,15 | 2 | 85 | 3 | |
| | Oil | 18 | 2 | | 5 | |
| | Surfactant | 1,5 | | | | |
| **228** | Gellan gum | 3 | 3 | 85-100 | 40 | |
| | Tap water | 100 | 1 | | | |
| | Salt | 0,15 | 2 | 85 | 3 | |
| | Oil | 18 | 2 | | 5 | |
| | Surfactant | 1,5 | | | | |
| **229** | Gellan gum | 3 | 3 | 85-100 | 40 | |
| | Tap water | 100 | 1 | | | |
| | Salt | 0,15 | 2 | 85 | 3 | |
| | Oil | 18 | 2 | | 5 | |
| | Surfactant | 1,5 | | | | |
| **230** | PVA | 12 | 3 | 20 | 60 | Oily |
| | Tap water | 100 | 1 | 20 | 10 | |
| | Salt | 0,15 | 1 | | | |

| | | | | | | |
|---|---|---|---|---|---|---|
| | Sodium acetate | 0,1 | 1 | | | |
| | Oil | 40 | 2 | | 5 | |
| | Surfactant | 5 | 2 | | | |
| **231** | PVA | 12 | 3 | 20 | 60 | Oily |
| | Tap water | 100 | 1 | 20 | 10 | |
| | Salt | 0,15 | 1 | | | |
| | Sodium acetate | 0,1 | 1 | | | |
| | Oil | 35 | 2 | | 5 | |
| | Surfactant | 4,5 | 2 | | | |
| **232** | PVA | 12 | 3 | 20 | 60 | Oily |
| | Tap water | 100 | 1 | 20 | 10 | |
| | Salt | 0,15 | 1 | | | |
| | Sodium acetate | 0,1 | 1 | | | |
| | Oil | 45 | 2 | | 5 | |
| | Surfactant | 5,2 | 2 | | | |
| **233** | PVA | 10 | 3 | 20 | 60 | More brittle |
| | Tap water | 100 | 1 | 20 | 5 | Turn off stove and continue mixing |
| | Salt | 0,15 | 1 | | | Precipitation of graphite |
| | Graphite | 35 | 1 | | | |
| | Acetone | | | | | |
| | Oil | 40 | 2 | | 5 | |
| | Surfactant | 5 | 2 | | | |
| | | | | | | |
| **234** | PVA | 15 | 2 | 20 | 60 | |
| | Tap water | 100 | 1 | 20 | 5 | |
| | Salt | 0,15 | 1 | | | |
| | Sodium acetate | 0,05 | 1 | | | |
| **235** | PVA | 15 | 2 | 20 | 60 | |
| | Tap water | 100 | 1 | 20 | 5 | |
| | Salt | 0,15 | 1 | | | |
| | Sodium acetate | 0,05 | 1 | | | |
| **236** | PVA | 15 | 2 | 20 | 60 | |
| | Tap water | 100 | 1 | 20 | 5 | |
| | Salt | 0,15 | 1 | | | |
| | Sodium acetate | 0,05 | 1 | | | |
| **237** | PVA | 15 | 2 | 20 | 60 | |
| | Tap water | 100 | 1 | 20 | 5 | |
| | Salt | 0,15 | 1 | | | |
| | Sodium acetate | 0,05 | 1 | | | |

| | | | | | | |
|---|---|---|---|---|---|---|
| **238** | Gellan gum | 3 | 2 | 85-100 | 40 | |
| | Tap water | 100 | 1 | | | |
| **239** | PVA | 15 | 2 | 20 | 60 | |
| | Tap water | 100 | 1 | 20 | 5 | |
| | Salt | 0,15 | 1 | | | |
| | Sodium acetate | 0,05 | 1 | | | |
| **240** | PVA | 17 | 2 | 20 | 60 | |
| | Tap water | 100 | 1 | 20 | 5 | |
| | Salt | 0,15 | 1 | | | |
| | Sodium acetate | 0,05 | 1 | | | |
| **241** | PVA | 20 | 2 | 20 | 60 | |
| | Tap water | 100 | 1 | 20 | 5 | |
| | Salt | 0,15 | 1 | | | |
| | Sodium acetate | 0,05 | 1 | | | |
| **242** | PVA | 15 | 2 | 20 | 60 | |
| | Tap water | 100 | 1 | 20 | 5 | |
| | Salt | 0,15 | 1 | | | |
| | Sodium acetate | 0,05 | 1 | | | |
| **243** | PVA | 15 | 2 | 20 | 60 | |
| | Tap water | 100 | 1 | 20 | 5 | |
| **244** | PVA | 15 | 2 | 20 | 60 | |
| | 0.36% saline | 100 | 1 | 20 | 5 | |
| | Sodium acetate | 0,05 | 1 | | | |
| **245** | PVA | 15 | 2 | 20 | 60 | |
| | Tap water | 100 | 1 | 20 | 5 | |
| | Sodium acetate | 5,5 | | | | |
| **246** | PVA | 20 | 2 | 20 | 60 | |
| | Tap water | 100 | 1 | 20 | 5 | |
| | Salt | 0,15 | 1 | | | |
| | Sodium acetate | 0,05 | 1 | | | |

*Phantom number in red, indicated failed phantom

**DEMI water = Demineralised water

## B2 Repeatability tests

**Results repeatability tests**

| Phantom number | Base material | Permittivity (%) | | | Conductivity (%) | | |
|---|---|---|---|---|---|---|---|
| | | Max. variation | Min. variation | Mean variation | Max. variation | Min. variation | Mean variation |
| 58 | Agar | 6.1 | 0 | 1.6 | 1.9 | 1.7 | 1.8 |
| 64 | Gellan gum | 17.7 | 5.7 | 14.5 | 8.2 | 7.6 | 8.1 |
| 66 | Gellan gum | 6.6 | 0 | 1.9 | 0.5 | 0.4 | 0.5 |
| 77 | PVA-C | 26.7 | 6.8 | 11.5 | 3.4 | 1.9 | 2.8 |
| 80 | Agar | 7.7 | 2.5 | 2.9 | 2.3 | 2.1 | 2.2 |
| 81 | Agar | 9.4 | 4.2 | 6.4 | 5.1 | 5.0 | 5.1 |
| 82 | Agar | 33.3 | 0 | 5.5 | 1.4 | 1.2 | 1.3 |
| 83 | Agar | 8.5 | 3.9 | 6.0 | 5.4 | 5.2 | 5.4 |
| 84 | Gellan gum | 4.7 | 1.2 | 2.3 | 1.6 | 1.5 | 1.6 |
| 87 | PVA-C | 7.8 | 1.7 | 3.3 | 2.2 | 2.1 | 2.2 |
| 89 | PVA-C | 8.9 | 2.0 | 5.4 | 3.4 | 3.3 | 3.4 |
| 98 | PVA-C | 12.1 | 0 | 5.9 | 4.8 | 42 | 4.5 |
| 100 | Gellan gum | 6.4 | 3.0 | 4.4 | 2.6 | 2.5 | 2.6 |
| 101 | Gellan gum | 16.7 | 0 | 6.2 | 2.9 | 2.0 | 2.7 |
| 102 | Gellan gum | 5.7 | 3.5 | 4.3 | 4.3 | 4.3 | 4.3 |
| 105 | Agar | 26.7 | 8.6 | 11.4 | 5.7 | 4.6 | 5.5 |
| 106 | Agar | 12.1 | 0 | 8.2 | 4.6 | 3.3 | 4.3 |
| 107 | Agar | 5.8 | 0 | 1.1 | 0.7 | 0.6 | 0.6 |
| 108 | Agar | 10.9 | 3.8 | 5.8 | 4.7 | 4.6 | 4.7 |
| 111 | PVA-C | 14.3 | 7.8 | 10.4 | 10.1 | 9.9 | 10.0 |
| 120 | Gellan gum | 7.5 | 1.3 | 5.2 | 3.0 | 2.9 | 3.0 |
| 122 | Gellan gum | 3.3 | 0.8 | 2.5 | 2.1 | 2.0 | 2.1 |
| 123 | Gellan gum | 6.5 | 0.9 | 4.5 | 1.6 | 1.3 | 1.5 |
| 136 | PVA-C | 16.7 | 0 | 5.9 | 3.5 | 2.7 | 3.2 |
| 137 | PVA-C | 8.3 | 7.2. | 8.0 | 8.3 | 7.2 | 8.0 |
| 138 | PVA-C | 1.8 | 1.7 | 1.7 | 1.8 | 1.7 | 1.7 |
| 154 | PVA-C | 9.0 | 0 | 1.7 | 1.3 | 1.2 | 1.2 |
| **Mean** | | **11.2** | **2.5** | **5.5** | **3.6** | **3.2** | **3.5** |

## B3 Shelf life

**Shelf life of phantoms with different storage conditions**

| Agar-based phantoms | | | | | |
|---|---|---|---|---|---|
| **Wt% agar** | **Preservative** | **Refrigerated** | **Stored in water** | **Sealed airtight** | **Shelf life** |
| < 2 | No | No | Yes | Yes | 2 weeks; becomes more brittle and eventually break |
| < 2 | No | No | No | No | 4 days; mould growth |
| 5,66 | No | Yes | No | Yes | 14 days; mould growth |
| 5,66 | Yes | Yes | No | Yes | 16 days; mould growth |
| 5,66 | No | Yes | Yes | Yes | 3 weeks; mould growth |

| Gellan gum-based phantoms | | | | | |
|---|---|---|---|---|---|
| **Wt% gellan gum** | **Preservative** | **Refrigerated** | **Stored in water** | **Sealed airtight** | **Shelf life** |
| < 2 | No | No | No | No | 5 days; mould growth |
| < 2 | No | No | Yes | No | 4 weeks; mould growth |
| 2,9 | No | Yes | No | Yes | 10 days; mould growth & drying out of phantom |
| 2,9 | No | No | No | No | 5 days; mould growth |
| 2,9 | No | Yes | No | Yes | 5 days; mould growth |
| 2,9 | Yes | Yes | No | Yes | 7 days; mould growth |
| 2,9 | No | Yes | Yes | Yes | 6 weeks; mould growth |
| 2,9 | Yes | Yes | Yes | Yes | 6 weeks; mould growth |

| PVA-based phantoms | | | | | |
|---|---|---|---|---|---|
| **Wt% PVA** | **Preservative** | **Refrigerated** | **Stored in water** | **Sealed airtight** | **Shelf life** |
| < 10 | No | No | No | No | 3 days; drying out of phantom |
| < 10 | No | Yes | No | Yes | 3 days; drying out of phantom |
| < 10 | No | Yes | Yes | Yes | > 1 month |
| < 10 | Yes | Yes | Yes | Yes | > 1 month |

## B4 Salt diffusion

**Results of impedance measurements of examination of salt diffusion**

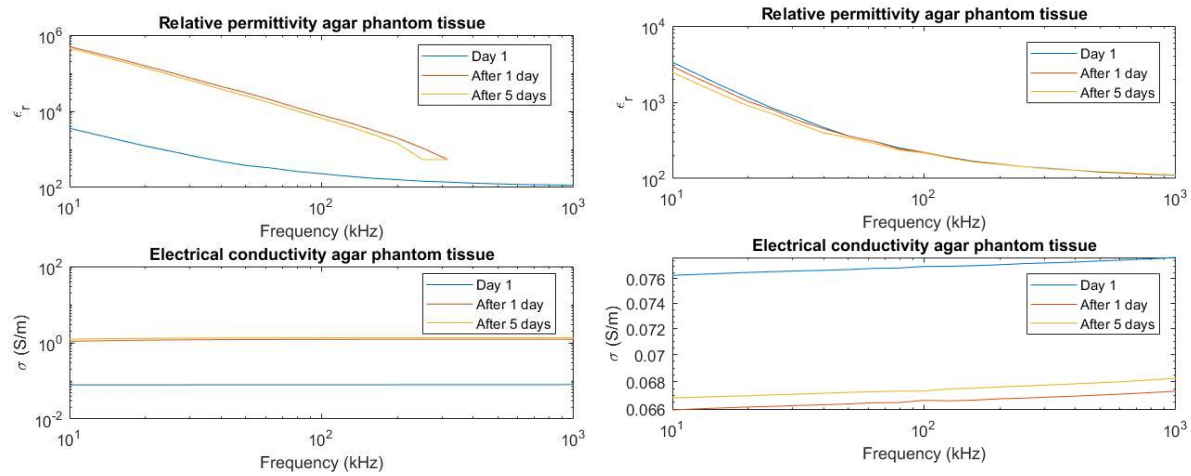


*Figure 65: Salt diffusion of agar phantoms prepared with 6g agar and 100ml tap water. Left: stored in 0.9% saline, right: stored in tap water*

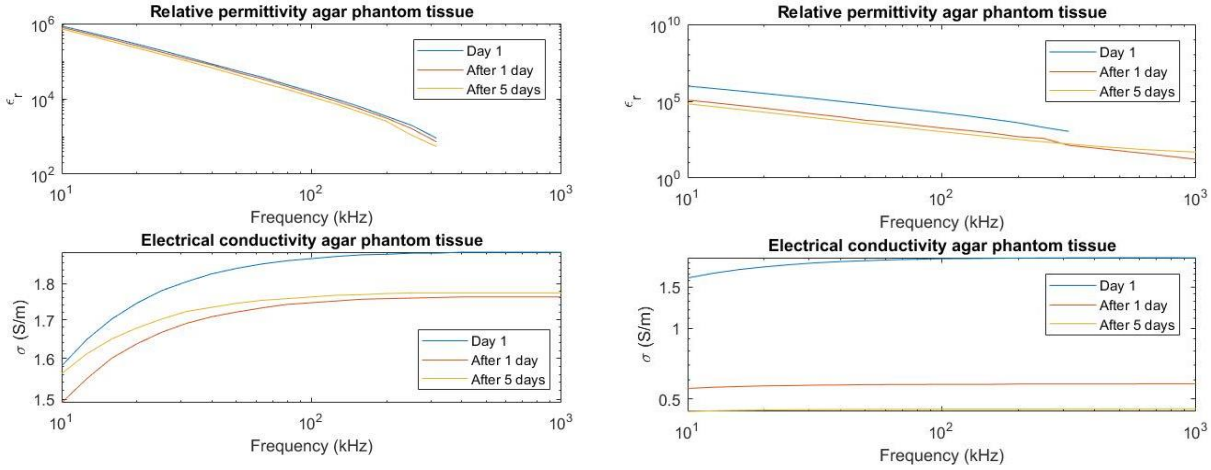


*Figure 66: Salt diffusion of agar phantoms prepared with 6g agar and 100ml 0.9% saline. Left: stored in 0.9% saline, right: stored in tap water*

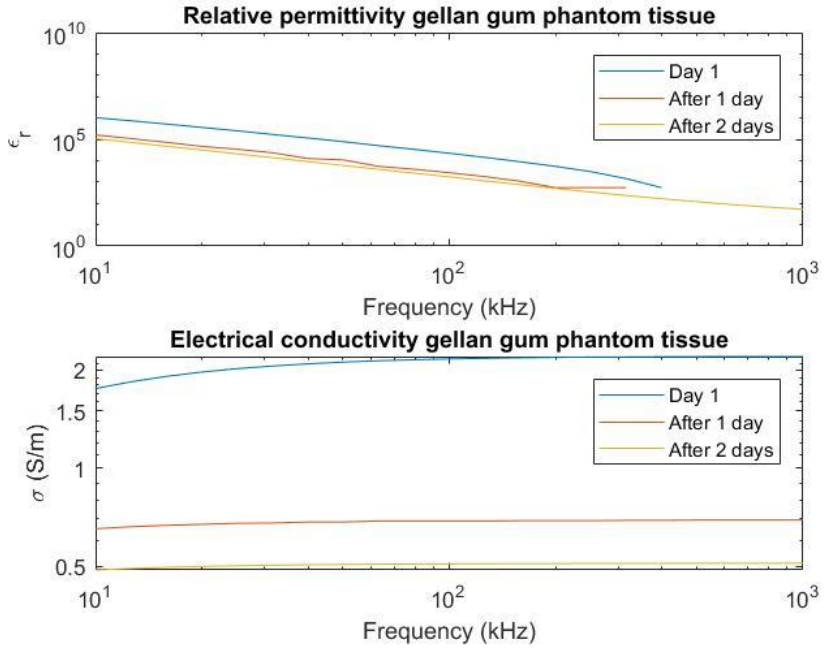


*Figure 67: Salt diffusion of gellan gum phantom prepared with 3g gellan gum powder and 100ml 0.9% saline solution, stored in tap water*

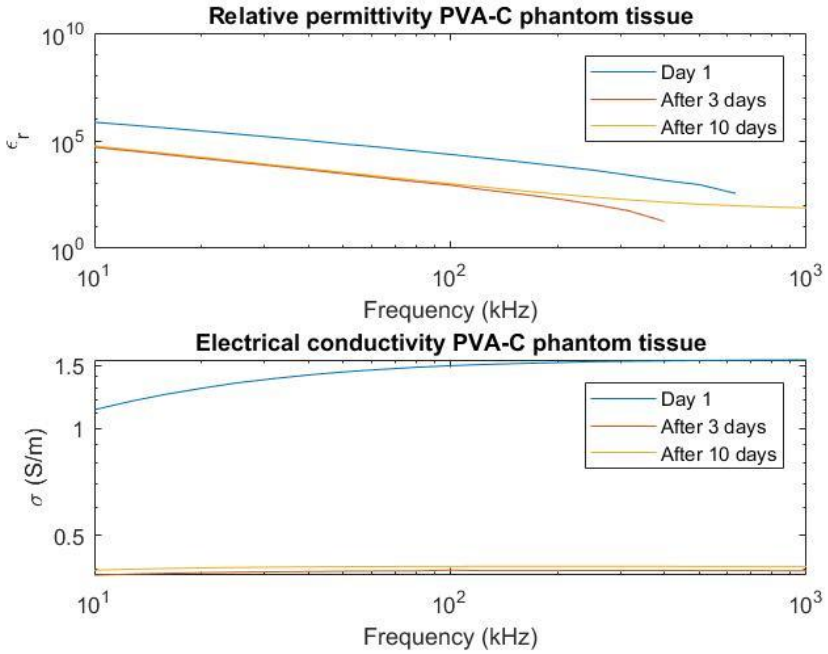


*Figure 68: Salt diffusion of PVA-C phantom prepared with 10g PVA powder and 100ml 0.9% saline solution, stored in tap water*

## B5 Base materials in comparison with target values

**Influence of amount of base material on the dielectric values**

Each figure shows multiple phantoms with the same liquid used for phantom preparation and a variety in amount of bae material. The liquid used for phantom preparation are tap water, tap water, deionized water, tap water and 0.9% saline solution respectively.

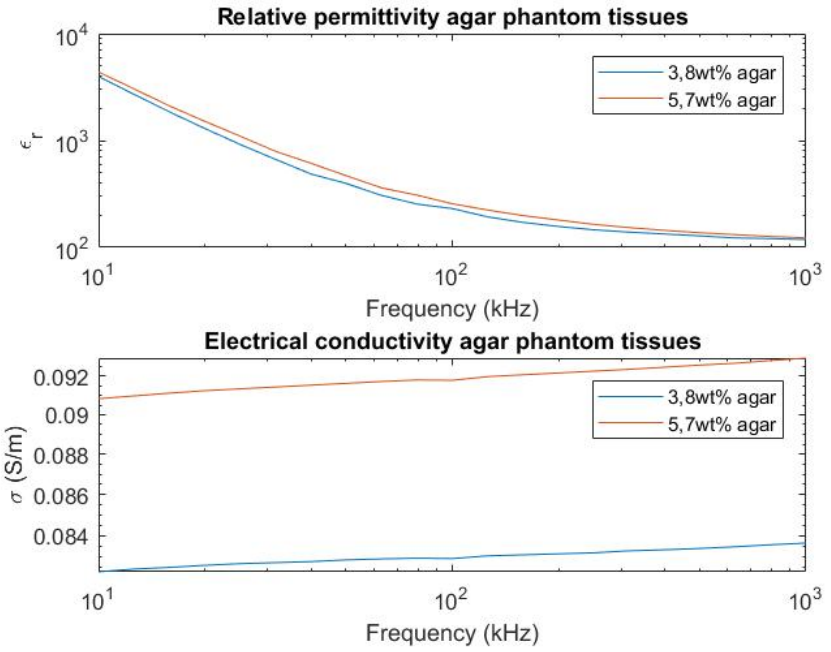


*Figure 69: Influence of wt% agar base material on dielectric values*

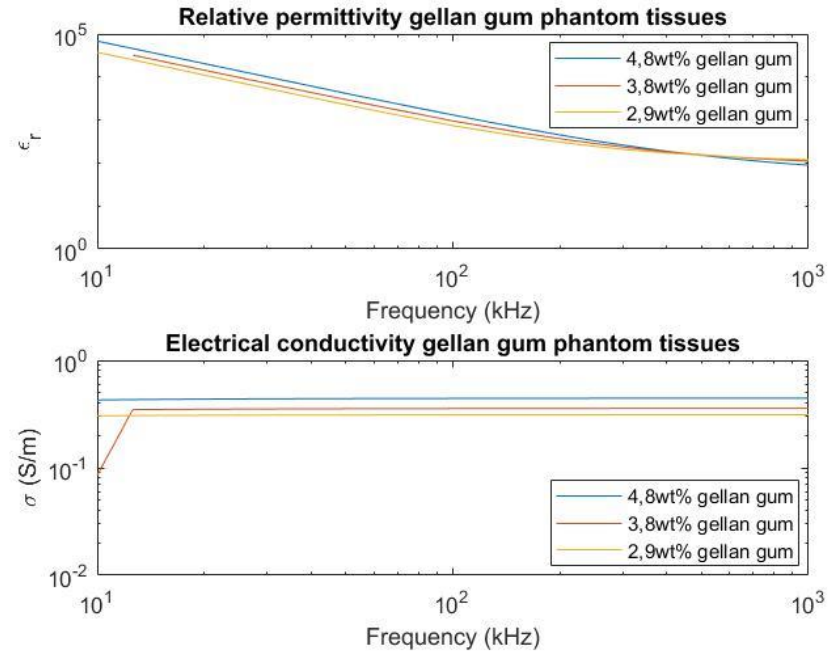


*Figure 70: Influence of wt% gellan gum base material on dielectric values*

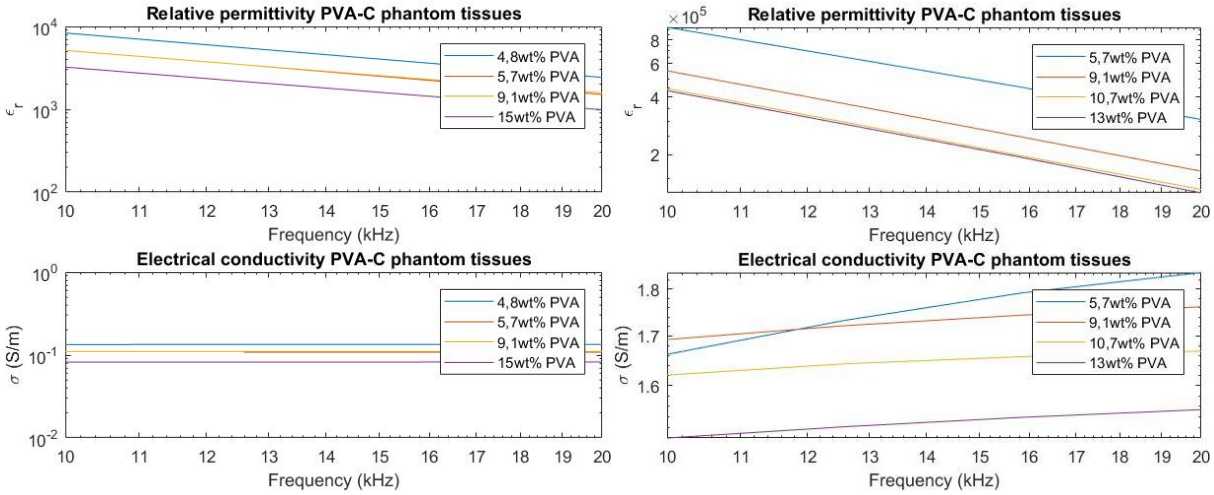


*Figure 71: Influence of wt% PVA base material on dielectric values*

## B6 Increase/decrease of additives

**Results of impedance measurements of the additives**

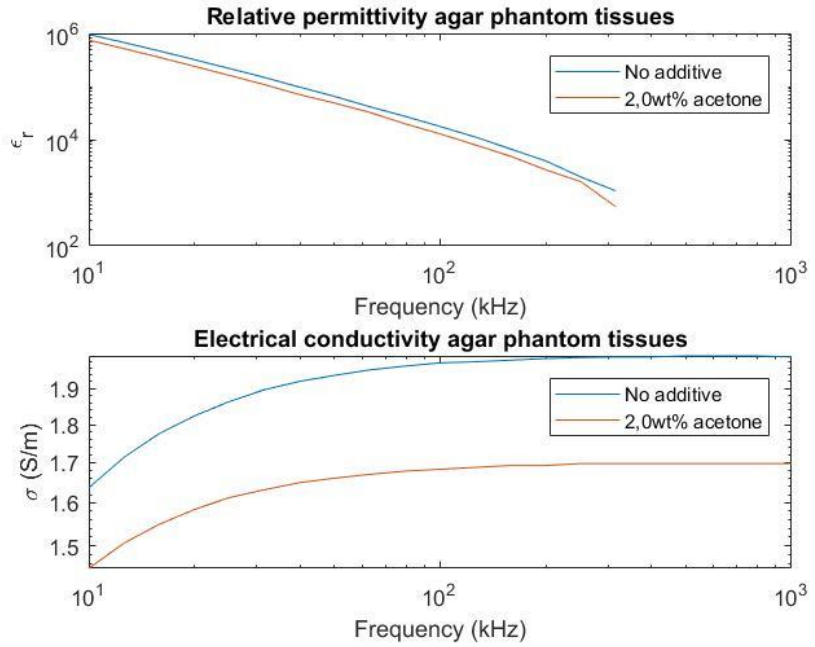


*Figure 72: Influence of acetone on dielectric values*

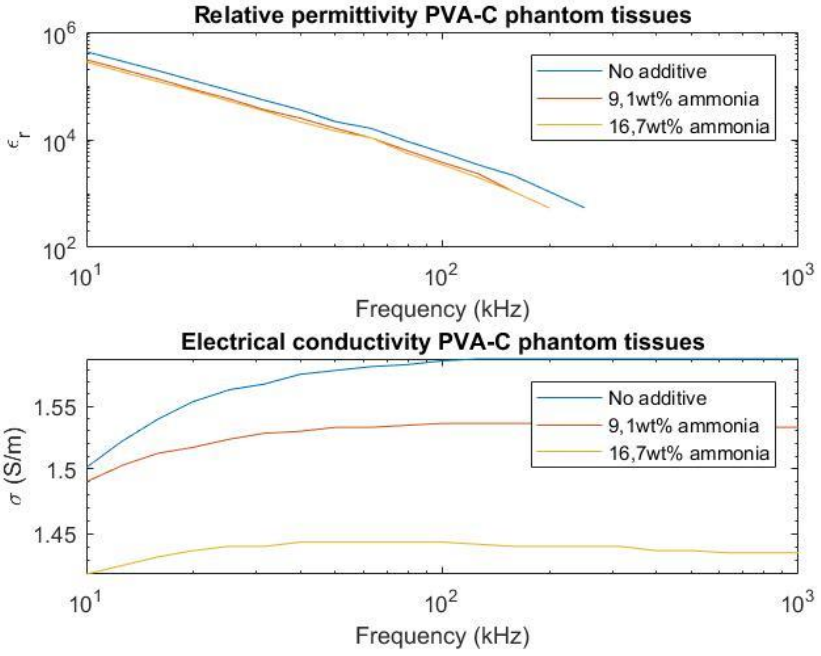


*Figure 73: Influence of ammonia on dielectric values*

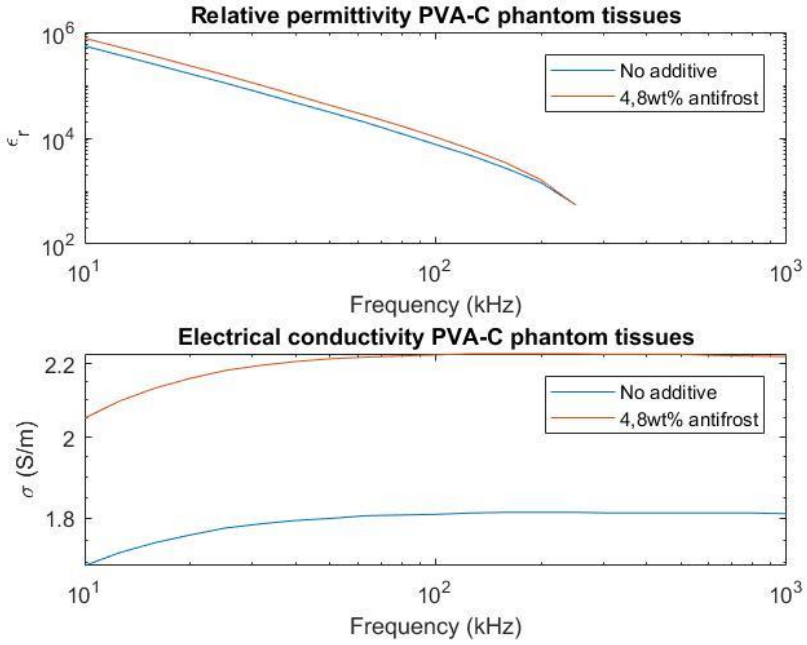


*Figure 74: Influence of antifrost on dielectric values*

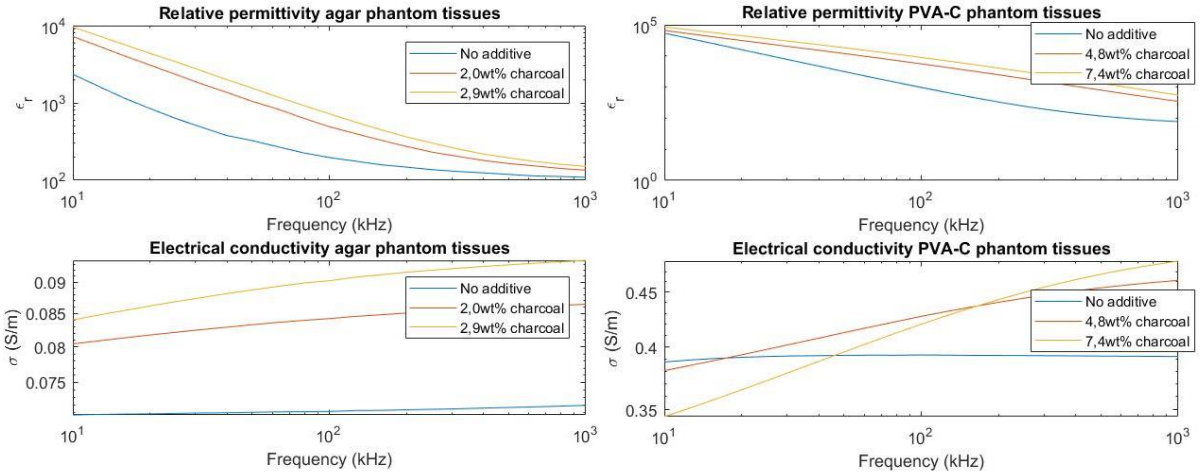


*Figure 75: Influence of charcoal powder on dielectric values*

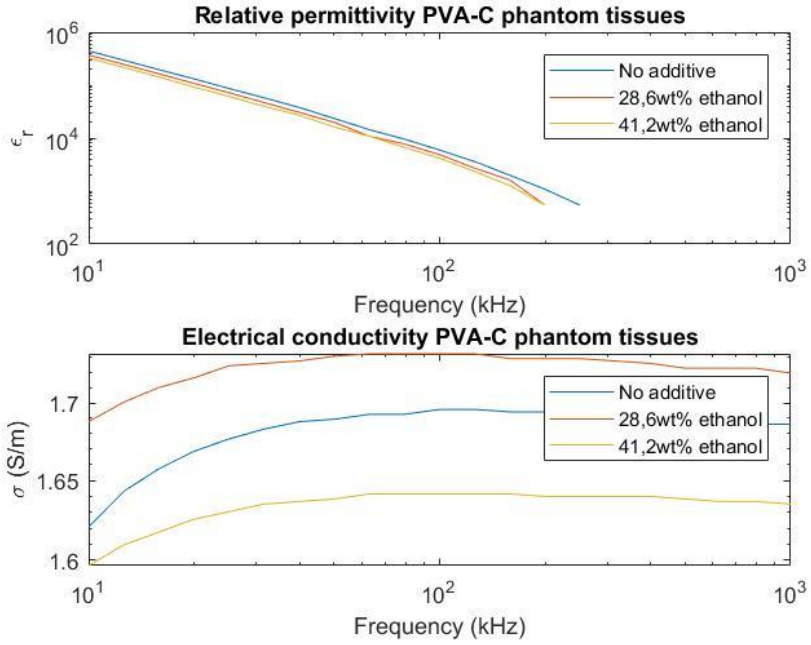


*Figure 76: Influence of ethanol on dielectric values*

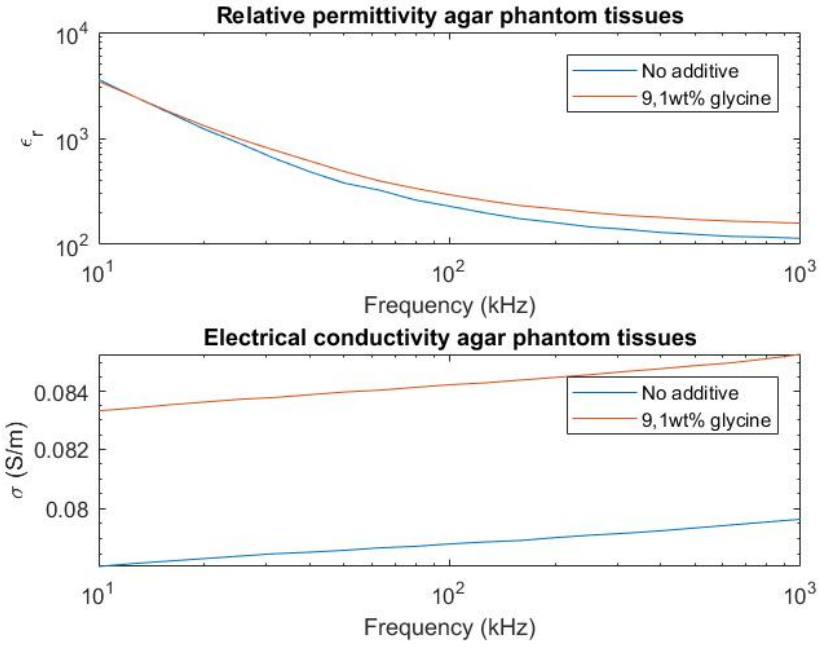


*Figure 77: Influence of glycine on dielectric values*

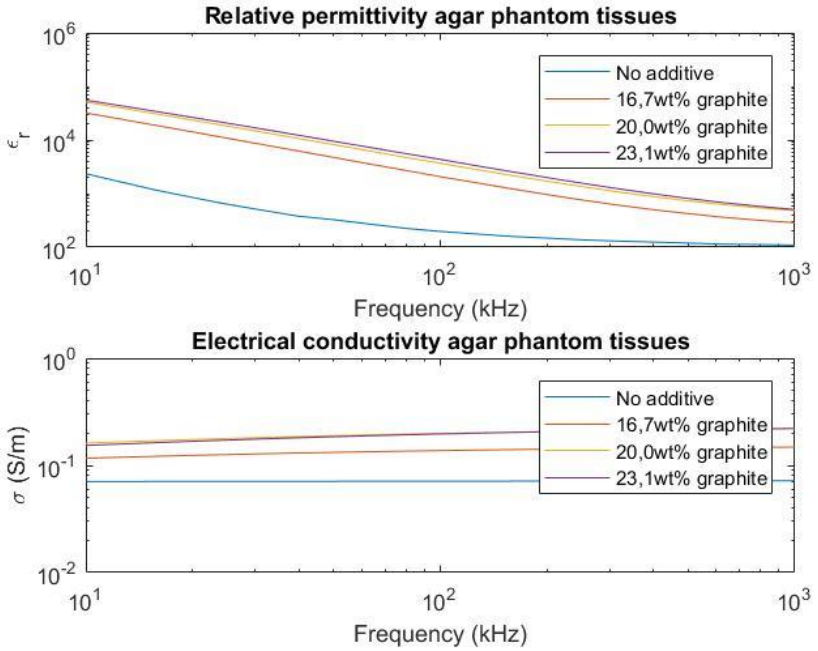


*Figure 78: Influence of graphite on dielectric values*

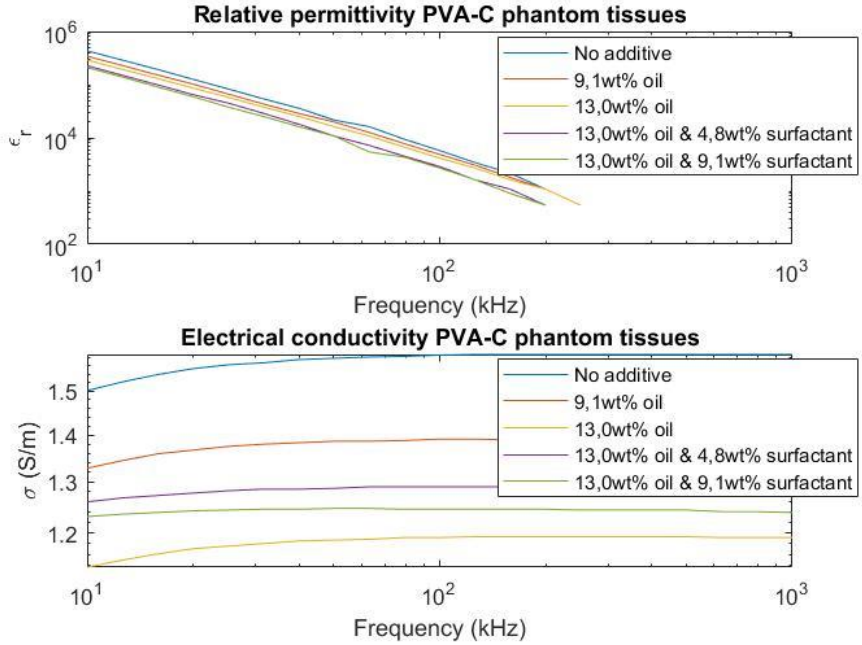


*Figure 79: Influence of oil and surfactant on dielectric values*

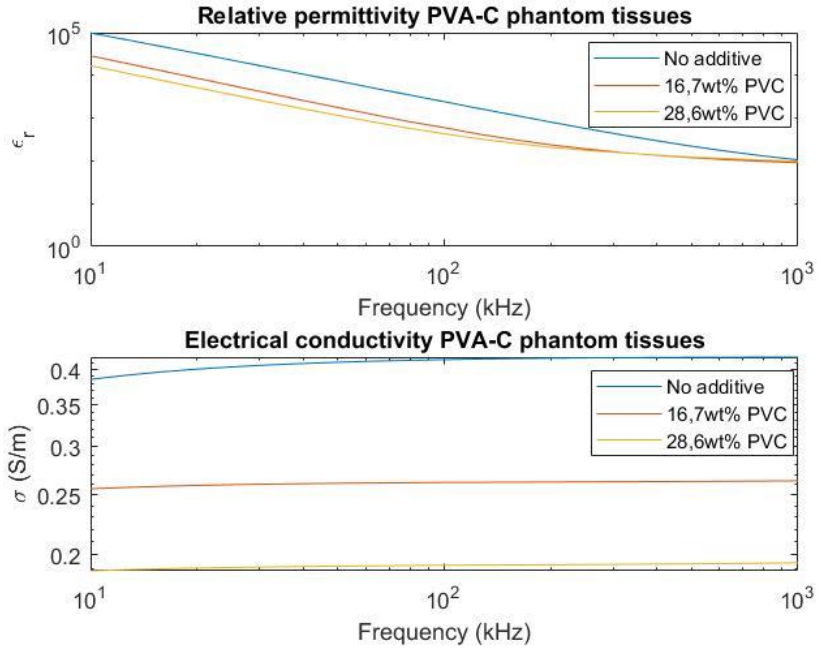


*Figure 80: Influence of PVC on dielectric values*

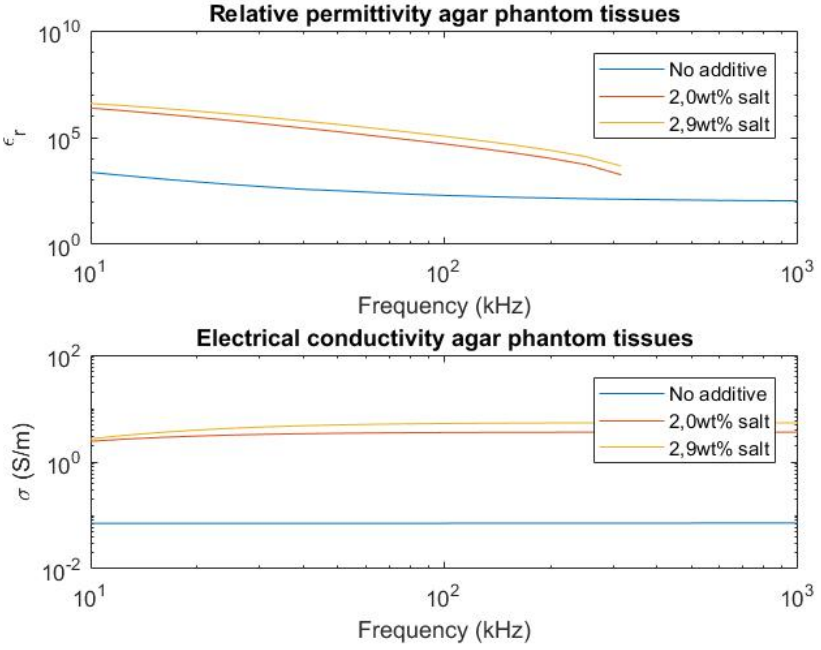


*Figure 81: Influence of salt on dielectric values*

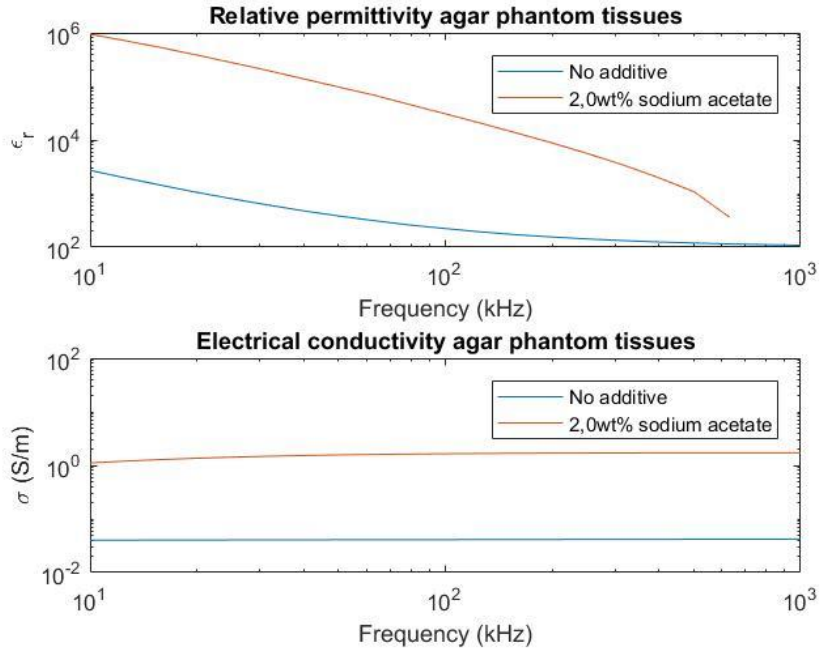


*Figure 82: Influence of sodium acetate on dielectric values*

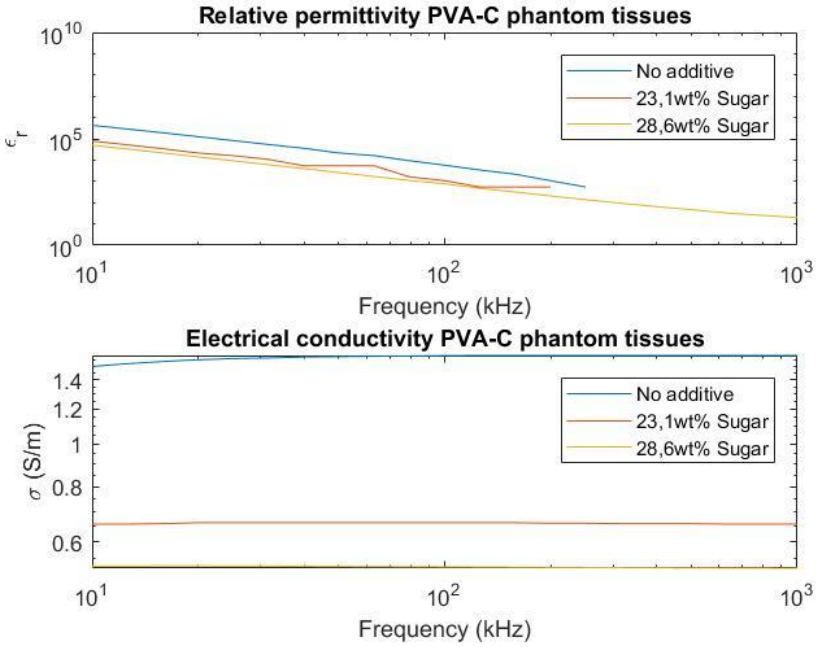


*Figure 83: Influence of sugar on dielectric values*

## B7 Sample phantoms

**Results of impedance measurements of all prepared sample phantoms**

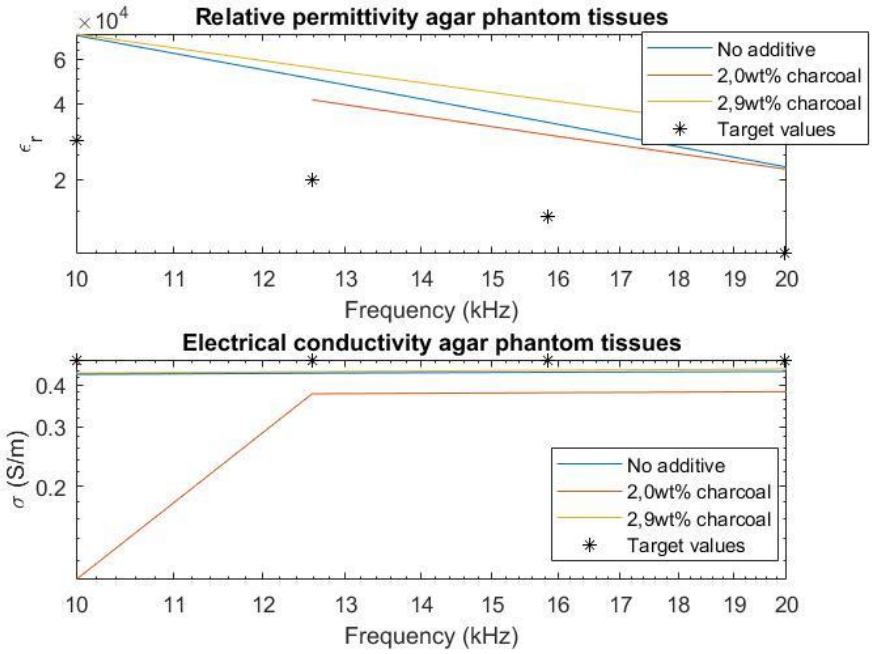


*Figure 84: Influence of different wt% charcoal on 5,7wt% agar phantom tissues*

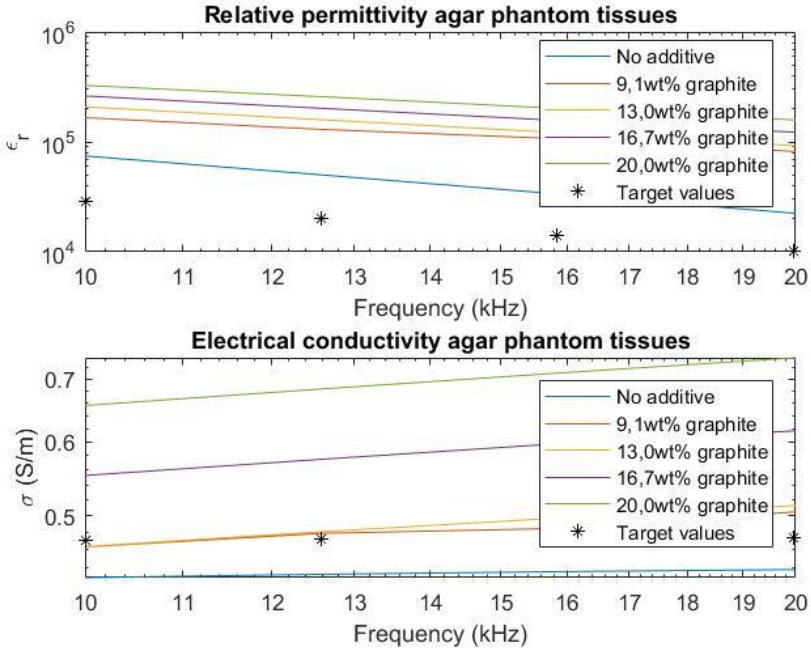


*Figure 85: Influence of different wt% graphite on 5,7wt% agar phantom tissues*

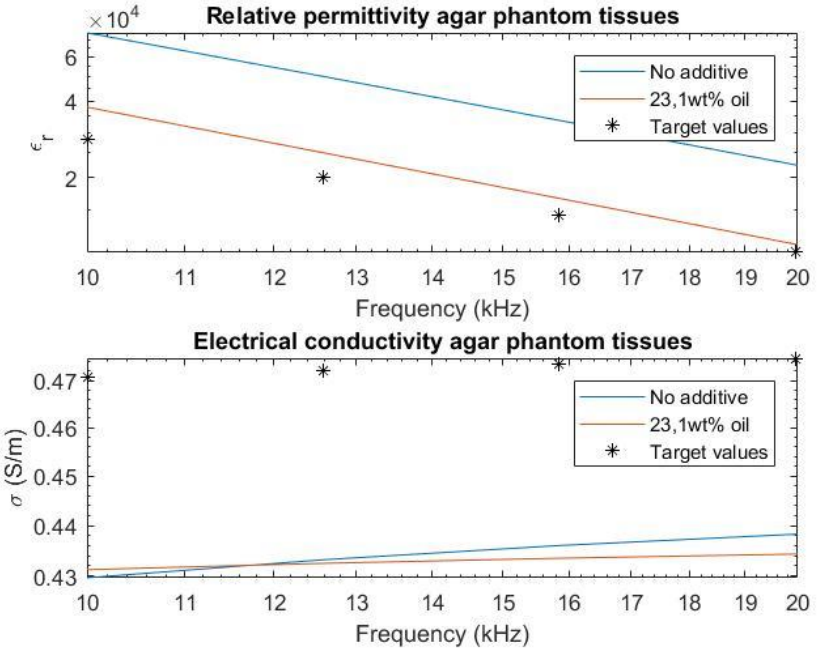


*Figure 86: Influence of different wt% oil on 5,7wt% agar phantom tissues*

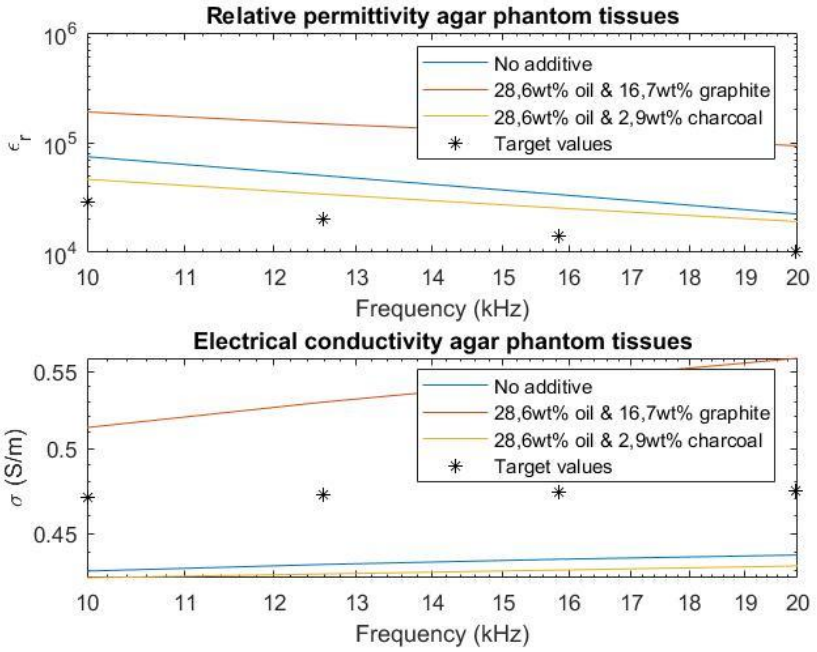


*Figure 87: Influence of different wt% charcoal & graphite in combination with oil on 5,7wt% agar phantom tissues*

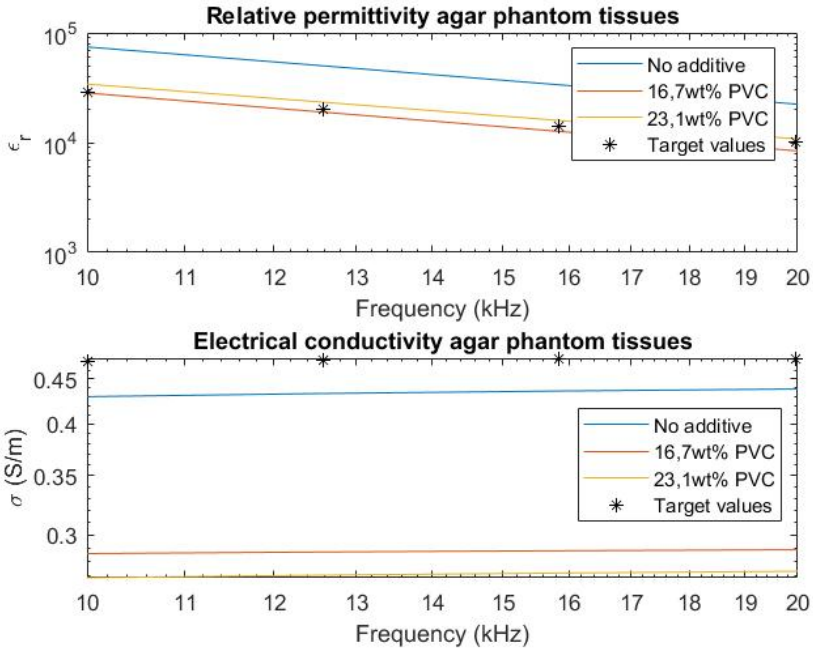


*Figure 88: Influence of different wt% PVC on 5,7wt% agar phantom tissues*

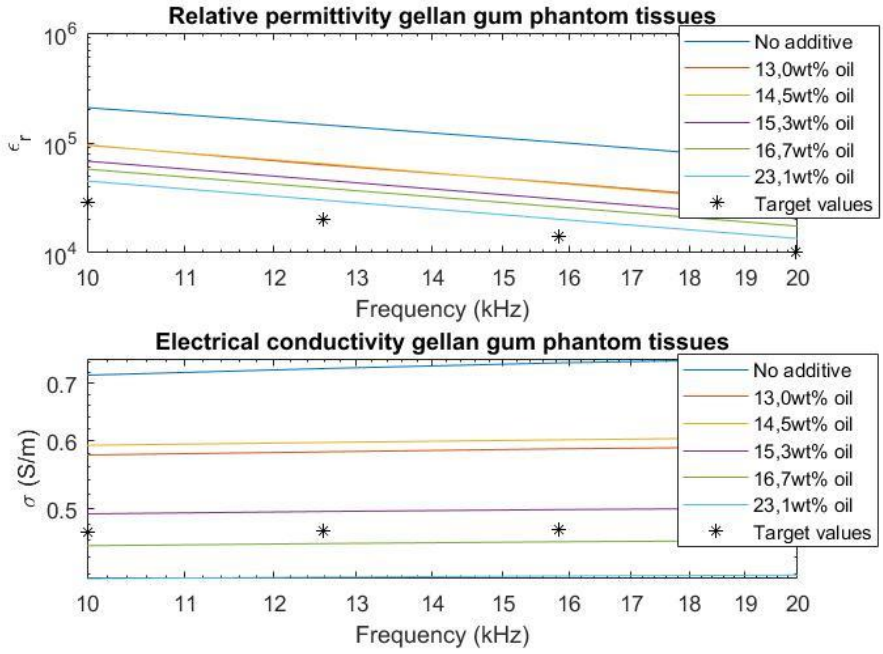


*Figure 89: Influence of different wt% oil on 2,9wt% gellan gum phantom tissues*

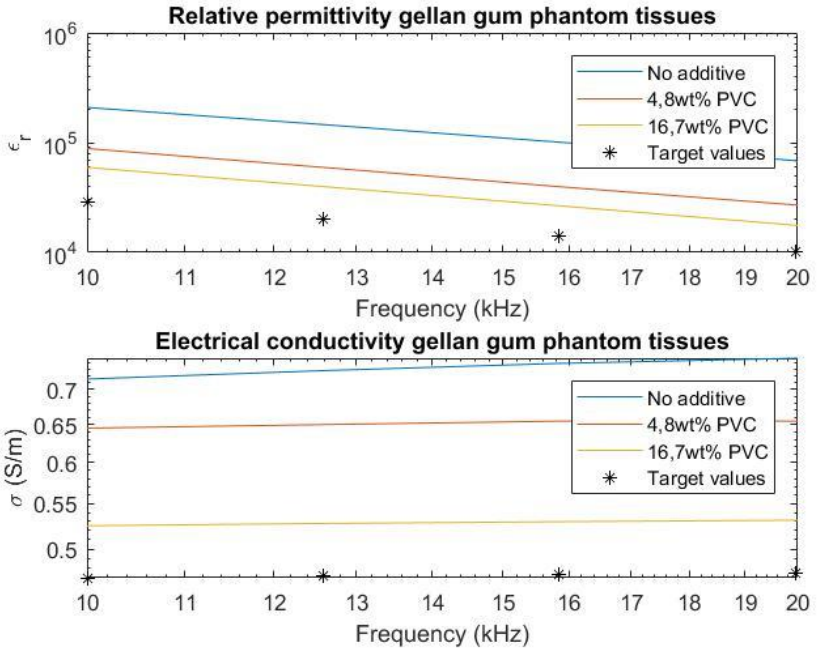


*Figure 90: Influence of different wt% PVC on 2,9wt% gellan gum phantom tissues*

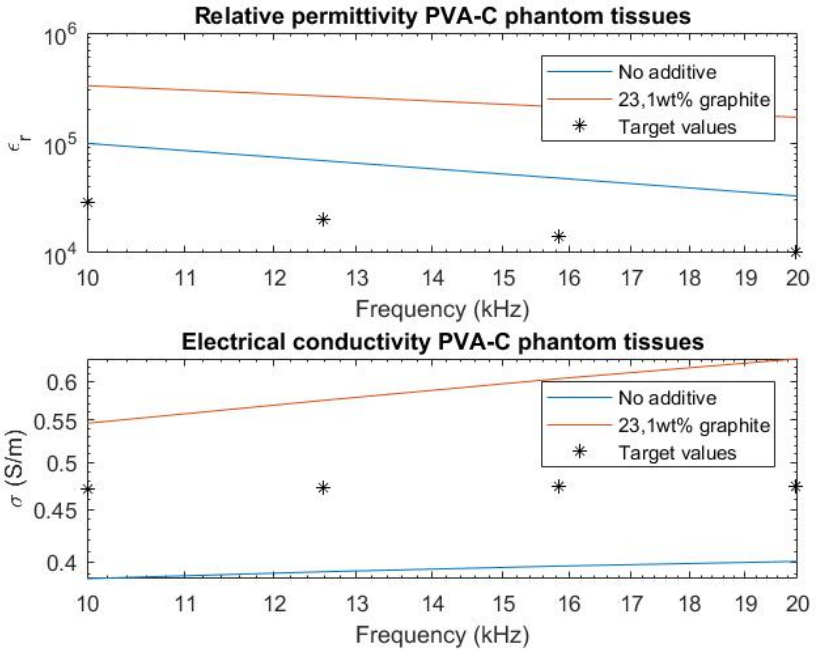


*Figure 91: Influence of graphite on 9,1wt% PVA-C phantom tissue*

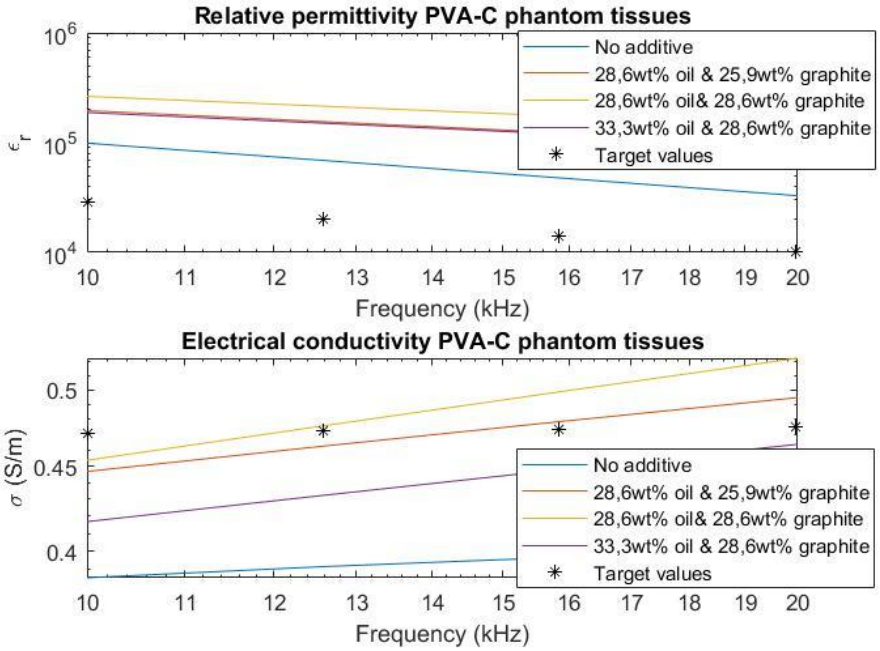


*Figure 92: Influence of different wt% oil & graphite on 9,1wt% PVA-C phantom tissue*

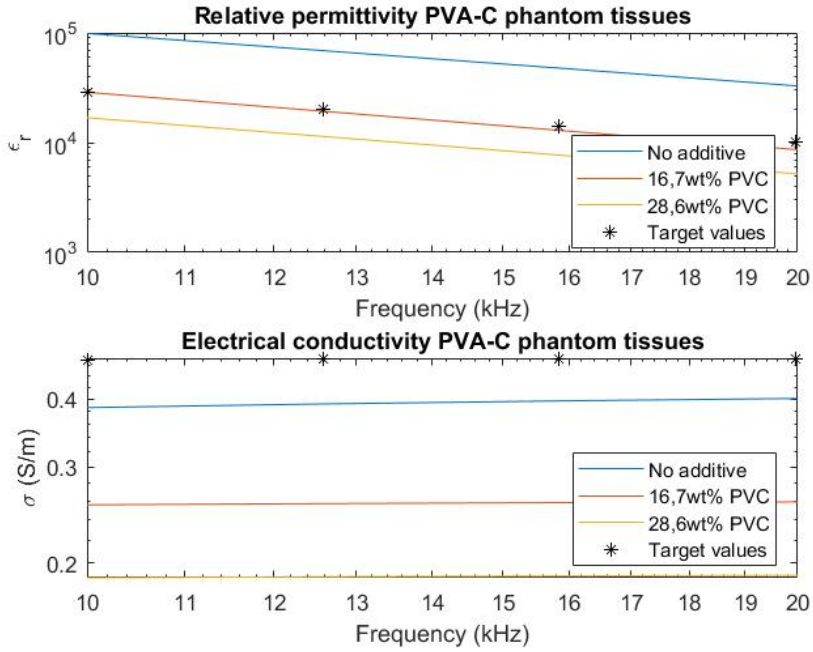


*Figure 93: Influence of different wt% PVC on 9,1wt% PVA-C phantom tissue*

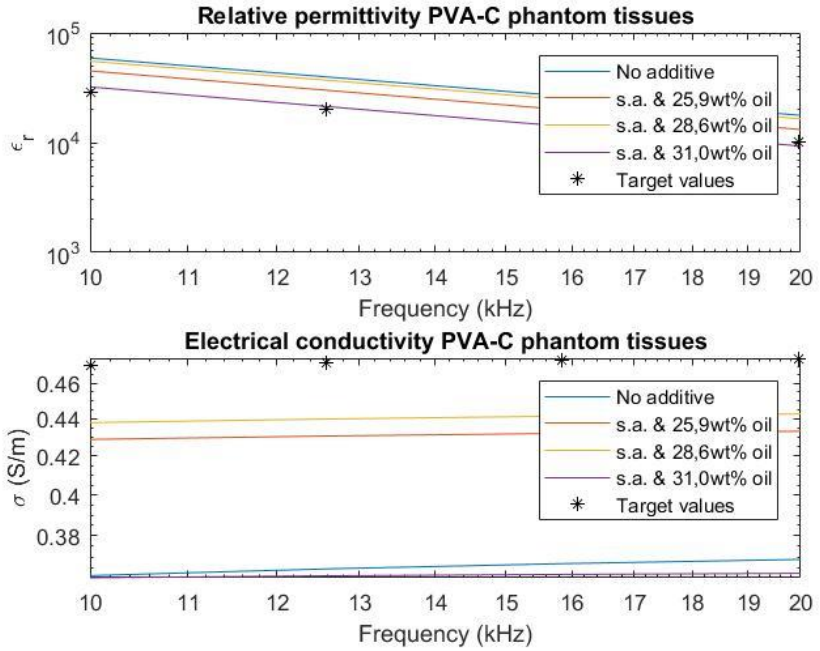


*Figure 94: Influence of different wt% sodium acetate (s.a.) & oil on 10,7wt% PVA-C phantom tissue*

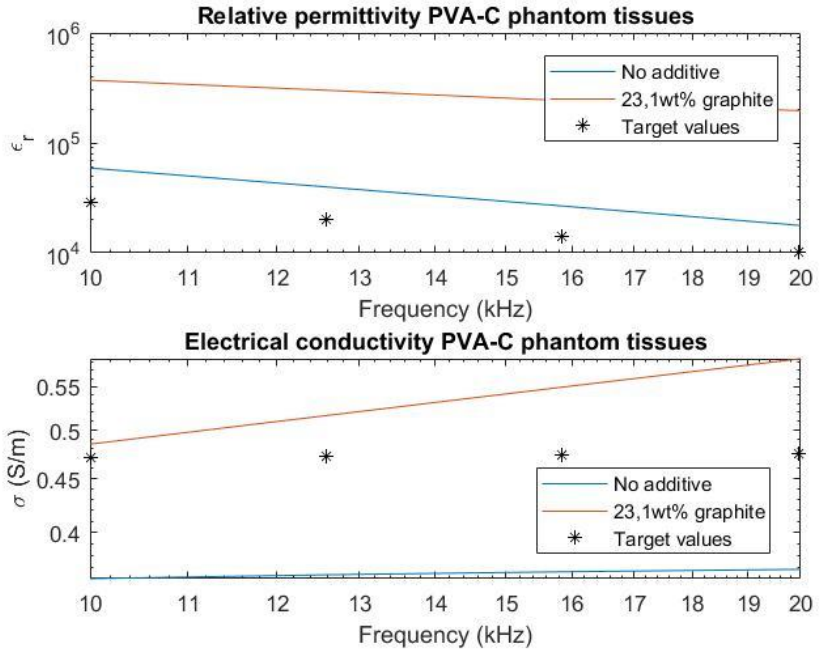


*Figure 95: Influence of graphite on 10,7wt% PVA-C phantom tissue*

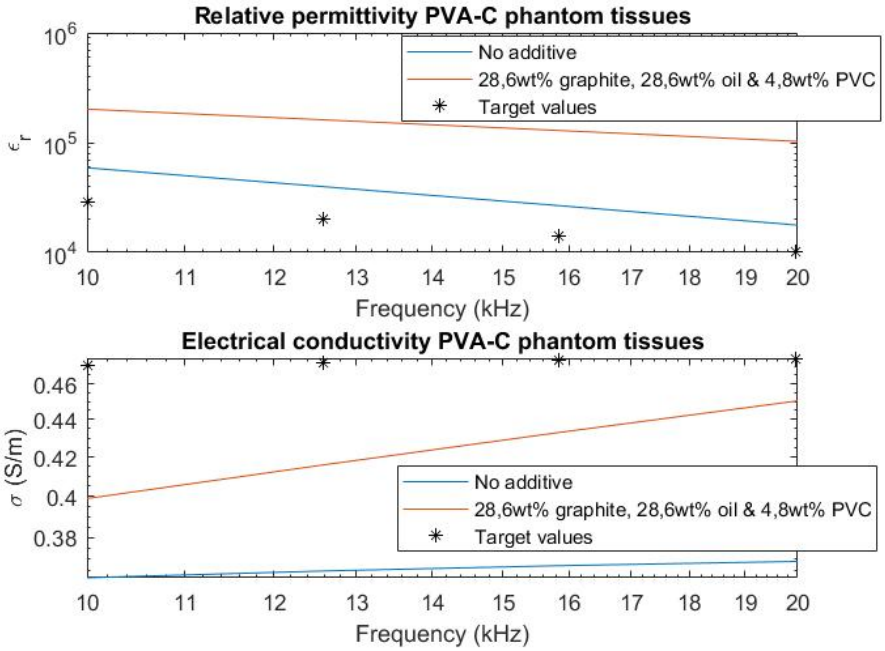


*Figure 96: Influence of graphite, oil & PVC on 10,7wt% PVA-C phantom tissue*

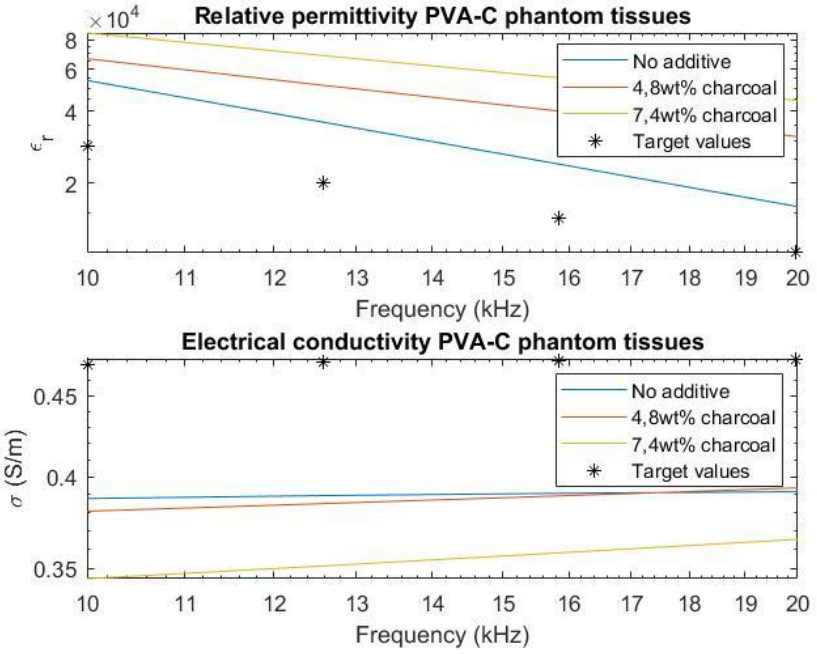


*Figure 97: Influence of different wt% charcoal on 13,0wt% PVA-C phantom tissue*

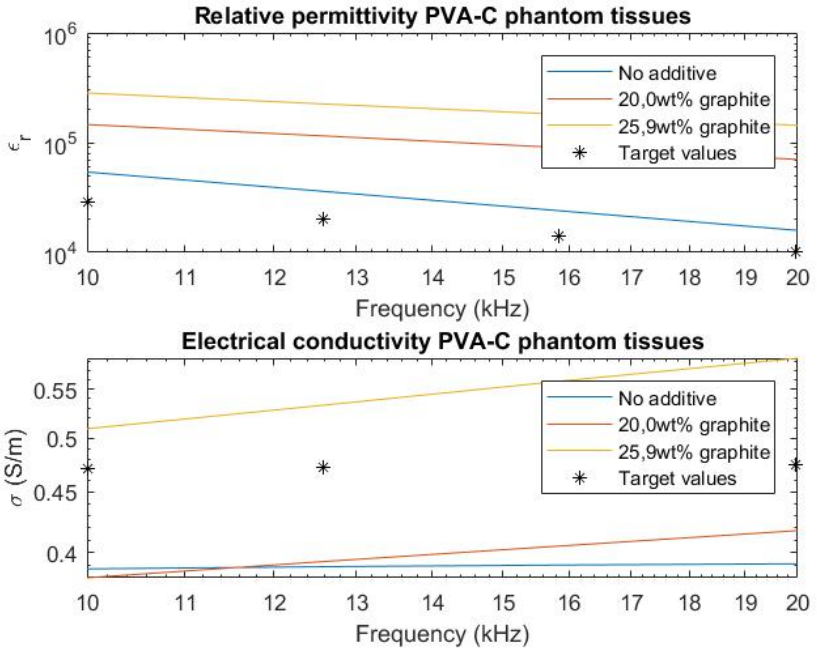


*Figure 98: Influence of different wt% graphite on 13,0wt% PVA-C phantom tissue*

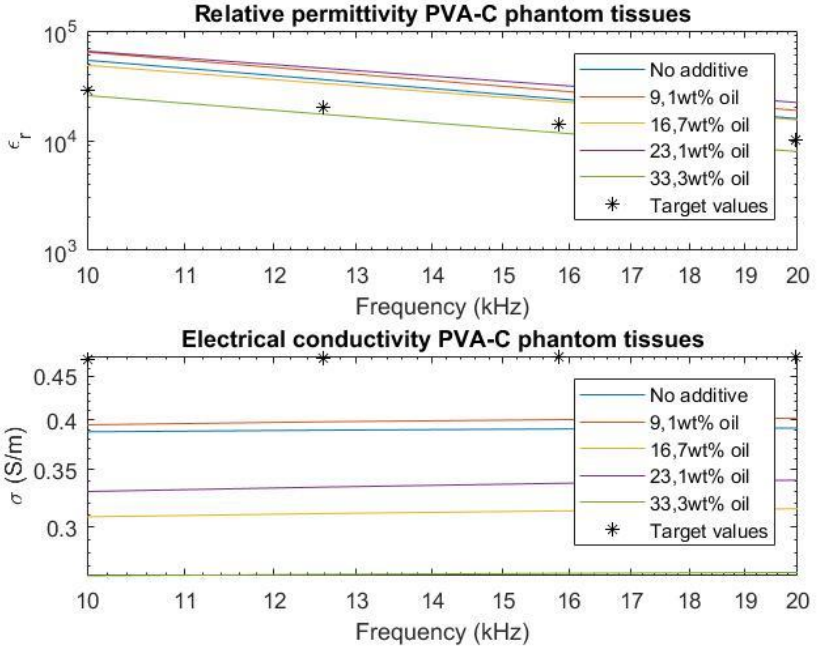


*Figure 99: Influence of different wt% oil on 13,0wt% PVA-C phantom tissue*

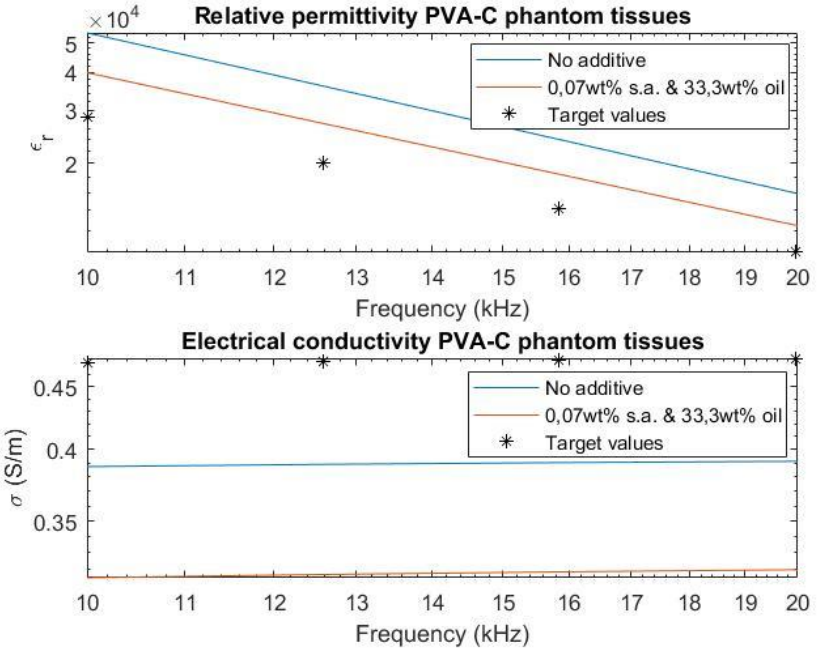


*Figure 100: Influence of sodium acetate (s.a.) & oil on 13,0wt% PVA-C phantom tissue*

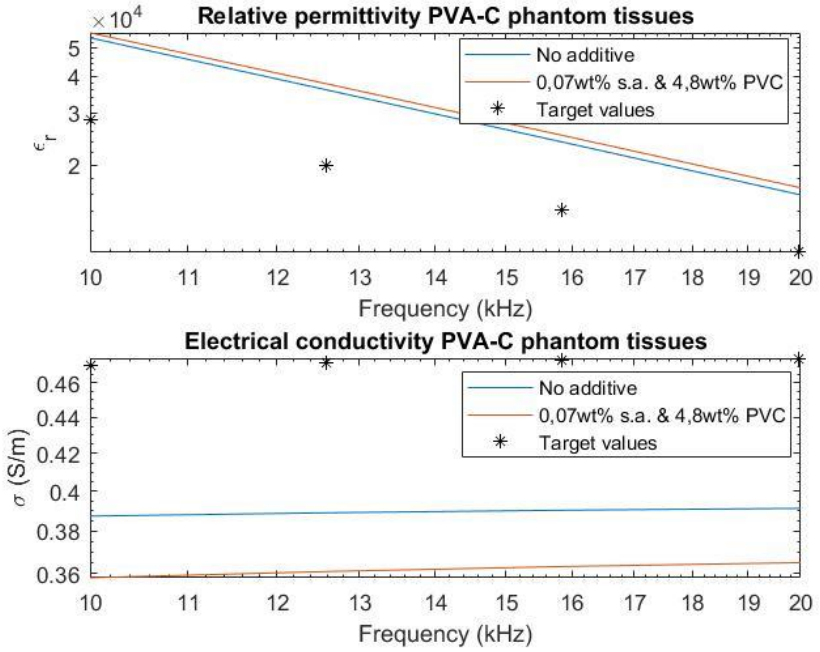


*Figure 101: Influence of sodium acetate (s.a.) & PVC on 13,0wt% PVA-C phantom tissue*

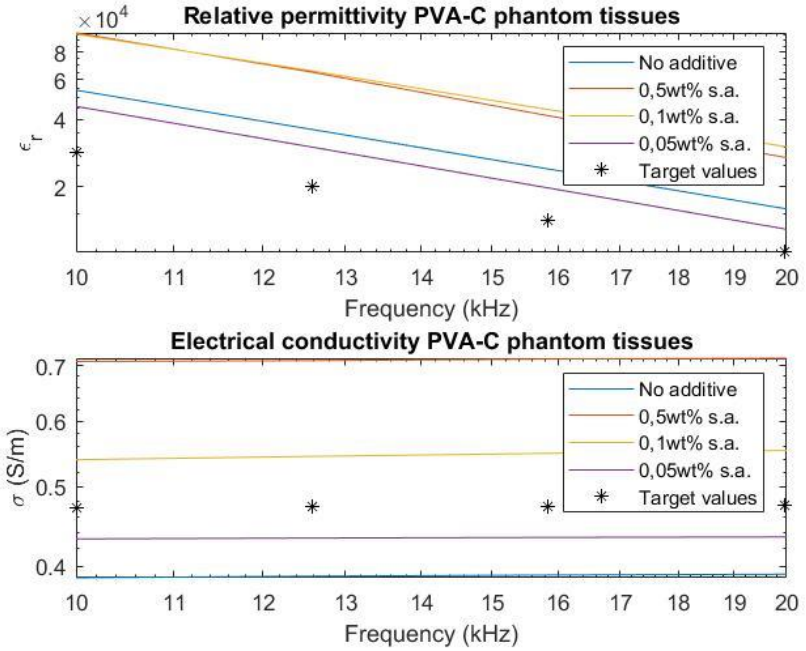


*Figure 102: Influence of different wt% sodium acetate (s.a.) on 13,0wt% PVA-C phantom tissue*

## B8 Boxplots of calculated Young's moduli of the cardiac phantom samples

**Boxplots of measured Young's moduli of the four cardiac phantom samples**

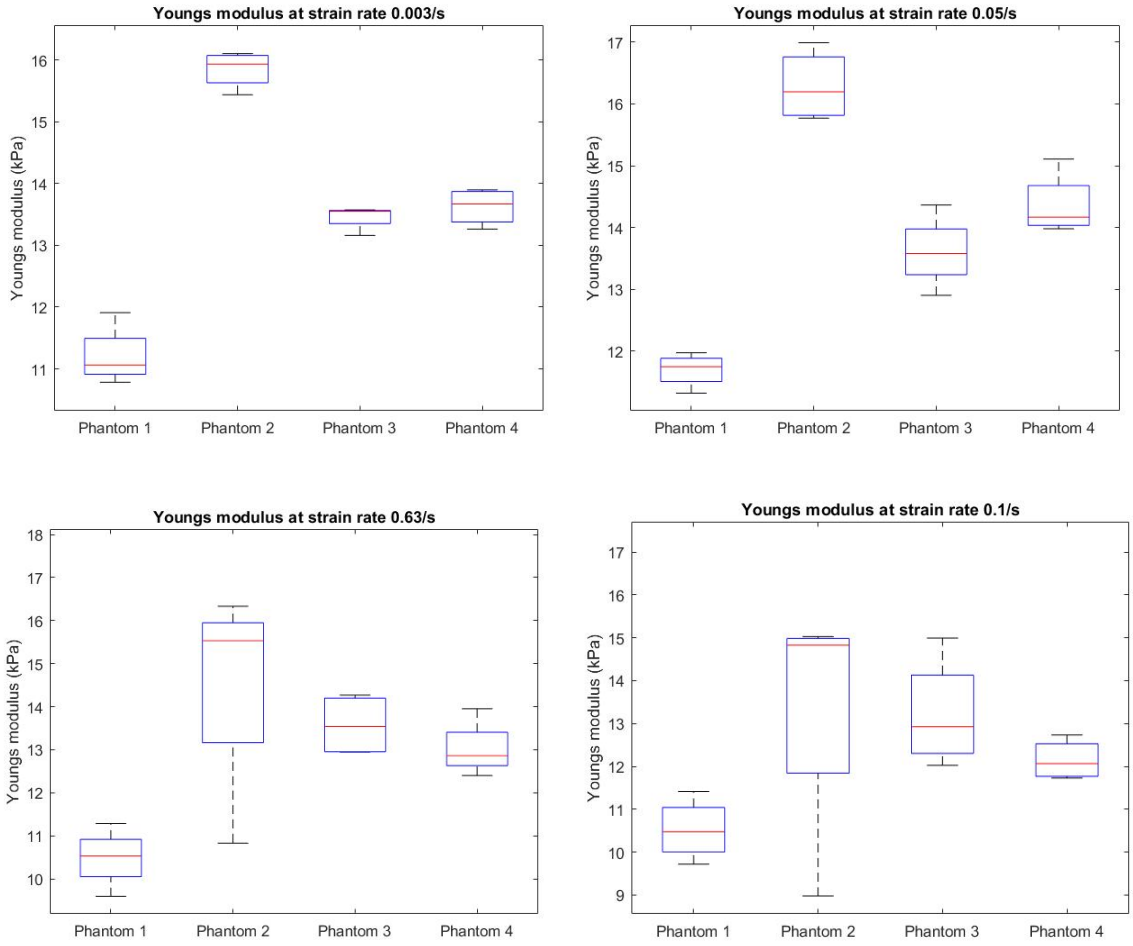


*Figure 103: Boxplots of all calculated Young's moduli at 15% strain of all four phantoms at all four strain rates*

## Appendix C

**Conductivity values measured with an EC-meter**

| Solution | Mean measured conductivity value* [uS/cm] |
|---|---|
| Deionized water | 2 |
| 0.9% saline | 4510 |
| Tapwater | 455 |
| 100ml tapwater + 0.15g salt | 6390 |
| 100ml tapwater + 0.16g salt | 8515 |

*All solutions were measured three times

# Appendix D

**Comparison between 3 electrodes methods**

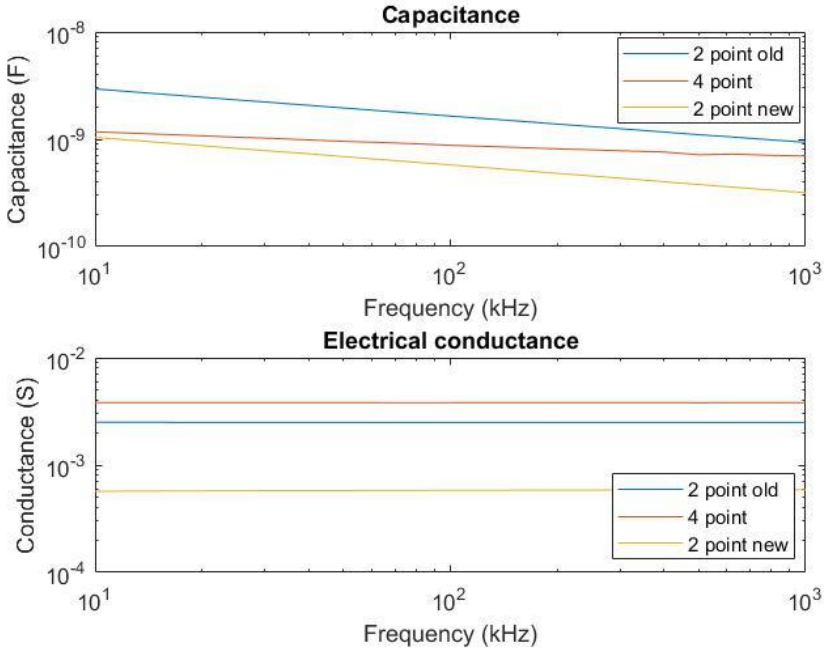


*Figure 104: Comparison between the 'old' 2-needle electrode (2 point old), the 4-needle electrode (4 point) and the 4-needle electrode functioning as a 2-needle electrode (2 point new)*

## Appendix E

**Comparison dielectric measurements of measured capacitance & conductance and measured magnitude & phase angle**

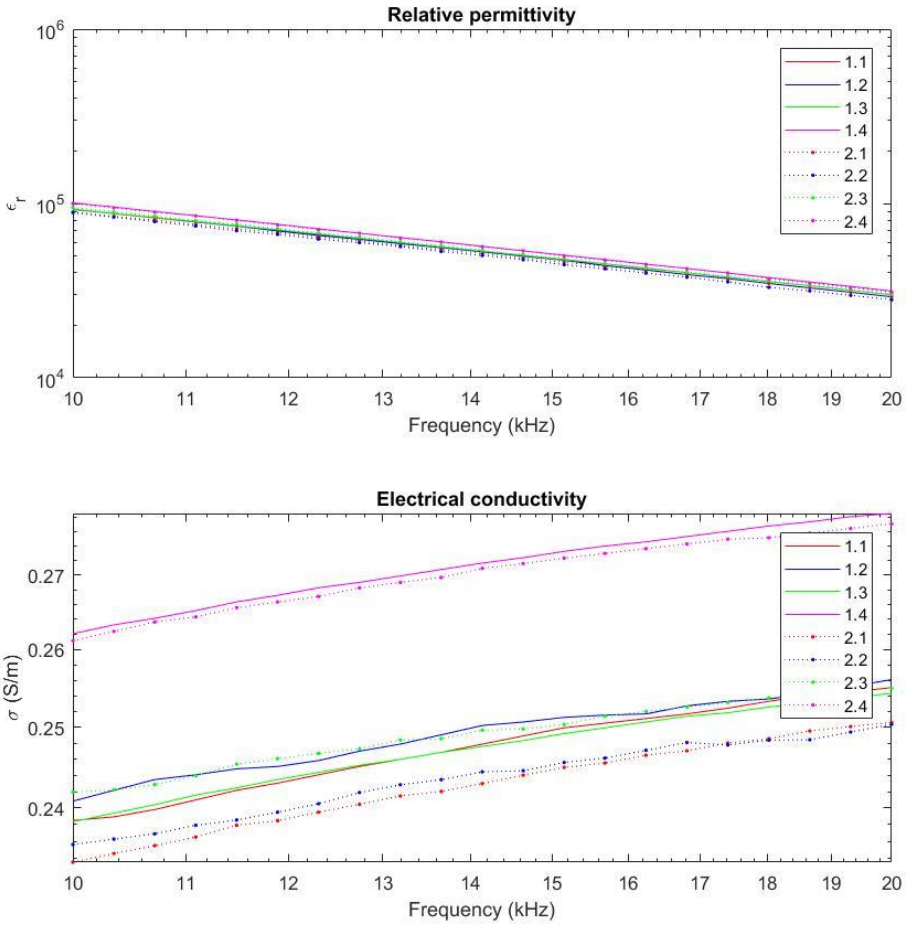


*Figure 105: Comparison between measured capacitance and conductance in parallel mode parameters (1.1 - 1.4) and measured magnitude and phase angle in series mode parameters (2.1 – 2.4)*

# Appendix F

**Notes of attention during mould preparation and filling of the mould**

## Mould preparation in 3D modelling software

1. When making the outer mould in 3D modelling software, make sure to slice the outer mould at every thickest part while the inner mould should be fitted inside the outer mould.
2. Secure the inner mould to the outer mould, in order to make sure the inner mould stays exactly in the middle of the outer mould during filling and solidification.
3. Include a filling hole and multiple holes to release air bubbles.
4. Include pins in truncated cone shapes to secure the different parts of the outer mould.
5. When making the truncated cones, make the pins with an offset of 0.5mm compared to the hollow truncated cone shape while the 3D prints will be printed with an approximate accuracy of 0.3mm.

## Dimensions of pins for connecting the different moulds

| Part | Part specifically | Dimensions (mm) |
|---|---|---|
| **Truncated cone bottom** | Bottom diameter | 3.5 |
| | Height | 4.0 |
| | Top diameter | 2.5 |
| **Truncated cone hole** | Bottom diameter | 4.0 |
| | Height | 4.5 |
| | Top diameter | 3.0 |

## Settings in Cura for 3D printing with the Ultimaker3

| | |
|---|---|
| **Extruder 1** | Generic PLA AA0.4 |
| **Extruder 2** | Generic PLA BB0.4 |
| **Infill density** | 20% |
| **Infill pattern** | Triangle |
| **Layer height** | 0.2 mm |
| **Support pattern** | Zig Zag |
| **Support density** | 15% |

When printing the inner core completely of PVA, make sure all 'Extruders' functions in Cura are set to Extruder 2.

## Filling of the mould

1. Coat the outer mould with XTC-3D Smooth-On Coating [120] to make the outer mould watertight.
2. Put Vaseline (Petrolium Jelly) between the outer moulds where they make contact, to make all sliced parts watertight at possible. Tape can be placed around the entire mould for extra securing and ensuring no phantom material will leak out of the mould.
3. Make sure to fill the mould with phantom material in one go. This can be done using a big syringe. Moreover, when filling the syringe make sure no air bubbles will get trapped in the syringe.

4. Inject the phantom material until only phantom material leaks out of all air holes (and no air bubbles anymore).
5. Close all holes to ensure no leakage of the phantom material.
6. Put the filled mould in the freezer and start the freeze-thaw cycle.

## Appendix G

**All cardiac phantom samples dielectric measurements**

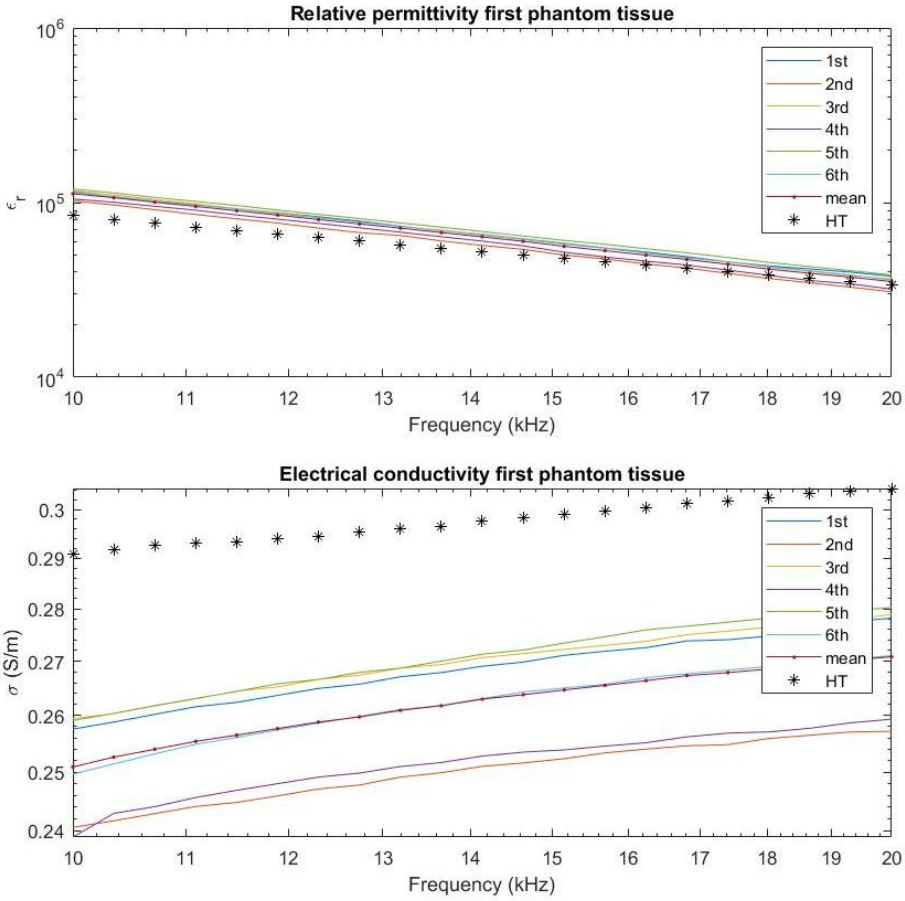


*Figure 106: Dielectric measurements of first cardiac phantom sample*

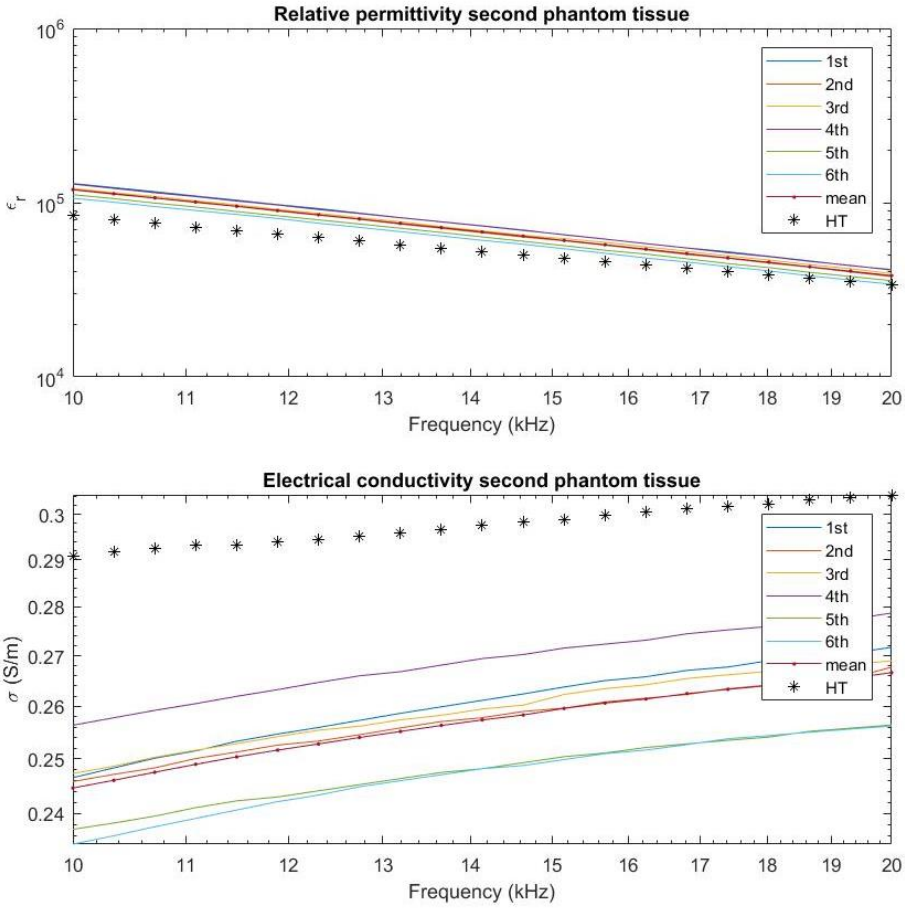


*Figure 107: Dielectric measurements of second cardiac phantom sample*

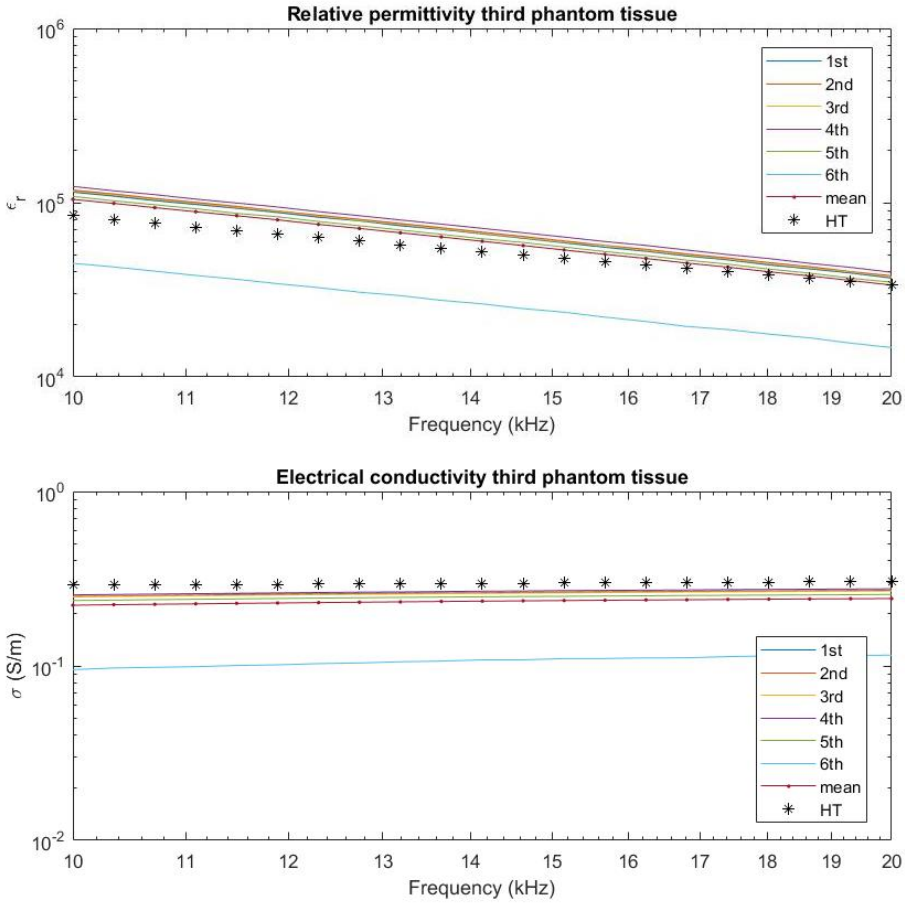


*Figure 108: Dielectric measurements of third cardiac phantom sample*

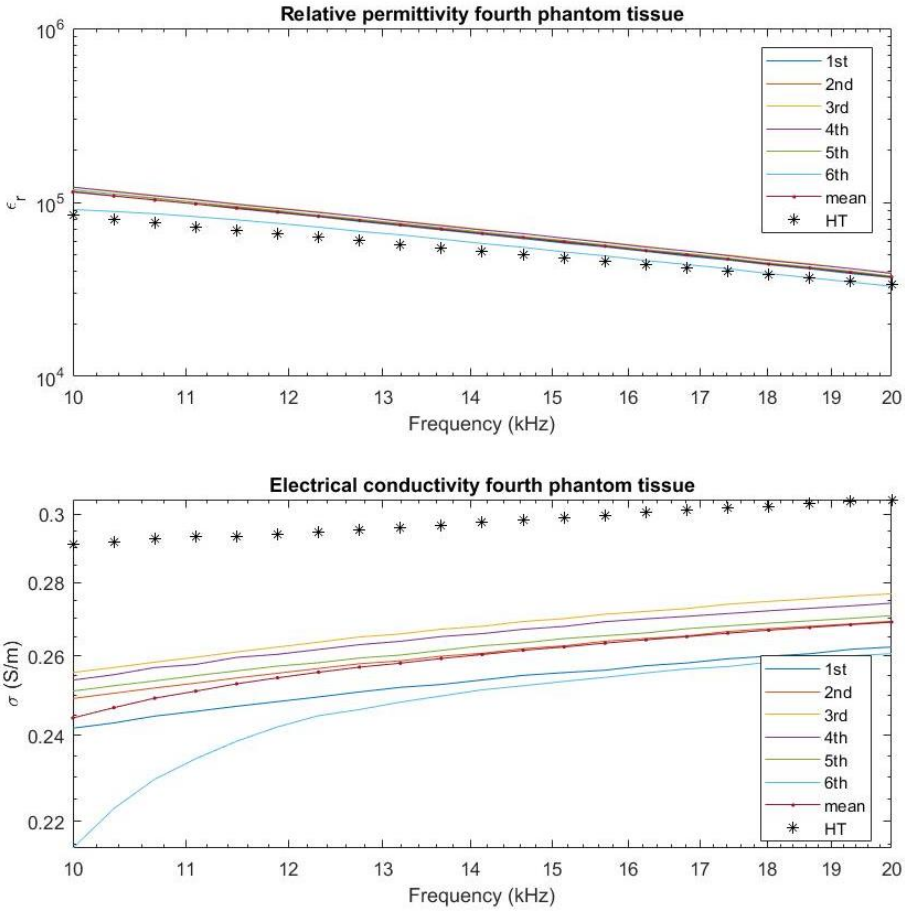


*Figure 109: Dielectric measurements of fourth cardiac phantom sample*